# Quantum Computing: From Theory to Practice

## KSETA 2026


**Lecturer: Benjamin Lienhard**

School of Natural Sciences – TU München

Walther-Meißner-Institut der Bayerischen Akademie der Wissenschaften

# Quantum Computing as a path to solve intractable problems

**“<u>hard</u>” / intractable problems:**
(exponentially increasing resources with problem size)

**Algebraic algorithms** (e.g. factoring, systems of equations)
for machine learning, cryptography,...
**Combinatorial optimization** (traveling salesman,
optimizing business processes, risk analysis,...)
**Simulating quantum mechanics** (chemistry, material science,...)

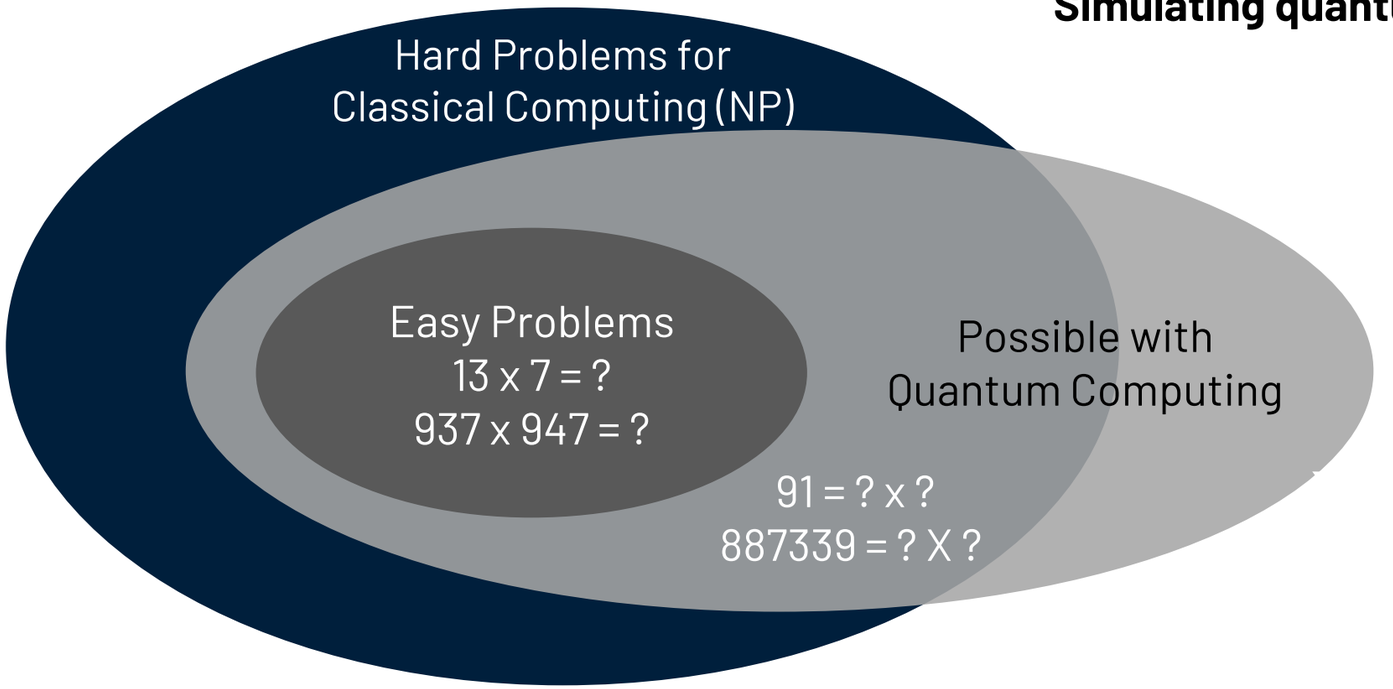



Material,
Chemistry


Machine
Learning

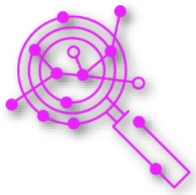
Optimization

# State of the art Quantum Computation

1st quantum computer prototypes are ‘on the market’ (>100 qubits)

Google AI

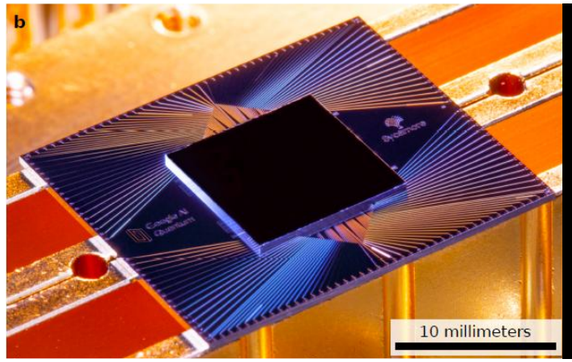


IBM

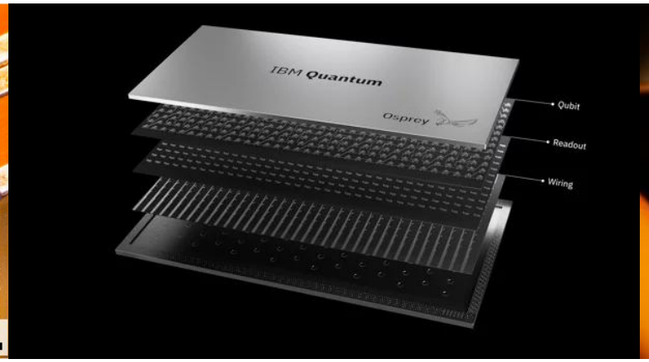


IonQ

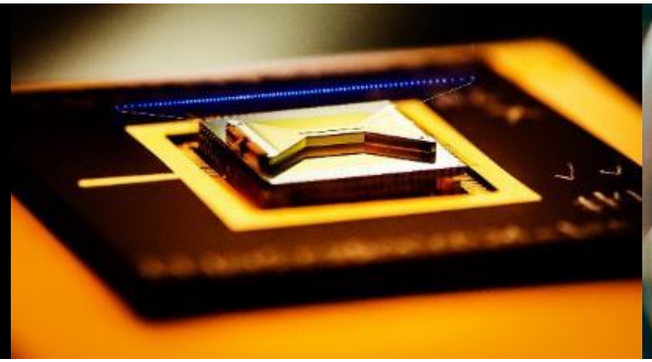

AQT

or in development ( OpenSuperQ GeQCoS MUNIQC-SC ... ) on different platforms: solid state systems (quantum dots, superconducting qubits), atomic systems (trapped ions, neutral atoms), photons, NV-centers

→ many challenges ahead (scaling, coherence, control & readout, system integration)

→ next milestones: practical quantum algorithm, logical qubits

# Quantum mechanics at the level of single particles

## Ultra-cold atoms

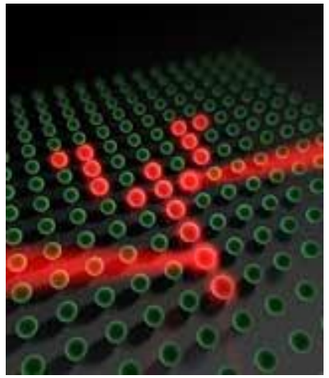

© S. Kuhr

## Trapped ions

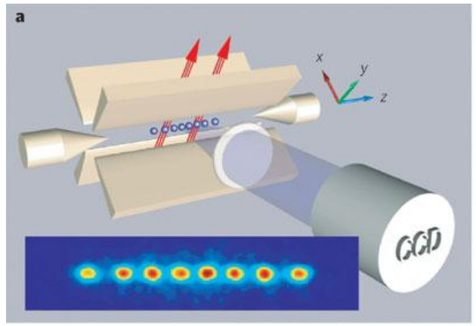


© Blatt & Wineland

## Photons

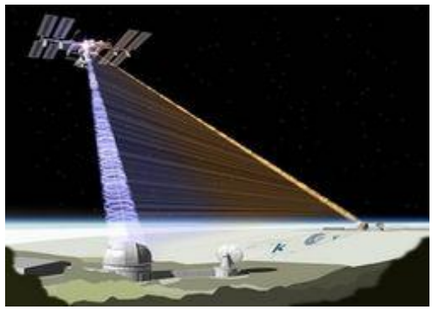

© QUEST, Zeilinger

## Nuclear spins (NMR)

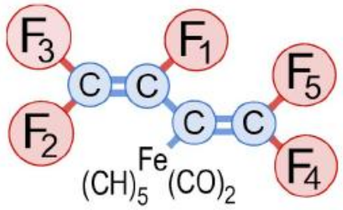


© Vandersypen, Chuang

## Quantum dots, NV-centers

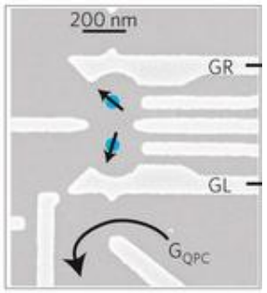


© Bluhm

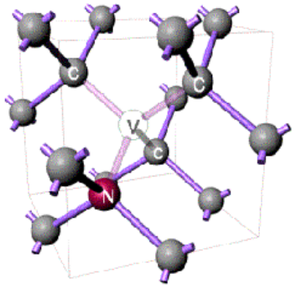


© Wrachtrup

## Superconducting qubits

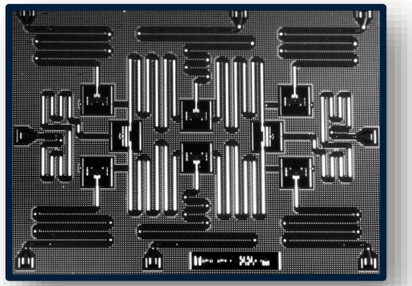

© IBM

# Exemplary Roadmap (IBM)

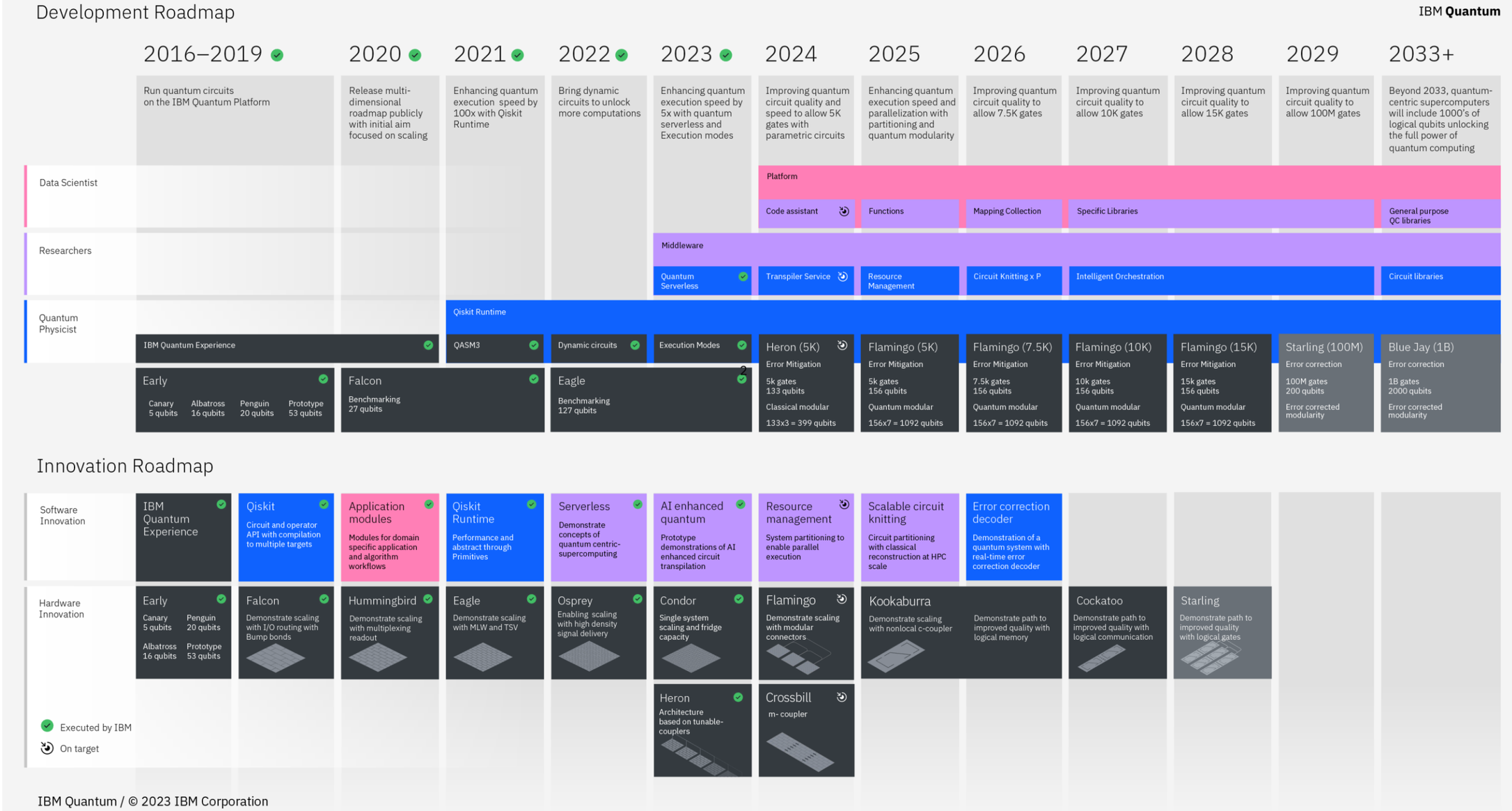

# Efforts at WMI


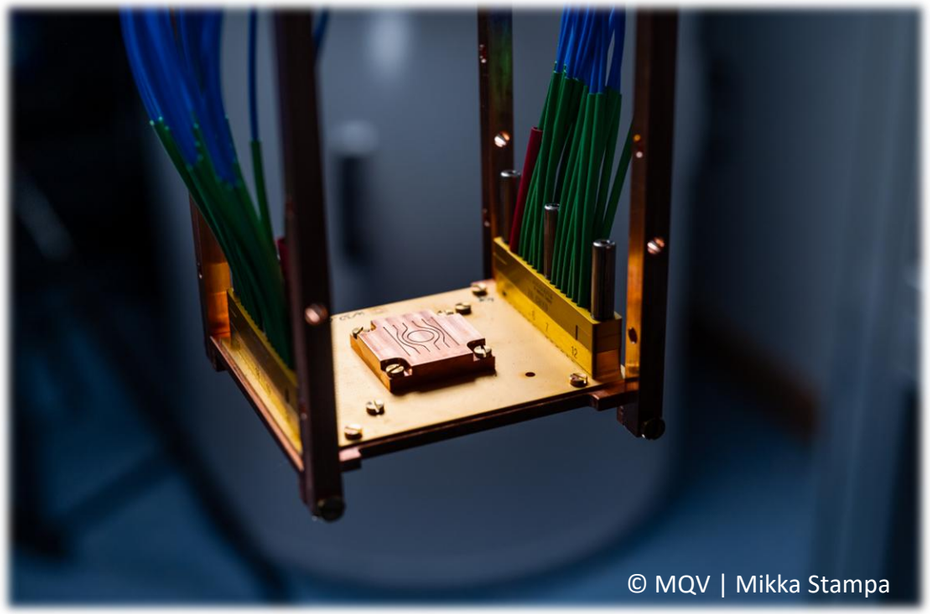


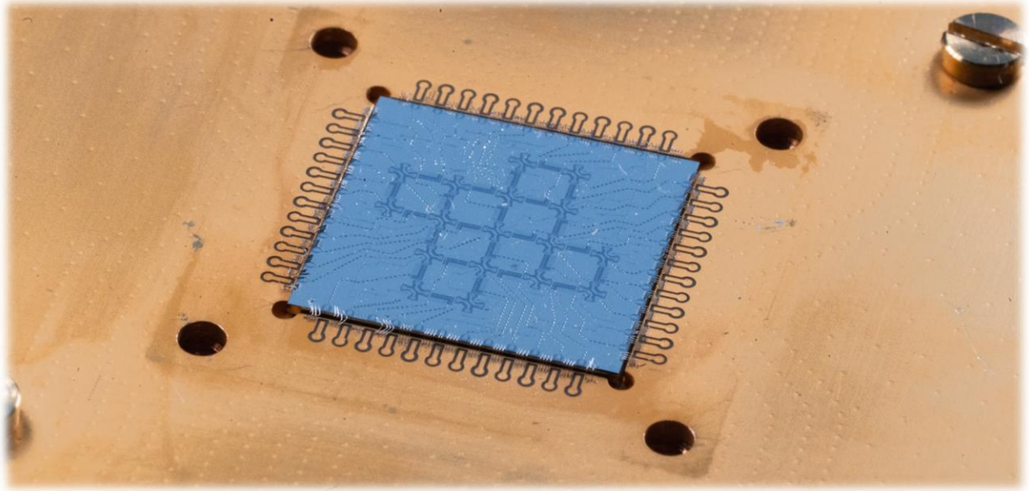

# The Future of Computing

1958

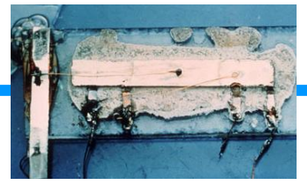

**First integrated circuit Size ~1 cm²**
**2 Transistors**

1971

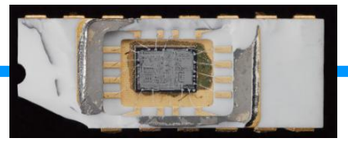

**Moore's Law is Born**
**Intel 4004**
**2,300 transistors**

2023

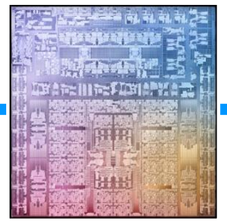

**Apple M3 Ultra**
**4 nm technology, 32 cores**
**184 Billion Transistors**

2024

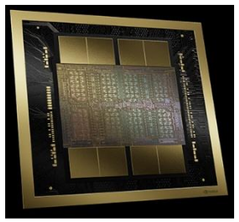

**NVIDIA Blackwell B100**
**4 nm technology**
**208 Billion Transistors**

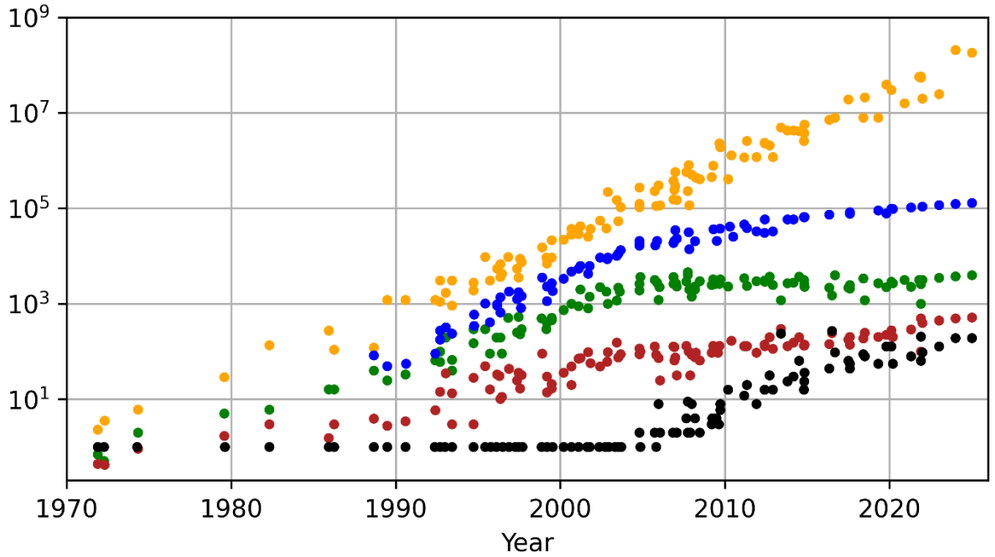


Original data up to year 2010 collected and plotted by M. Horrowitz, F. Labonte, O. Shacham, K. Olukotun, L. Hammond, C. Batten
Data from 2010 to 2020 by K. Rupp: github.com/karlrupp/microprocessor-trend-data
Data from 2020 to 2025 collected by OpenAI ChatGPT

alternative (co-existing) architectures:
next generation systems ('More than Moore')

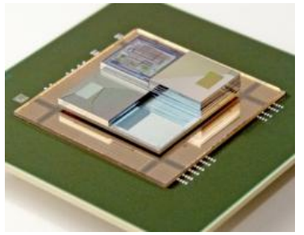

neuromorphic (cognitive)

quantum computing

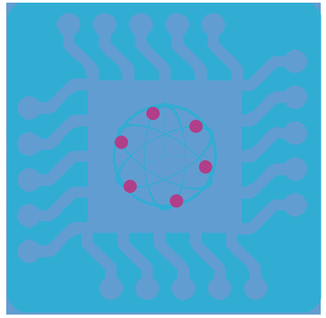

# Evolution of (Classical) Computing Technology

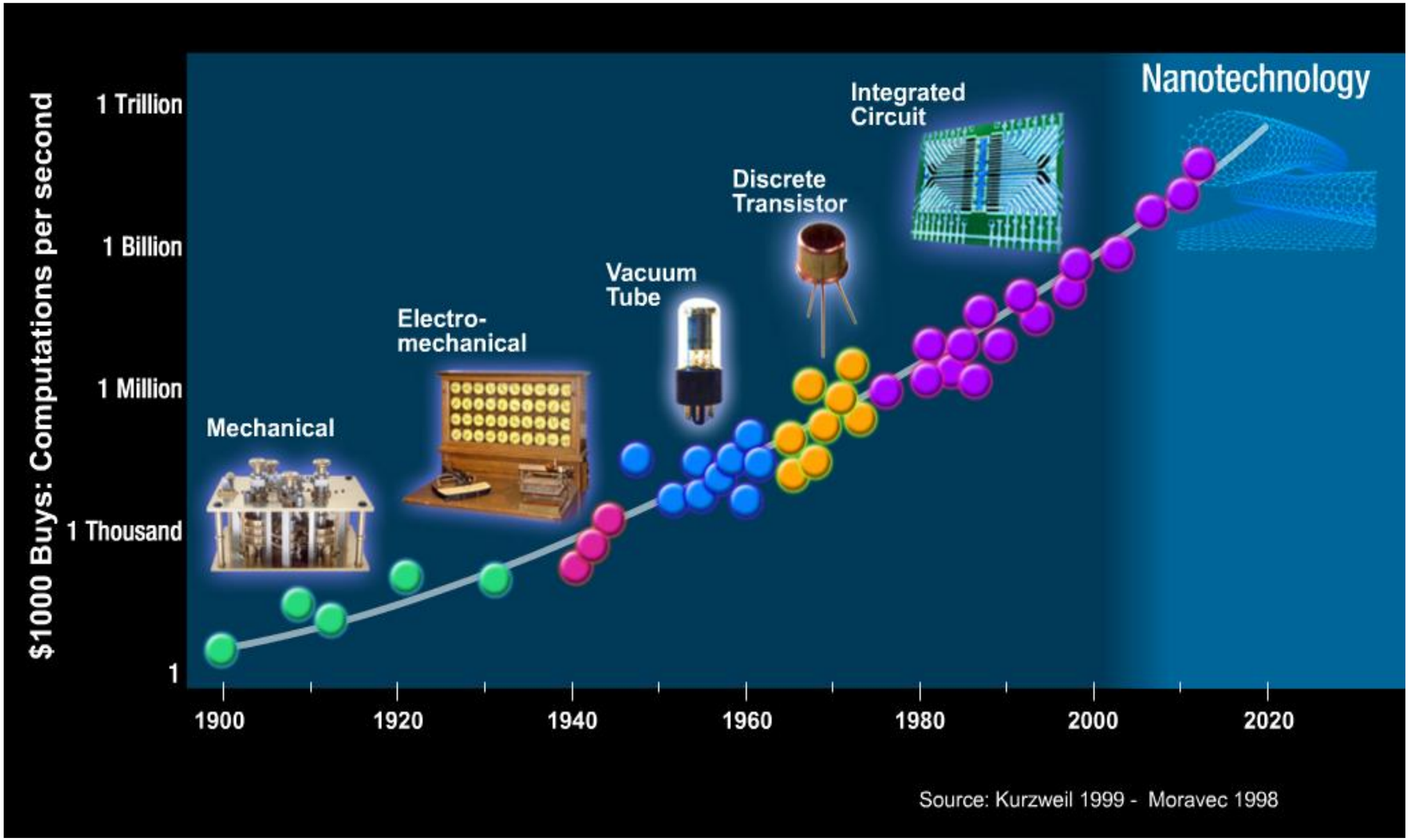

# Evolution of Silicon Technology

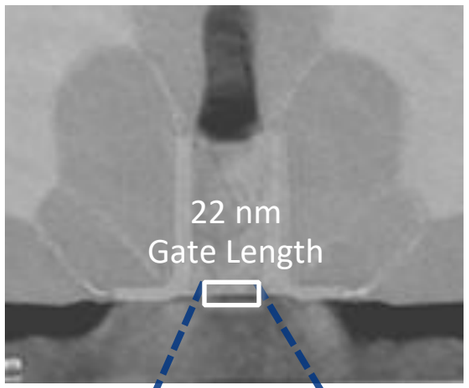


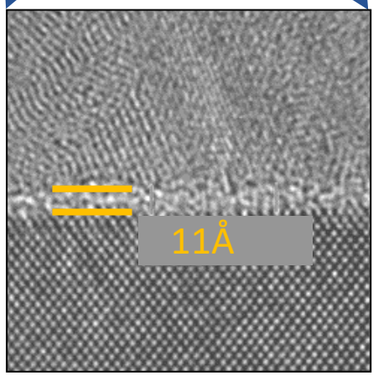


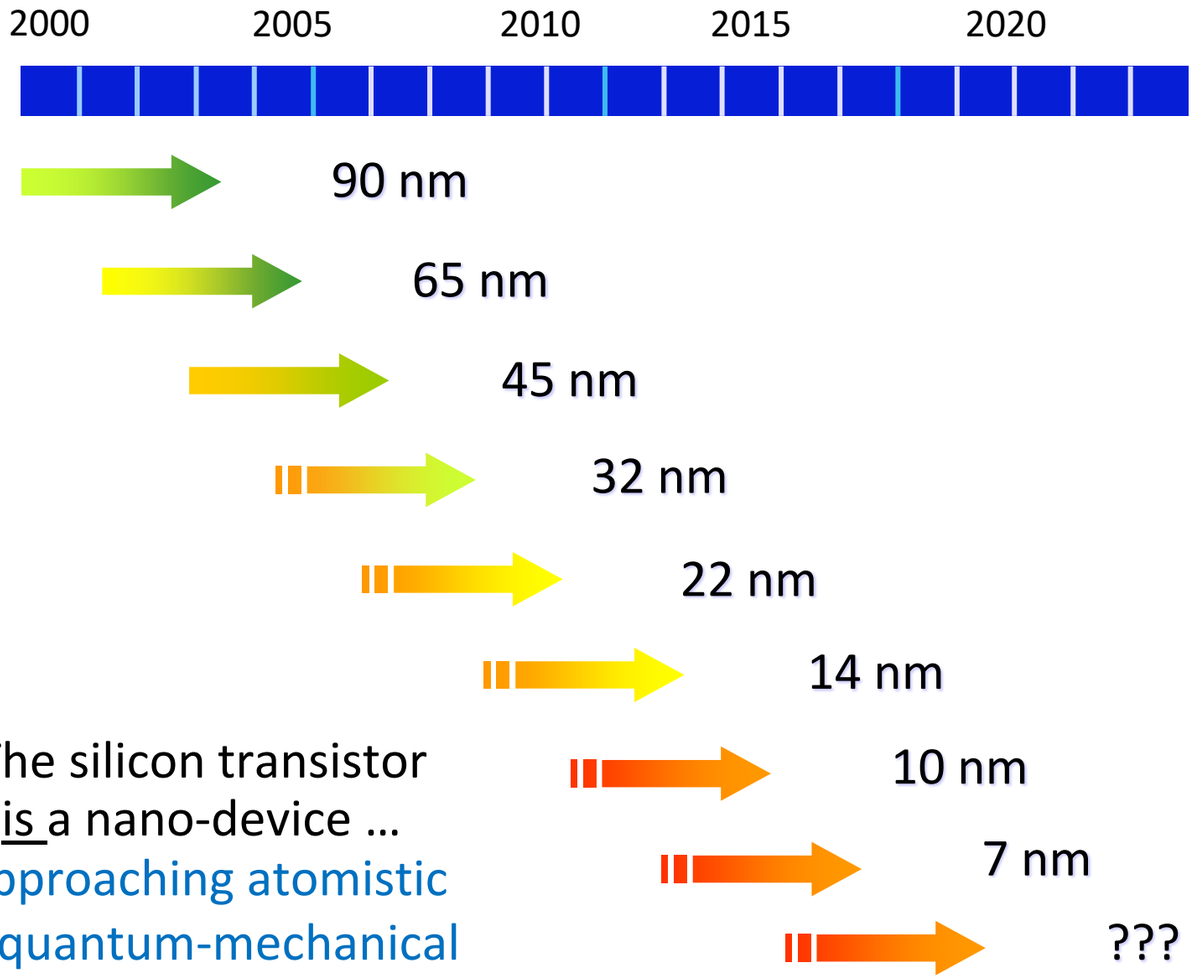


The silicon transistor
is a nano-device …
… approaching atomistic
and quantum-mechanical
boundaries

… approaching
molecular dimensions.

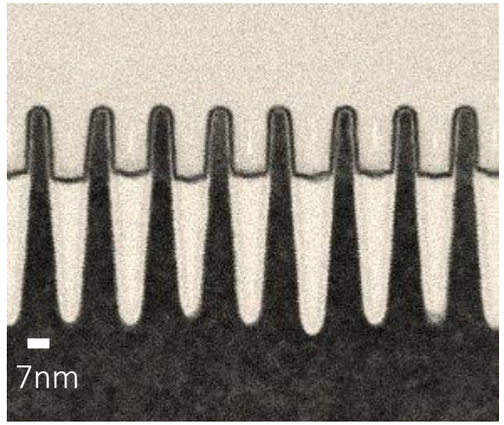


7 mm finFET (IBM; 2016)

# Size of a transistor

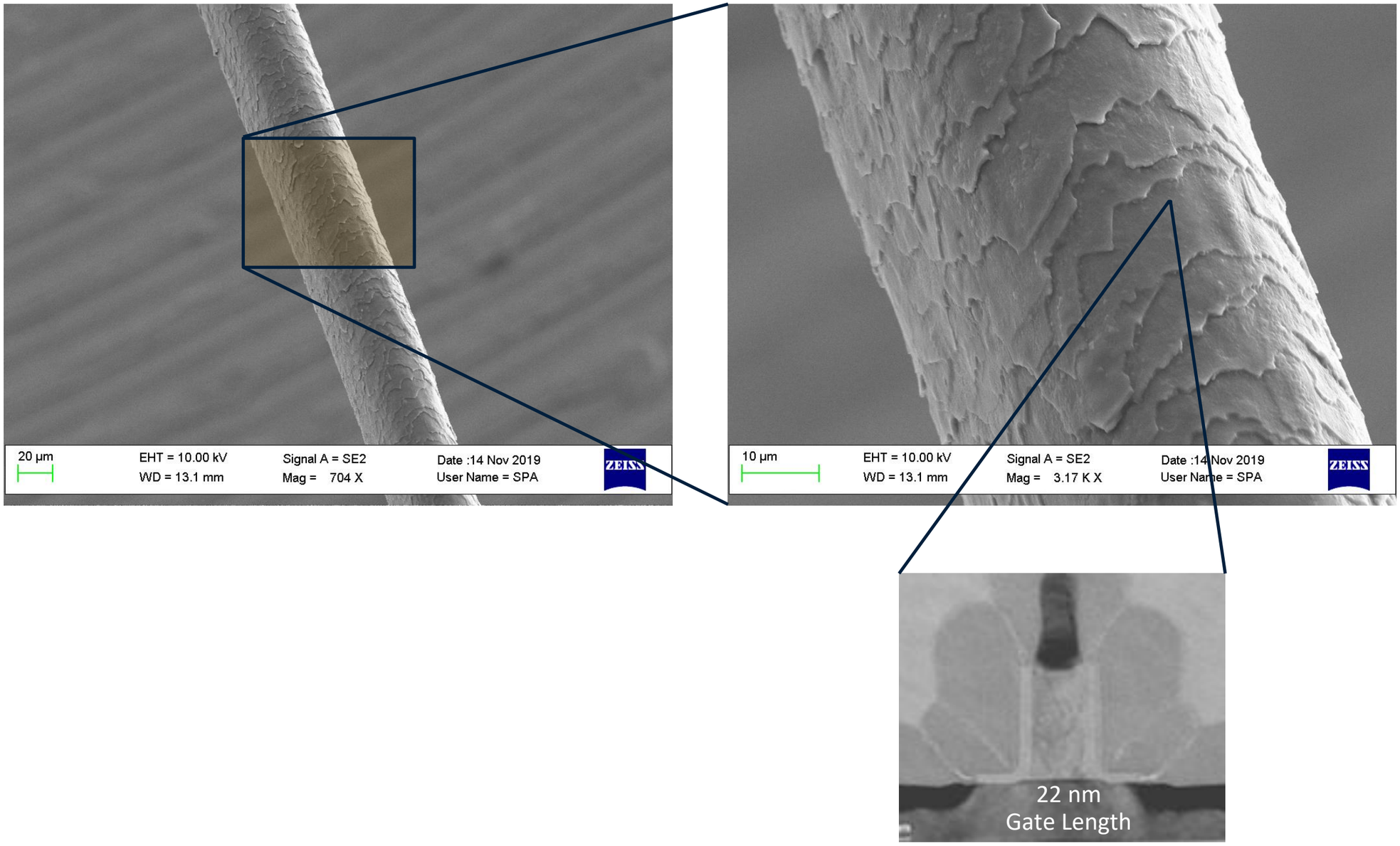

# History of Computing

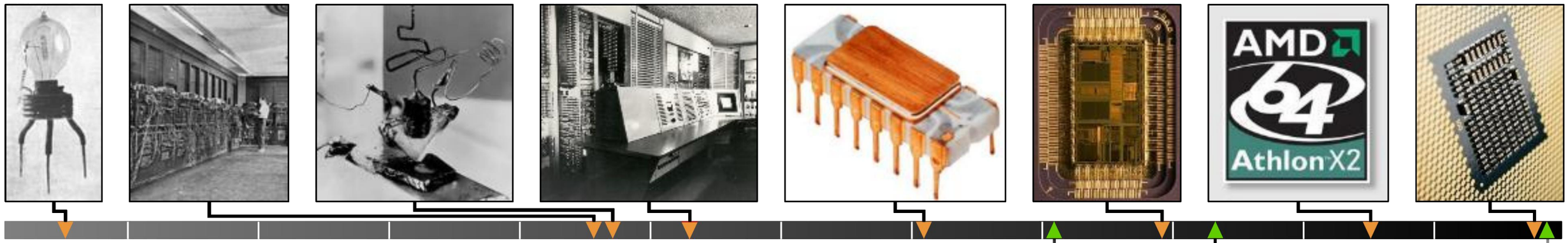


**Today's classical computers required >100 years of engineering.**
**Quantum computing is still in its infancy.**

Idea of quantum computer

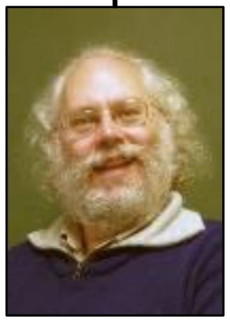

Factoring algorithm

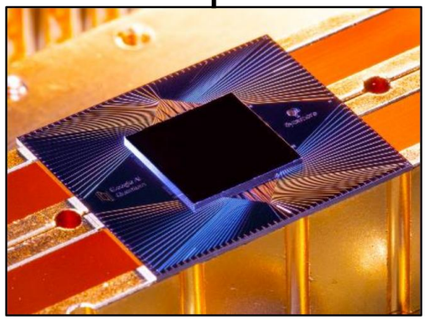

Quantum supremacy (53 qubits)

# Computation Theory

Computational complexity theory: studies the required computational resources (e.g., time, memory, power) to solve a given problem

**Problem: algorithm A run on machine M**

**→ resource requirements are computer architecture dependent**

**Turing machine: abstract machine (mathematical model of computation) able to manipulate symbols on a tape according to a program**

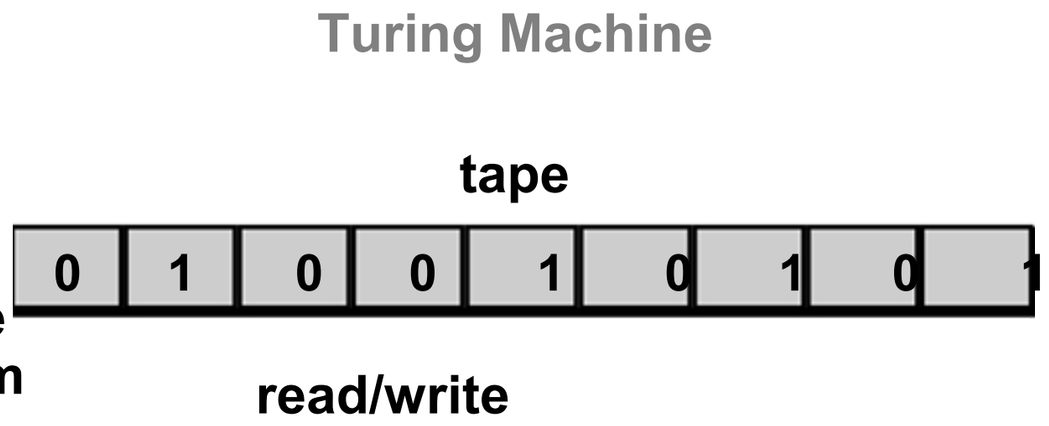


**Resources:**

**Time: number of steps taken by Turing machine**

**Space: number of cells on tape used**

**Turing, A. M., Proceedings of the LMS 2, 41 (1936)**

# Complexity Classes

**P: Polynomial-Time** (Class of feasible problems for classical computers)
Class of decision problems solvable in polynomial time by a deterministic Turing machine

**BQP: Bounded-Error Quantum Polynomial-Time** (Class of feasible problems for quantum computers)
Class of decision problems solvable in polynomial time by a quantum Turing machine, with at most 1/3 probability of error

**NP: Nondeterministic Polynomial-Time**
Class of decision problems solvable by a nondeterministic polynomial-time Turing machine such that
- If the answer is "yes," at least one computation path accepts (verifiable in polynomial time)
- If the answer is "no," all computation paths reject.

**NP-Complete: Nondeterministic Polynomial-Time Complete** ("brute-force search")
Class of decision problems that are in NP and every problem in NP that can be reduced to it
NP-complete problems: most difficult problems in NP

**PSPACE: Polynomial space**
Class of decision problems that can be solved by a Turing machine using a polynomial amount of space

**https://complexityzoo.uwaterloo.ca/Complexity_Zoo**

# Complexity Classes Overview

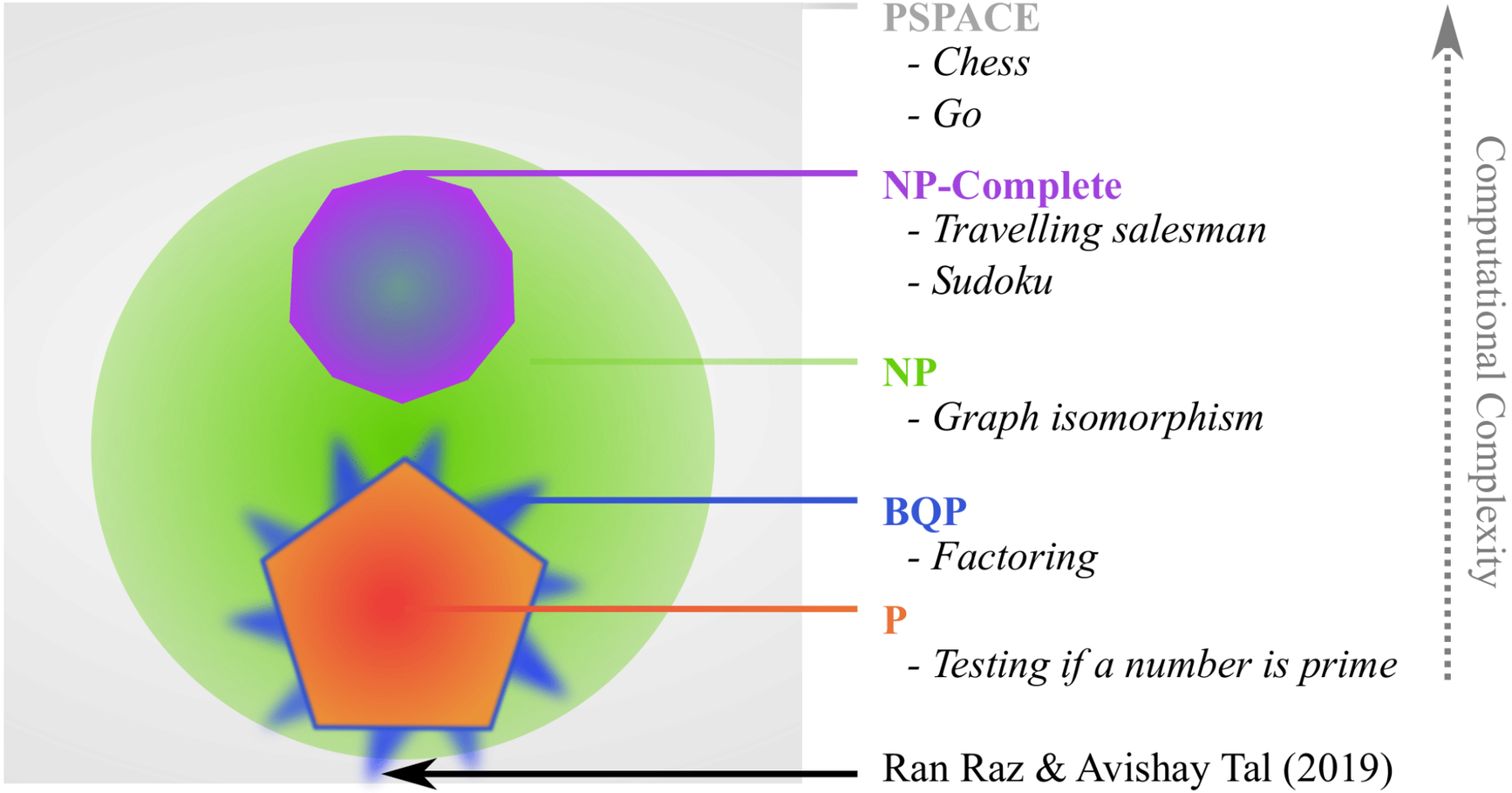


**Quantum computer is more powerful than classical computer**

# Encryption - Decryption

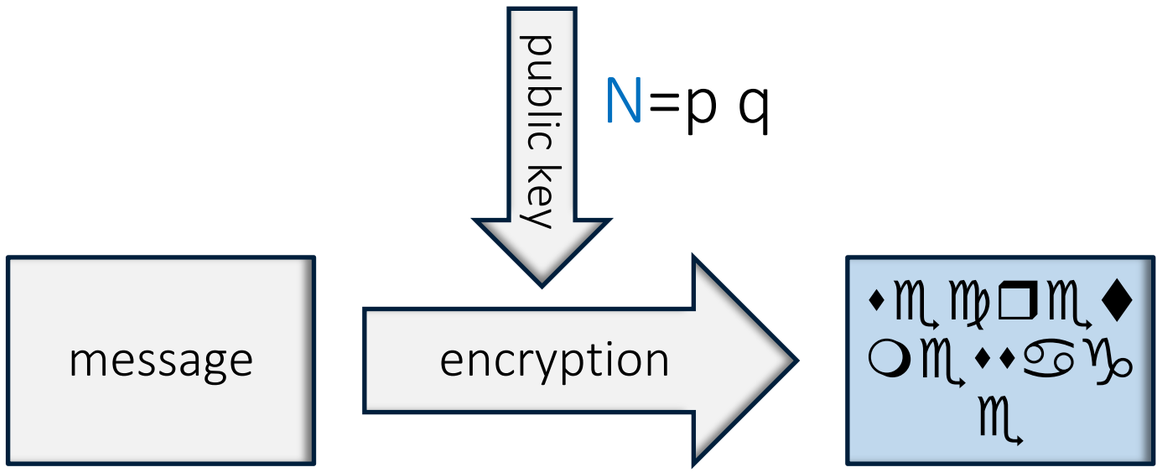


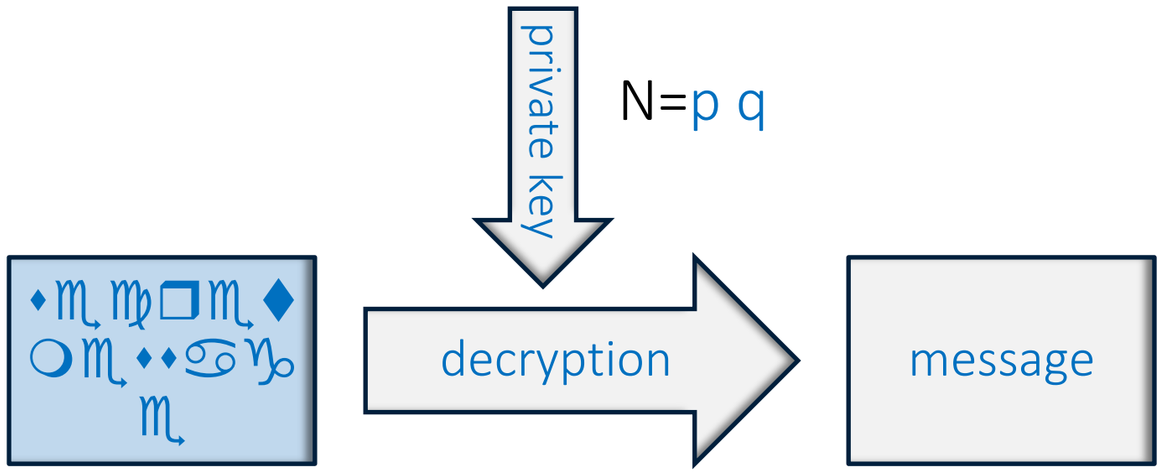

# Factoring Numbers (Shor's Algorithm)

The problem of multiplication vs factoring:

3 x 5 = ?15
29 x 47 = ?1363
→ easy!

Vs.

35 = ?3 x 7
1711 = ?29 x 59
→ hard!

1024 bit – number:
6840125346266703910299476456048009922209314 9893310302951659314435991353018017220121470 6541320995449942227909375021886099382522828 8592859849846037390163982097843793610808523 3562256872463491965682468501271183246657037 2812969247294818566930469719541057172136556 1012039354241537540883074873955926591234907 3090

**= p × q**

→ just short of impossible

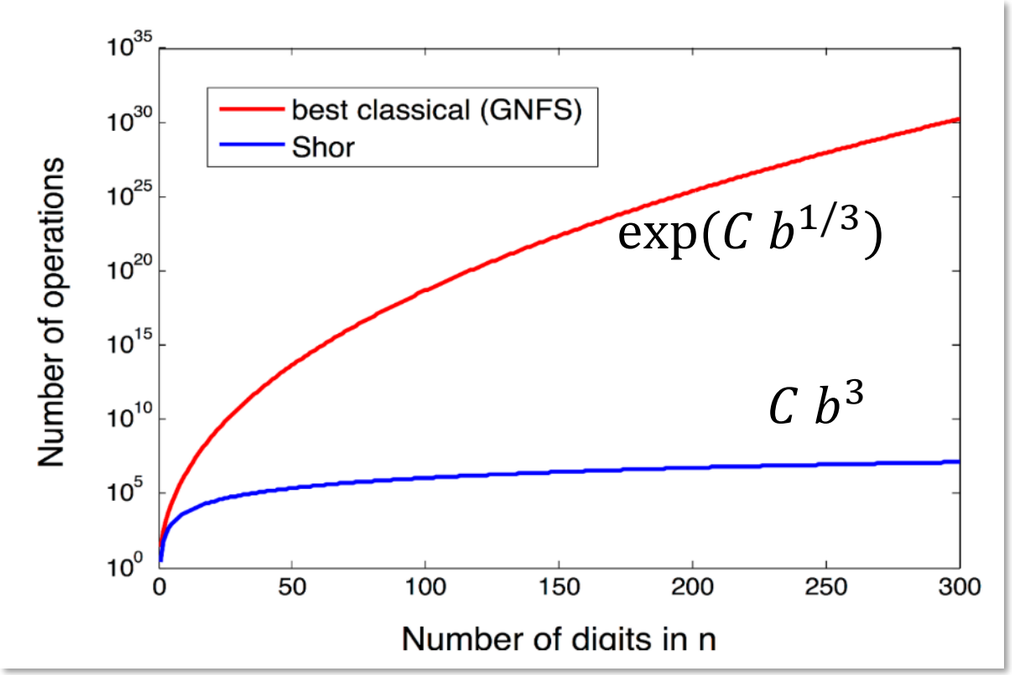


**Exponential speed-up:**
A task taking 300 years ($2^{33}$ seconds) on a classical computer might take a minute (~ 30 seconds) on a quantum computer

Shor's algorithm jumpstarted interest in quantum computing!

# Quantum chemistry – Why is it a challenge?

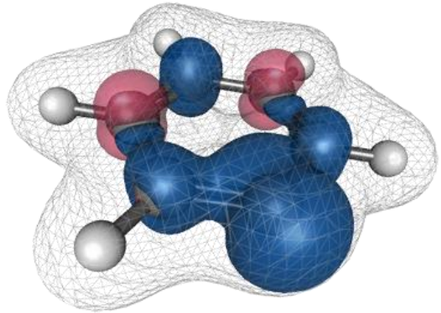

Electrons can occupy different orbitals in many possible combinations (e.g. in hydrogen $H_2$)

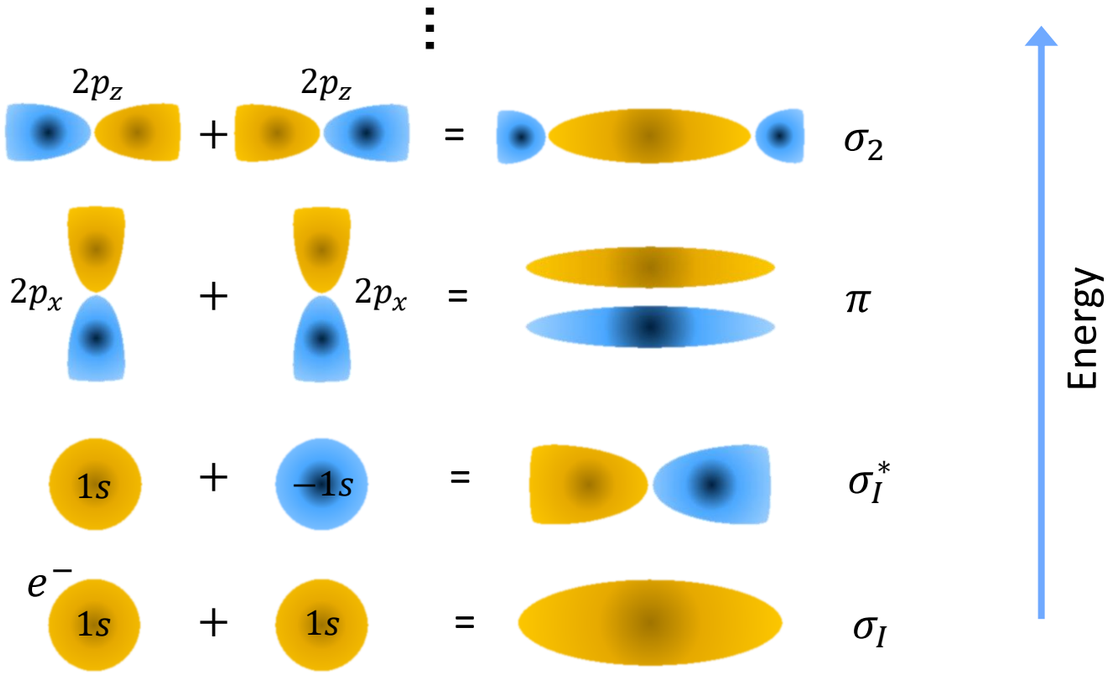

# Electron configurations

How many possibilities are there to arrange N electrons in M orbitals?

*a)* $\frac{M!}{(M-N)!N!}$

*b)* $M \cdot N$

*c)* $e^{M \cdot N}$

# Quantum chemistry – Why is it a challenge?

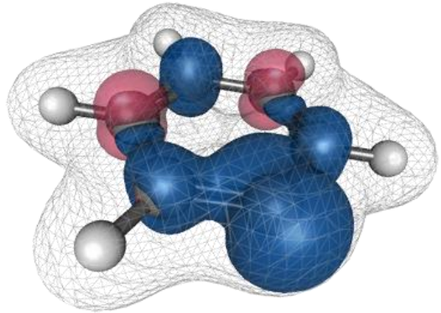

Electrons can occupy different orbitals in many possible combinations (e.g. in hydrogen $H_2$)

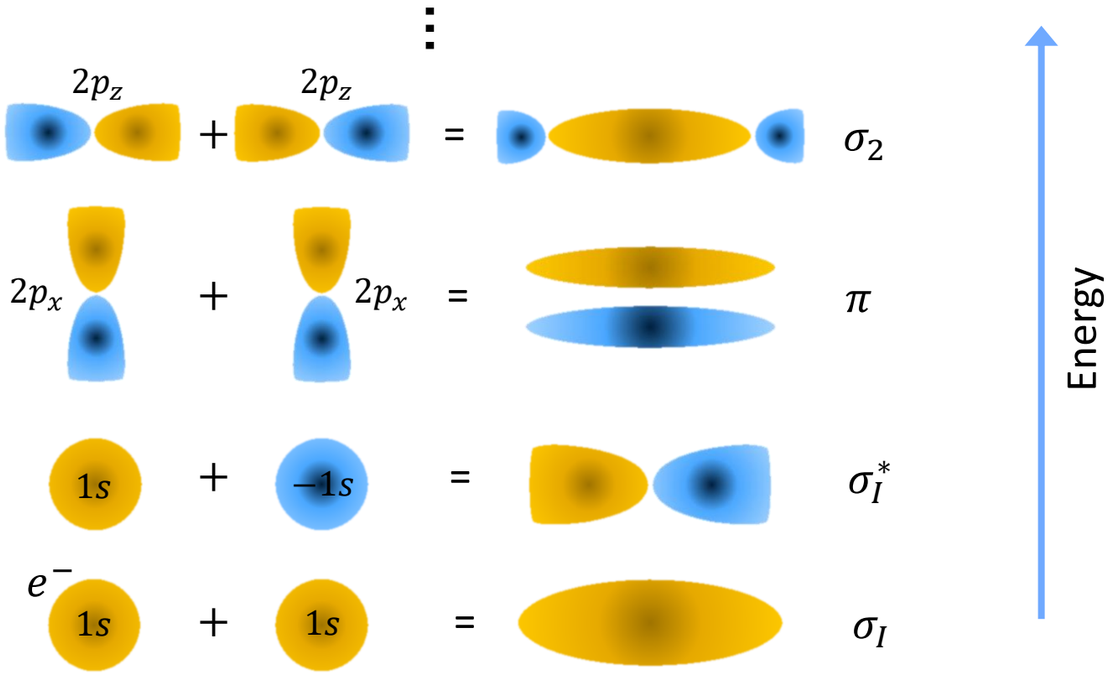


$$\frac{M!}{(M-N)!\,N!}$$

M: # orbitals

N: # electrons

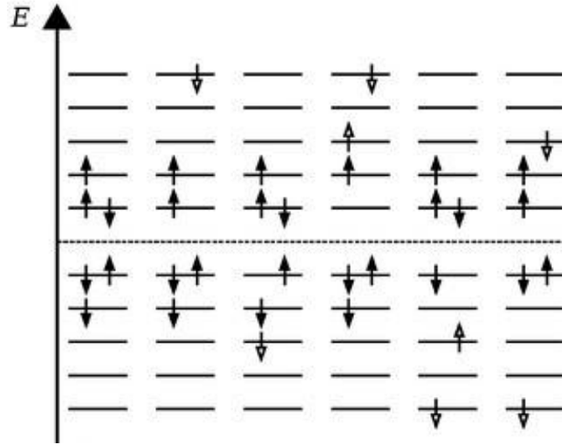


$\approx 2^{65}$ possibilities

for M=82,N=22

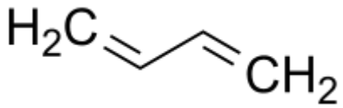


(Butadien)

**Exponential quantum advantage** when electron wavefunction is stored directly in a quantum system

# Quantum computing vison

A) What is needed to make quantum computers useful is more **hardware** development?

B) What is needed to make quantum computers useful is more **software/applications** development?

C) Quantum computing won’t work at all, but it will certainly lead to **new useful technology.**

# Outline - 1. Introduction to Qubits and QIP

- What is quantum computing?
- What is a qubit?
- What is entanglement?
- How can entanglement be created (e.g., CNOT)?
- What is a projective measurement?
- What are the basic components of a quantum computer?

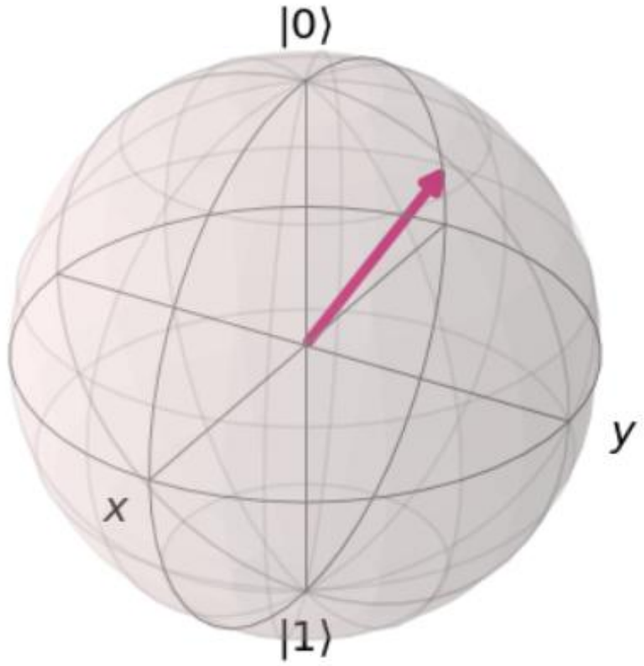

# Outline - 2. Qubits

- What is a superconducting qubit?
- What is a Josephson junction?
- How to realize different types of superconducting qubits? (CPB, transmon)
- What properties do the different types of qubits have?

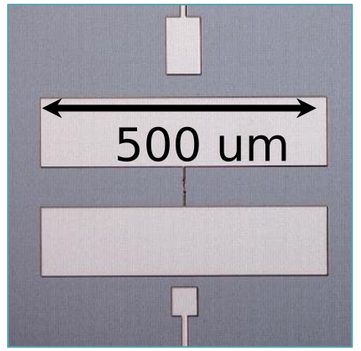

# Outline - 3. Qubit design and fabrication

- How to fabricate superconducting circuits?
- Which materials and which processes are used?
- What kind of losses and decoherence channels are there?

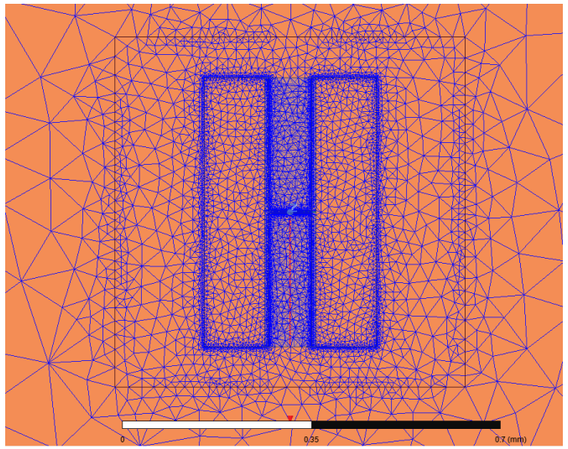

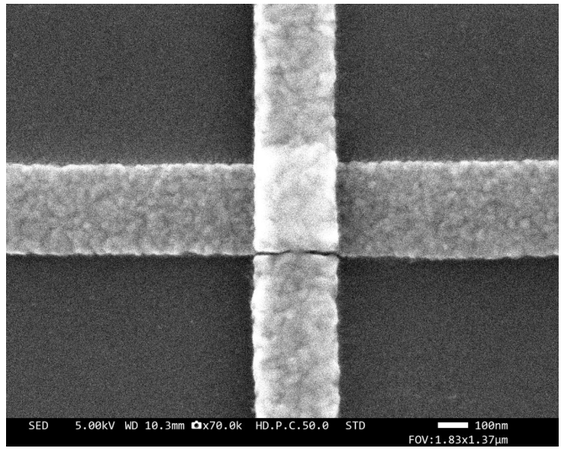


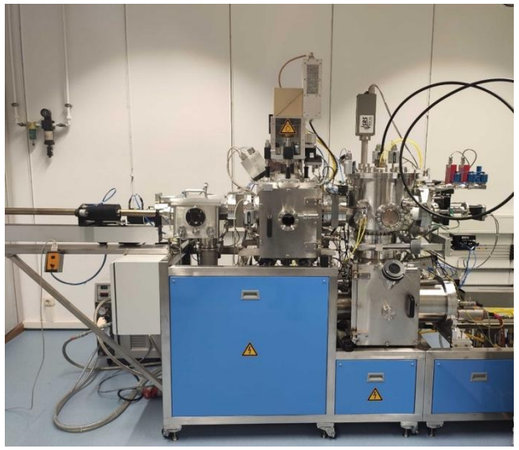

# Outline - 4. Qubit Readout, Control, and Correction

- How to readout a qubit?
- How to control a qubit?
- How to correct errors?
- What are the open challenges?

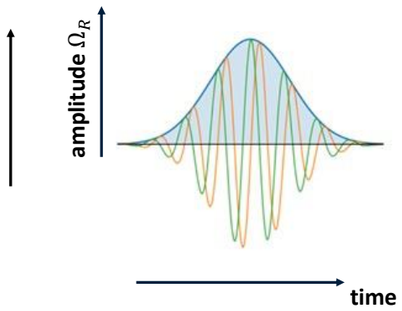


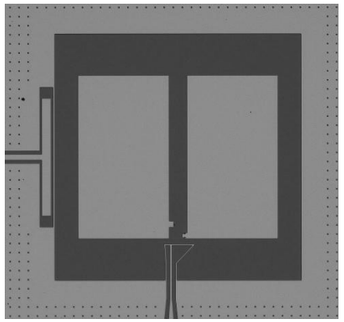

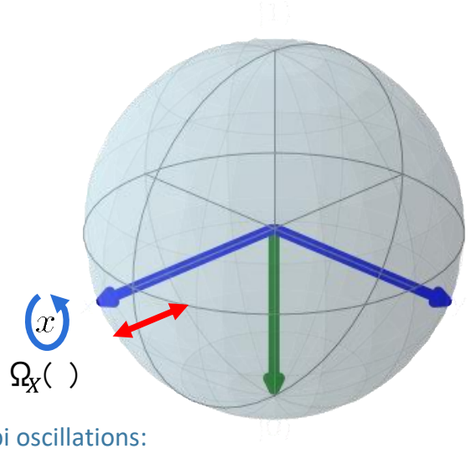


Rabi oscillations:

# Quantum Computing

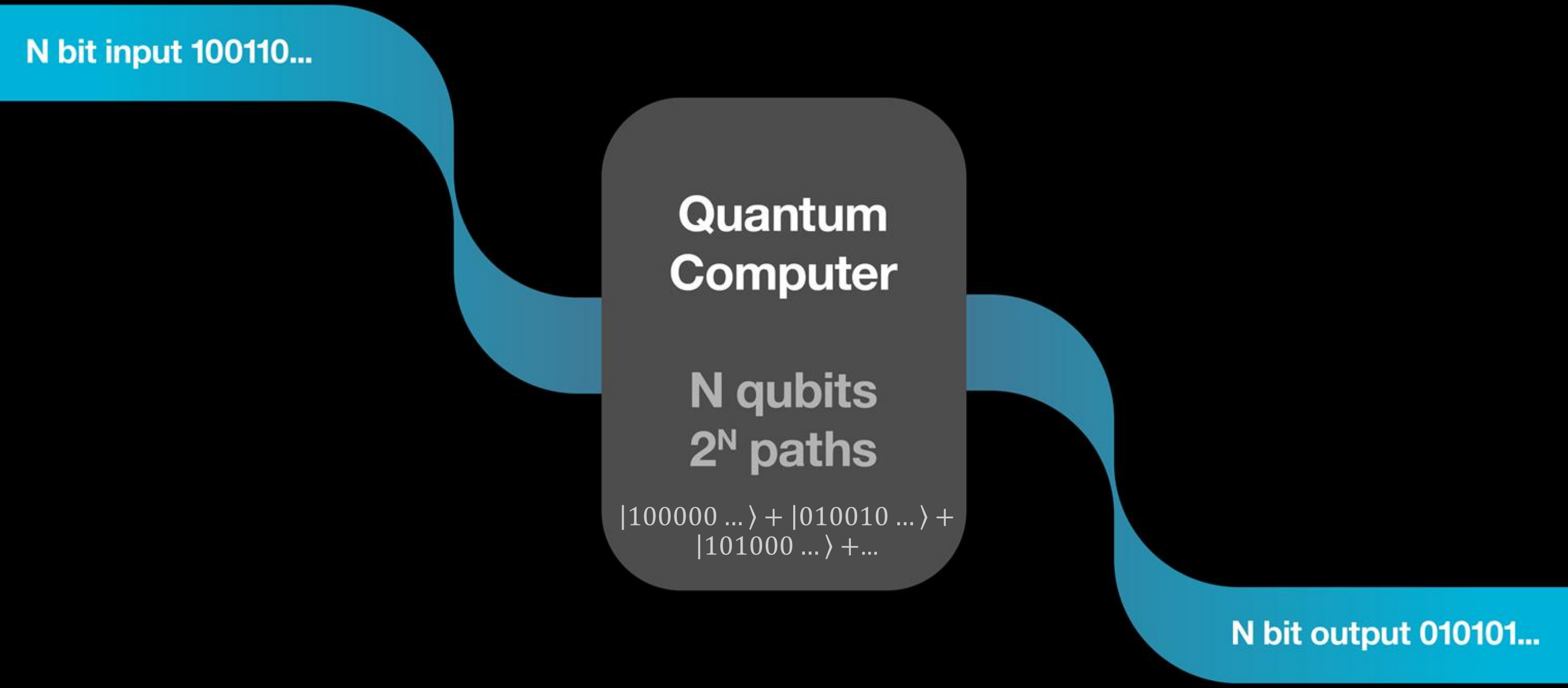
N bit input 100110...
Quantum Computer
N qubits
$2^N$ paths
$|100000 \ldots\rangle + |010010 \ldots\rangle + |101000 \ldots\rangle + \ldots$
N bit output 010101...

# Types of Quantum Computing

## Quantum Annealing

### Optimization Problems

- Machine learning
- Fault analysis
- Resource optimization
- etc...

$$H(t) = H_0 t + (1-t)H_t$$

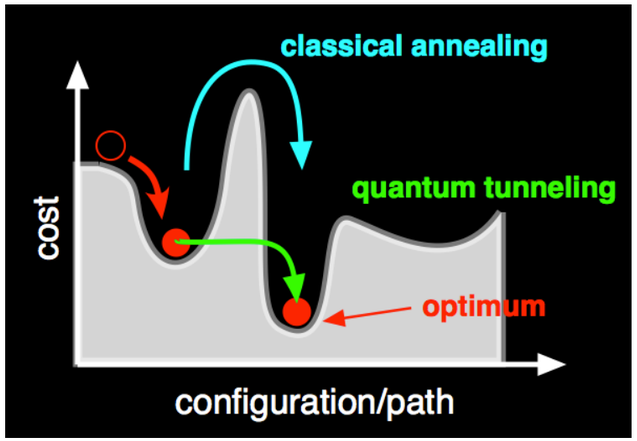


Many 'noisy' qubits can be built;
large problem class in optimization;
amount of quantum speedup unclear

## Approximate Q-Comp. (NISQ)

### Simulation of Quantum Systems, Optimization

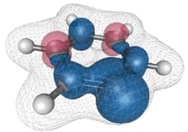

- Material discovery
- Quantum chemistry
- Optimization (logistics, time scheduling,...)
- Machine Learning

$$E_t = \langle \psi_t | H | \psi_t \rangle$$

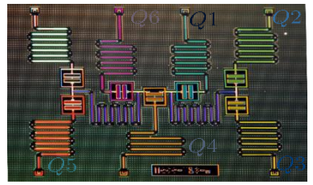


Hybrid quantum-classical approach;
already 50-100 "good" physical qubits
could provide quantum speedup.

## Fault-tolerant Universal Q-Comp.

### Execution of Arbitrary Quantum Algorithms

- Algebraic algorithms
  (machine learning, cryptography,...)
- Combinatorial optimization
- Digital simulation of quantum systems

$$|\psi_t\rangle = U_n \dots U_1 |\psi_0$$

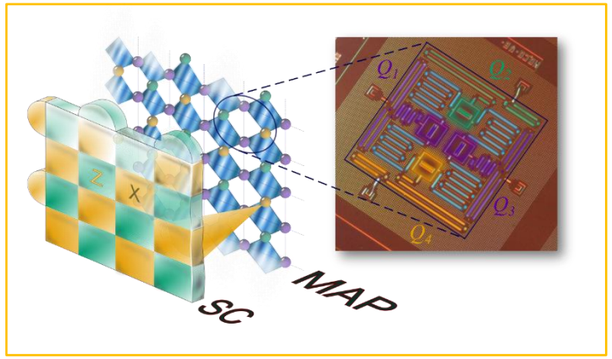


Surface Code: Error correction in a Quantum Computer

Proven quantum speedup;
error correction requires significant
qubit overhead.

# Quantum Computing: Extra power from interference

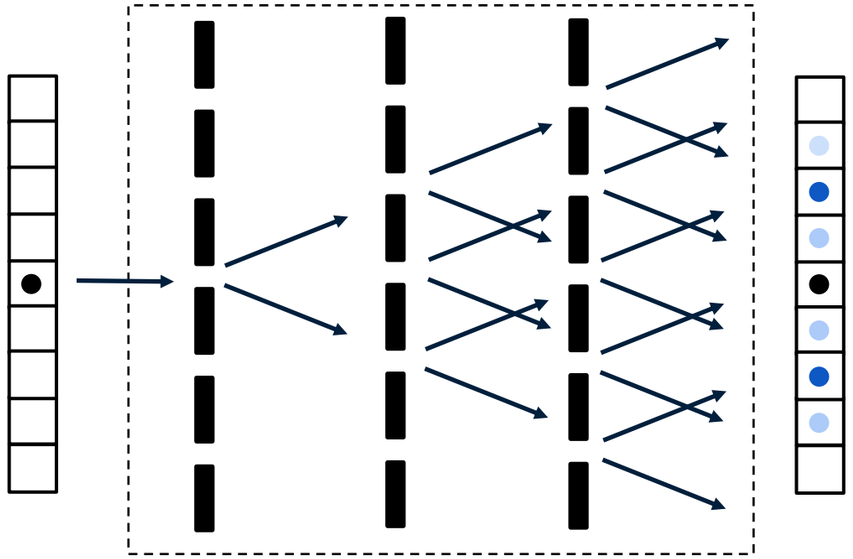

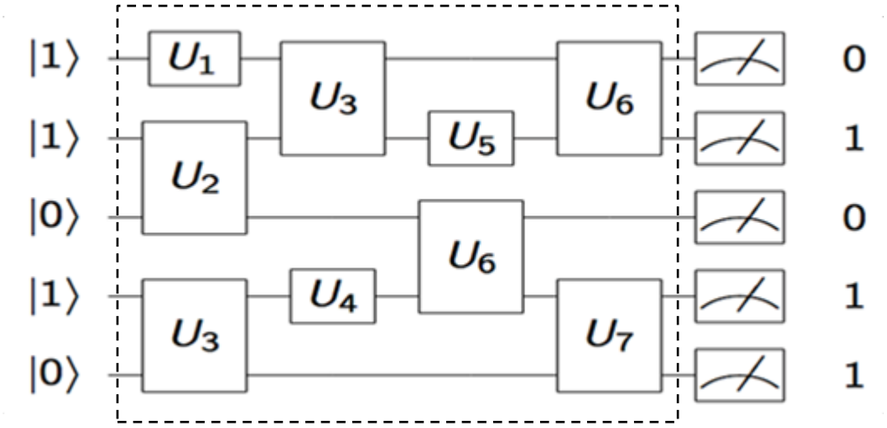


- Many computational paths from initial state to each final state
- Each path accumulates a complex phase, e.g. $1, -1, i, e^{i\pi/4}, \ldots$
- Output probability: concentrated at the final states where (almost) all paths arrive with (approximately) the same phase.

# Quantum Computer Building Blocks

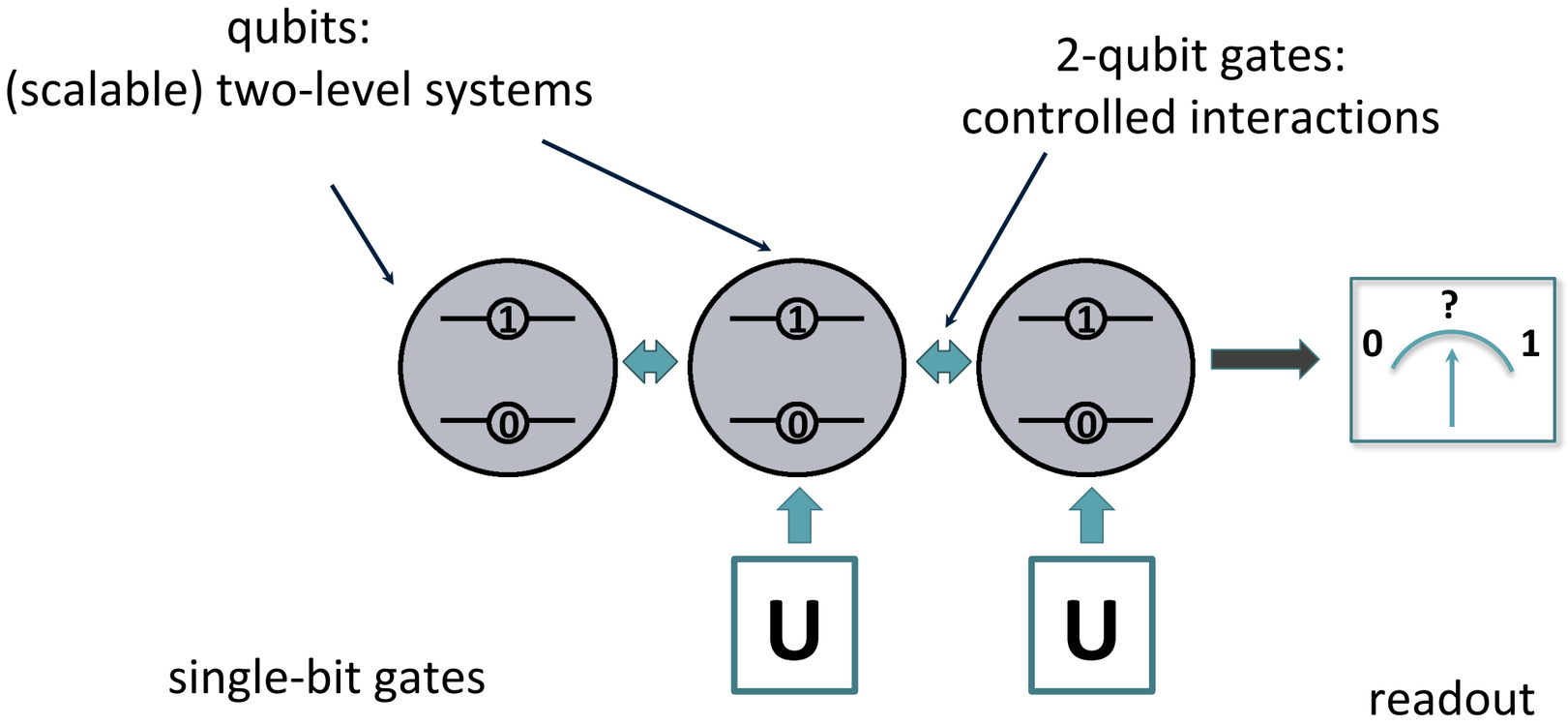


- Quantum information processing requires excellent qubits, gates & readout
- Conflicting requirements: good isolation from environment while maintaining good addressability

# DiVincenzo Criteria

for Implementing a quantum computer in the standard (circuit approach) to quantum information processing (QIP):

#1. A **scalable** physical system with well-characterized qubits.

#2. The ability to **initialize** the state of the qubits.

#3. **Long (relative) coherence** times, much longer than the gate-operation time.

#4. A **universal set** of quantum gates.

#5. A qubit-specific **measurement** capability.

plus two criteria requiring the possibility to transmit information:

#6. The ability to **interconvert** stationary and mobile (or flying) qubits.

#7. The ability to faithfully **transmit** flying qubits between specified locations.

# ‘Circuit-approach’ to quantum computing

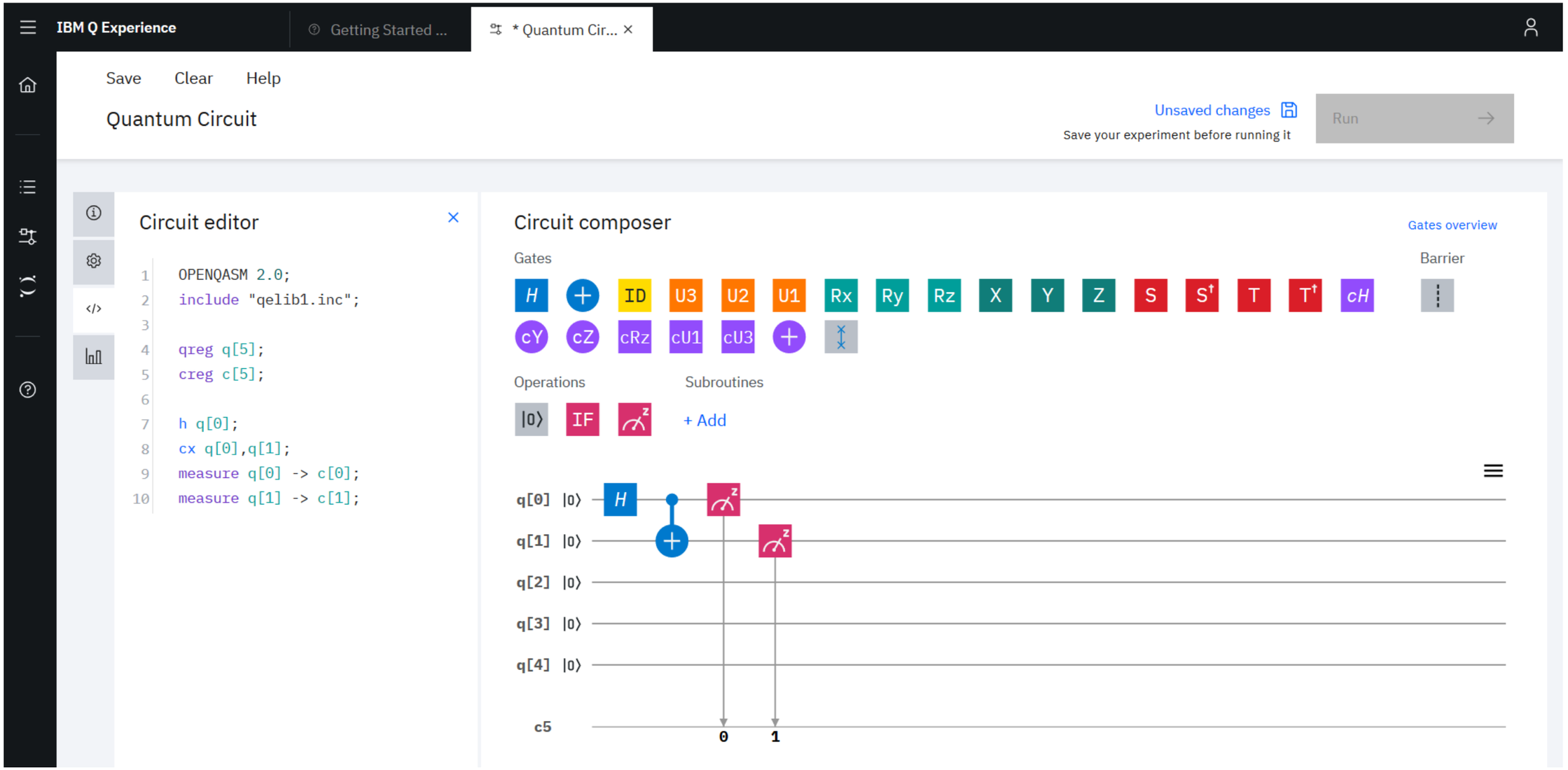


https://quantum-computing.ibm.com/

# Qubits

# What are the basic units of information?

## Classical Bit


0 or 1

## Quantum Bit (Qubit)

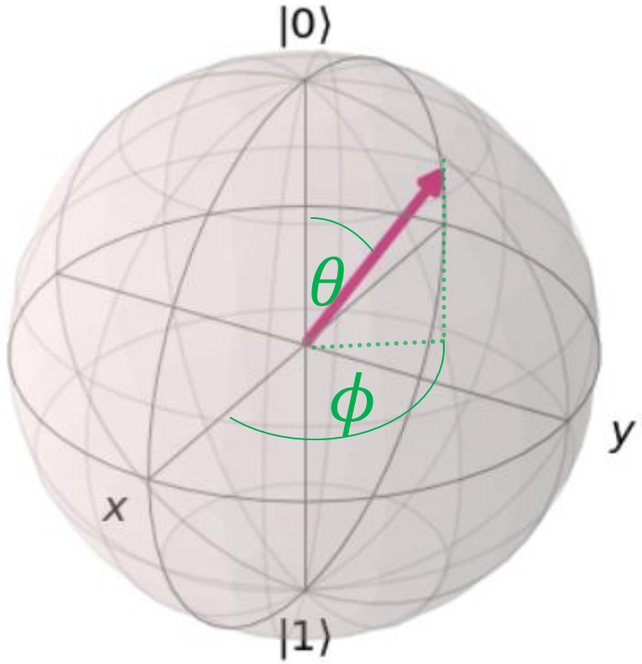


0 and 1, at the same time

represented by point on (Bloch-)Sphere

’superposition’

# What are the basic units of information?

## 2 Classical Bits

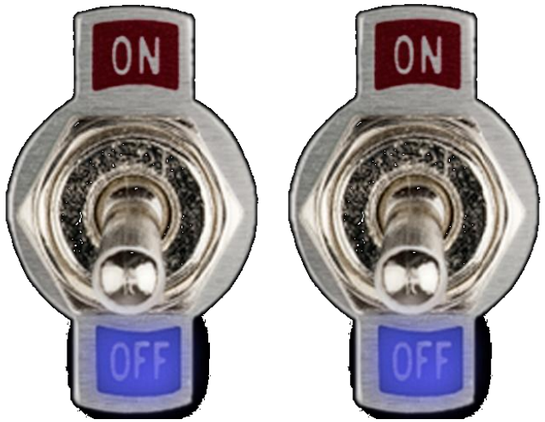


00, 01, 10, or 11

## 2 Quantum Bits (Qubits)

$$\alpha|00\rangle+\beta|01\rangle+\gamma|10\rangle+\delta|11\rangle$$

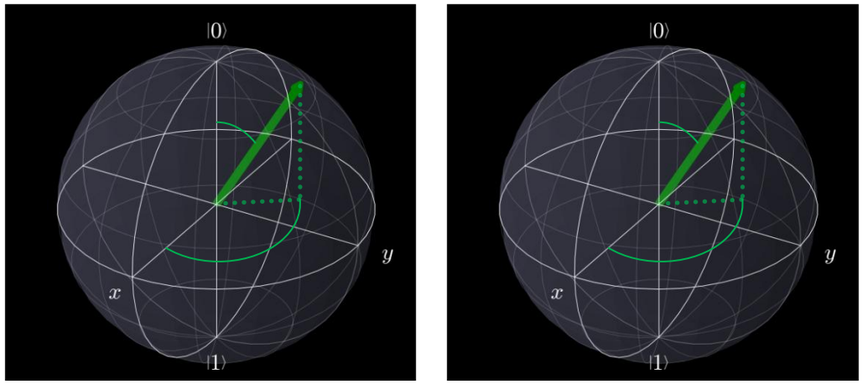


00, 01, 10 and 11 at the same time

with probability $|\alpha|^2$, $|\beta|^2$, $|\gamma|^2$ and $|\delta|^2$

**Superposition + Entanglement**

# 1 qubit – 2 basis states

$$\alpha|0\rangle + \beta|1\rangle$$

where $\alpha$ and $\beta$ are complex numbers

$2^1$

## 1 qubit – 2 basis states

$$\alpha|0\rangle + \beta|1\rangle$$

## 2 qubits – 4 basis states

$$\alpha|00\rangle + \beta|01\rangle + \gamma|10\rangle + \delta|11\rangle$$

where $\alpha, \beta, \gamma, \delta$ are complex numbers

$$2^2$$

## 1 qubit – 2 basis states

$$\alpha|0\rangle + \beta|1\rangle$$

## 2 qubits – 4 basis states

$$\alpha|00\rangle + \beta|01\rangle + \gamma|10\rangle + \delta|11\rangle$$

## 3 qubits – 8 basis states

$$\alpha|000\rangle + \beta|001| + \gamma|010\rangle + \delta|011\rangle + \epsilon|100\rangle + \zeta|101| + \eta|110\rangle + \theta|011\rangle$$

**where $\alpha$, $\beta$, ...$\theta$ are complex numbers**

$2^3$

Exponential growth

$$2^n$$

# $2^{50} \sim 8EB$

# (8 million GB)

Basis states
50 qubit system

1125899906842624

$$2^{275}$$

More basis states than there are atoms in the observable universe

607084028820540334662331845882349658325752137203793600391191378043407589126627 65568

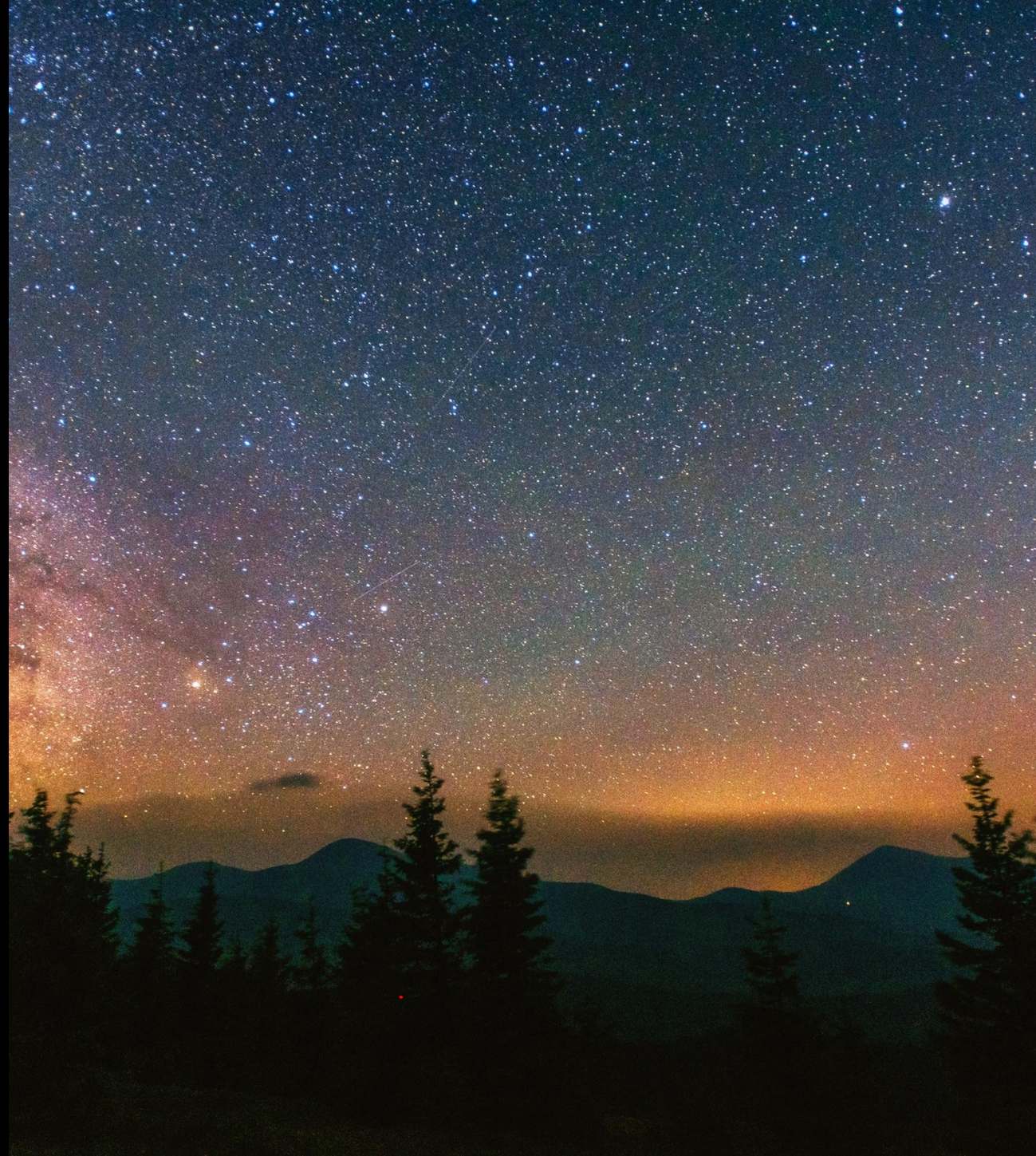

# Exponential growth of state space

***How much memory is needed to store a quantum state?***

| # qubits | quantum state | coefficients | # bytes |
|---|---|---|---|
| 1 | $a\|0\rangle + b\|1\rangle$ | $2^1 = 2$ | 16 Bytes |
| 2 | $a\|00\rangle + b\|01\rangle + c\|10\rangle + d\|11\rangle$ | $2^2 = 4$ | 32 Bytes |
| 8 | | $2^8 = 256$ | 2kB |
| 16 | … | $2^{16} = 65'536$ | 512 kB |
| 32 | … | ~4 billion | 32 GB |
| 64 | … | ~ information in internet | 128 EB (134 million GB) |
| 256 | … | ~ # of atoms in universe | … |

# Classical logical operations

**Classical bit:**

- possible values are 0 or 1
- physical realizations:

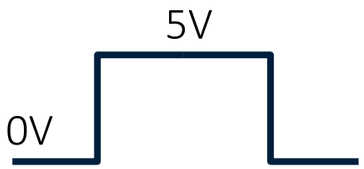


Voltage level in a circuit


Switch

Relais

VacuumTube

Transistor

- manipulation of bits via a **physical** process:

Harddisc write heat

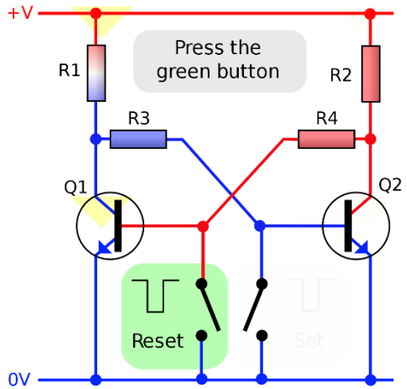


Flip-flop circuit
https://en.wikipedia.org/wiki/Flip-flop_(electronics)

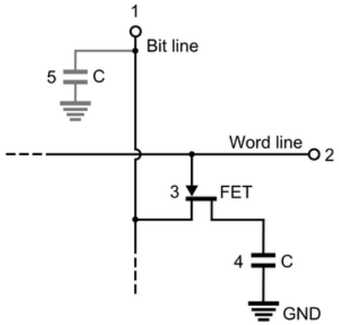


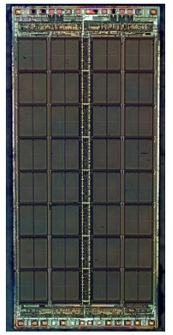

DRAM – memory cell
https://en.wikipedia.org/wiki/Memory_cell_(computing)

# Classical logic operations

Any classical operation can be decomposed into single and two-bit gates!

Single-bit gates:

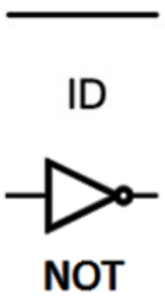


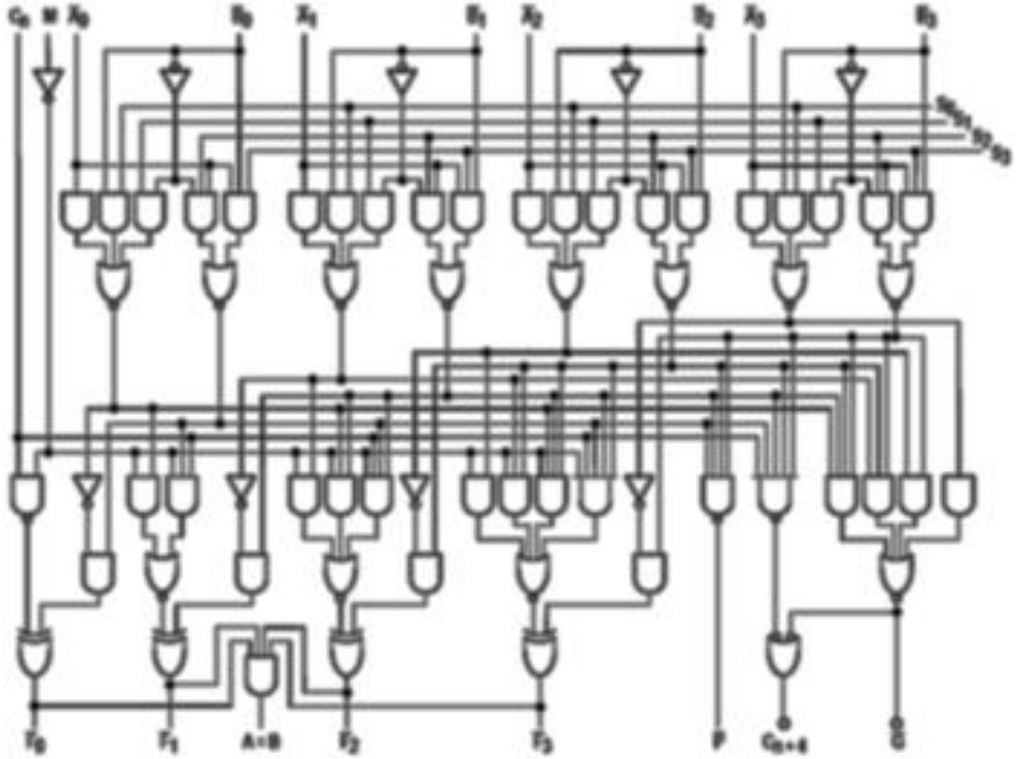

Two-bit gates:

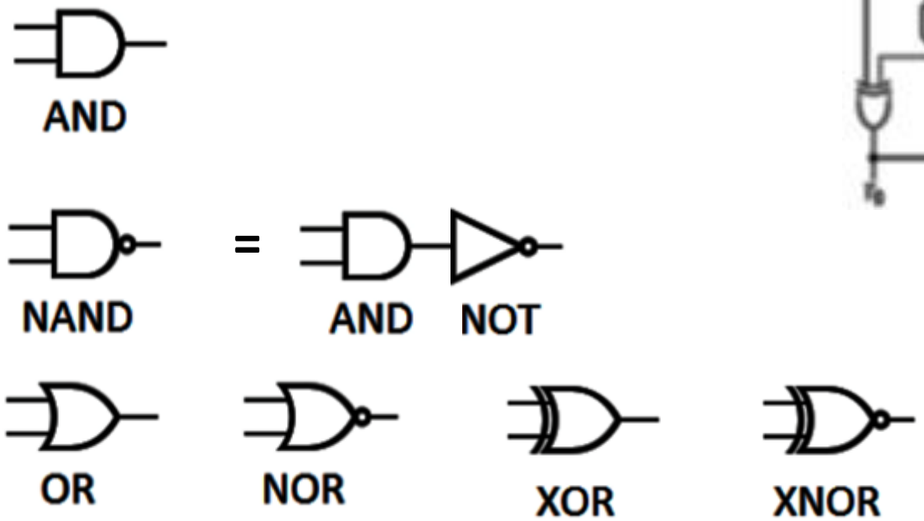

# Classical logical operations

**Universal logic gates:** NOR, NAND

Any other gate can be built from using only NOR (or only NAND) gates:

**Circuit Representation** of ‘a AND b’ in terms of NAND gates

**Truth table:**

| a | b | a AND b |
|---|---|---|
| 0 | 0 | 0 |
| 0 | 1 | 0 |
| 1 | 0 | 0 |
| 1 | 1 | 1 |

| a | b | a NAND b |
|---|---|---|
| 0 | 0 | 1 |
| 0 | 1 | 1 |
| 1 | 0 | 1 |
| 1 | 1 | 0 |

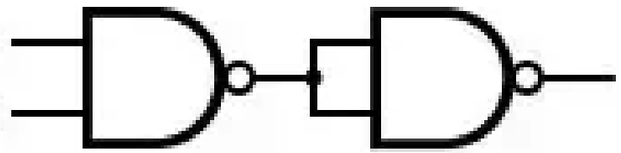

**Properties of a classical computer**

- Bits can be copied (FANOUT)
- Additional working bits are allowed (ANCILLAS)
- Values of bits can be interchanged (CROSSOVER / SWAP)
- Number of output bits may be smaller than # of input bits

# Digital vs. Analog Computing

Why is digital computing so much better than analog computing?

- Resilience to errors
- Universality (applicable to many applications)

Example for specific use of analog computer:
Water integrator (Lukyanov, 1936)
(https://www.amusingplanet.com/2019/12/vladimir-lukyanovs-water-computer.html )

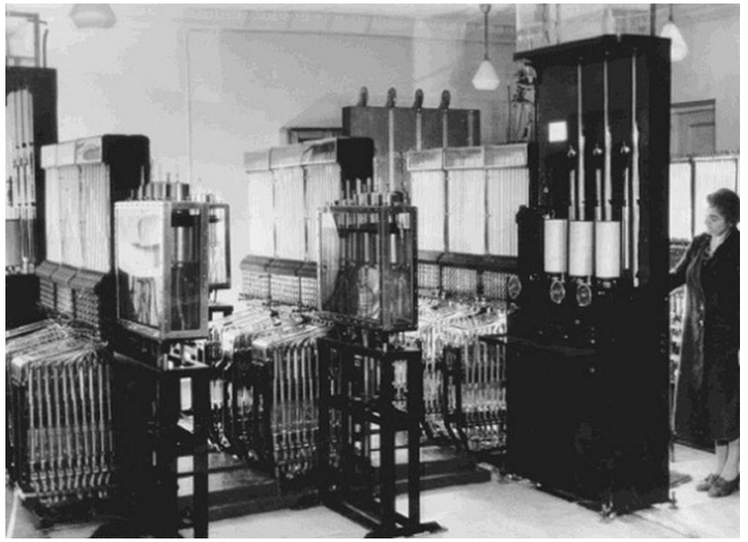

© amusingplanet.com

# Gates and Operations

$\alpha|0\rangle + \beta|1\rangle$

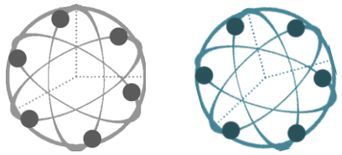

**superposition**

**quantum physics:**

**discrete quantum states (qubits)**

**+ unitary evolution**

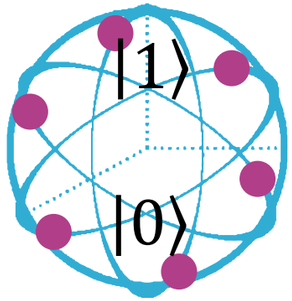


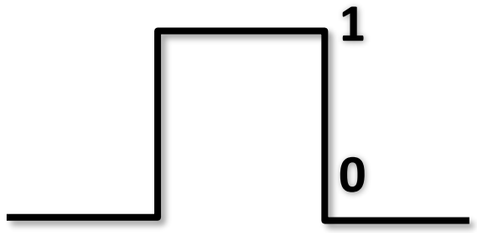


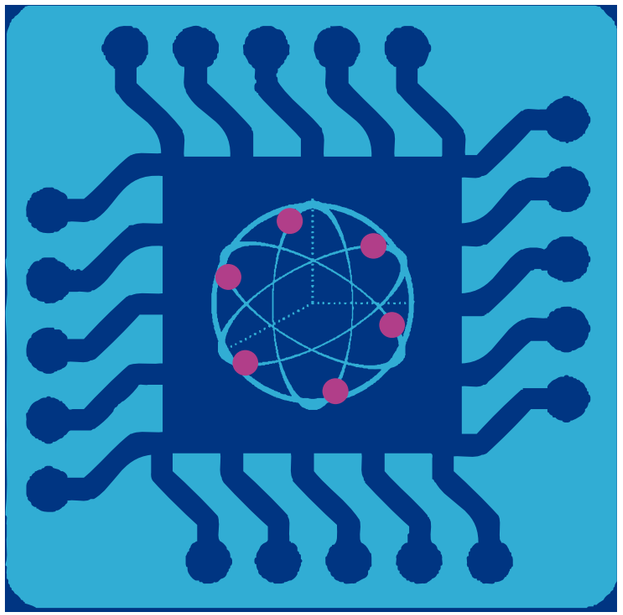

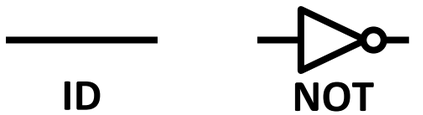


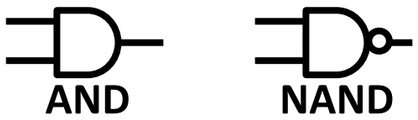



1-qubit gates

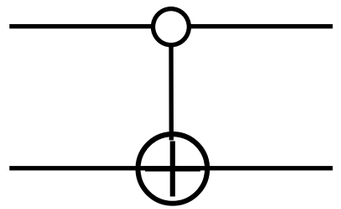

2-qubit gates

**entanglement**

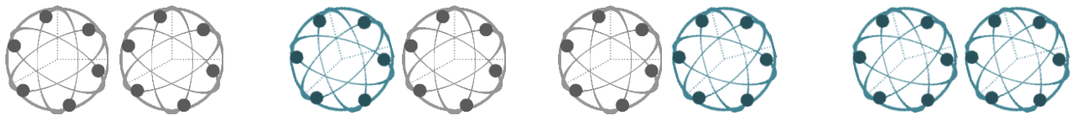

$\alpha|00\rangle + \beta|10\rangle + \gamma|01\rangle + \delta|11\rangle$

# No Cloning theorem

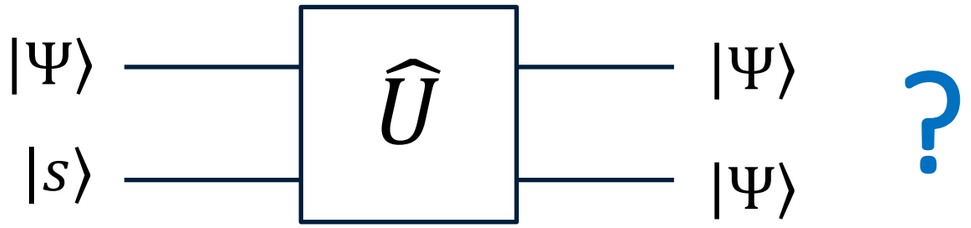


Cloning = copying of a general state is not possible:

This would imply $|0\rangle \rightarrow |0\rangle|0\rangle$ and $|1\rangle \rightarrow |1\rangle|1\rangle$ and by linearity

$$\alpha|0\rangle + \beta|1\rangle \rightarrow \alpha|0\rangle|0\rangle + \beta|1\rangle|1\rangle$$

$$\neq$$

$$(\alpha|0\rangle + \beta|1\rangle)(\alpha|0\rangle + \beta|1\rangle)$$

Alternative proof:

$$\hat{U}|\Psi_1\rangle|s\rangle = |\Psi_1\rangle\,|\Psi_1\rangle$$

$$\hat{U}|\Psi_2\rangle|s\rangle = |\Psi_2\rangle\,|\Psi_2\rangle$$

$$\boxed{\langle\Psi_2|\Psi_1\rangle} = \langle\Psi_2|\Psi_1\rangle\langle s|s\rangle = \langle\Psi_2|\langle s|\hat{U}^\dagger\hat{U}|\Psi_1\rangle|s\rangle = (\langle\Psi_2|\Psi_1\rangle)(\langle\Psi_2|\Psi_1\rangle) = \boxed{(\langle\Psi_2|\Psi_1\rangle)^2}$$

# Classical vs. quantum bit

Name the (main) difference(s) between classical and quantum bits.

- States do not live indefinitely
- Phase matters
- Parallelism: operations act on many states at once
  (for $n$ qubits, up to $2^n$ states)

# What is a quantum bit?

## Classical Bits:

Relais

Vacuum Tube

Transistor

## Quantum Bits:

Two-Level Systems

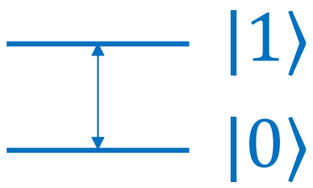


Example:
Atom orbitals with different energetic levels

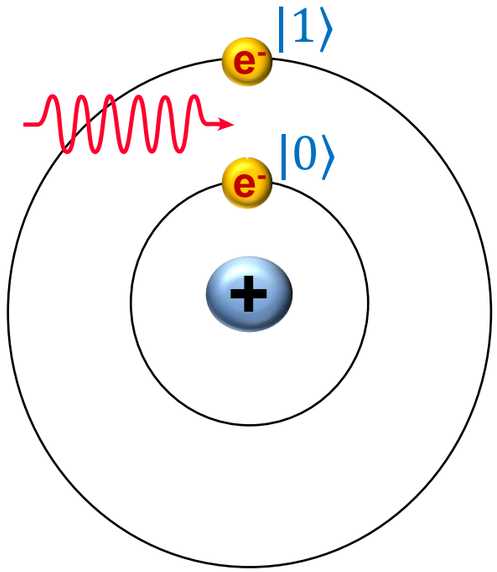


Neutral Atoms

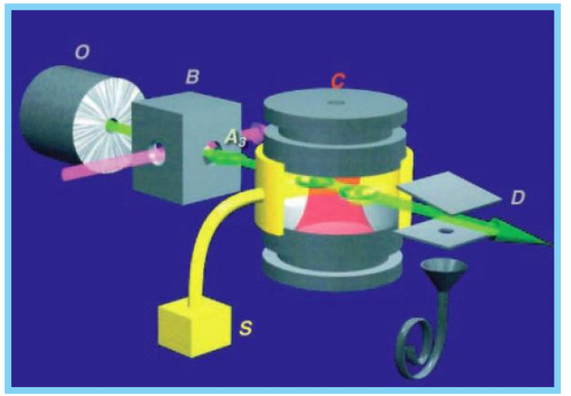


© Haroche

Ion Traps

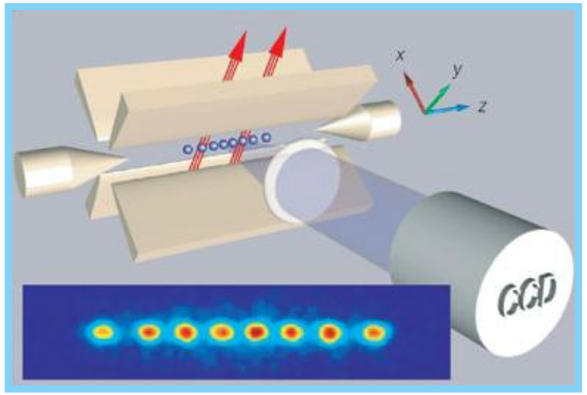


© Blatt & Wineland

Quantum Dots

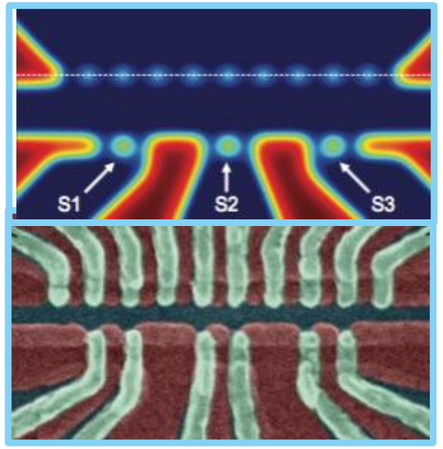


© Petta

Superconducting Circuits

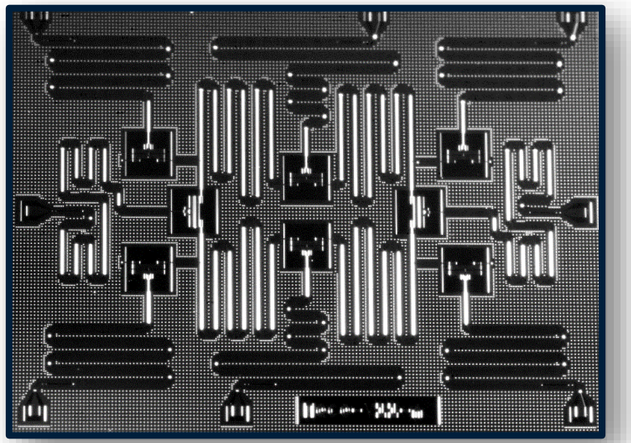

© IBM

# The quantum bit

**Representation of qubit state:** vectors in Hilbert space (2-dim, complex)

$$|0\rangle = \begin{pmatrix} 1 \\ 0 \end{pmatrix} \widehat{=} |\downarrow\rangle \widehat{=} |H\rangle$$

$$|1\rangle = \begin{pmatrix} 0 \\ 1 \end{pmatrix} \widehat{=} |\uparrow\rangle \widehat{=} |V\rangle$$

$|.\rangle$ … Dirac notation
$(.)$ … vector notation

**Most general qubit state:** $|\psi\rangle = \alpha|0\rangle + \beta|1\rangle \; with \; \alpha, \beta \in \mathbb{C}$

- superposition state of $|0\rangle$ & $|1\rangle$
- probability to find system in 0 or 1:

$$P_0 = |\alpha|^2, \qquad P_1 = |\beta|^2$$

- Laws of probabilities: $P_0 + P_1 = 1 \rightarrow$ Normalization: $|\alpha|^2 + |\beta|^2 = 1$

# Bloch Sphere

- **Representation of a state:** $|\psi\rangle = \alpha|0\rangle + \beta|1\rangle$ with $|\alpha|^2 + |\beta|^2 = 1$
- **3 parameters:**

$$\alpha = \cos\frac{\theta}{2}e^{i\phi_\alpha}, \quad \beta = \sin\frac{\theta}{2}e^{i\phi_\beta}$$

$$|\psi\rangle = \cos\frac{\theta}{2}e^{i\phi_\alpha}|0\rangle + \sin\frac{\theta}{2}e^{i\phi_\beta}|1\rangle$$

$$= e^{i\phi_\alpha}\left(\cos\frac{\theta}{2}|0\rangle + e^{i\phi}\sin\frac{\theta}{2}|1\rangle\right)$$

→ **Global phase** $e^{i\phi_\alpha}$ is immaterial
(at least for a single qubit)

- **2 parameters:**

$\theta \in [0, \pi[$... polar angle

$\phi \in [0, 2\pi]$... azimuthal angle

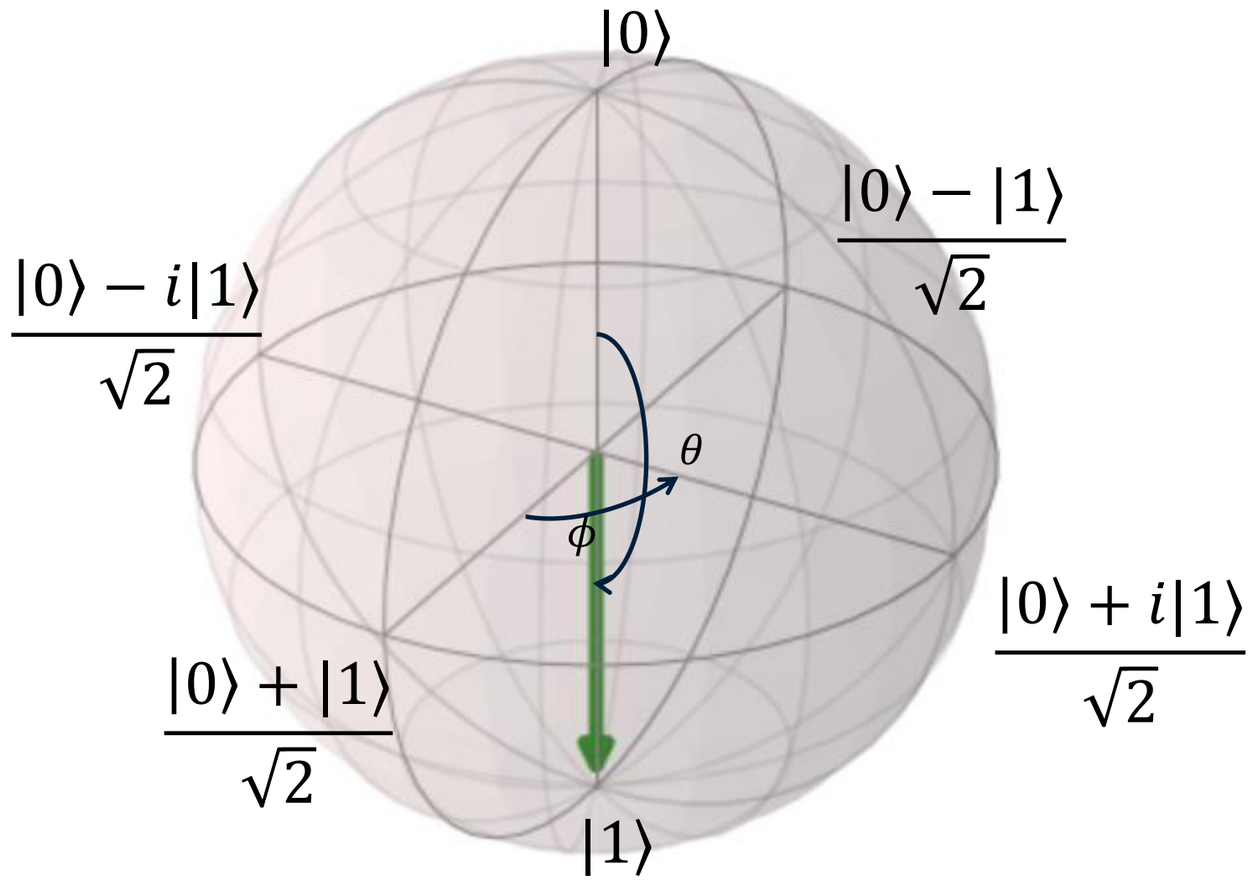

# Single Qubit Gates

Circuit representation:

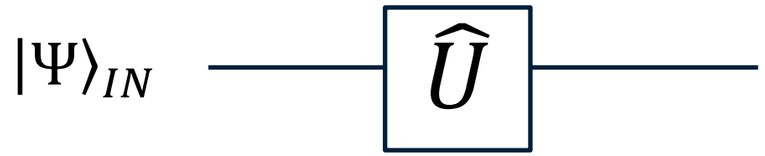


- Identity operation: $\hat{U} = \hat{I} = 1_2 = \begin{pmatrix} 1 & 0 \\ 0 & 1 \end{pmatrix}$
- Bit flip operation: $\hat{U} = \hat{X} = \sigma_x = \begin{pmatrix} 0 & 1 \\ 1 & 0 \end{pmatrix}$ ($\hat{=}$ NOT operation)
  (rotation by $\pi$ about x-axis)
- Phase flip operation: $\hat{U} = \hat{Z} = \sigma_z = \begin{pmatrix} 1 & 0 \\ 0 & -1 \end{pmatrix}$
  (rotation by $\pi$ about z-axis)
- Bit-phase flip operation: $\hat{U} = \hat{Y} = \sigma_y = \begin{pmatrix} 0 & -i \\ i & 0 \end{pmatrix}$
  (rotation by $\pi$ about y-axis)

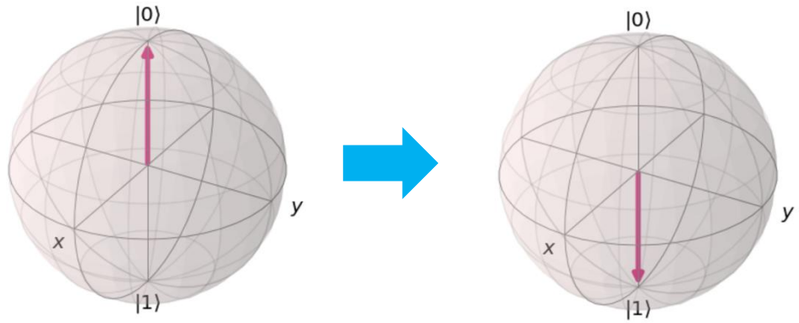


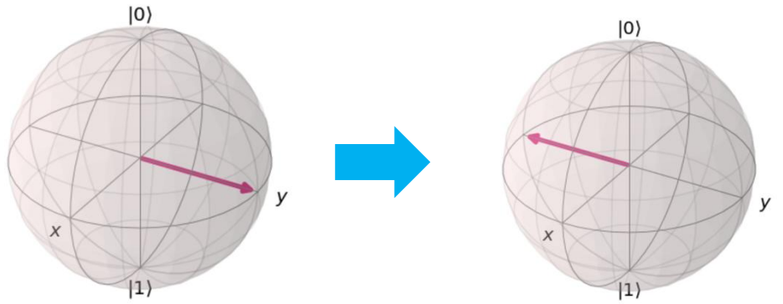


$\sigma_x, \sigma_y, \sigma_z$... Pauli matrices; $\{1, \sigma_x, \sigma_y, \sigma_z\}$... basis set for operators on a single qubit

# Single Qubit Dynamics

Time-evolution given by Schrödinger equation:

$$\hat{H}|\psi\rangle = i\hbar \frac{\partial}{\partial t}|\psi\rangle$$

Simple(st) example: single spin-1/2 particle in a magnetic field ($\mu_B = \frac{e\hbar}{2m_e}$... Bohr magneton):

$$\hat{H} = -\vec{\mu}\cdot\vec{B} = \mu_B \begin{pmatrix}\hat{\sigma}_x\\ \hat{\sigma}_y\\ \hat{\sigma}_z\end{pmatrix}\cdot\begin{pmatrix}B_x\\ B_y\\ B_z\end{pmatrix} = \mu_B\,(\hat{\sigma}_x B_x + \hat{\sigma}_y B_y + \hat{\sigma}_z B_z)$$

Unitary evolution: $\hat{U} = e^{\frac{i\omega_L t}{2}\vec{n}\cdot\hat{\sigma}} = \hat{1}\cdot\cos\frac{\omega_L t}{2} + i\,\vec{n}\cdot\hat{\sigma}\sin\frac{\omega_L t}{2}$ (Larmor frequency $\omega_L = \frac{2\mu_B|B|}{\hbar}$)

For $\vec{B} = B_z$: $\hat{U}_z = e^{\frac{i\omega_L t}{2}\hat{\sigma}_z} = \begin{pmatrix} e^{\frac{i\omega_L t}{2}} & 0 \\ 0 & e^{-\frac{i\omega_L t}{2}}\end{pmatrix}$

[see e.g., Haken & Wolf, Atom- & Quantenphysik, ch. 14]

# Quantum gates

How do you realize a bit flip that brings

$$|0\rangle \rightarrow |1\rangle?$$

A) Apply a static B-field that is orthogonal to the quantization axis z.

B) Apply a B-field that is oscillating at the Larmor frequency  orthogonal to the z axis.

C) Both.

D) None of the above.

# Quantum gates

What is the evolution of the state $|0\rangle$ (on the Bloch sphere), when $\vec{B} = B_z$ ?

A) Remains constant.

B) Obtains a phase $e^{i\frac{\omega t}{2}}$ .

C) Both.

D) None of the above.

# Measurement and Readout

**Generic measurement setup:**

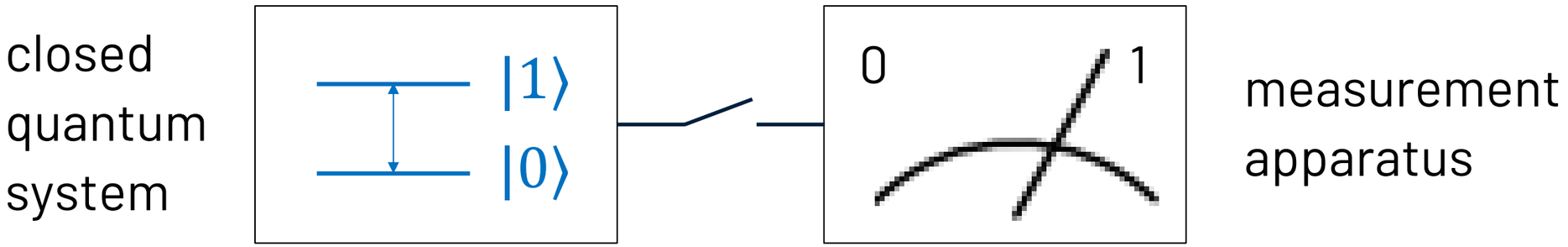


**Goal:** faithful representation of quantum state

**Properties** of an ideal measurement apparatus:

- high ON/OFF ratio: no interaction in OFF, strong interaction in ON state
- High fidelity of mapping of quantum system to measurement apparatus

- Fast measurement with respect to dissipation
- Repeatability (quantum non-demolition)

# Projective Measurement

- Described by an 'observable' (=Hermitian operator) $\widehat{M}$

$\hat{S}_z$ ... spin along z-axis

$\hat{S}^2$ ... absolut value squared of spin

Example: Stern-Gerlach apparatus to measure spins
(magnetic gradient field leads to deflection of particles with different spins)

Measurement operator (observable): $\hat{S}_z = \frac{\hbar}{2}\sigma_z$

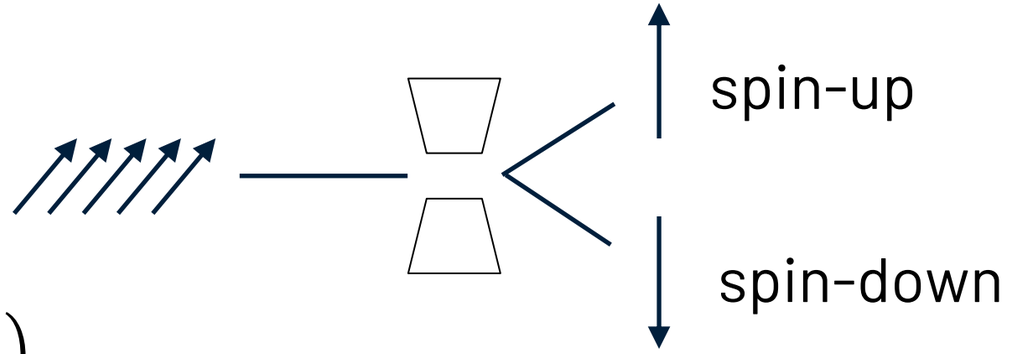


with Pauli-Matrix $\sigma_z = 1 \cdot |0\rangle\langle 0| - 1 \cdot |1\rangle\langle 1| = \begin{pmatrix} 1 & 0 \\ 0 & -1 \end{pmatrix}$

"Bohr is right after all." – Stern to Gerlach

# Measurement

Is the measurement of $\sigma_z$ sufficient to determine the state completely?

e.g., one cannot learn the phase of a state $|\psi\rangle = \frac{1}{\sqrt{2}}\left(|0\rangle + e^{i\phi}|1\rangle\right)$,

*Measure $\sigma_x, \sigma_y$ in addition -> State tomography*

Can one perform different measurements simultaneously on a single particle?

*If a measurement is done, the state is destroyed. We can only measure different observables on an* ***ensemble*** *of equally prepared states.*

# Multi-qubit states

Exponential growth of Hilbert space:

- **Classical bits:** only one state is realized at any given time
- **Quantum bits:** quantum register can be in any superposition of basis states

| # qubits | quantum state | coefficients | # bytes |
|---|---|---|---|
| 1 | $a\|0\rangle + b\|1\rangle$ | $2^1 = 2$ | 16 Bytes |
| 2 | $a\|00\rangle + b\|01\rangle + c\|10\rangle + d\|11\rangle$ | $2^2 = 4$ | 32 Bytes |
| 8 | | $2^8 = 256$ | 2kB |
| 16 | … | $2^{16} = 65'536$ | 512 kB |
| 32 | … | ~4 billion | 32 GB |
| 64 | … | ~ information in internet | 128 EB (134 million GB) |
| 256 | … | ~ # of atoms in universe | … |

**Tensor product:** $|\psi\rangle = |A\rangle \otimes |B\rangle = |AB\rangle$

e.g. for two qubits $|A\rangle = \alpha_A|0\rangle + \beta_A|1\rangle$ & $B = \alpha_B|0\rangle + \beta_B|1\rangle$

$\rightarrow |\psi\rangle = \alpha_A\alpha_B|00\rangle + \alpha_A\beta_B|01\rangle + \beta_A\alpha_B|10\rangle + \beta_A\beta_B|11\rangle$

with $\Sigma_{ij}|\alpha_{ij}|^2 = 1$ (normalization)

# Multi-qubit state

Does it matter how close two quantum systems are in order to assign a tensor product state to the systems, $|A\rangle \otimes |B\rangle$?

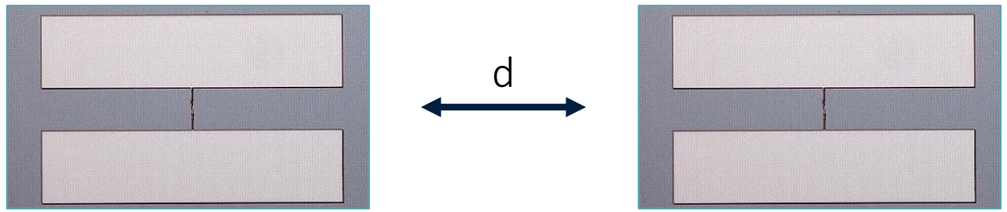

# Entanglement

**Definition:** An **entangled** state of a composite system is a state that **can not** be written as a tensor product state of the component systems.

**Product state (separable state):**

$$|\psi\rangle = |A\rangle \otimes |B\rangle$$

$$= \alpha_A\alpha_B|00\rangle + \alpha_A\beta_B|01\rangle + \beta_A\alpha_B|10\rangle + \beta_A\beta_B|11\rangle$$

$$\text{with } |A\rangle = \alpha_A|0\rangle + \beta_A|1\rangle \;\&\; B = \alpha_B|0\rangle + \beta_B|1\rangle$$

**Entangled state**:

$$|\psi\rangle = \frac{1}{\sqrt{2}}(|00\rangle + |11\rangle)$$

**Proof:** It cannot be written in the form above!

$$\alpha_A\alpha_B = \beta_A\beta_B = \frac{1}{\sqrt{2}}$$

$$\rightarrow \alpha_A\beta_B \neq 0 \text{ or } \beta_A\alpha_A \neq 0!$$

# Multi-qubit state

How many coefficients are required to describe a separable (product) state of N qubits, $|\psi_{sep}\rangle = |A_1\rangle \otimes |A_2\rangle \otimes \cdots \otimes |A_N\rangle$?

How many coefficients are required to describe a general entangled state of N qubits $|\psi_{ent}\rangle$?

# Superconducting Circuits

# Classical and Quantum Circuits

basic circuit elements:

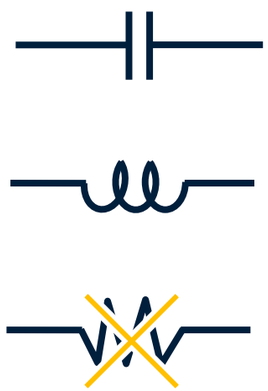

charge on a capacitor:

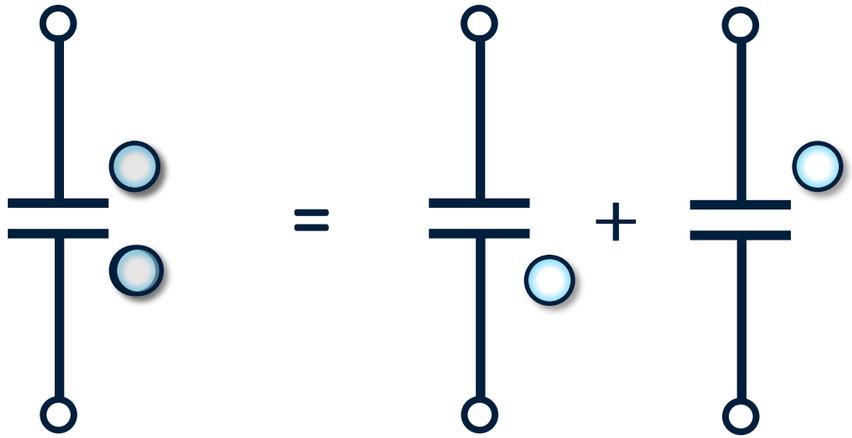

(Quantum) degrees of freedom:

- Charge $Q$
- Current / magnetic flux $\phi$

current or magnetic flux in an inductor:

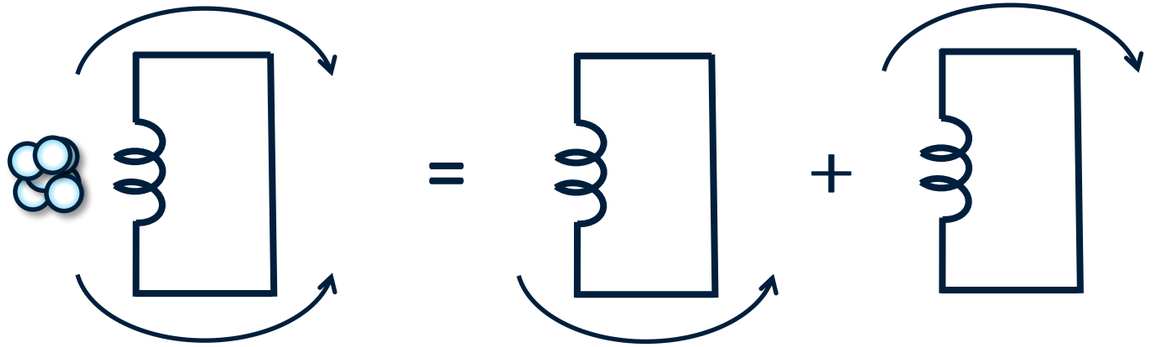

# Quantum electronic circuits – excitation modes

- Circuit elements: capacitors, inductors, ~~resistors (which we want to avoid because of dissipation),~~ Josephson junction

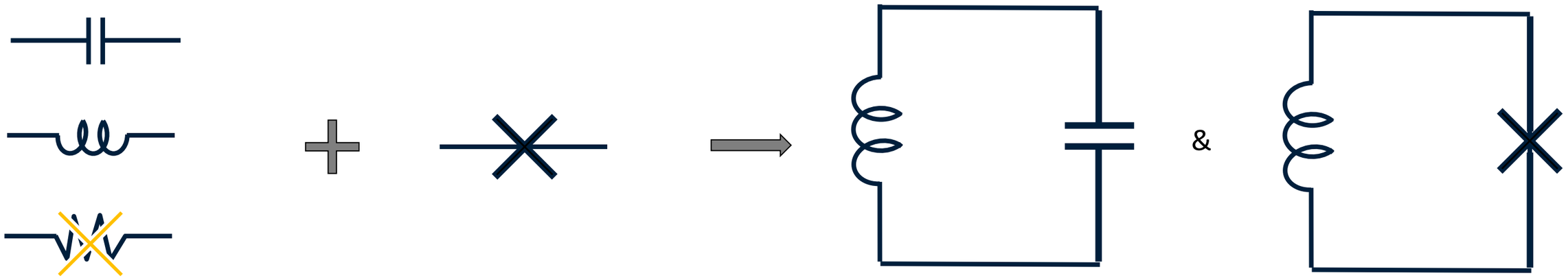


- Superconducting elements: electrons form Cooper pairs and condense in ground state with excitation gap $2\Delta$

  → current flow without dissipation
  → dramatic reduction of degrees of freedom
  → objects which behave like single-electron 'artificial atoms' although comprising $10^9 - 10^{12}$ electrons

- Uniform electron gas (Jellium model): Coulomb interaction suppresses low-excitation modes (below plasma frequency $\omega_p$)

[M. Devoret, Quantum Fluctuations in Electrical Circuits, Les Houches Lecture Notes (1995); Vool and Devoret, arXiv: 1610.03438; Steve Girvin's Les Houche Lecture Notes]

# Superconductivity

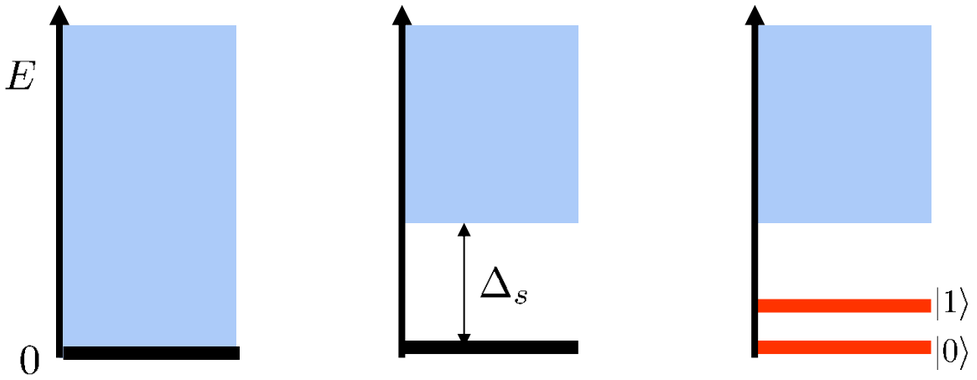


normal metal superconductor How to make a qubit?

single non-degenerate macroscopic ground state, thanks to phonon-assisted attractive interactions between electrons with opposite spin (Cooper pairs)

Superconducting materials (for electronics):

Niobium (Nb): $2\Delta/h = 725\ GHz, T_c = 9.2\ K$

Aluminum (Al): $2\Delta/h = 100\ GHz, T_c = 1.2\ K$

Cooper pairs:
bound electron pairs

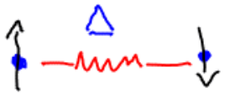

Bosons (S=0, L=0)

2 chunks of superconductors


macroscopic wave function

$$\psi_i = \sqrt{n_i^{CP}} e^{i\delta_i}$$

Cooper pair density $n_i$
and global phase $\delta_i$

# Mechanical harmonic oscillator

Hamiltonian: $H = \underbrace{\frac{p^2}{2m}}_{\text{kin.}} + \underbrace{\frac{k}{2}x^2}_{\text{pot.energy}} = \frac{Q^2}{2C} + \frac{\Phi^2}{2L}$

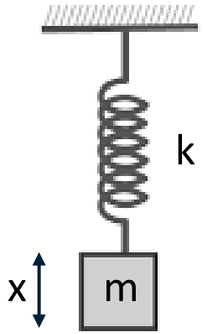


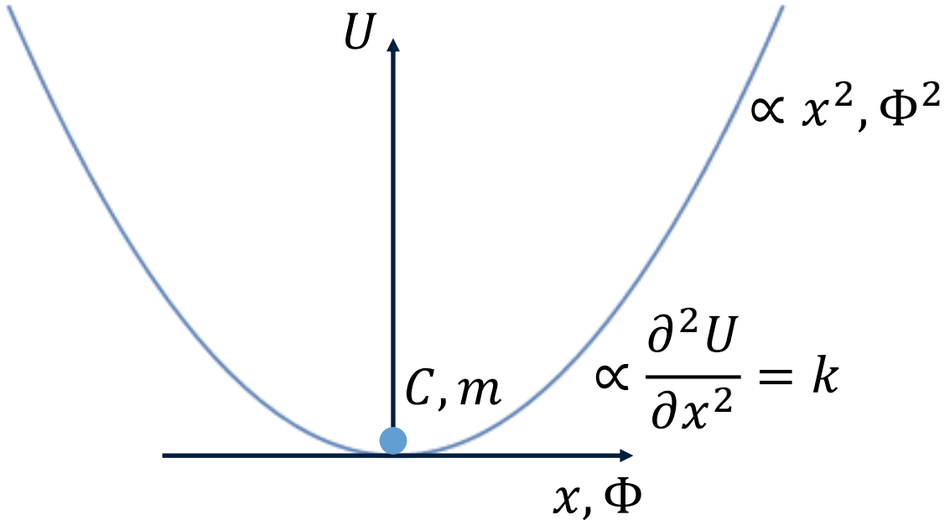


| Characteristic variables: | |
|---|---|
| **Mechanical** | **electronic** |
| Position x | Flux $\Phi$ |
| Momentum p | Charge q |
| Mass m | Capacitance C |
| Spring Constant k | Inv. Inductance 1/L |
| Frequency $\omega = \sqrt{\frac{k}{m}}$ | $\omega = \frac{1}{\sqrt{LC}}$ |

(∗) conjugate momenta

(virtual) particle of mass m (C) moving in quadratic potential

# LC circuit

## Parallel LC oscillating circuit:

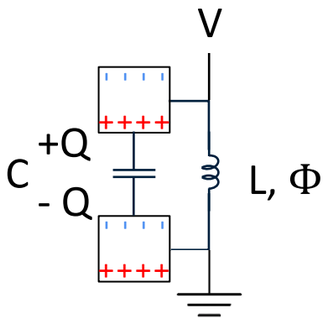


Voltage across oscillator: $V = \frac{Q}{C} = -\frac{d\Phi}{dt} = -L\frac{dI}{dt}$

Energy stored in the circuit (Hamiltonian):

$$H = \underbrace{\frac{1}{2}CV^2}_{\text{Capacitive (electrostatic) energy (→ T)}} + \underbrace{\frac{1}{2}LI^2}_{\text{Inductive (magnetic) energy (→ W)}} = \frac{1}{2}\frac{Q^2}{C} + \frac{1}{2}\frac{\Phi^2}{L}$$

$\Phi$ … magnetic flux stored in inductor ($\Phi = L\,I$)
$Q$ … charge stored on the capacitor ($Q = CV$)

$\Phi, Q$ … conjugate variables

Equations of motion:

$$-\dot{\Phi} = V = -L\frac{\partial I}{\partial t} = \frac{\partial H}{\partial Q} = \frac{Q}{C} \text{ (Faraday's law)}$$

$$\dot{Q} = I = \frac{\partial H}{\partial \Phi} = \frac{\Phi}{L}$$

# Realization I: Lumped Element

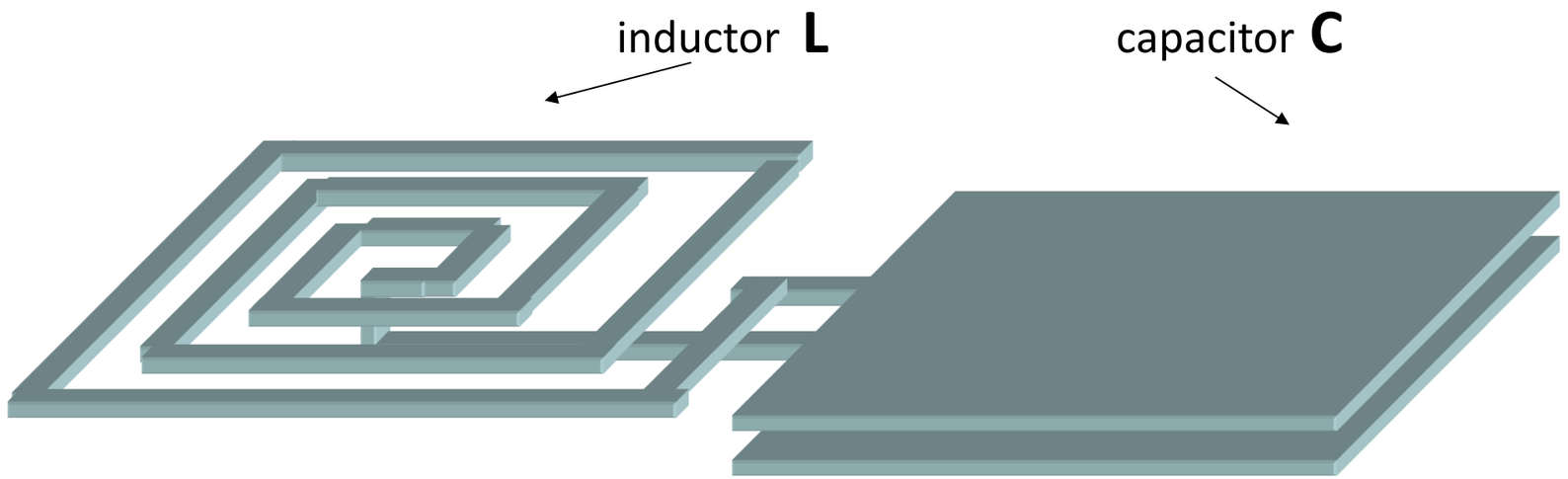


a harmonic oscillator

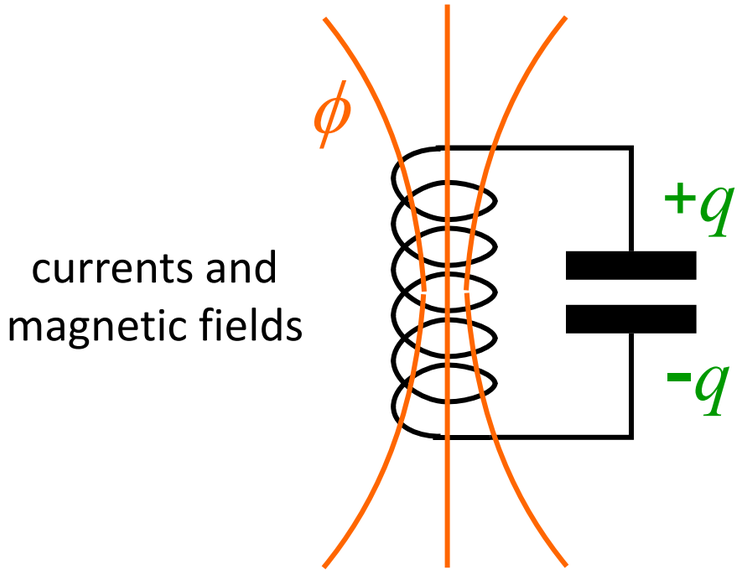


currents and magnetic fields

charges and electric fields

# Realization II: Transmission Line Resonator

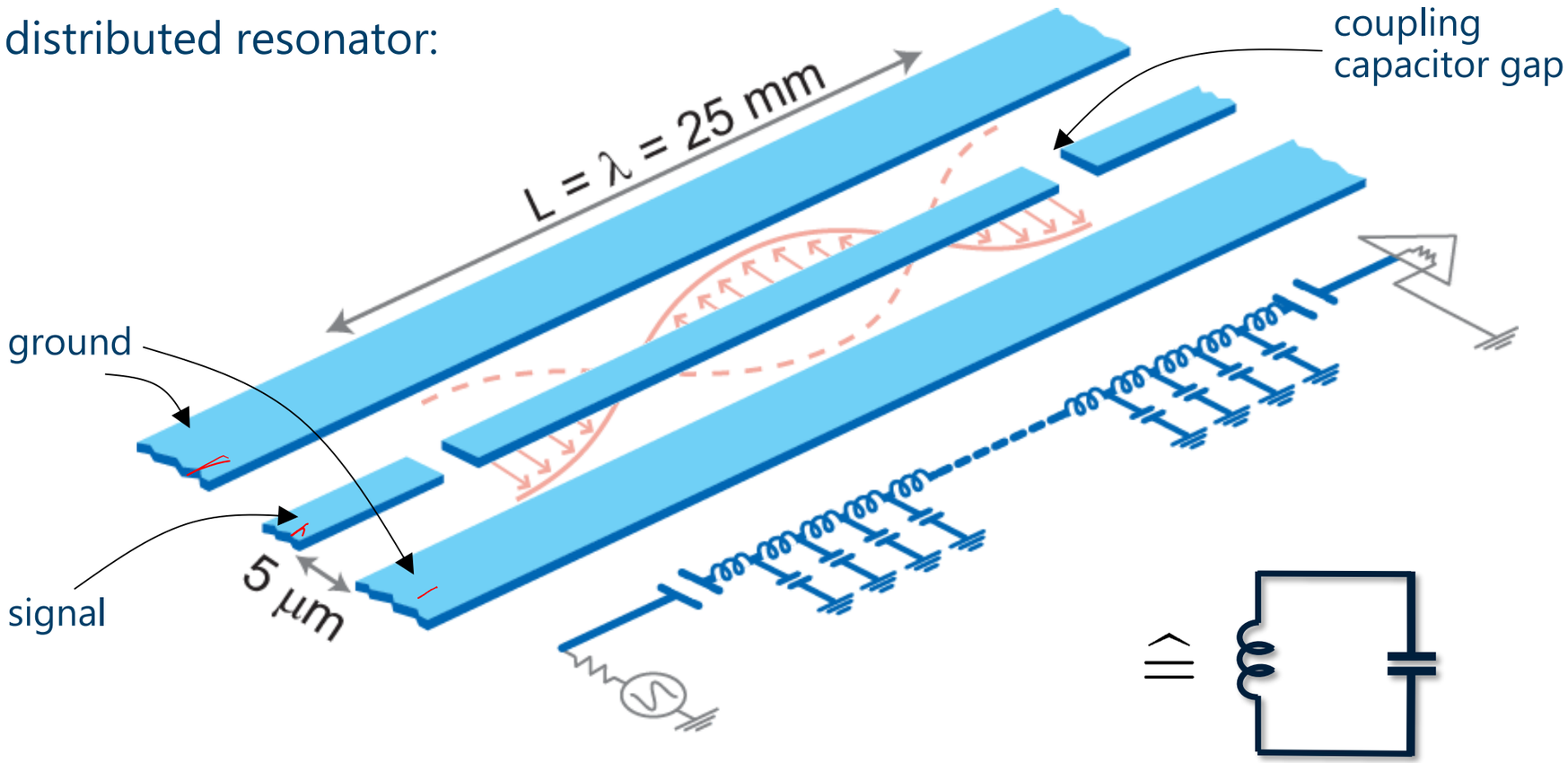


- coplanar waveguide resonator
- close to resonance: equivalent to lumped element LC resonator
- transmission line resonator = microwave cavity

[M. Goeppl *et al.*, *Journal of Applied Physics* **104**, 113904 (2008)]

# Realization III: 3D Cavity

Transmon in a three-dimensional cavity:

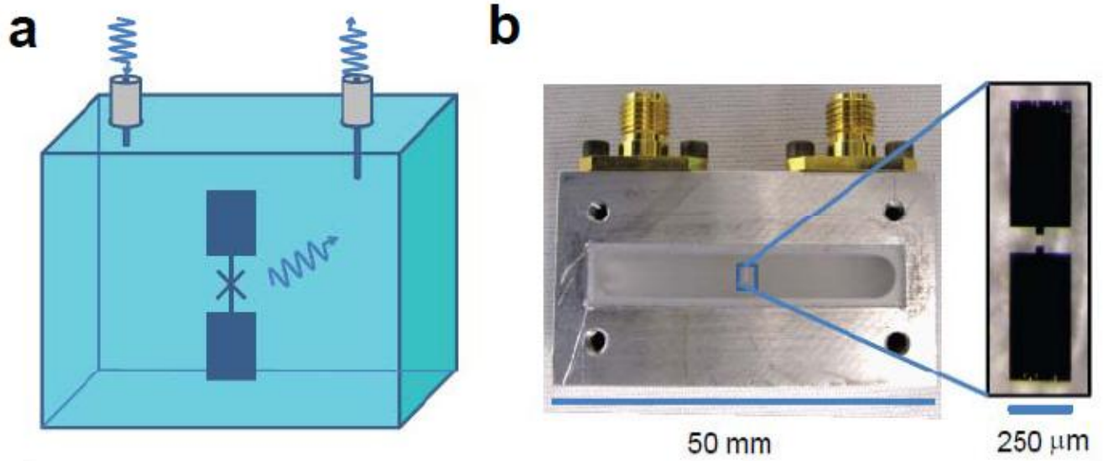


H. Paik et al., PRL (2012)

[Pozar – Microwave Engineeering]

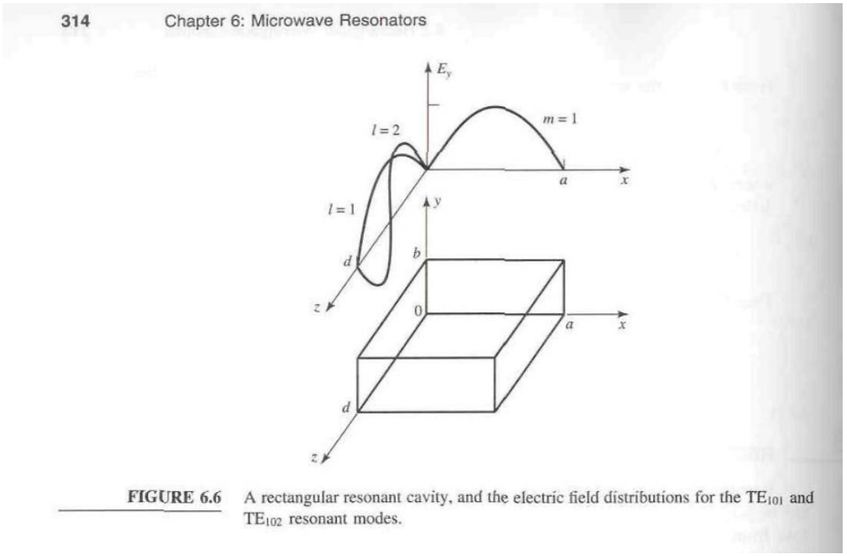


- mode structure and frequency determined by cavity dimensions
- close to resonance: equivalent to lumped element LC resonator
- long coherence times (lower field density at surfaces -> lower losses)

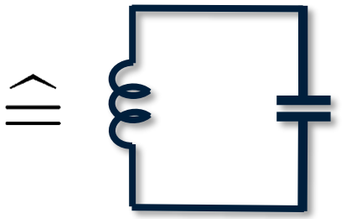

# Realizations of Superconducting Qubits

| charge | charge/phase (transmon) | fluxonium | (C-shunt) flux | phase |
|---|---|---|---|---|
| 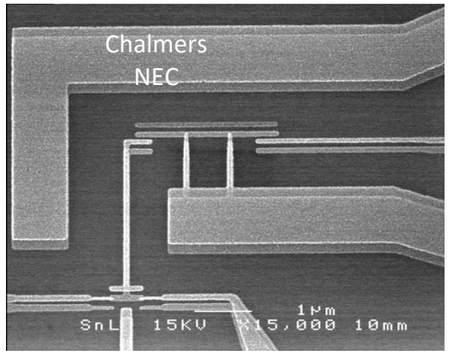  | 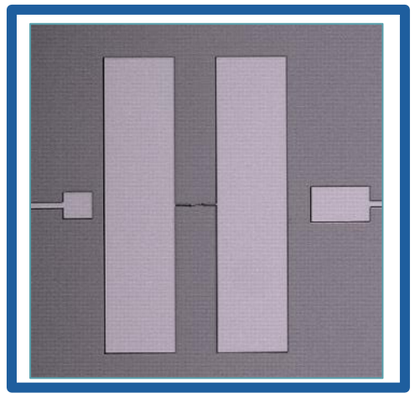 | 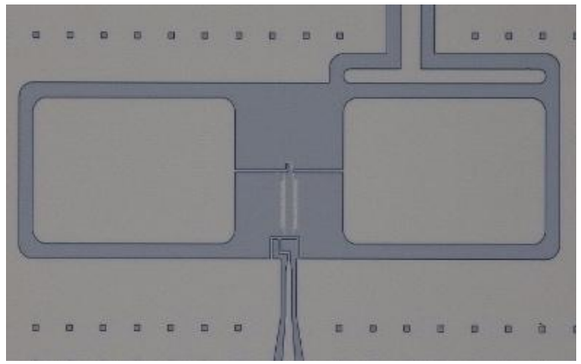 | 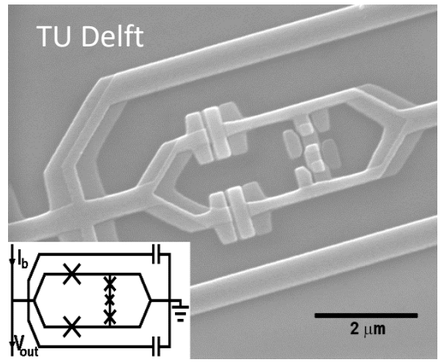  | 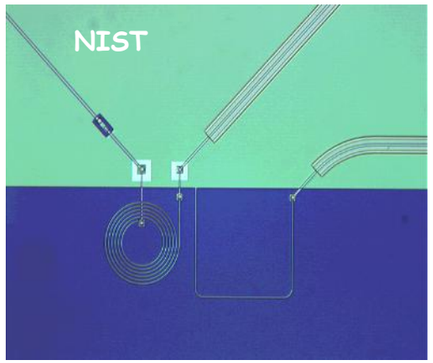  |
| NEC, Chalmers, Yale,... | Yale, ETHZ, Google, IBM, Rigetti, WMI,... | Yale, KIT, WMI, EPFL,... | Delft, WMI, MIT, ... | NIST, Santa Barbara, Maryland,... |


[Nakamura, Pashkin, Tsai *et al. Nature* **398**, **421**, **425** (1999, 2003, 2003);

Chiorescu, van der Wal, Mooij, Orlando, S. Lloyd *et al. Science* **285**, **290, 299** (1999, 2000, 2003);

Vion, Esteve, Devoret *et al. Science* **296** (2002);

Martinis, Simmonds, Lang, Nam, Aumentado, Urbina *et al. Phys. Rev. Lett.* **89**, **93** (2002, 2004);

Manucharyan, Science **326** (2009)]

Clarke & Wilhelm, Superconducting quantum bits. Nature 453 (2008)]

# Harmonic Oscillator: equally spaced energy levels

harmonic LC oscillator

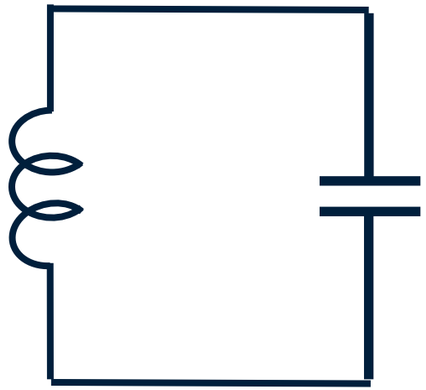

quantum:

$$\hat{H} = \frac{\hat{\phi}^2}{2L} + \frac{\hat{Q}^2}{2C} = \hbar\omega\left(\hat{a}^\dagger\hat{a} + \frac{1}{2}\right)$$

$$\left[\hat{\phi}, \hat{Q}\right] = -i\hbar$$

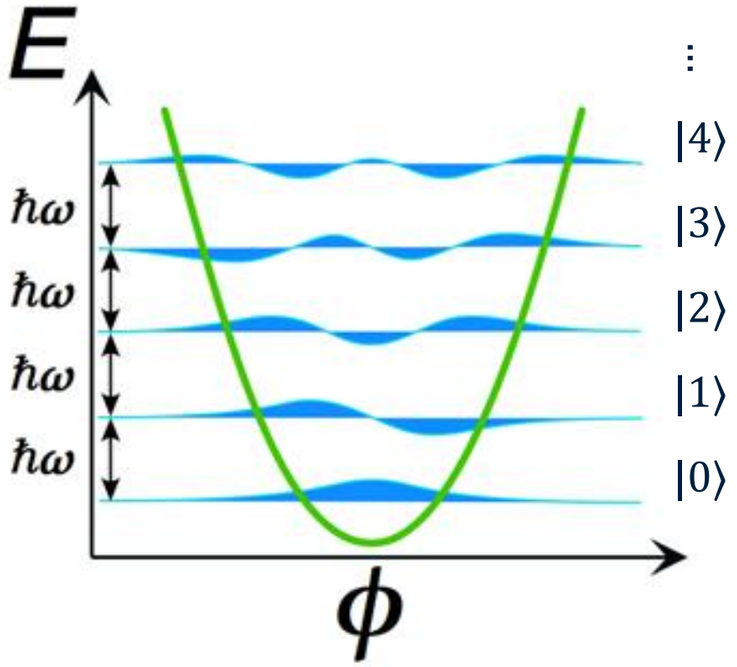


→ (loss-less) non-linearity required to form a qubit

# Typical frequencies

## What is the typical frequency of a microscopic LC circuit?

(assume thin wire approx. 1nH/mm, Al-Oxide $\epsilon_r = 10$ and $\epsilon_0 = 8.8\ 10^{-12}$)

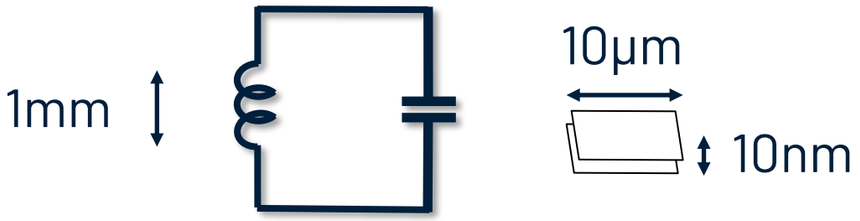


typical inductor: $L = 1\ nH$

a wire in vacuum has inductance $\sim 1\ nH/mm$

typical capacitor: $C = 1\ pF$

a capacitor with plate size 10 $\mu$m x 10 $\mu$m and dielectric AlOx ($\epsilon = 10$) of thickness $10\ nm$ has a capacitance $C \sim 1\ pF$

$$\rightarrow \omega \sim \sqrt{\frac{1}{10^{-21}}} \sim 10^{10} \rightarrow \nu \sim 5\ GHz$$

# An-harmonic quantum oscillator (=qubit)

basic circuit elements:

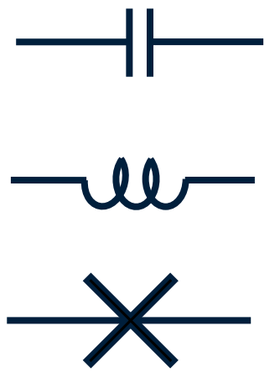

an-harmonic LC oscillator

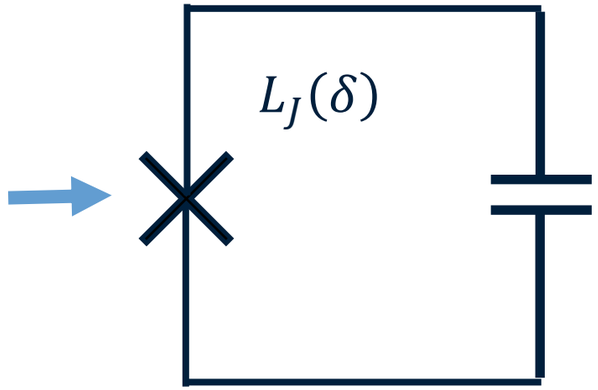


Josephson junction circuit = (transmon) qubit

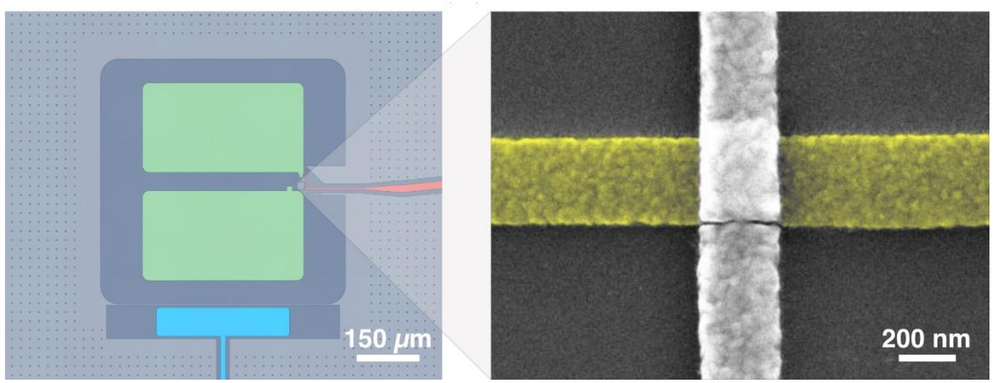


Josephson junction:

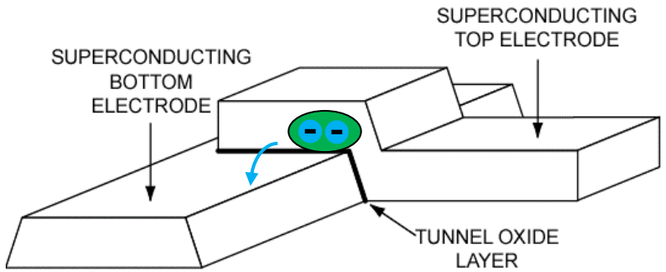


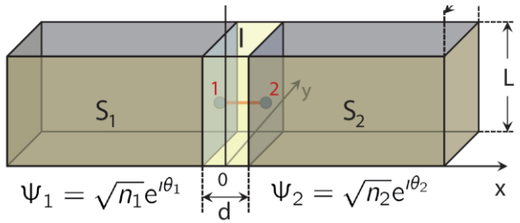


$$\hat{H} = \frac{\hat{q}^2}{2C} + \frac{\phi_0 I_c}{2\pi}\cos\frac{\hat{\phi}}{\varphi_0}$$

$$= \hbar\left[\frac{\omega_q}{2} + \left(\omega_q + \alpha\hat{a}^\dagger\hat{a}\right)\hat{a}^\dagger\hat{a}\right]$$

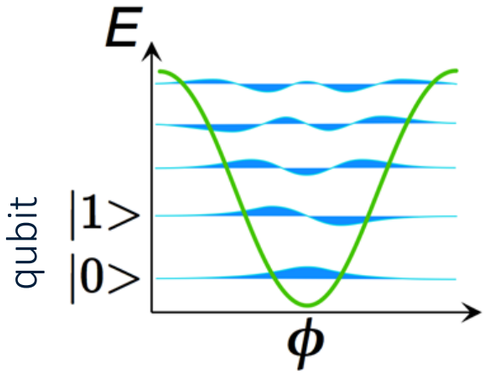

# Phase/Flux Quantization

Flux quantization in a superconducting loop

$$\psi(r,\theta) = \psi(r,\theta + 2\pi)$$

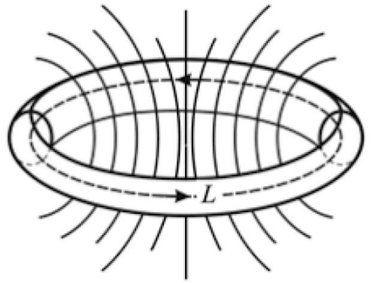


© http://www.supraconductivite.fr/en/index.php?p=applications-squid-quantification

**Aharonov-Bohm effect:**

Electron ($2e^-$ charge) taken along a closed loop acquires phase proportional to enclosed magnetic flux

$$\delta = \frac{2e}{\hbar}\oint \vec{A}\cdot d\vec{s} = \frac{2e}{\hbar}\Phi$$

→ single-valued wavefunction: $\delta = j\ 2\pi$

→ flux quantization

$$\delta = \frac{2\mathrm{e}}{\hbar}\Phi = j\ 2\pi \ \rightarrow\ \Phi = j\frac{h}{2e} \equiv j\phi_0;\ \delta = \frac{2\pi\Phi}{\phi_0} \equiv \frac{\Phi}{\varphi_0}\mathrm{d}$$

Phase-number commutator:

$$\left[\frac{2\pi\hat{\Phi}}{\mathrm{h}}2\mathrm{e}, \frac{\hat{Q}}{2\mathrm{e}}\right] = \left[\frac{2\pi\hat{\Phi}}{\phi_0}, \frac{\hat{Q}}{2e}\right] =$$

$$\left[\hat{\delta}, \hat{N}\right] = -i$$

($\phi_0$ ... magnetic flux quantum $\frac{h}{2e}$ = (2.067 10-15 Wb))

($\phi_0$ ... magnetic flux quantum $\frac{h}{2e}$)

# Josephson effect

1 superconducting electrode

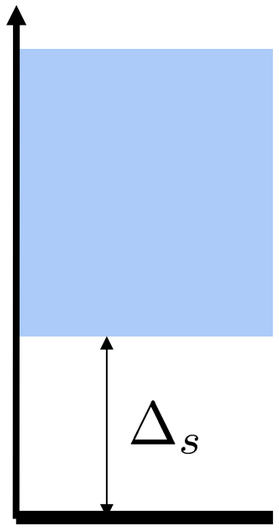


Continuum of quasi-particle excitations

Superconducting energy gap

One unique ground state with a fixed number of cooper-pairs $|N\rangle$

# Josephson effect

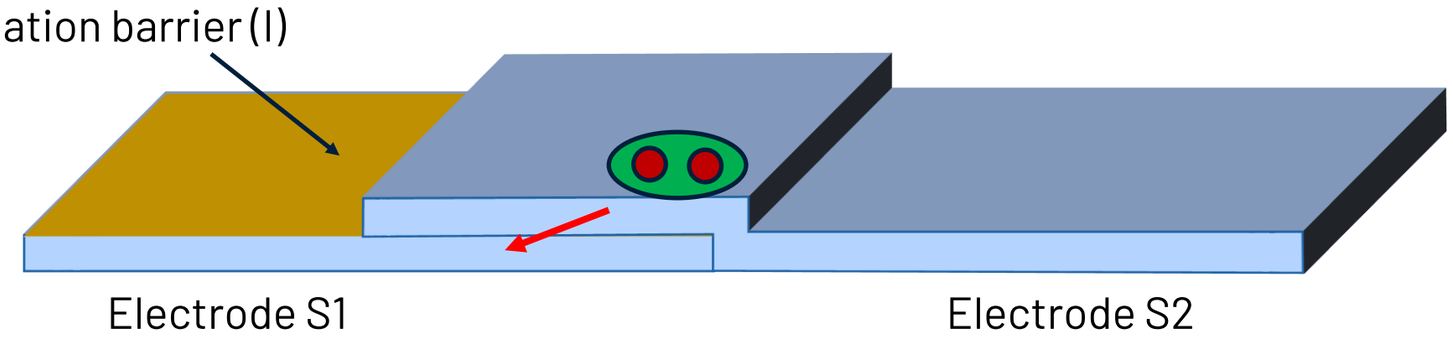


Josephson (SIS) junction

Total number of Cooper pairs $N = N_1 + N_2$ is fixed, difference can vary.

.

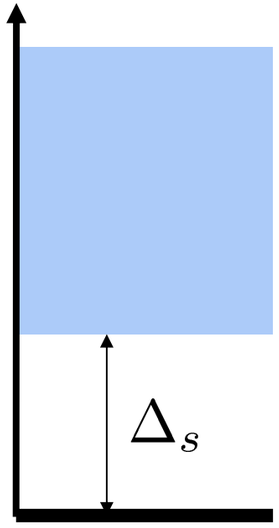


Continuum of quasi-particle excitations

Superconducting energy gap

# Josephson effect

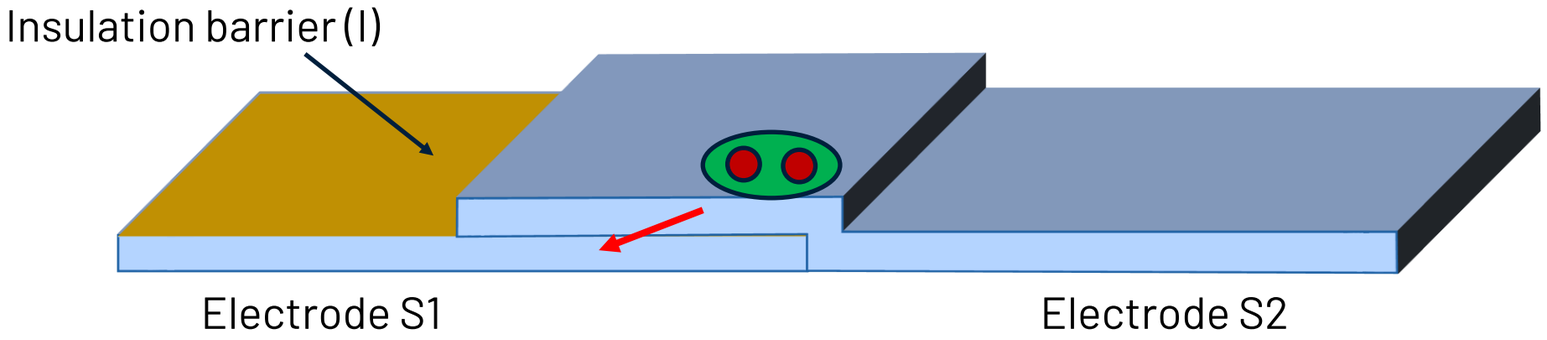


Josephson (SIS) junction

Total number of Cooper pairs $N = N_1 + N_2$ is fixed, difference can vary.
→ state defined as $|n\rangle = |N_1 - n, N_2 + n\rangle$ with the number of Cooper pairs $n$ having passed through the barrier.

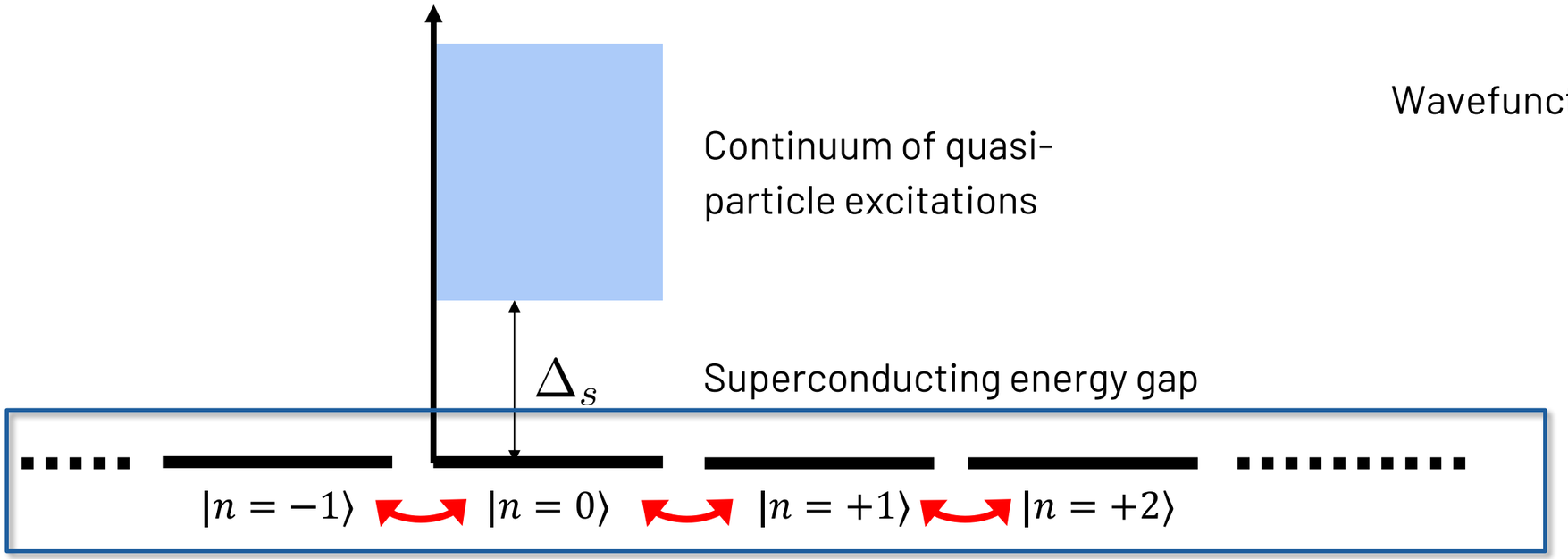


Hilbert space

Wavefunction in the 'number representation':

$$|\Psi\rangle = \sum_n c_n |n\rangle$$

# Ground state of Josephson junction

Which energy terms are important to describe the physics of a Josephson junction?

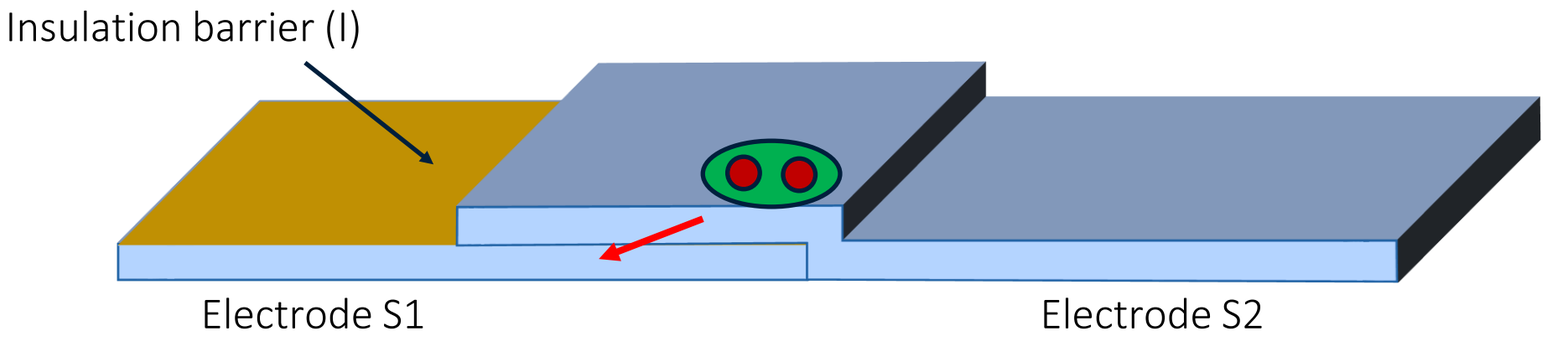


Josephson (SIS) junction

# Interaction / tunneling energy – Josephson Energy

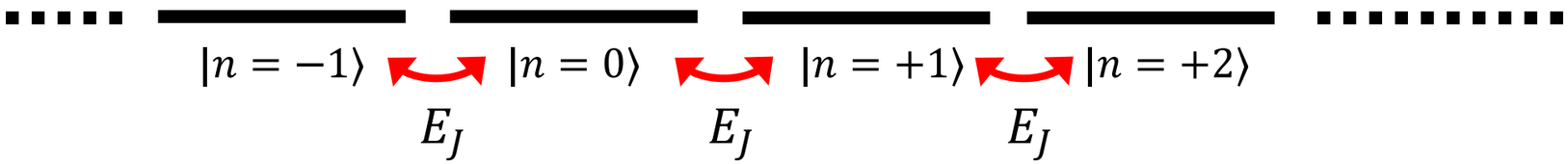


## Josephson Hamiltonian

(can be derived from the tunneling of electrons and BCS theory of superconductivity)

$$H_J = -\frac{\mathrm{E_J}}{2}\sum_n \left[\left[|n\rangle\langle n+1\right] + |n+1\rangle\langle n|\right]$$

with tunneling rate/energy $E_J = \frac{1}{2}\frac{h}{(2e)^2}\frac{\Delta}{\mathrm{R_N}}$ and normal state resistance $R_N$

($R_N$ depends on junction parameters (size, thickness))

→ leads to periodic potential $H_j \propto \cos\delta$ and Bloch bands

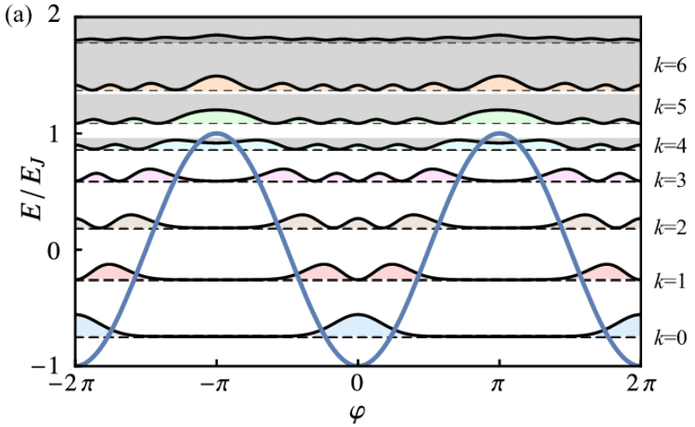


[Pietikäinen et al., PRA 99 (2019)]

# 1st Josephson relation

$$\hat{H}_J = -\frac{\mathrm{E_J}}{2}\sum_n [|n\rangle\langle n+1| + |n+1\rangle\langle n|]$$

(unnormalized) eigenstates: $|\delta\rangle = \sum_{n=-\infty}^{n=+\infty} e^{in\delta}|n\rangle$

**'phase states'** (coherent state) with well defined amplitude and phase $\delta$, but uncertain number

$\delta$... phase difference $\delta_2 - \delta_1$ across the junction (Note: $|\delta + 2\pi\rangle = |\delta\rangle$)

Eigenvalues: $\hat{H}_J|\delta\rangle = -E_J \cos\delta\,|\delta\rangle \rightarrow$ Hamiltonian $\hat{H}_J \equiv -E_J \cos\hat{\delta}$

Current operator: change of charge $(2\mathrm{e})\hat{n}$ per time step ($\hat{n} = \sum n|n\rangle\langle n|$)

$$\hat{I} = 2e\frac{d\hat{n}}{dt} = 2\mathrm{e}\frac{1}{i\hbar}[\hat{n}, \hat{H}] = -i\frac{e}{\hbar}E_J\sum_n [|n\rangle\langle n+1| - |n+1\rangle\langle n|]$$

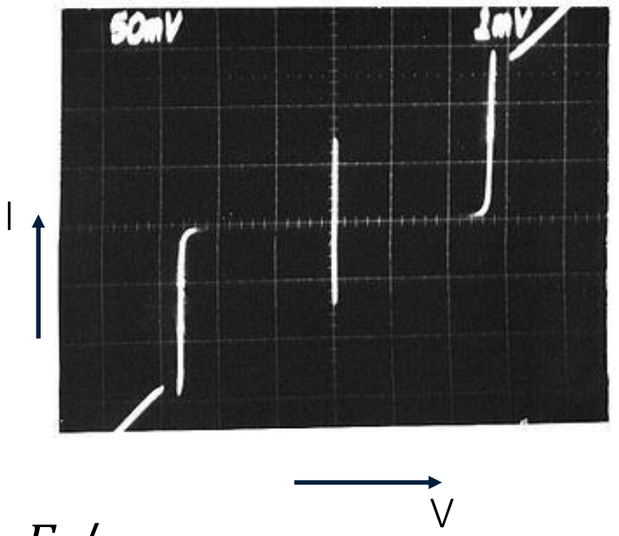


**1st Josephson relation:** $\hat{I}|\delta\rangle = I_c \sin\delta\,|\delta\rangle$ with $I_c = \frac{2e}{\hbar}E_J = E_J/\varphi_0$

→ dissipationless supercurrent $I_0 \sin\delta$ across junction at zero applied voltage

# 2nd Josephson relation

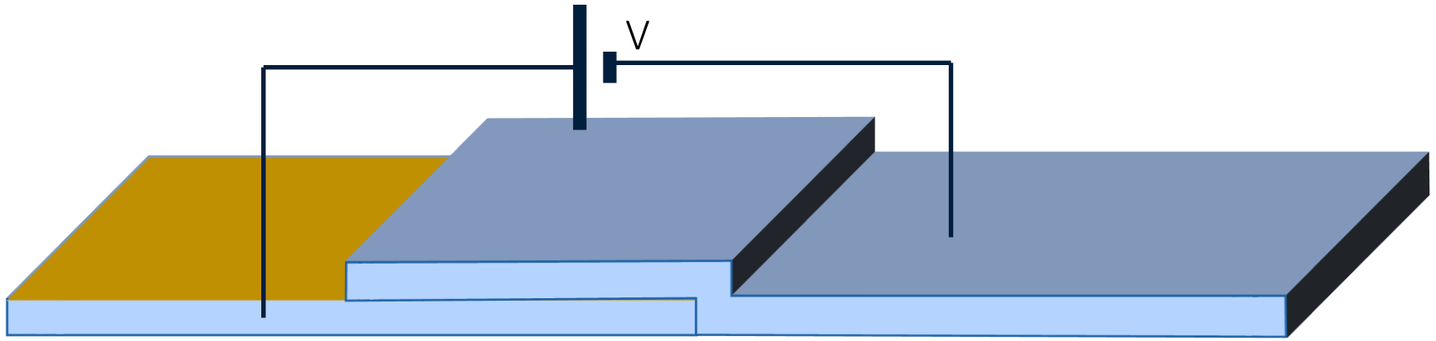


Electrostatic energy for passing $\hat{n}$ Cooper pairs across the barrier is $-(2e)V\hat{n}$ (semiclassical regime)

Total Hamiltonian of the junction is $\hat{H} = -\mathrm{E_J}\cos\hat{\delta} - 2e\,V\,\hat{n}$

**2nd Josephson relation:** $\frac{d\hat{\delta}}{dt} = \frac{1}{i\hbar}\left[\hat{H},\hat{\delta}\right] = -\frac{2eV}{i\hbar}\left[\hat{n},\hat{\delta}\right] = \frac{1}{\varphi_0}V$

'reduced flux quantum': $\varphi_0 = \frac{\hbar}{2e}$ $[\varphi_0 = \frac{\phi_0}{2\pi}]$;
flux quantum $\phi_0$ with $1/\phi_0 = 483.597891\ \mathrm{MHz}/\mu V]$

(superconducting phase change proportional to applied voltage)

Relation between superconducting phase $\hat{\delta}$ and electrodynamic flux $\hat{\Phi} \equiv \int \hat{V}(t')dt' = \varphi_0\hat{\delta}$

(remember Faraday's law of induction $V = -d\Phi/dt$ [up to a sign convention])

# Josephson Inductance

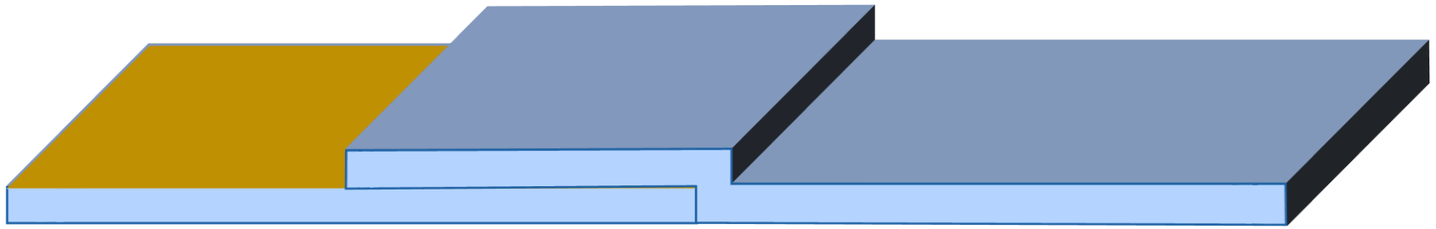

Josephson relations (in the classical limit):

$$I = I_c \sin\delta$$
$$V = \varphi_0 \dot{\delta}$$

recall:

$$V = -\frac{d\Phi}{dt} = L\frac{dI}{dt}$$

combined: $\frac{dI}{dt} = I_c\dot{\delta}\,\cos\delta \;\rightarrow\; V = \frac{\varphi_0}{I_c\delta}\frac{dI}{dt} = L_J(\delta)\frac{dI}{dt}$ (to leading order in $\delta$)

**Josephson inductance:**

$$L_J = \frac{\varphi_0}{I_c\delta} = \frac{\varphi_0}{I_c\sqrt{1-\left(\frac{I}{I_c}\right)^2}}$$

→ A Josephson junction behaves as a non-linear inductance!

# CPB & Transmon Qubit

# Cooper Pair Box Qubit

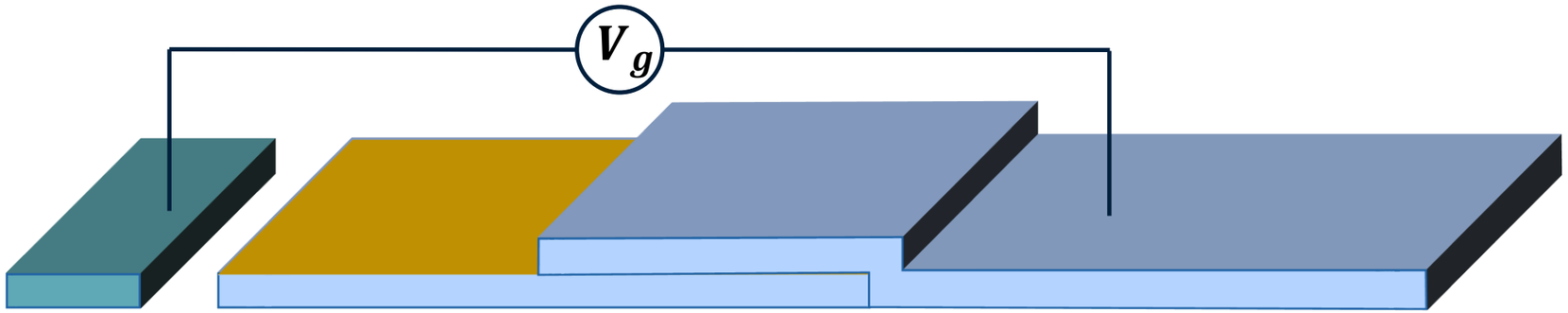


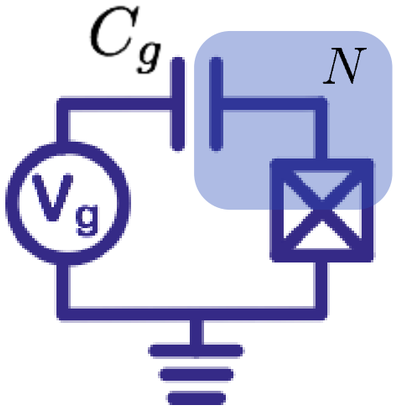


$$H = 4E_C\left(\hat{n} - n_g\right)^2 - E_J \cos\hat{\varphi}$$

$$H = \sum_N \left[4E_C\left(n - n_g\right)^2 |n\rangle\langle n| - \frac{E_J}{2}|n\rangle\langle n+1| + |n+1\rangle\langle n|\right]$$

Charging energy: $E_C = \frac{e^2}{2\,C_\Sigma}$ Gate charge: $n_g = \frac{C_g V_g}{2e}$

Josephson energy: $E_J = \frac{I_0\phi_0}{2\pi} = \frac{h\Delta}{8e^2R_J}$

2-state (qubit) approximation: at $n_g = 0.5$,

$\tilde{H}_2 = -\frac{E_J}{2}\sigma_z$ … spin-1/2 / effective 2-level system

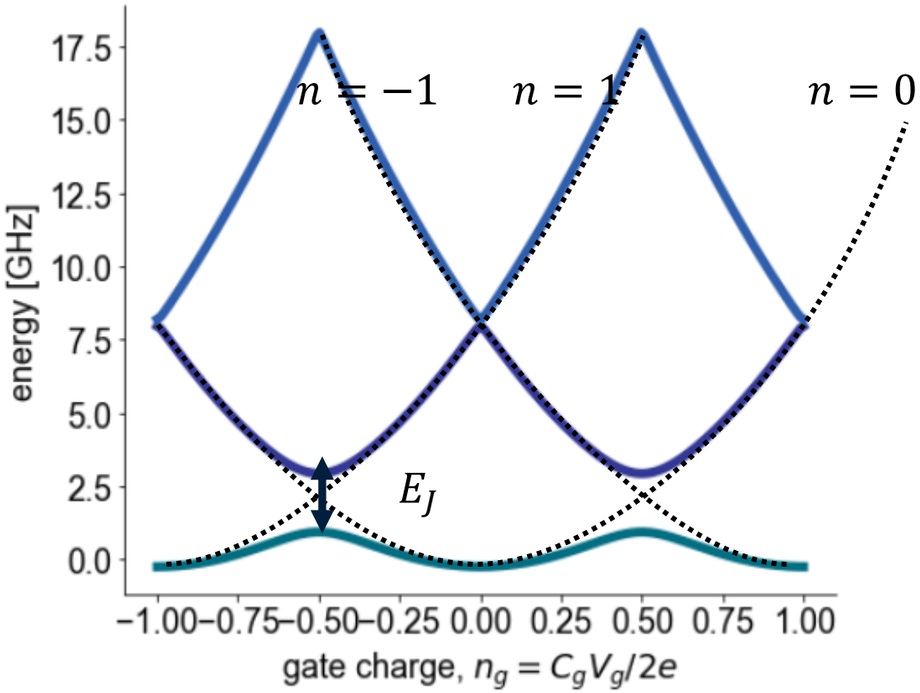

# Cooper Pair Box Qubit – Summary

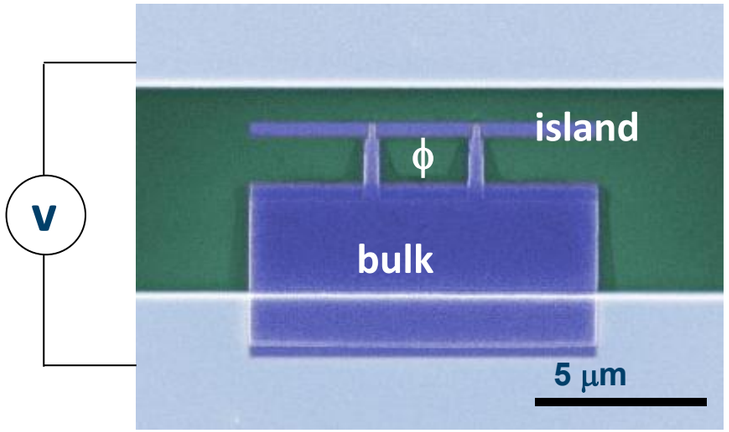


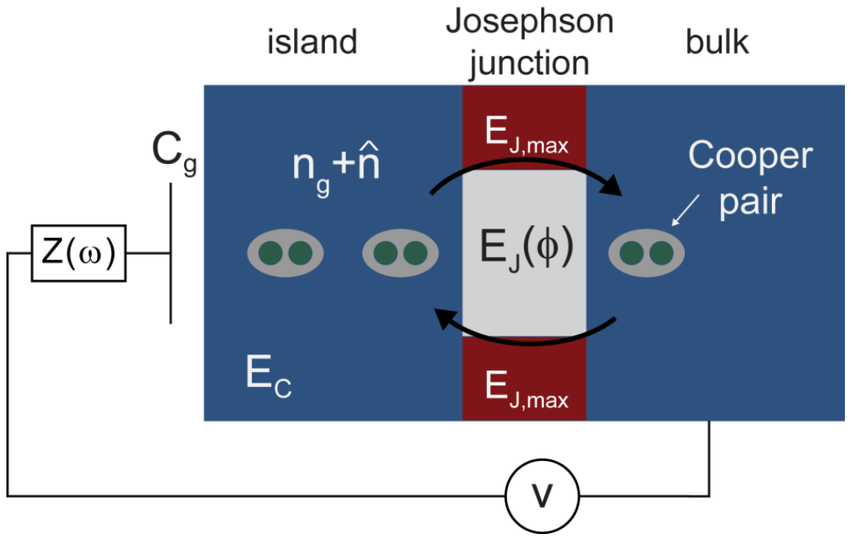


- superconducting island connected via Josephson junctions to grounded reservoir (bulk)
- Cooper pairs can tunnel onto island
- relevant degree of freedom: number of excess Cooper pairs on island (n)
- polarization charge $n_g$ adjustable via voltage bias
- energy scales:
  - charging/electrostatic energy $E_C$ (energy to add another Cooper pair)
  - Josephson energy $E_J$ (coupling energy)

[Bouchiat, Vion, Joyez, Esteve, Devoret, *Physica Scripta* T76, 165 (1998).]

# Two State Approximation

$$H = 4E_C\left(\hat{n} - n_g\right)^2 - E_J \cos\hat{\delta}$$

$$\widehat{=} \sum_N \left[4E_C\left(n - n_g\right)^2 |n\rangle\langle n| - \frac{E_J}{2}\left(|n\rangle\langle n+1| + |n+1\rangle\langle n|\right)\right]$$

2-dim Hilbert space: $\hat{n} = \begin{pmatrix} 0 & 0 \\ 0 & 1 \end{pmatrix} = \frac{\hat{1} - \hat{\sigma}_z}{2}$

$$\rightarrow \hat{\sigma}_z = -2\hat{n} + \frac{\hat{1}}{2};\ \cos\hat{\delta} = \frac{\sigma_x}{2}$$

$$\rightarrow\ H_2 = -E_C\left(1 - 2n_g\right)\sigma_z - \frac{E_J}{2}\sigma_x$$

Bias point: $n_g = \frac{1}{2}$; basis transformation $\sigma_x \rightarrow \sigma_z$

$$\rightarrow\ \widetilde{H}_2 = -\frac{E_J}{2}\sigma_z$$ … spin-1/2 / effective 2-level system

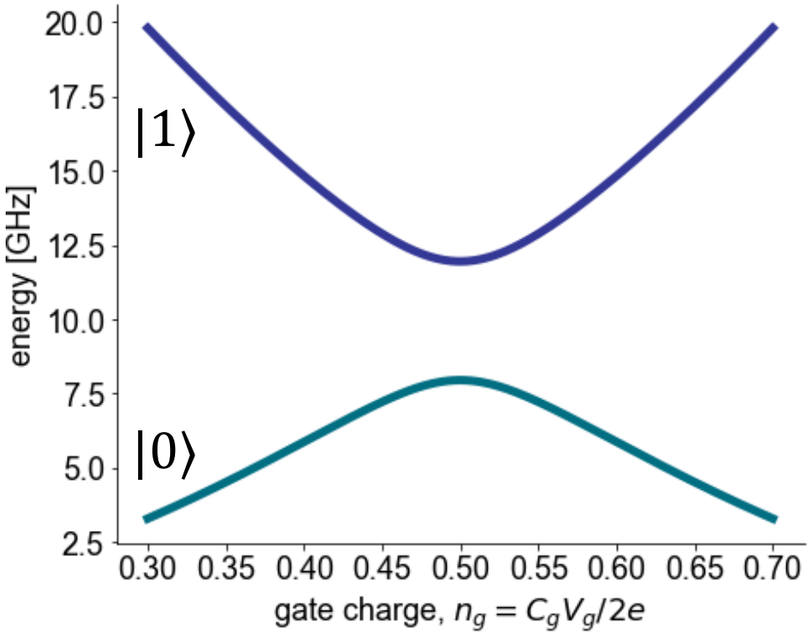


[Shnirman *et al., Phys. Rev. Lett.* **79**, 2371 (1997)]

# Phase Quantization – SQUID as a tunable junction

## SQUID: flux-tunable Josephson junction

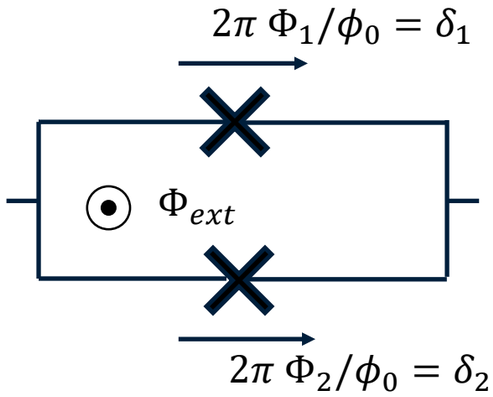


$$\delta_1 - \delta_2 - \frac{2\pi\,\Phi_{ext}}{\phi_0} = j \cdot 2\pi$$

**Recall:**

Aharonov-Bohm effect $\delta = \frac{2e}{\hbar}\oint \vec{A}\cdot d\vec{s} = \frac{2e}{\hbar}\Phi_{\mathrm{ext}}$

& single-valuedness of wavefunction $\delta = j\,2\pi$

Critical current tunable via external magnetic field:

$$I_{tot} = I_1 + I_2 = \mathrm{I_{c1}}\sin\delta_1 + I_{c2}sin\delta_2$$

$$I_c(\Phi_{ext}) = 2I_c\left|\cos\left(\frac{\pi\Phi_{ext}}{\phi_0}\right)\right|\sin\tilde{\delta}$$

(for $I_{c1} = I_{c2} = I_c$)

# Tuning the Josephson Energy

split Cooper pair box in perpendicular field: SQUID modulation of Josephson energy

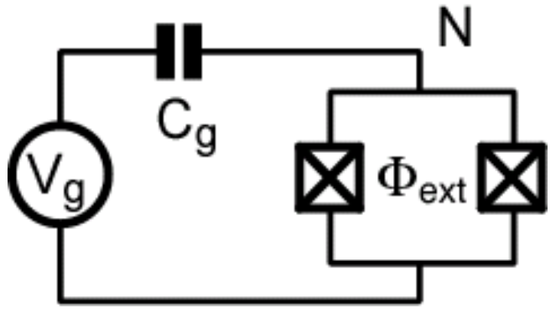


$$H = 4E_C\left(\hat{n} - n_g\right)^2 - \overbrace{E_{J,max}\left|\cos\left(\frac{\pi\Phi_{ext}}{\Phi_0}\right)\right|}^{E_J}\cos\hat{\varphi}$$

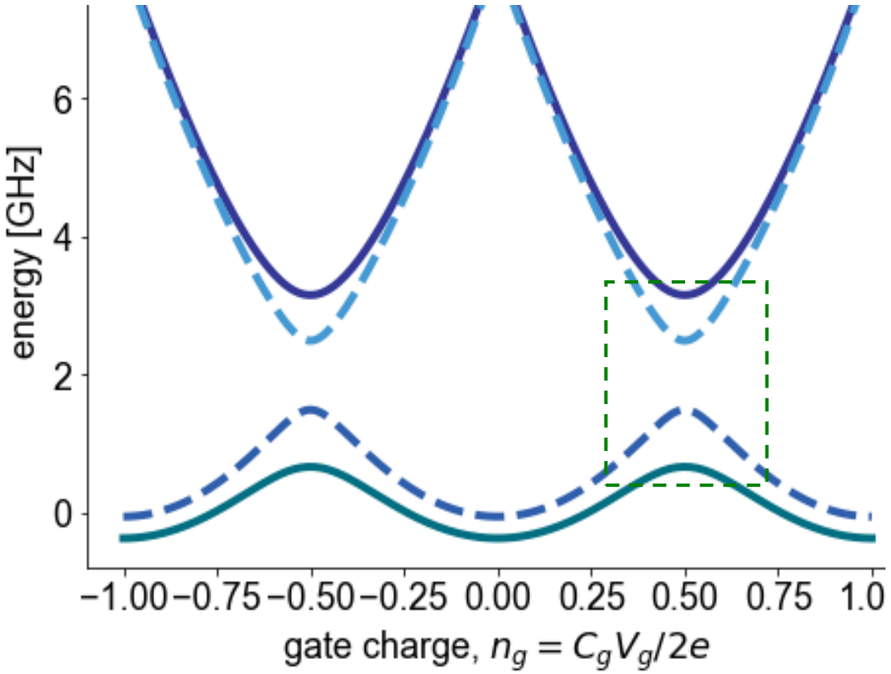


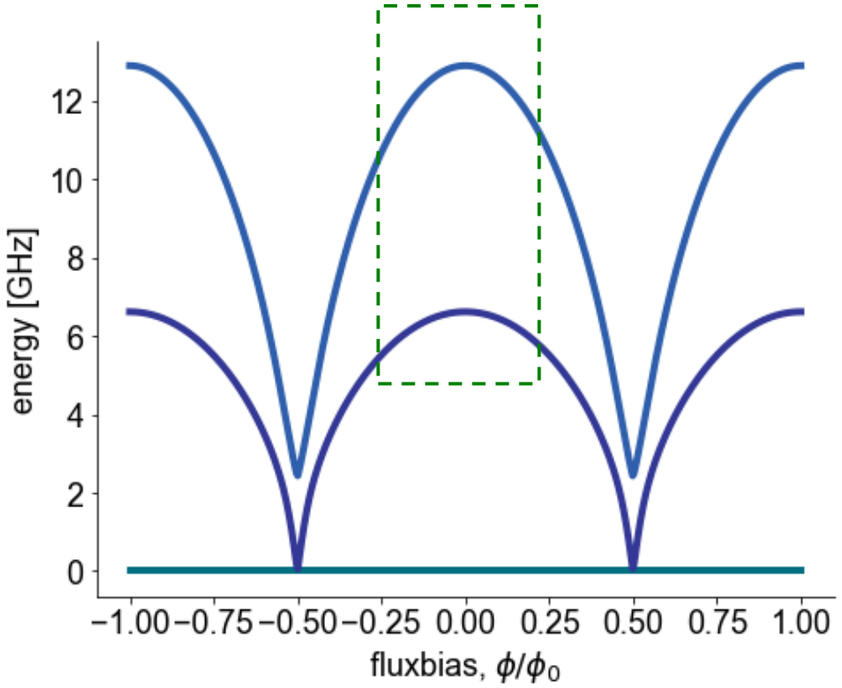


[J. Clarke, *Proc. IEEE* **77**, 1208 (1989)]

# Charge and Phase Wave Functions ($E_J \sim E_C$)

$|\psi_1\rangle$

$|\psi_0\rangle$

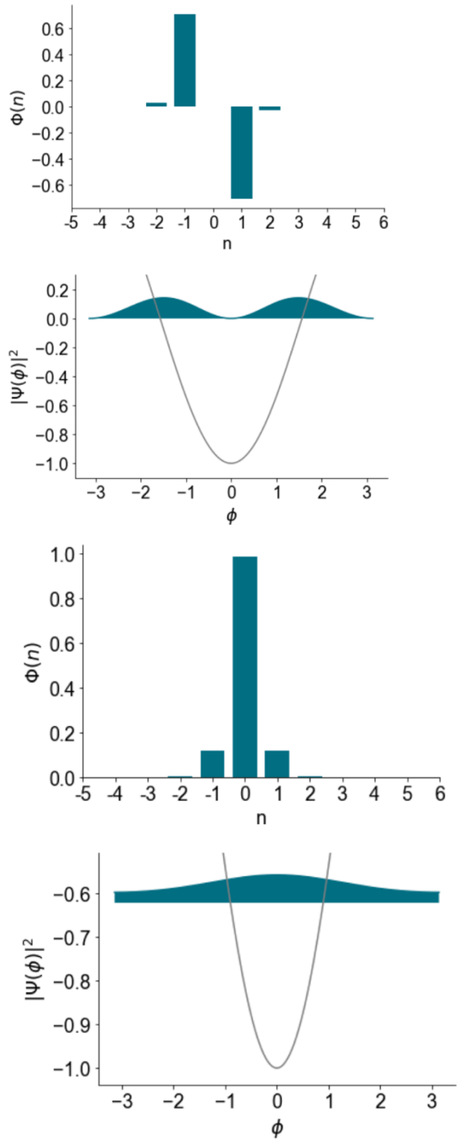


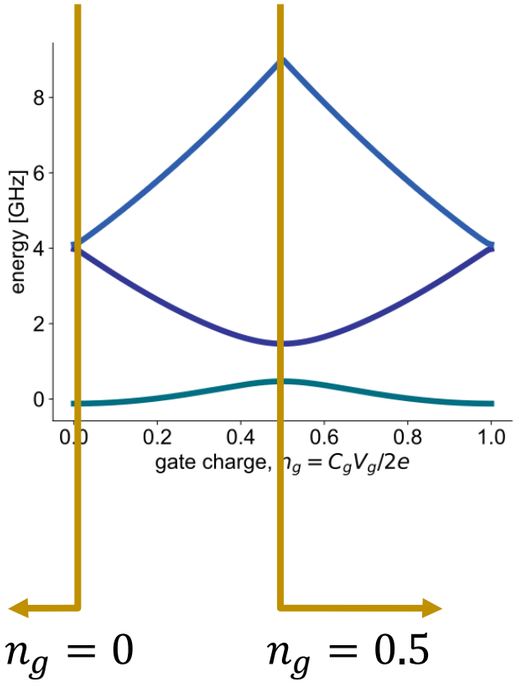


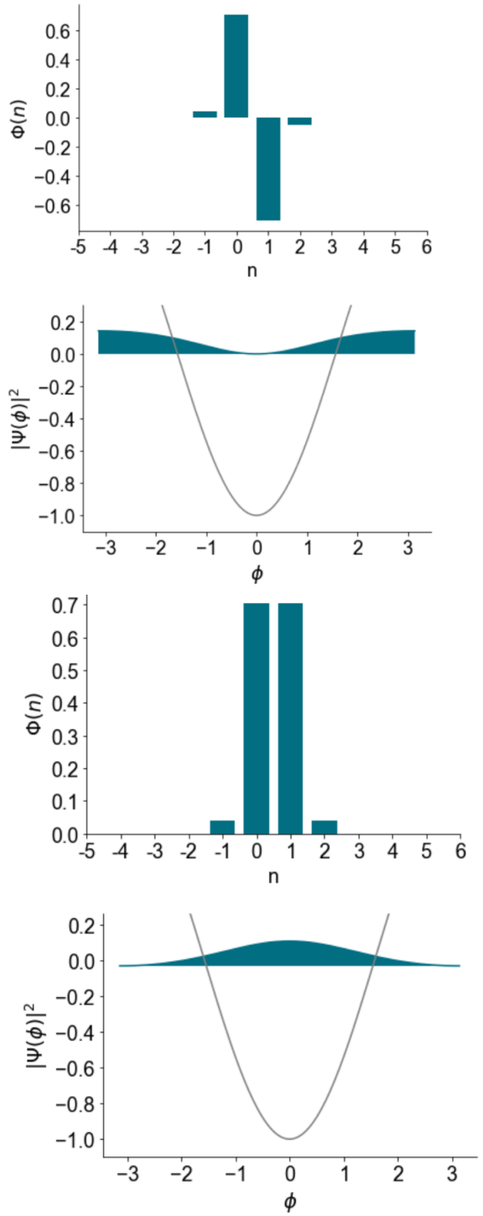


$|\psi_1\rangle$

$|\psi_0\rangle$

# Charge and Phase Wave Functions ($E_J \gg E_C$)

Transmon regime:

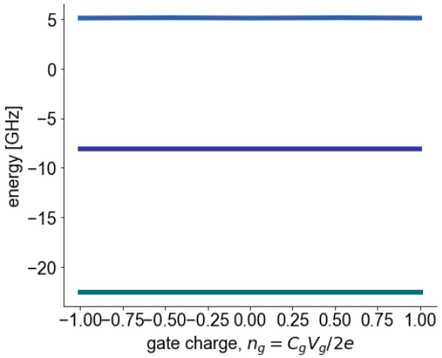


ground state $|0\rangle$

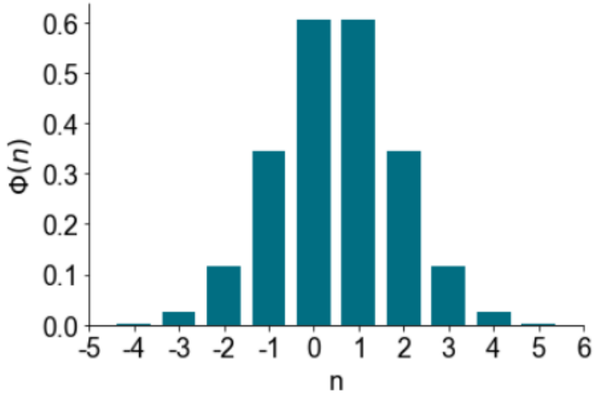


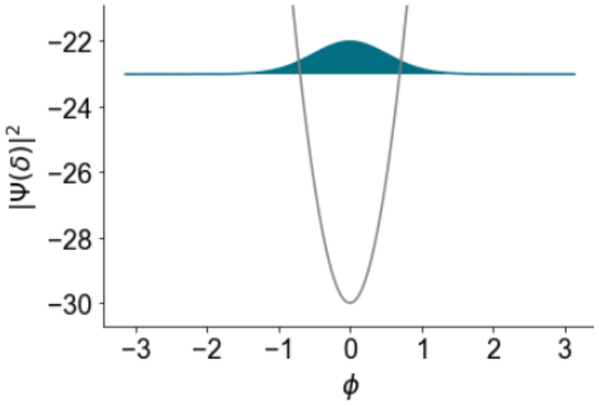


1st excited state $|1\rangle$

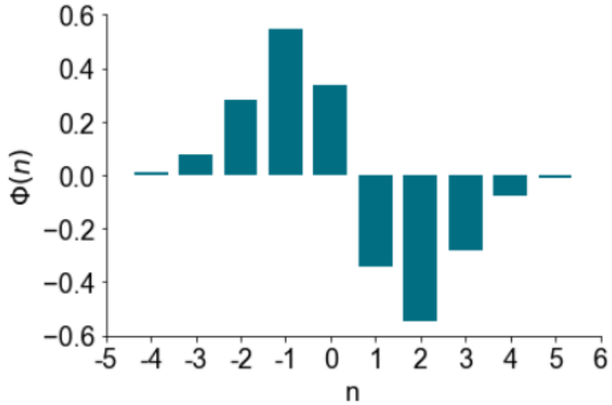


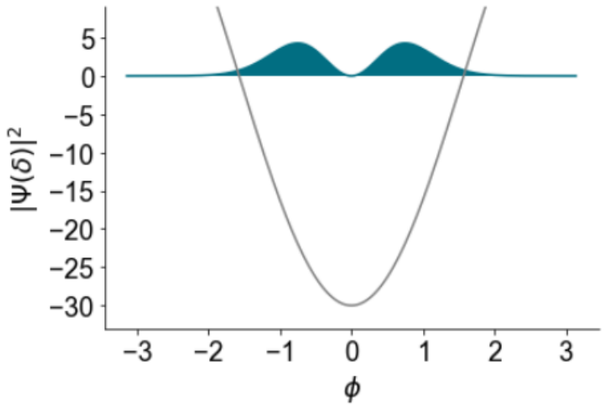


2nd excited state $|2\rangle$

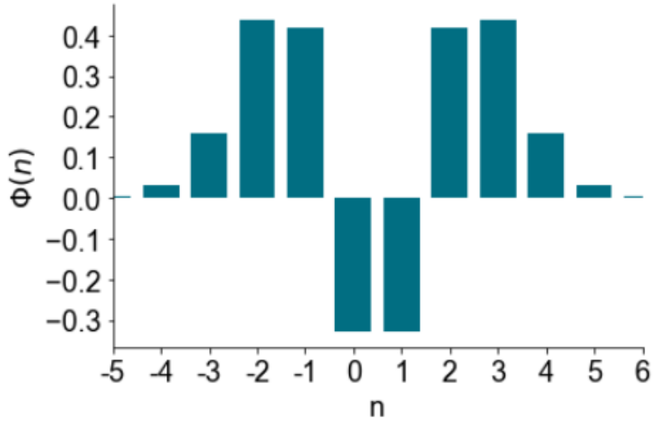


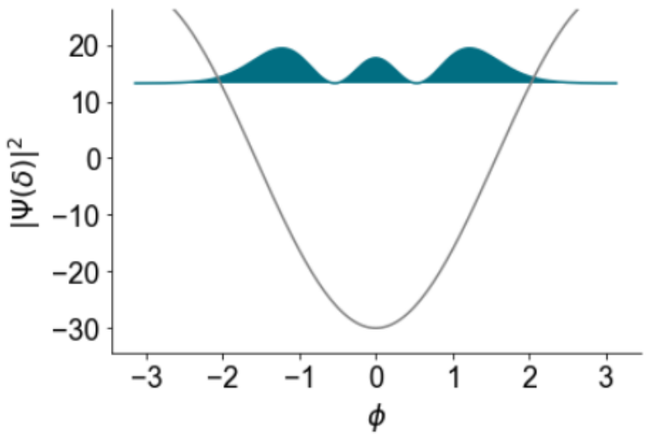

# Transmon qubit – a charge noise resilient qubit

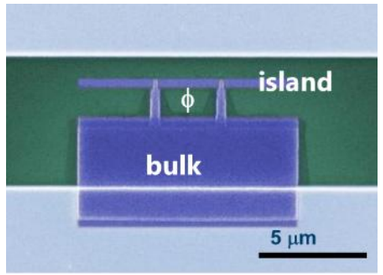


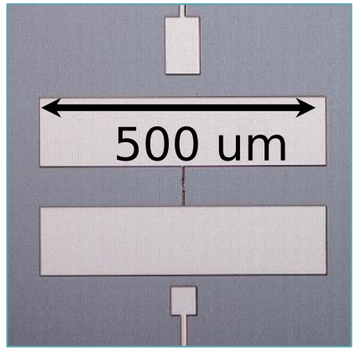


- shunting capacitor reduces $E_c$
- Increased $E_J/\,Ec$ ratio flattens energy bands
- Less sensitivity to charge noise

$$E_C = \frac{e^2}{2\,C_\Sigma}$$

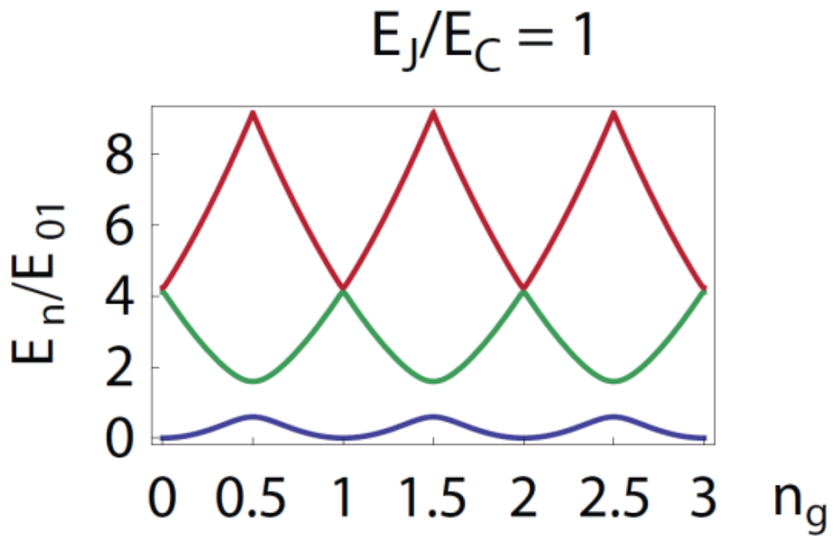


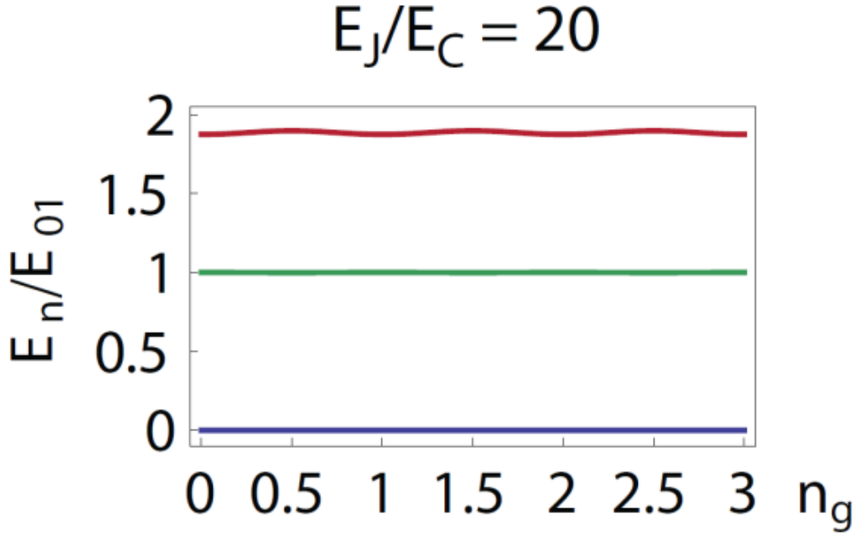


$$H = E_C\left(\hat{n} - n_g\right)^2 - E_j \cos\hat{\delta}$$

BUT: anharmonicity $\alpha \equiv \omega_{12} - \omega_{01}$ decreases (polynomially) with increasing $E_J/E_C$ !!

[Koch *et al. PRA 76, 042319 (2007)*; Schreier *et al. PRB (2008)*]

# Transmon qubit – Anharmonicity

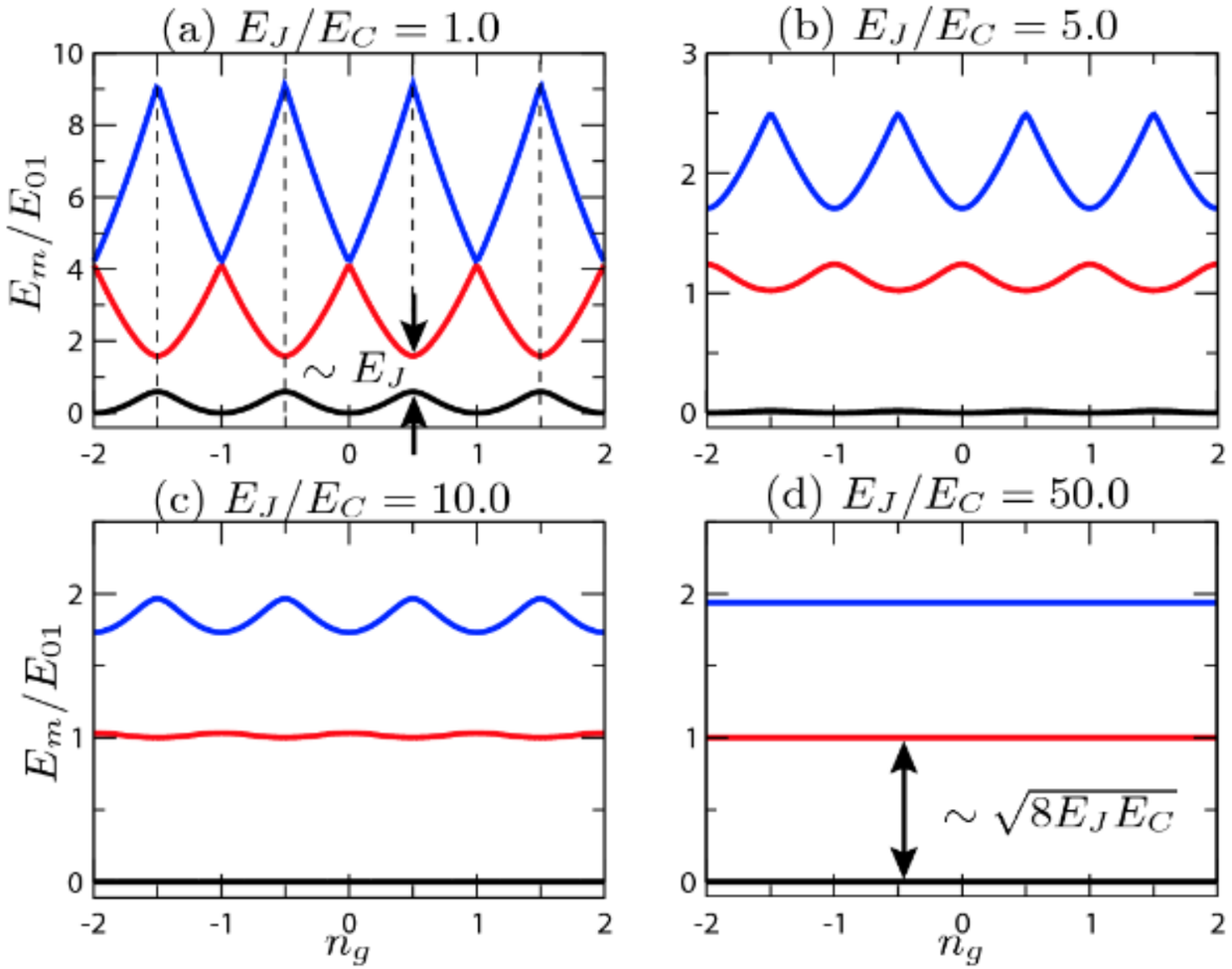


$$E_{01} = \sqrt{[4E_C(2n_g - 1)]^2 + E_J^2}$$

$$\alpha \equiv E_{12} - E_{01}$$
$$\alpha_r \equiv \alpha/E_{01}$$

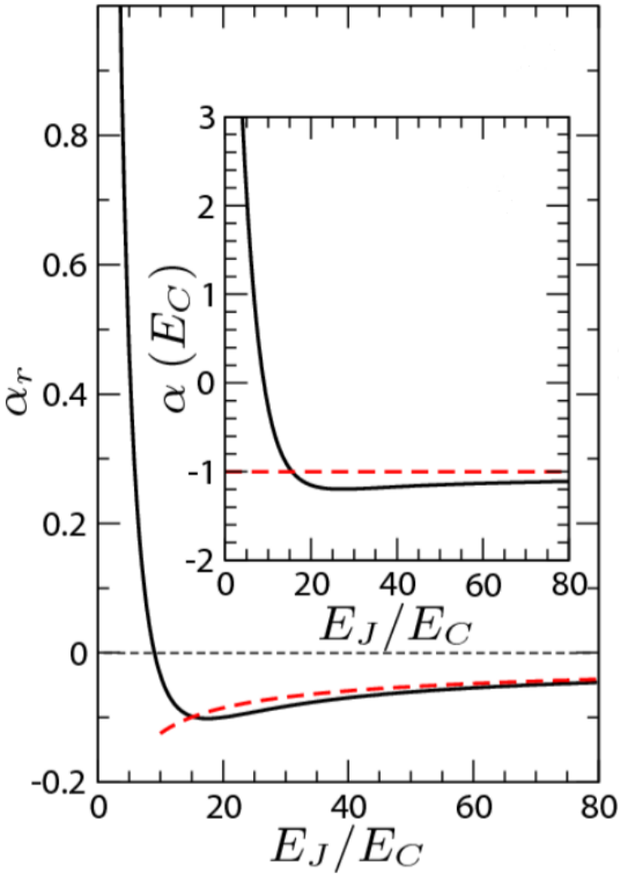


[Koch *et al. PRA 76, 042319 (2007)*; Schreier *et al. PRB (2008)*]

# Charge dispersion

- Transmon qubit with tunable $E_J(\Phi_x)$
- record qubit frequency as a function of gate charge $n_g$

  for different $\frac{E_J}{E_C} = (a)28.6, (b)16.3, (c)13.3, (d)10.4$

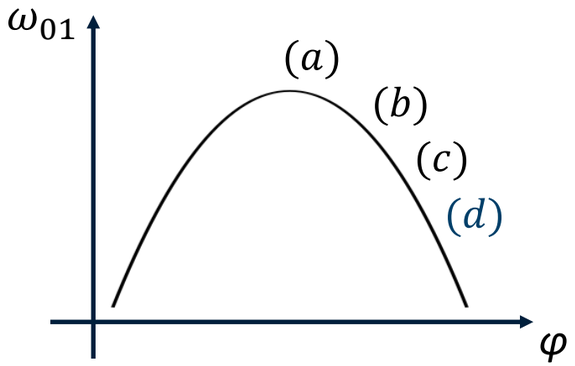


- Two possible frequencies $\omega_{01} \pm \delta_c$
  (extra electron= quasi-particle on island)

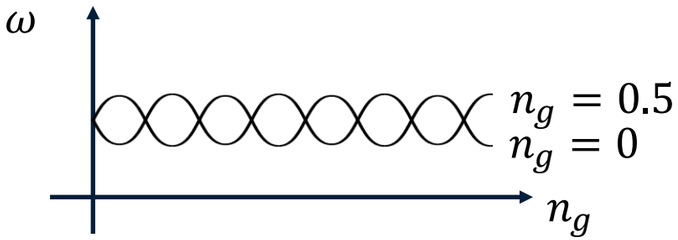


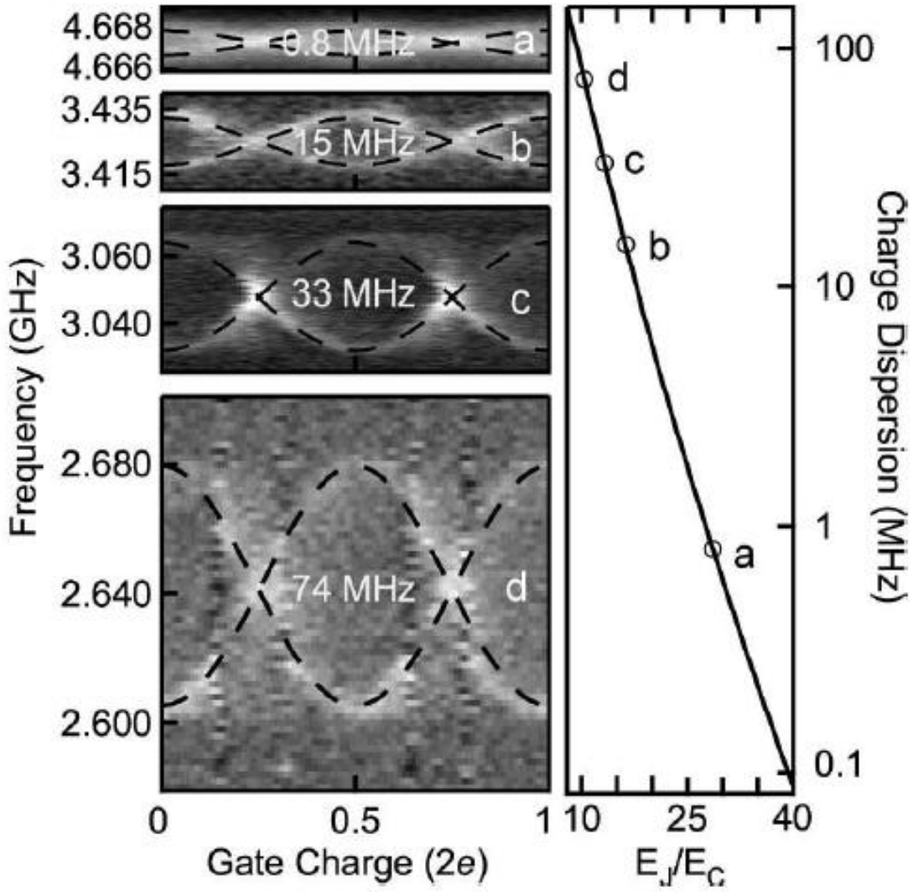


[Schreier *et al. PRB (2008)*]

# Charge dispersion qubit

Why does one observe two distinct lines and not a broad transition?

a) Because the time scale of quasi-particle tunnelling is **slower** than each experiment but **faster** than the whole experiment (with n repetitions).

b) Because the time scale of quasi-particle tunnelling is **faster** than each experiment but **slower** than the whole experiment (with n repetitions).

# Transmon Tunability

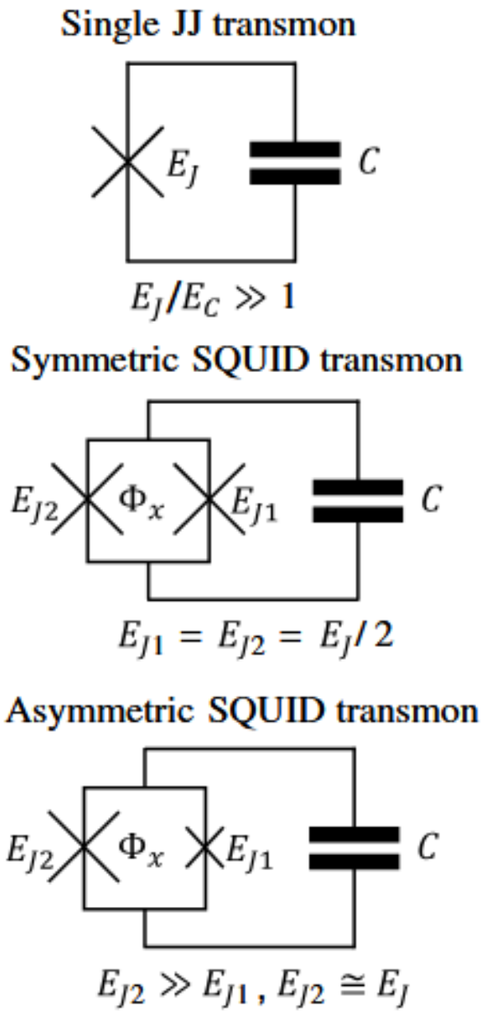


[Chavez-Garcia *et al. PRAppl (2022)]*

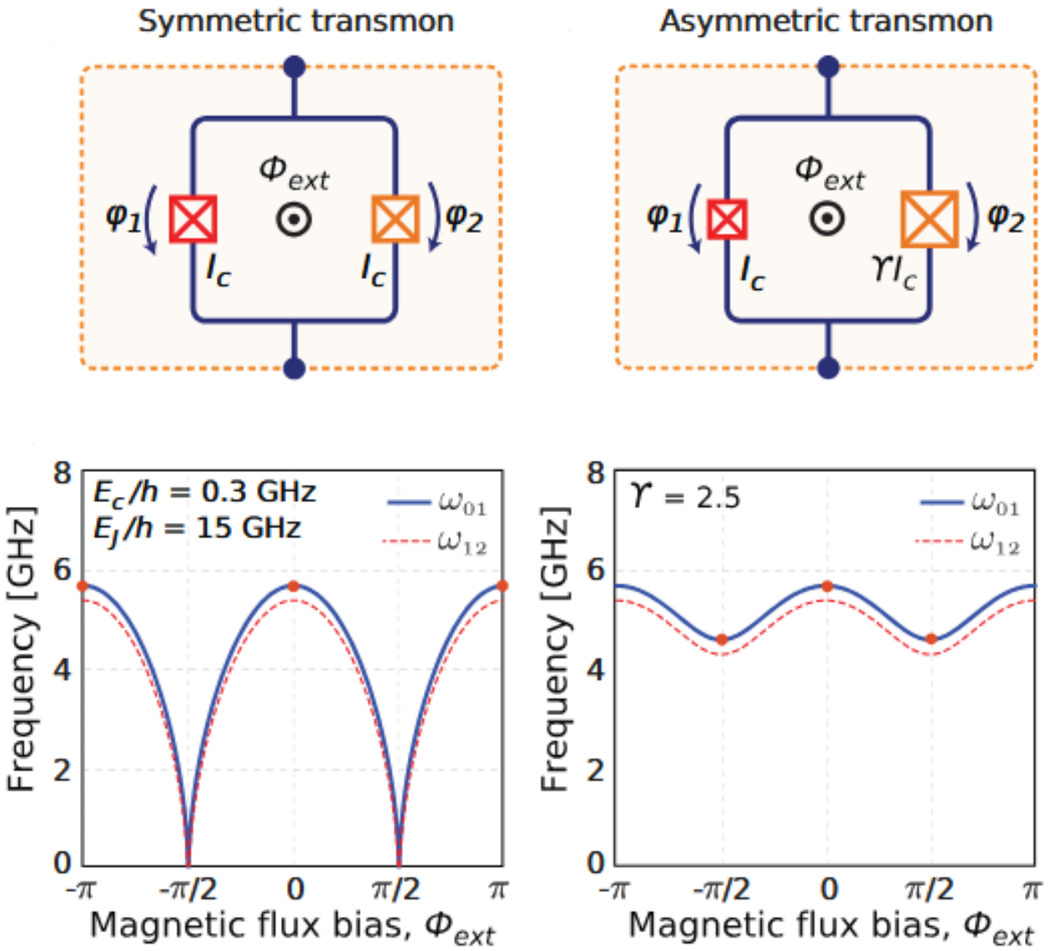


[Krantz *et al. Appl. Phys. Rev. (2019)]*

# Ta-on-Si Transmon Qubits with Relaxation Times Exceeding 1 ms

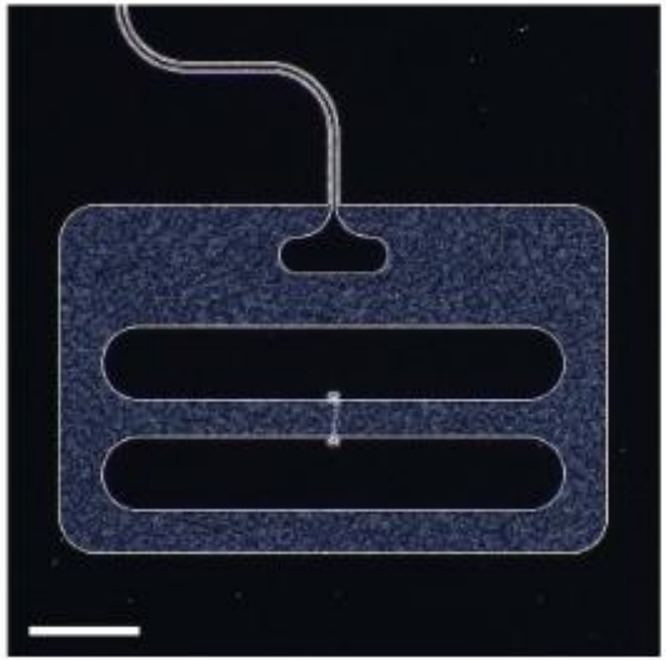

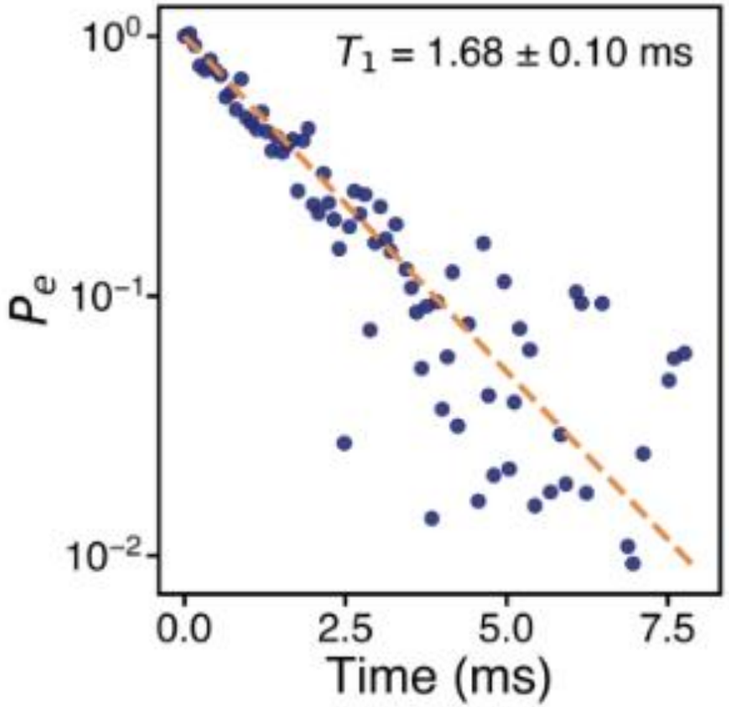


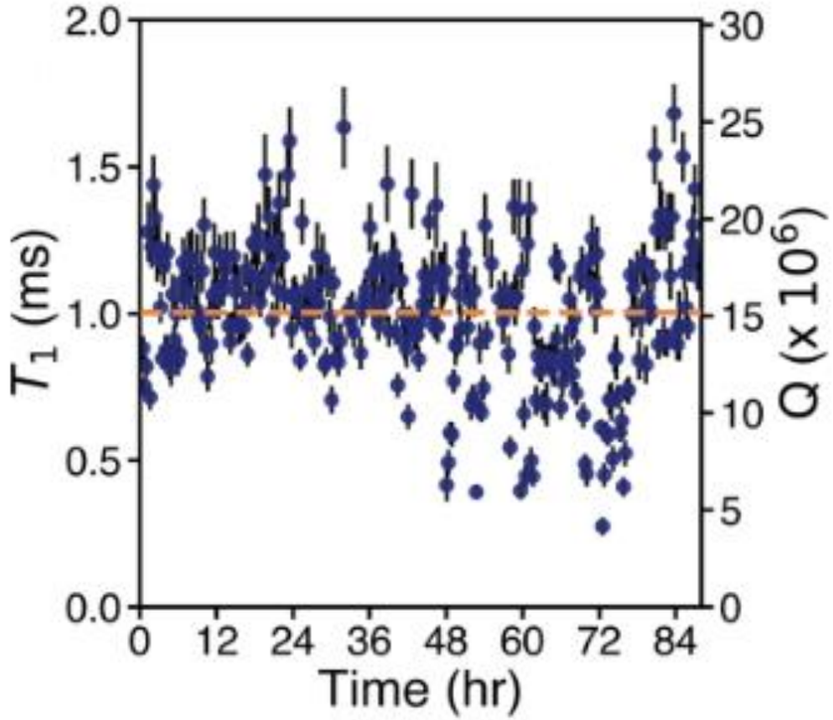


[Bland *et al. arXiv2503,14798 (2025)]*

# Fabrication

# Microscope image of transmon qubit

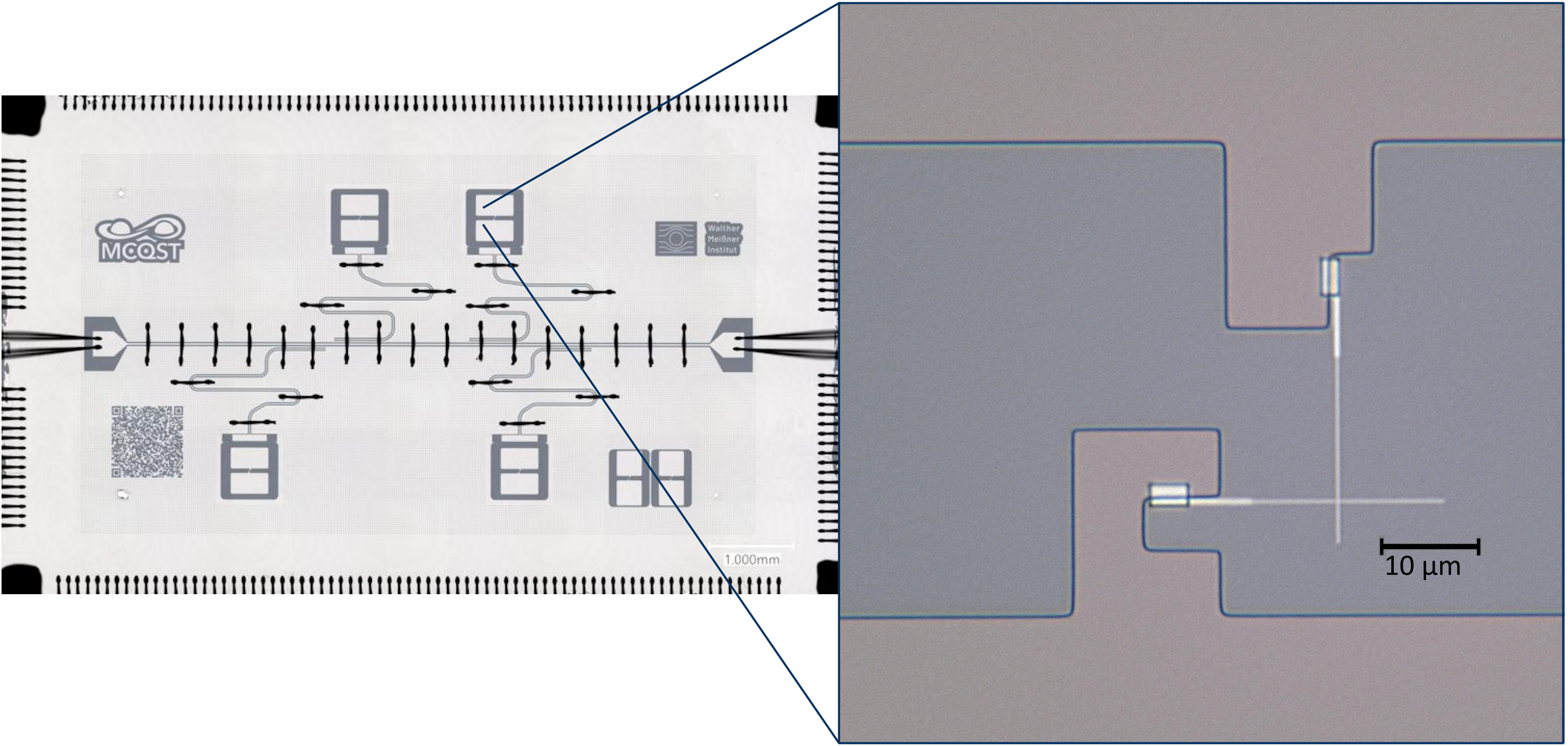

# Clean room

Controlled environment with strict specifications on

- temperature stability
- humidity
- particles per $m^3$

ISO 14644-1 Cleanroom Standards

| Class | Maximum Particles/$m^3$ | | | | | | FED STD 209E equivalent |
|---|---|---|---|---|---|---|---|
| | >=0.1 µm | >=0.2 µm | >=0.3 µm | >=0.5 µm | >=1 µm | >=5 µm | |
| ISO 1 | 10 | 2 | | | | | |
| ISO 2 | 100 | 24 | 10 | 4 | | | |
| ISO 3 | 1,000 | 237 | 102 | 35 | 8 | | Class 1 |
| ISO 4 | 10,000 | 2,370 | 1,020 | 352 | 83 | | Class 10 |
| ISO 5 | 100,000 | 23,700 | 10,200 | 3,520 | 832 | 29 | Class 100 |
| ISO 6 | 1,000,000 | 237,000 | 102,000 | 35,200 | 8,320 | 293 | Class 1,000 |
| ISO 7 | | | | 352,000 | 83,200 | 2,930 | Class 10,000 |
| ISO 8 | | | | 3,520,000 | 832,000 | 29,300 | Class 100,000 |
| ISO 9 | | | | 35,200,000 | 8,320,000 | 293,000 | Room Air |

LEAST STRINGENT

MOST STRINGENT

# Qubit fabrication steps

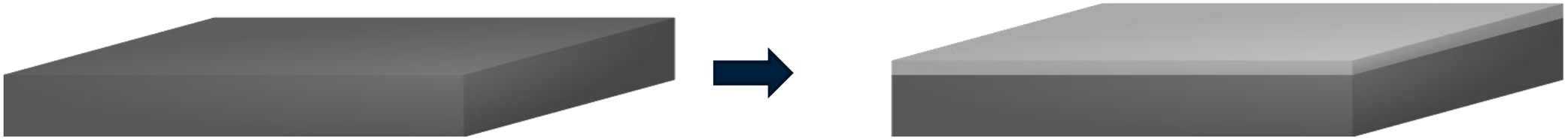

**Base metallization (> 1 µm)**

- High-ohmic Si (100) substrate
- Piranha (mix of sulfuric acid and hydrogen peroxide), to remove organic carbon compunds
- Buffered Oxide Etch (BOE, mix of hydrofluoric acid and ammonium fluoride), to remove native Si oxides
- DC magnetron sputtering 150 nm niobium
- Resist writing via optical lithography
- pattern transfer via RIE
- Resist removal and 30 s BOE cleaning

# Sputter deposition

Ultra-high vacuum system

1. load clean silicon substrate into deposition tool, via load lock
2. deposit 150 nm metallization layer
   (e.g. Niobium, Tantalum or other superconducting materials)

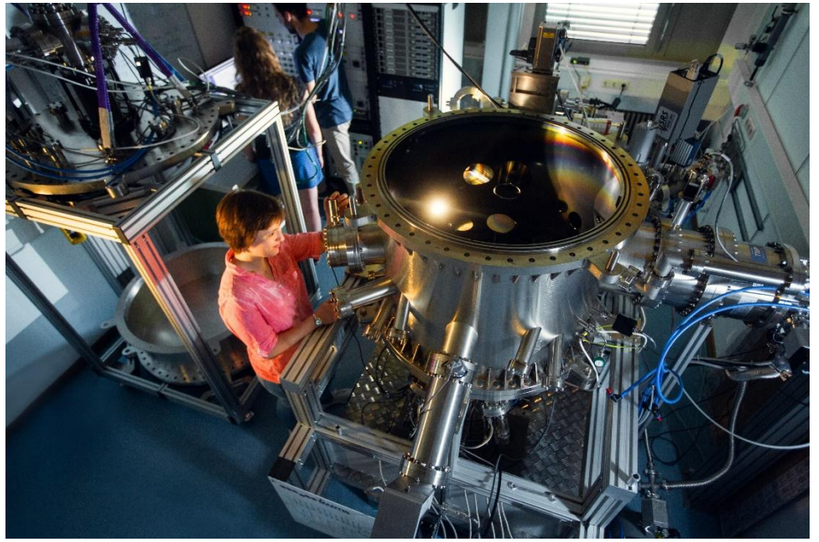

DC magnetron sputtering tool

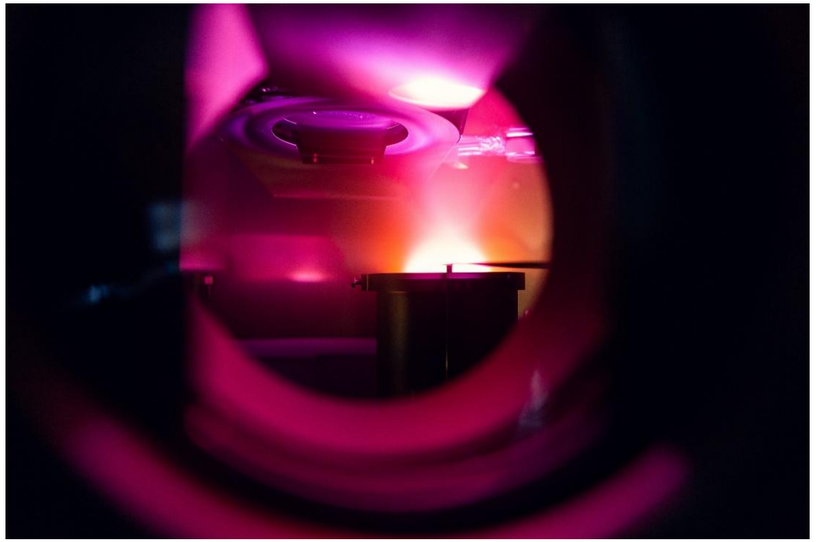

Ignited plasma during deposition

# Sputter deposition

- apply high voltage between a target material (the superconducting material) and substrate (silicon)
- introduce argon into process chamber
- high voltage ignites plasma of $Ar^+$ ions that are accelerated onto target material
- atoms sputtered off the target due to kinetic energy of ions
- atoms condense on the substrate and form a thin film
- film quality determined by temperature and pressure

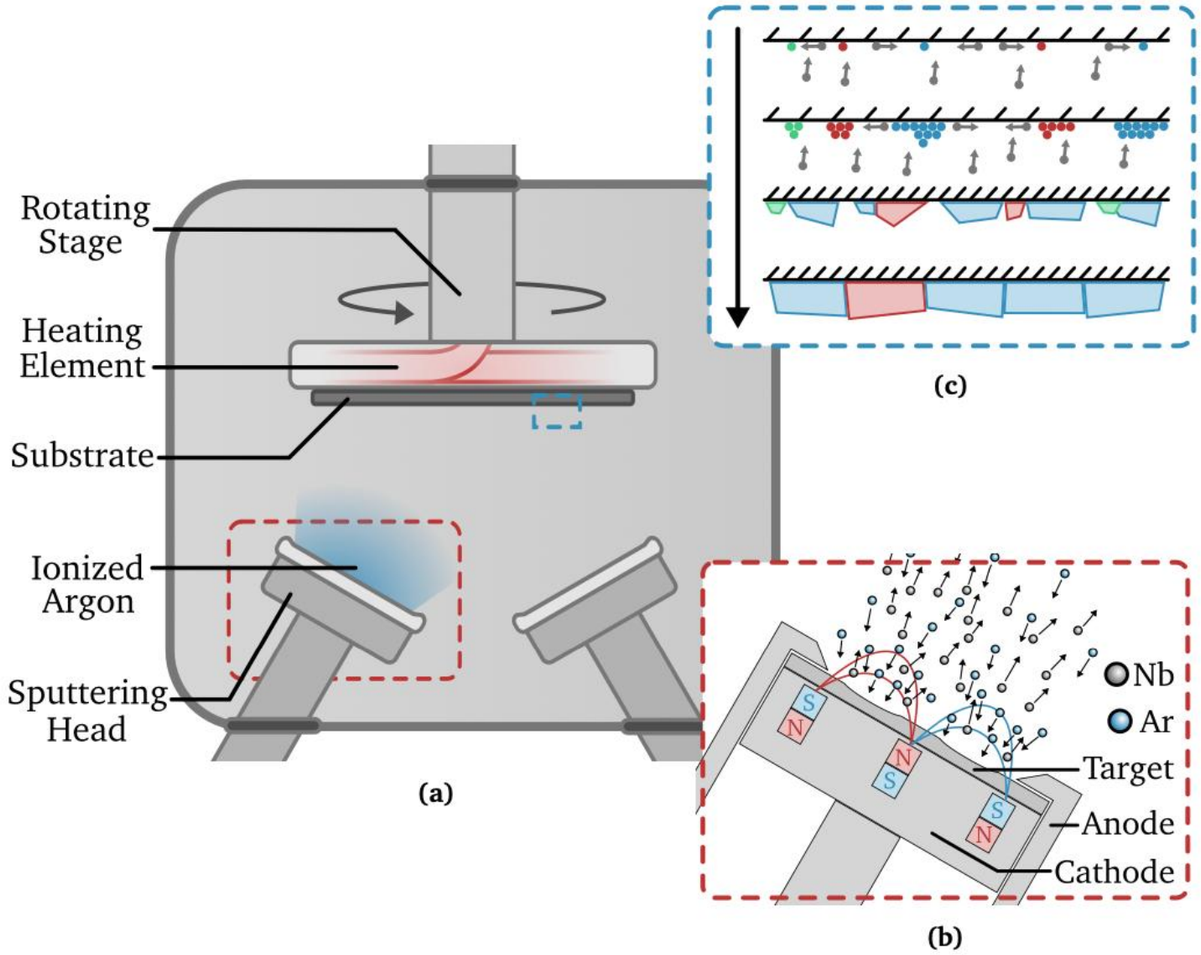


(a) sputtering chamber.
(b) magnetron sputtering head.
(c) illustration of the thin film growth process (colours represent various crystal orientations)

# Optical lithography – spin coating

Either via direct laser writer or via mask-aligner process

Structure sizes limited by (optical) wavelength

1. spin coat photoresist onto metallized substrate
    - Thickness set by rotation speed and resist properties
    - Sensitive to temperature and humidity

Photoresist

- light sensitive organic material (typically consist of resin, sensitizer and solvent)
- Exists in two polarities: positive and negative
    - Positive: exposed area is soluble in developer
    - Negative: exposed are is insoluble in developer

Spincoating resist

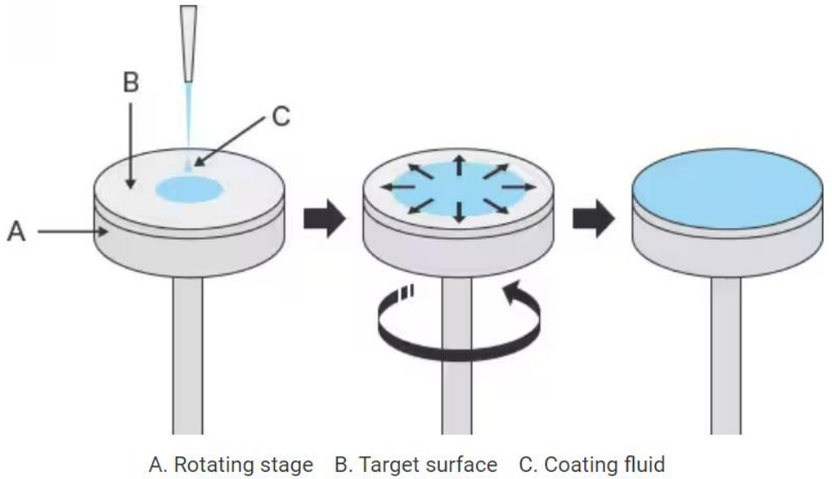

# Optical lithography – patterning first layer

Either via mask-aligner process, direct laser writer or maskless aligner (using a DMD)

Structure sizes limited by (optical) wavelength

Spincoating resist | Optical lithography | Etching

1. spin coat positive optical resist
   onto metallized substrate
   - Sensitive to temperature and humidity
2. expose the resist with laser light
   in areas defined by a layout
   → exposure leads to chemical
   changes in exposed resist
3. dip the sample into developer
   → removes resist in exposed areas (positive resist)
4. etch sample via reactive ion etching or wet chemical etching
   → unexposed areas are protected by the remaining resist
   → micro structure from mask is transferred into metal layer


# Reactive Ion Etching

Combination of physical sputtering (similar to thin film deposition) and chemical etching
('dry etching')

- oscillating RF electric field between upper and lower electrode
  → ignites plasma (e.g. sulfur hexafluoride $SF_6$)
- oscillating electromagnetic field initiates the plasma
- electrons create a large potential difference (low mass)
  (discharge to ground on upper electron, charges are collected on lower electrode/blocking capacitor; ions are mostly stationary)
- voltage difference → positive ions (ion sheat) move towards sample
  → chemical reactions and sputtering at the same time
- Optional: Inductively coupled plasma source for higher plasma densities


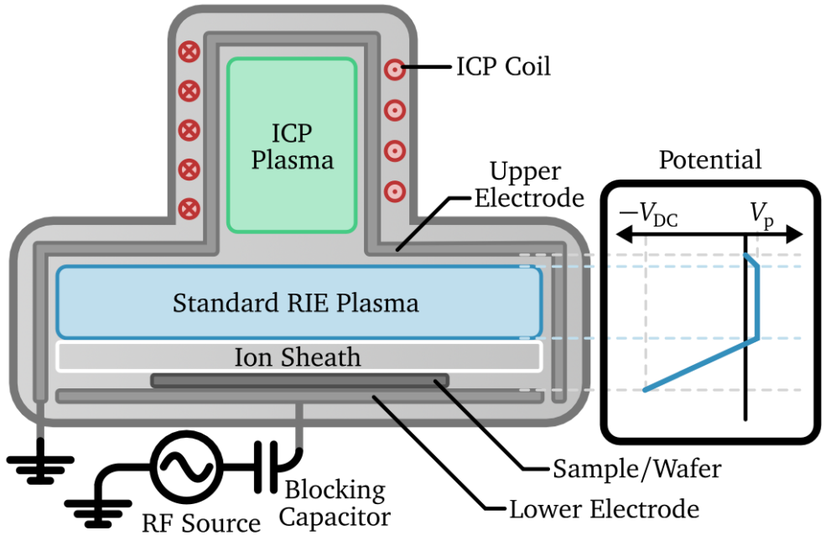


RIE chamber including ICP (inductively coupled plasma) unit.
Negative potential accelerates plasma towards the sample.

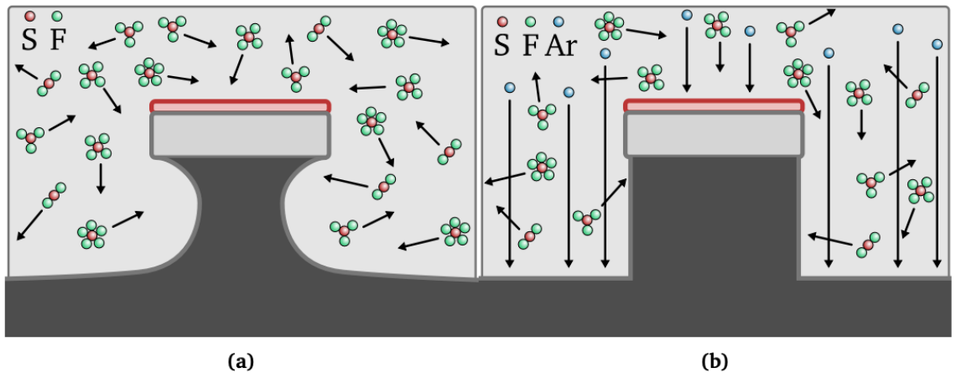


(a) Isotropic etch profile vs
(b) an-isotropic etch profile due to momentum of argon ions.

# Josephson Junction fabrication steps

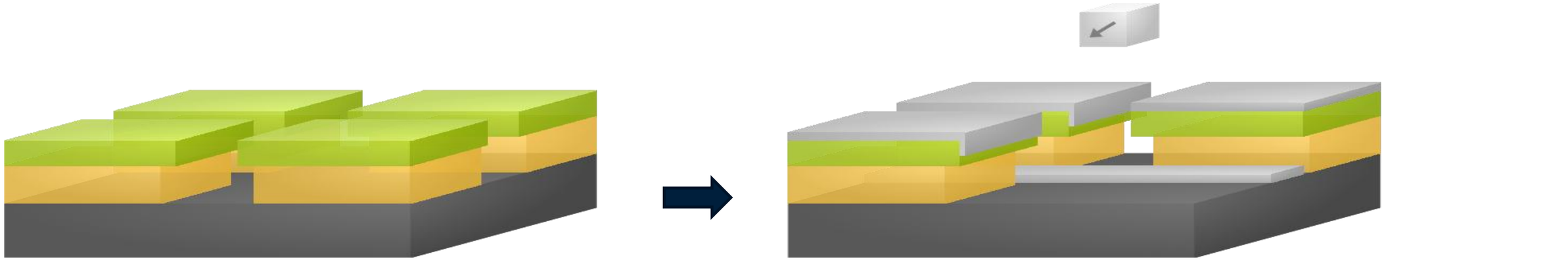

**Junction fabrication (< 1 µm)**

- Bilayer resist system (e.g. CSAR and PMMA)
- Evaporation and dynamic oxidation
- Evaporation of second aluminum layer
- Resist stripping and metal lift-off

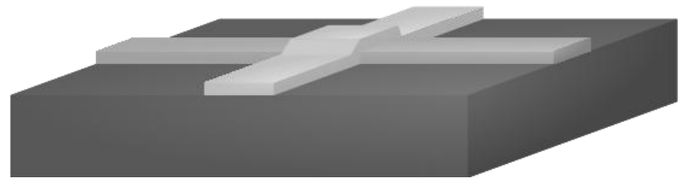

# E-beam lithography – defining Josephson Junctions

Similar to optical lithography but for nm – sized structures

→ suitable to define Josephson junctions

(typical dimensions 50x50 $nm^2$ to 300x300 $nm^2$)

- Sensitive to temperature, vibrations, electric/magnetic fields

1. spin coat two resist layers onto the sample
2. load the sample into a UHV e-beam writing tool
3. expose resist in predefined areas by electron irradiation
4. develop the resist structure

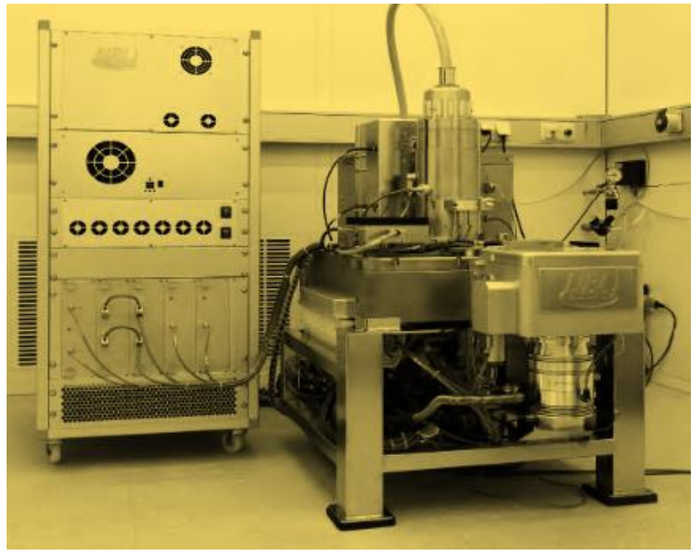

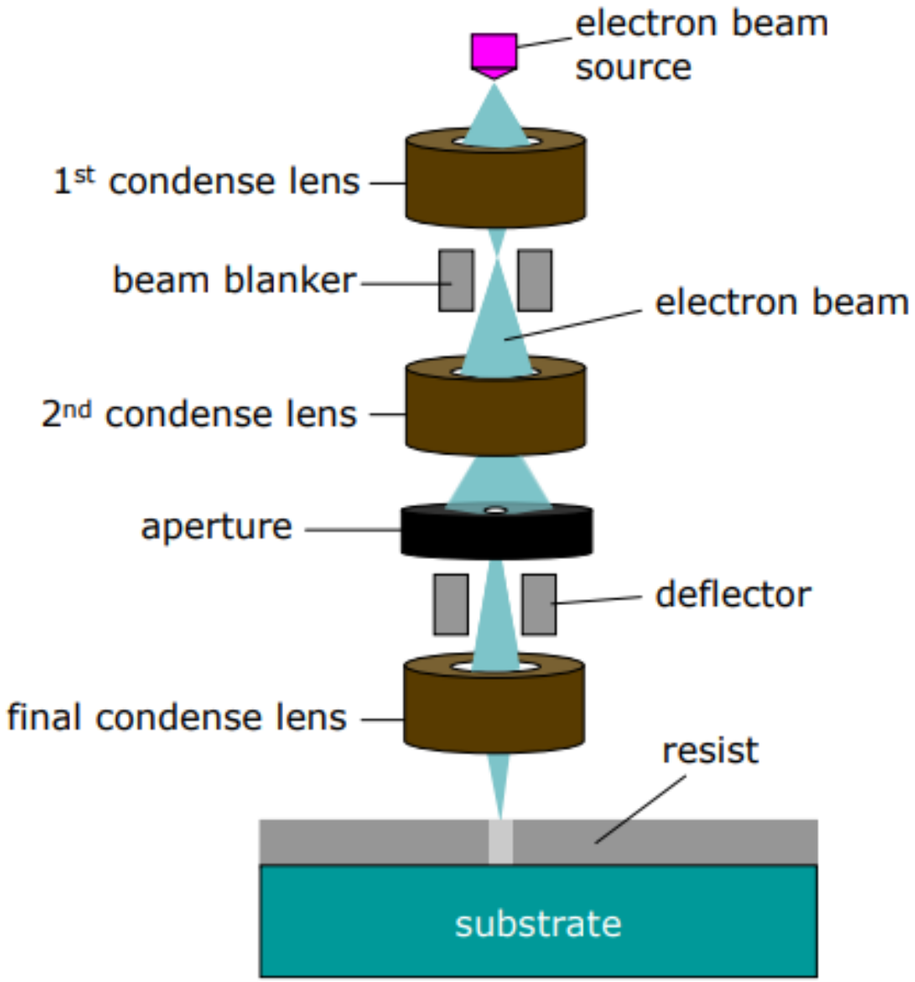

# Deposition of Al-AlOx-Al trilayer

Aluminium is deposited via electron beam evaporation

- high kinetic energy electron focused onto aluminium target
  → sublimation of aluminium
- aluminium is directed to substrate
  → condenses as thin film

Oxidation through controlled inlet of oxygen into chamber

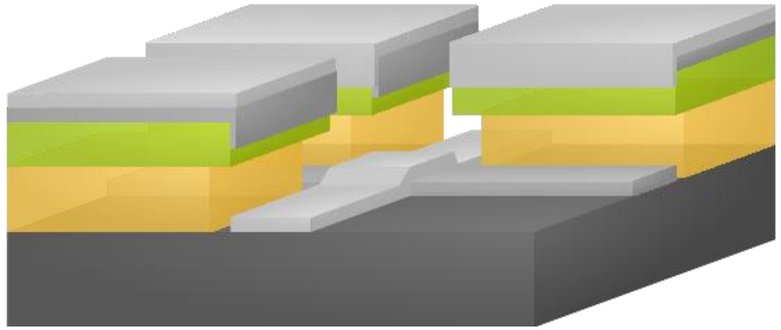

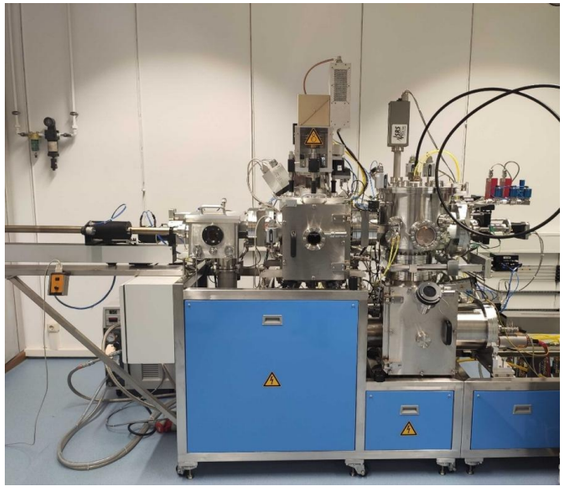

1. load sample with resist mask into Al evaporation tool
2. pump ultra high vacuum ($< 10^{-8} mbar$)
3. deposit first junction arm via e-beam evaporation (20 nm thickness)
4. dynamically oxidize the surface of this first junction arm
5. tilt and rotate sample
6. deposit second junction arm (60 nm thickness)

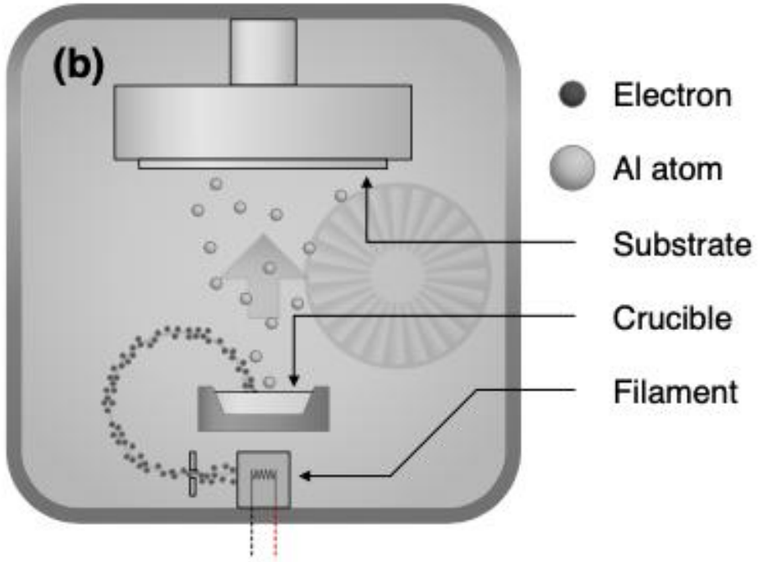

# Lift-off – removing excess aluminium

1. Put sample into acetone to dissolve resist
2. Generate a flow to „wash away“ excess aluminium
3. rinse and dry sample

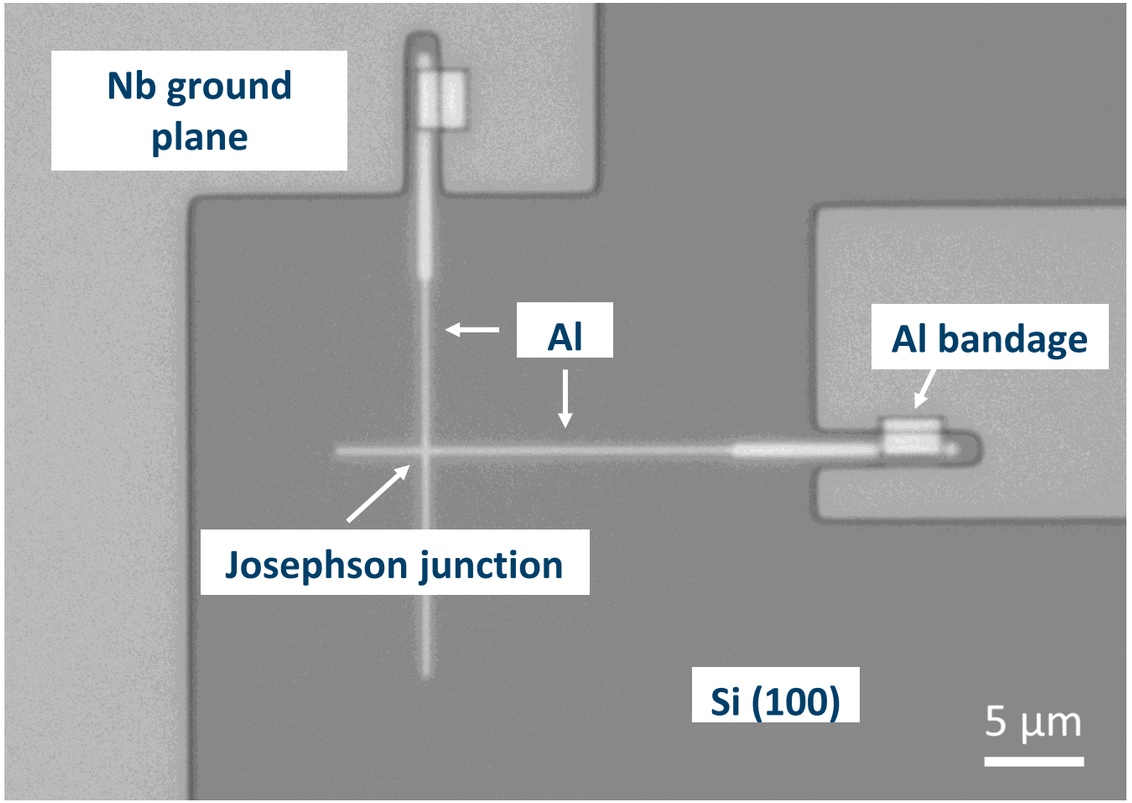


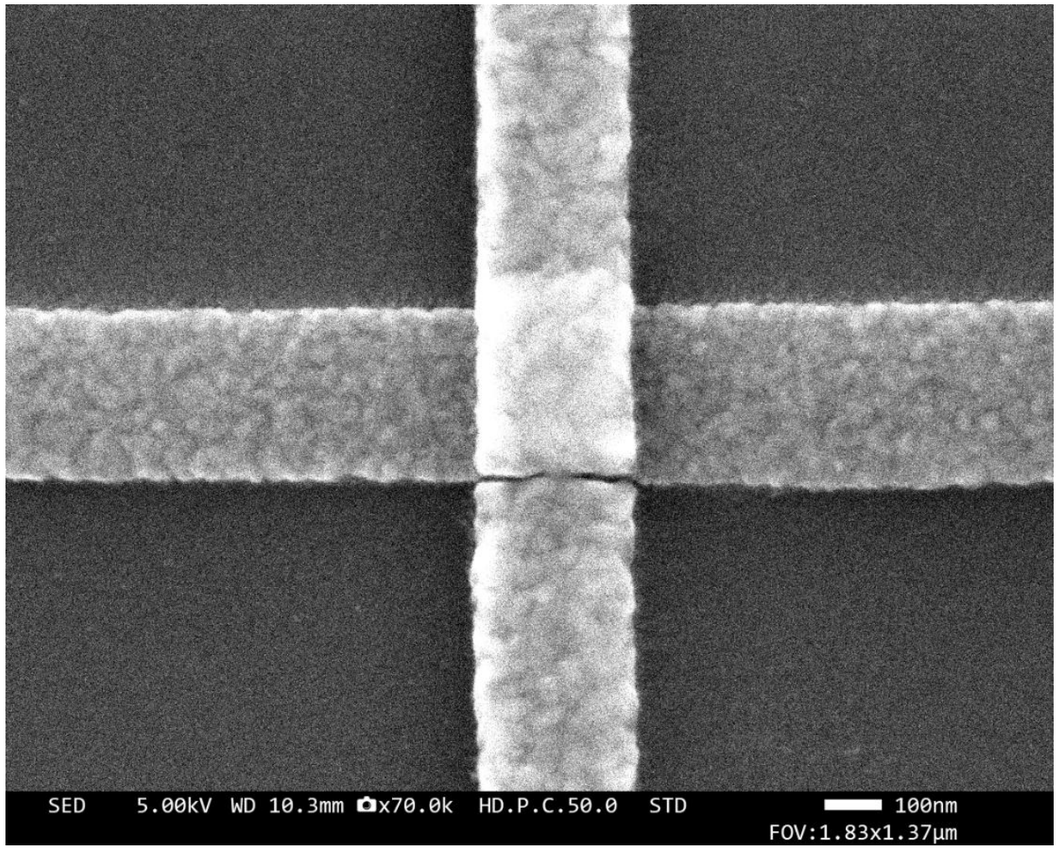

# Adding bandages

Ensure contact between Nb base layer and junction arms

1. spin coat resist layers onto the sample
2. load sample again into a UHV e-beam writing tool
3. expose resist in predefined areas
   (purple areas in the picture) by electron irradiation
4. develop the resist structure
5. load sample into Al evaporation tool
6. etch away surface oxides by Ar-Ion milling
7. deposit aluminium for galvanic contact between first metallization layer and junction arms
8. Lift-off excess aluminium

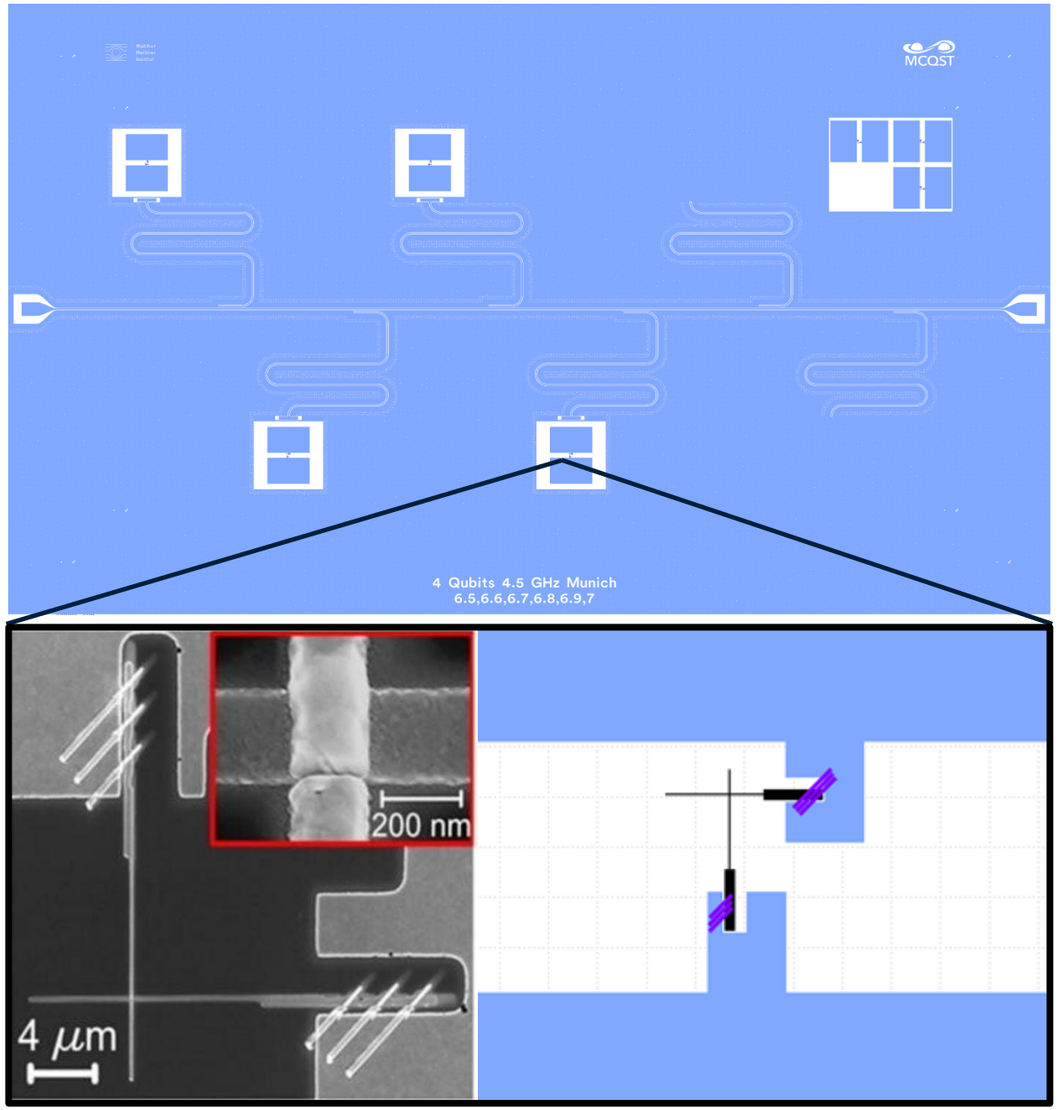

# Process flow

Sputtering Nb

Spincoating resist

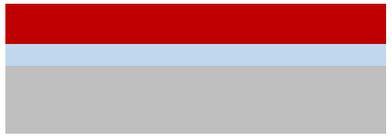

Optical lithography

Etching

Stripping resist

Photoresist
Niobium
Substrate
E-beam resist 1
E-beam resist 2
Aluminum
Aluminum oxide
Bandages
Airbridges

Spincoating resist

E-beam lithography

Evaporation 1

Oxidation +Evap. 2

Lift-off

Side view of Josephson Junction

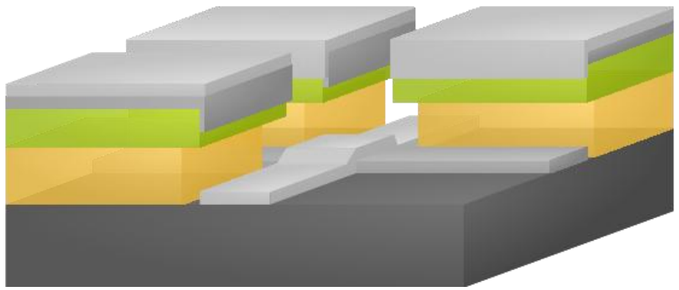

Top view

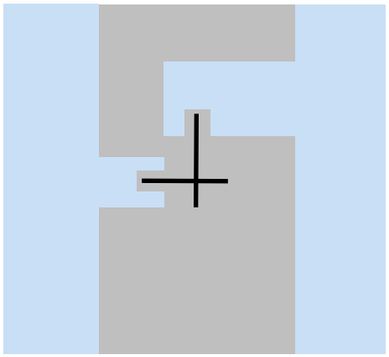

Bandages

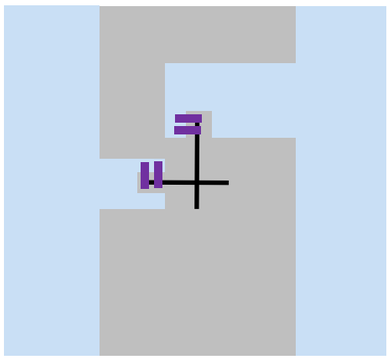

Air bridges

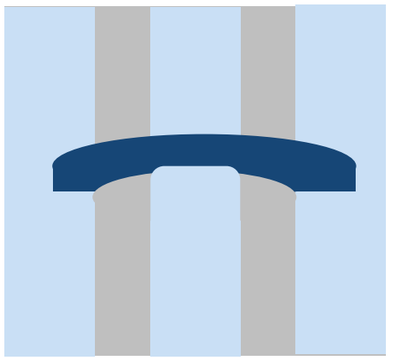

# Scaling: 3D integration and I/O

Requirement for scalability:

- addressability of all qubits (3-5 controls per qubit)
  → would require $> 10^6$ signal lines for universal QC
- reduction of modes in large chips
- reduction of cross-talk

## Air bridges

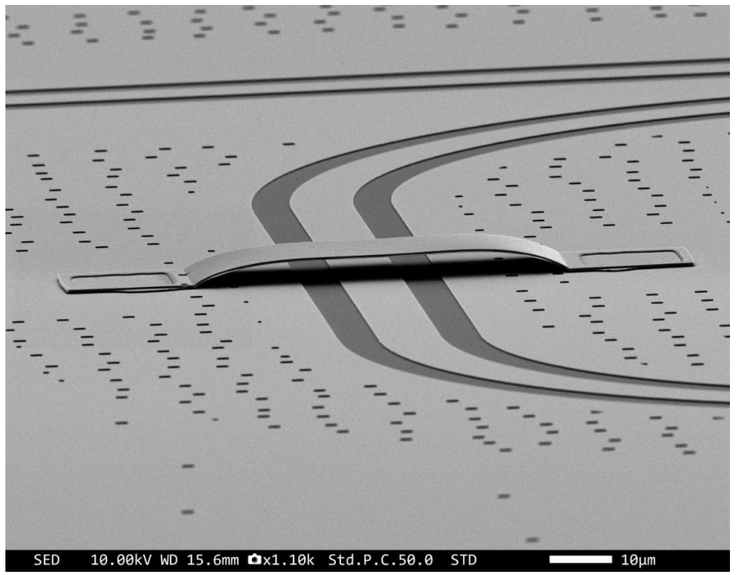


## Indium bump flip-chip bonding

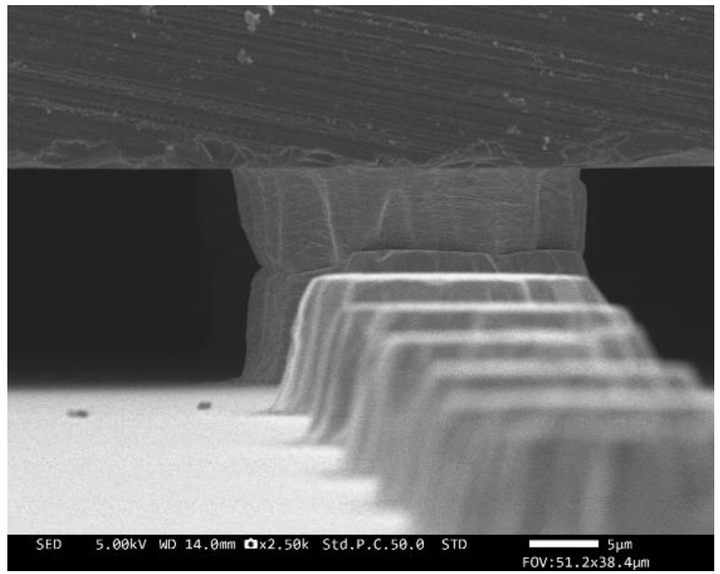


## Through-silicon-Via (TSV)

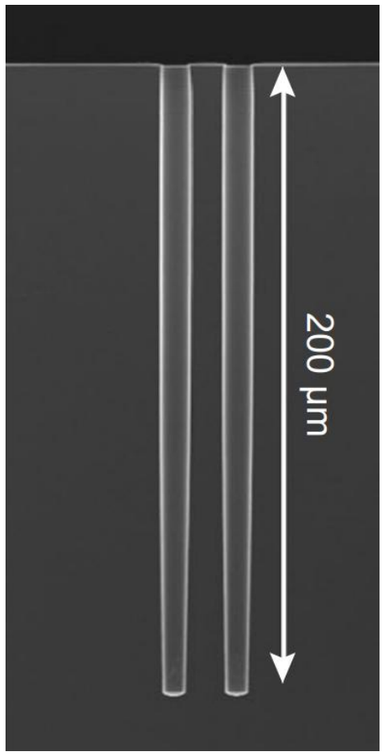

# Scaling: Air bridge process

To connect grounds on the chip and to route signal lines

1. spin coat optical resist on pre-patterned substrate
2. define a structure by optical lithography, develop the structure and „reflow“ the resist by melting it
3. deposit metallization layer on top
4. spin coat and define a second structure by optical lithography
5. etch away the excess material
6. release the air bridge by dissolving remaining resist

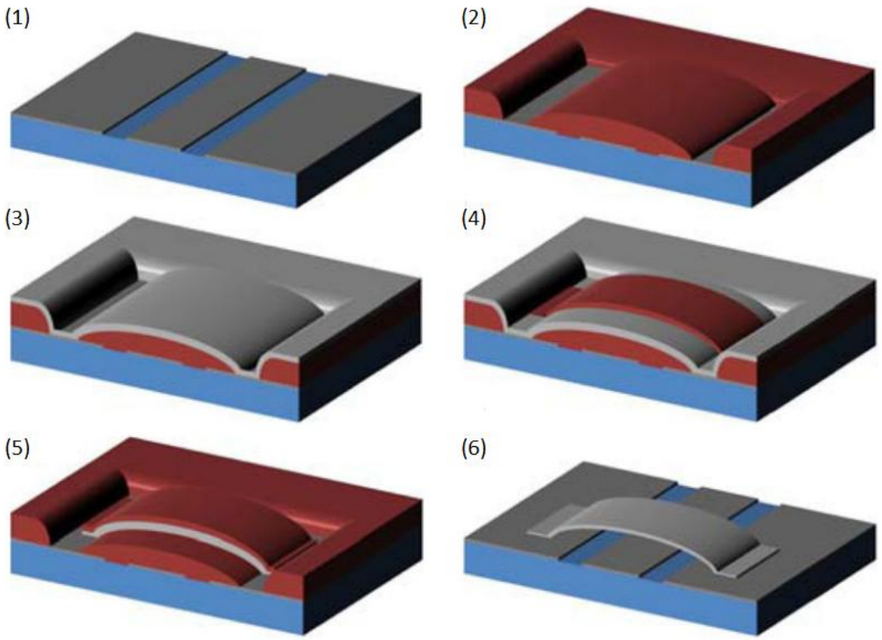


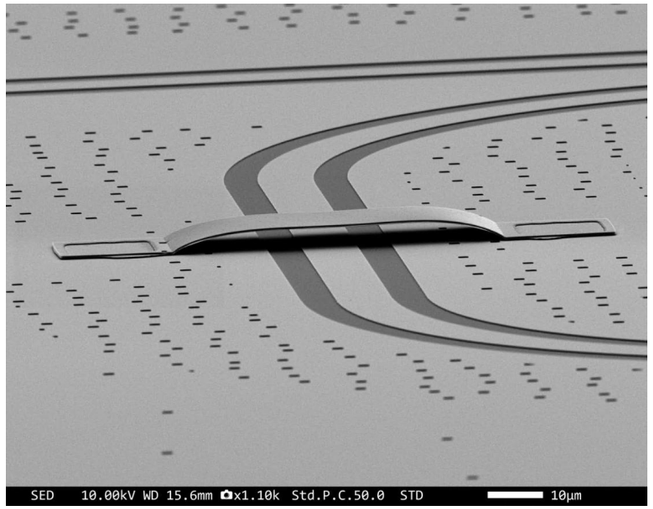

# Scaling: Indium bump flip-chip bonding

Two Si chips connected by indium bumps

- Bottom chip for routing
- Top chip for qubits and couplers
- ~ 10 µm chip spacing, precise tilt control is key

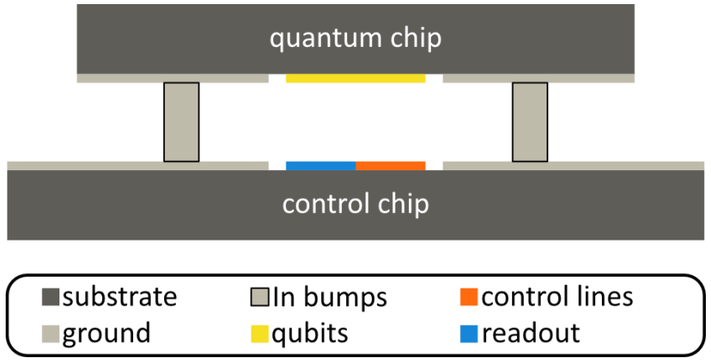


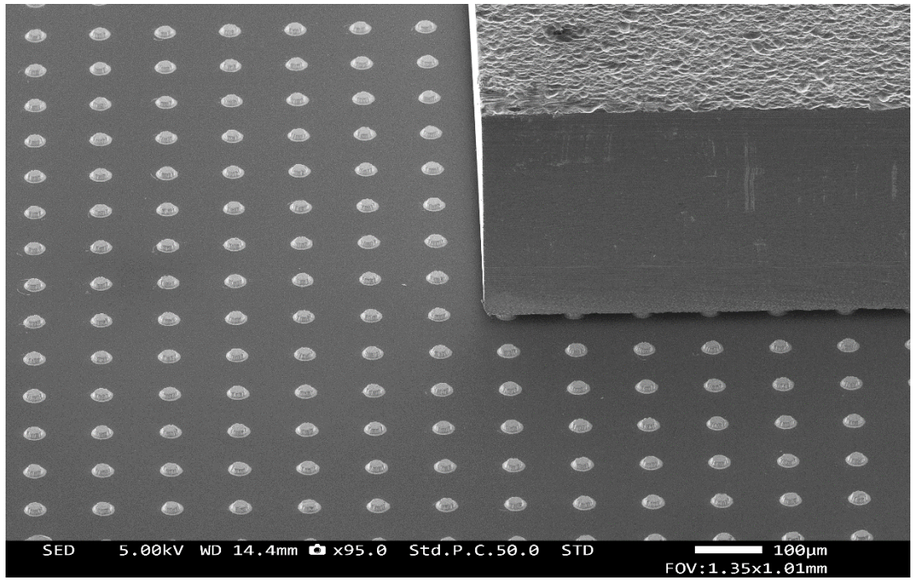


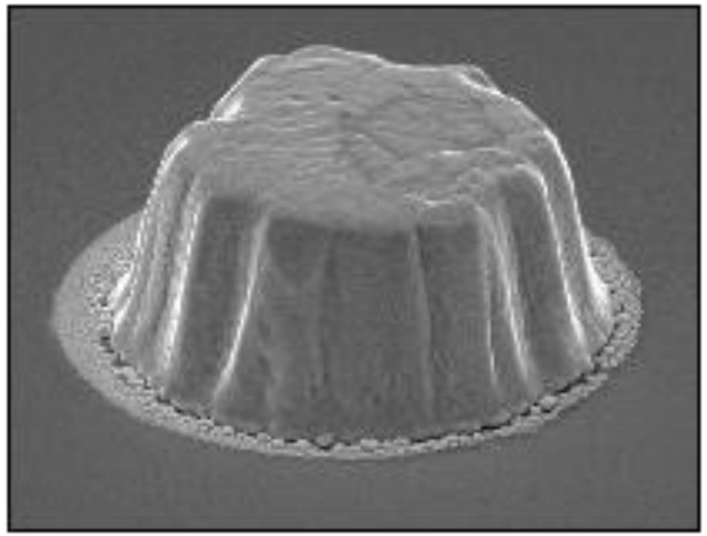

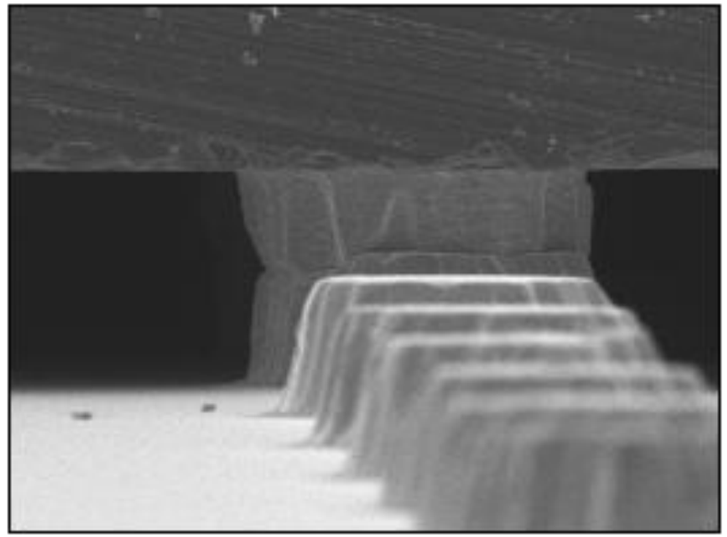

# Scaling: Through-Silicon-Via etching

RIE Bosch process:

- Cyclic etch process which enables etching of deep trenches in Si

1. SF6 gas to etch small amount of initial silicon
2. C4F8 gas to passivate surface (PTFE/Teflon)
3. Switch to SF6 (& Ar), the anisotropic physical component facilitates breaking of the polymer at the bottom
4. Cycle between SF6 and C4F8

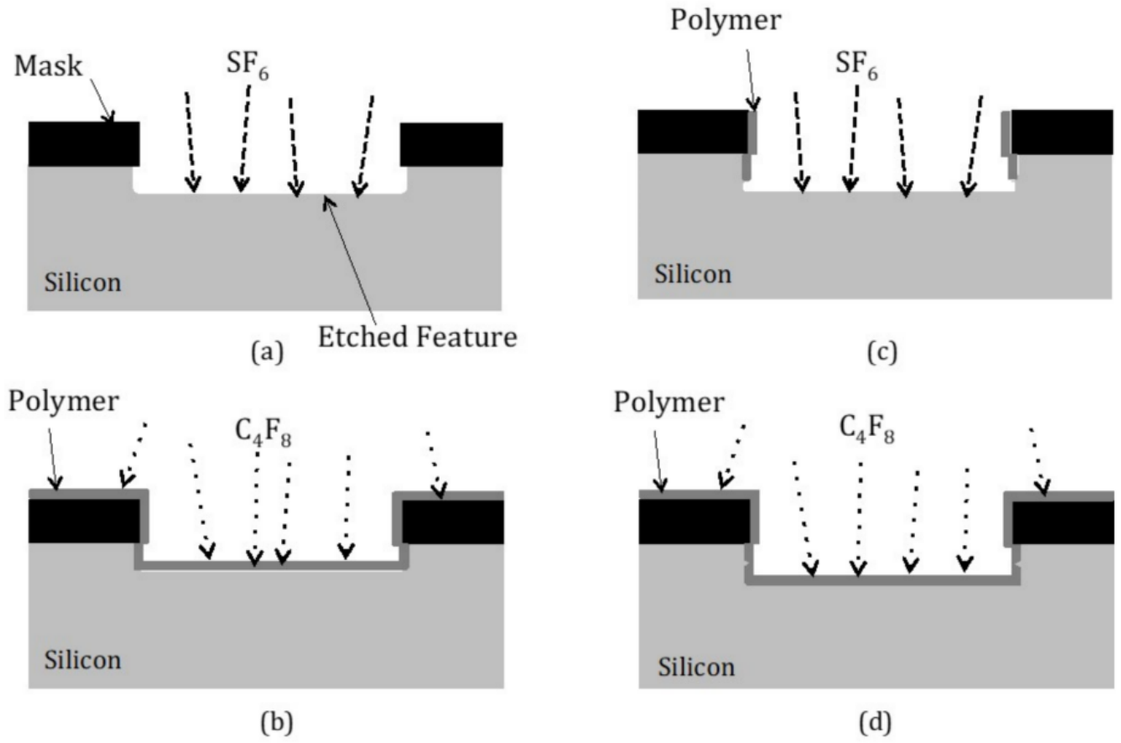


**Through-silicon-Via (TSV)**

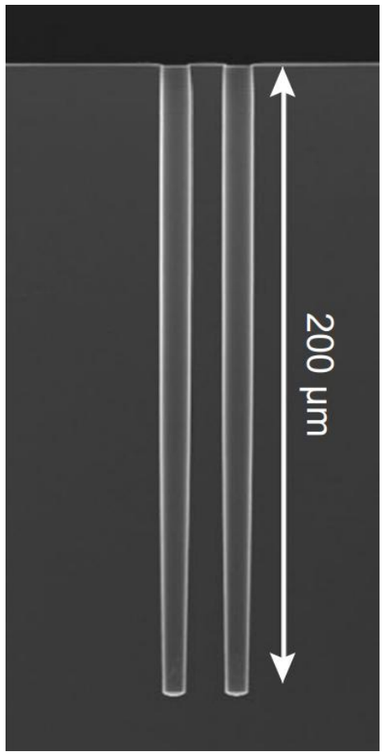

# Scaling: Atomic Layer Deposition

ALD process (Al2O3 as example):

- Pulse with precursor (TMAl) which forms a monolayer (ideally)
- Purge reactor chamber
- Pulse reactant (H2O)
- Purge reactor chamber
- One layer of Al2O3 has now been deposited, repeat cycle
- Advantages: High thickness control, conformal deposition
- For TSVs for qubits applications, materials such as TiN and NbN are of interest


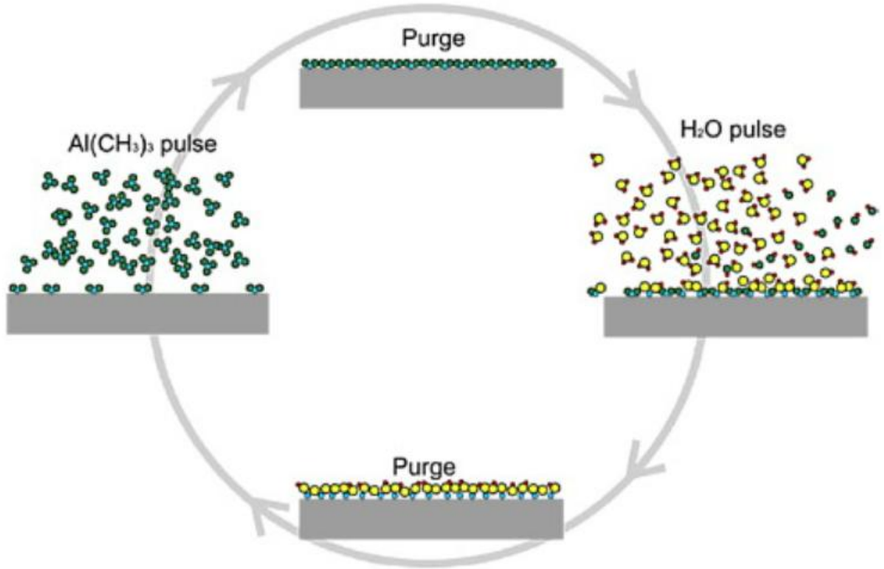


**Through-silicon-Via (TSV)**

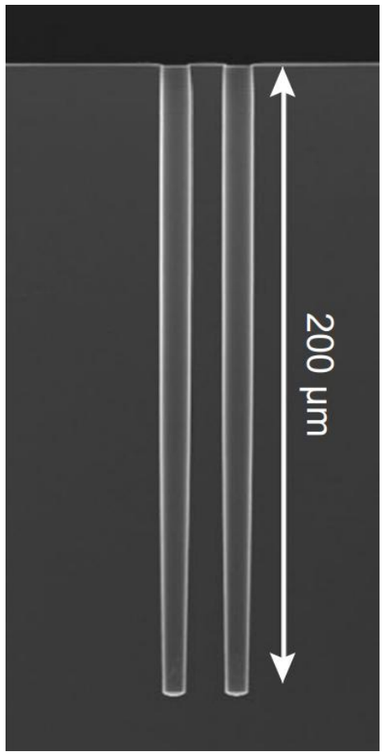

# Scaling: 3D integration and I/O

**Qubit chip**
- Qubit capacitor pads
- Josephson junctions

**Interposer/control chip**
- Resonators
- Flux lines
- Drive lines

**Multichip Module**
- Cryo CMOS
- SFQ
- TWPAs
- Packaging

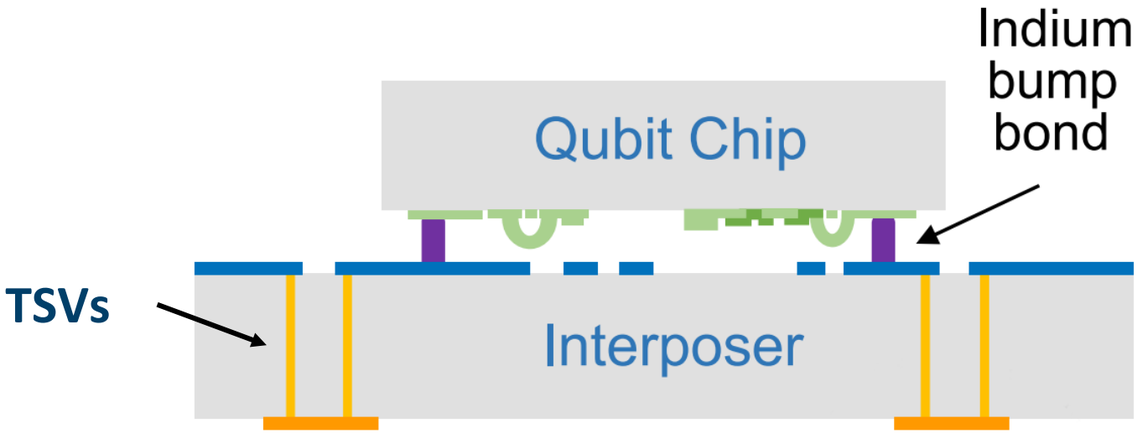


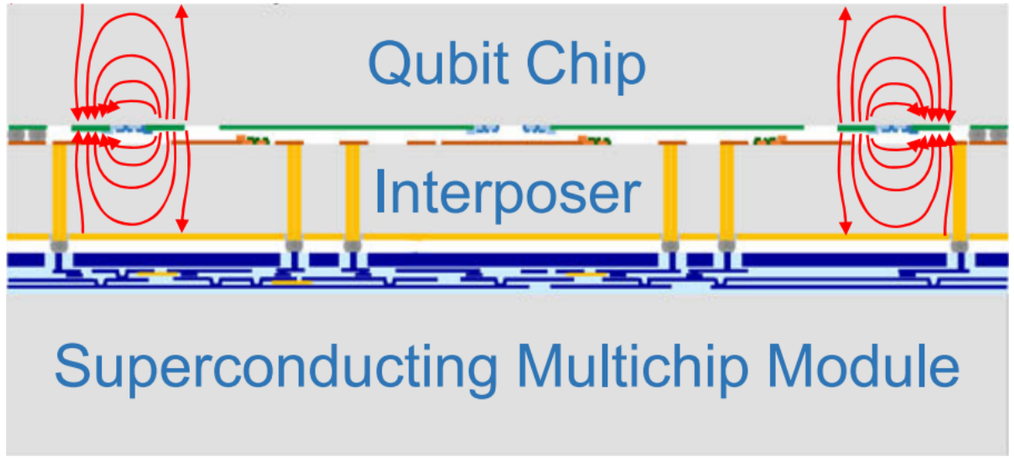

# Clean room impressions @WMI

Reactive Ion Etcher


Wet bench

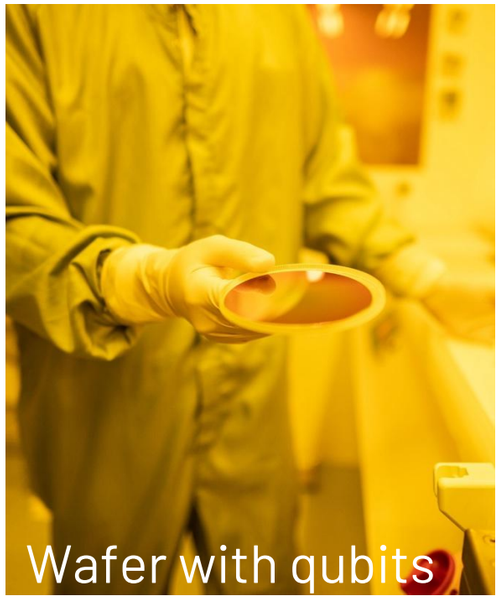
Wafer with qubits


Optical lithography

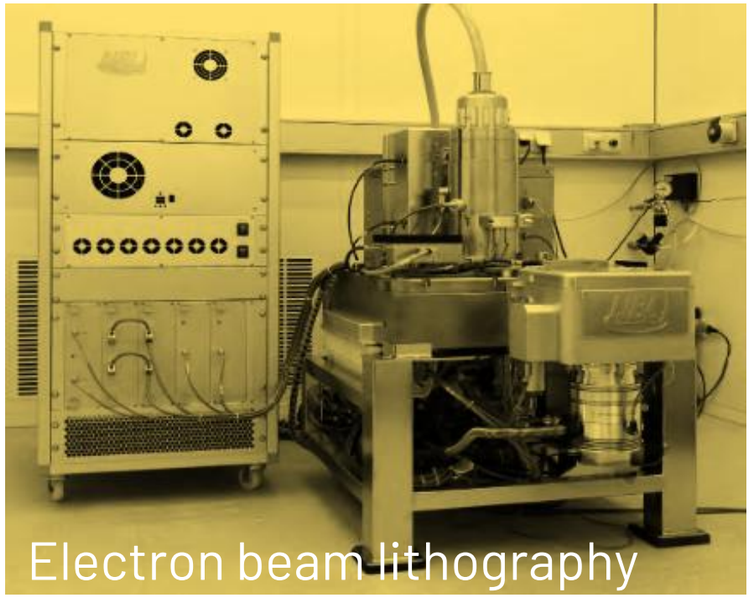
Electron beam lithography

Wafer saw/dicer

# Characterization tools


Optical microscope

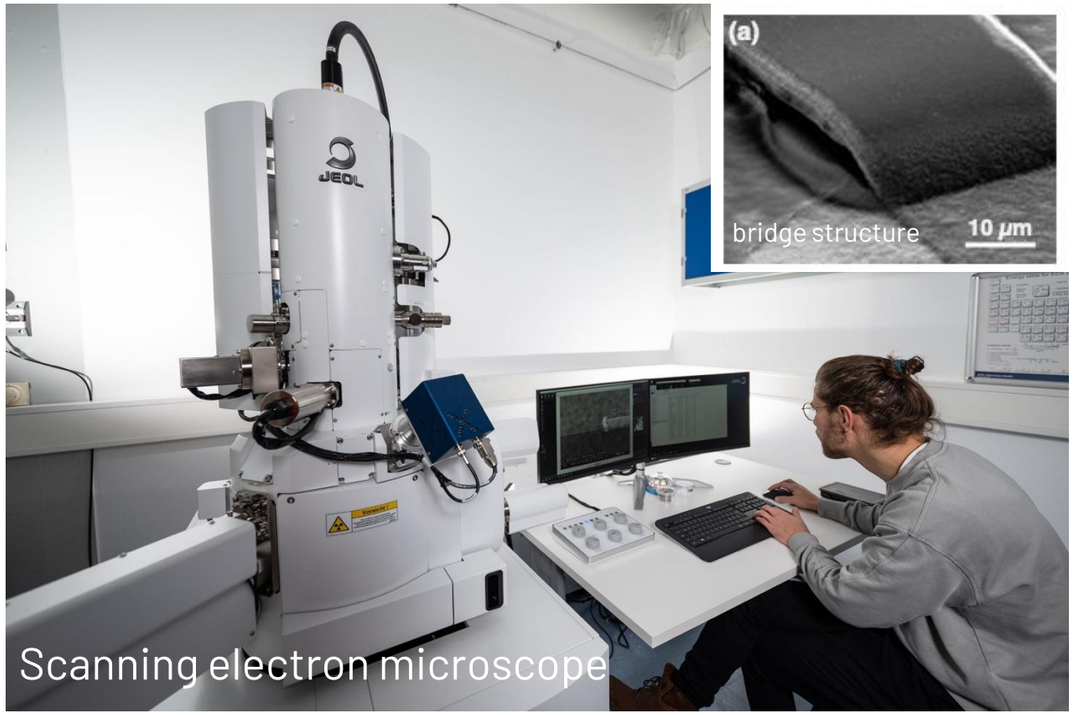



Scanning electron microscope

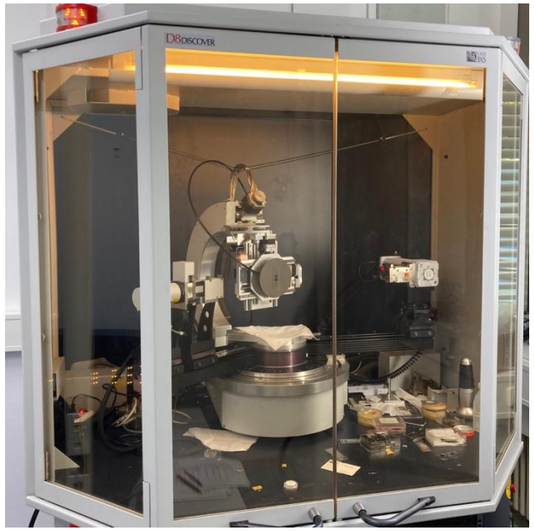

X-Ray diffractometer

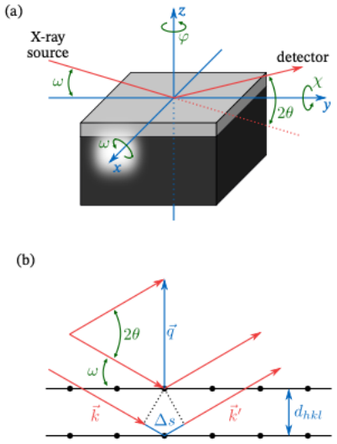



Atomic force microscope

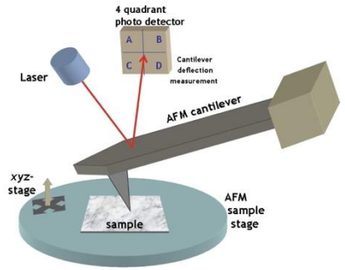


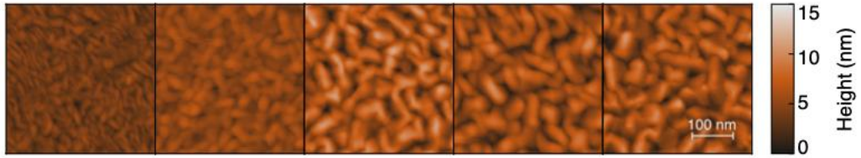

# Sample preparation / Packaging

Wire bonder:


Wafer dicer:


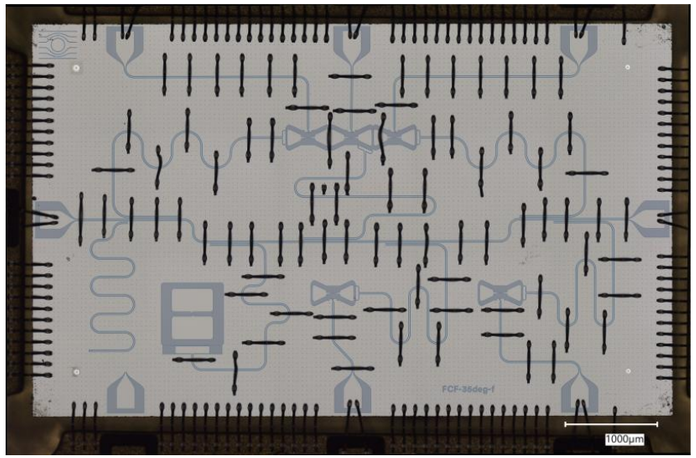


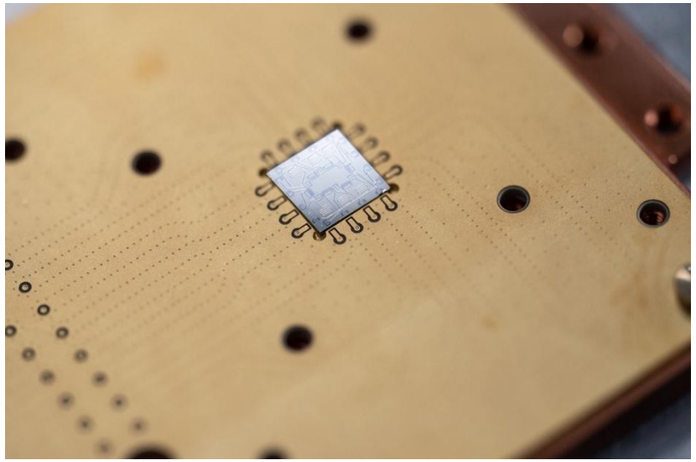

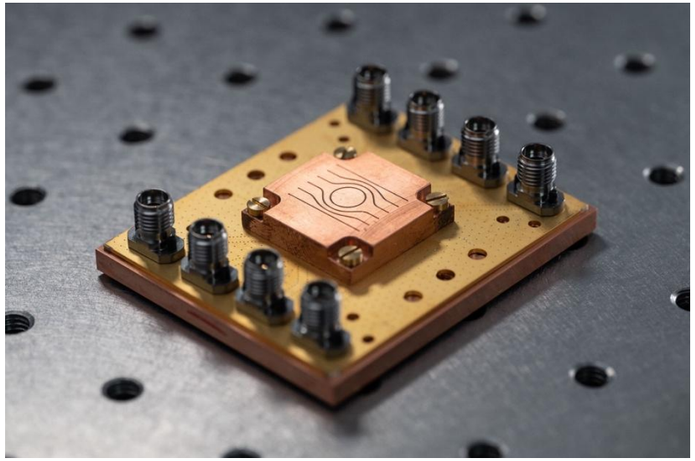

# Surface Losses & Decoherence

# Bloch sphere representation

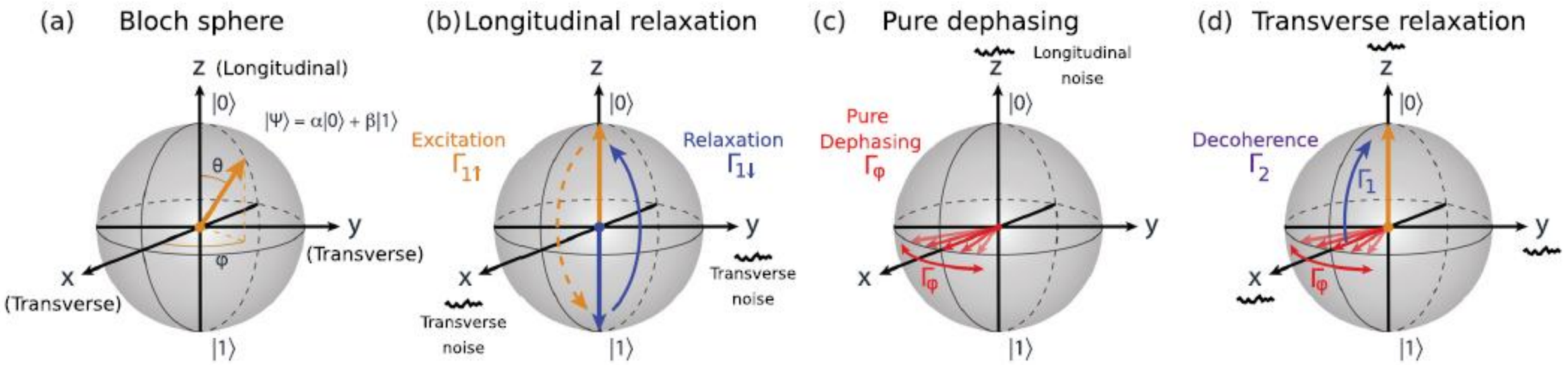


[Krantz *et al., Appl. Phys Rev* **6** (2019)]

Longitudinal relaxation rate: $\Gamma_1 \equiv \frac{1}{T_1}$

Pure dephasing rate: $\Gamma_\phi$

Transversal relaxation rate $\Gamma_2 \equiv \frac{1}{T_2} = \frac{\Gamma_1}{2} + \Gamma_\phi$

Bloch-Redfield dynamics:

Two-level system weakly coupled to noise sources with short correlation time

$$\rho_{BR} = \begin{pmatrix} 1 + (|\alpha|^2 - 1)e^{-\Gamma_1 t} & \alpha\beta^* e^{-\Gamma_2 t} \\ \alpha^*\beta e^{-\Gamma_2 t} & |\beta|^2 e^{-\Gamma_1 t} \end{pmatrix}$$

# Longitudinal relaxation

[Krantz *et al.*, *Appl. Phys Rev* **6** (2019)]

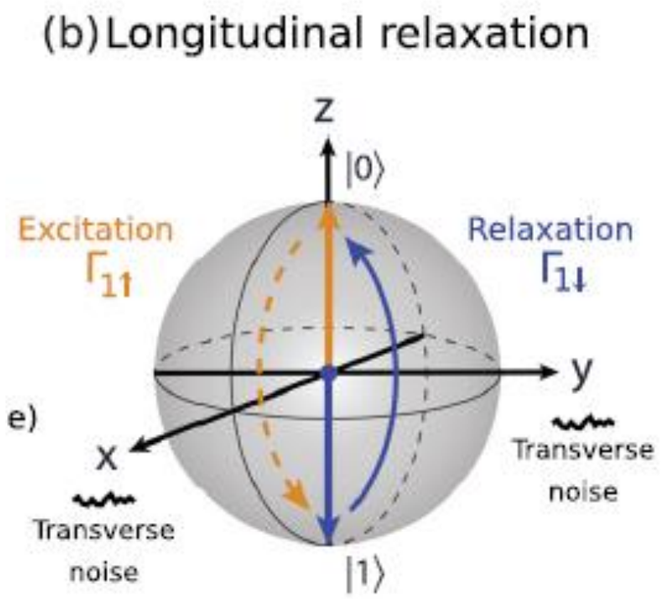


- Energy decay or energy relaxation into ground state $|0\rangle$ (or steady state if environment is at non-zero temperature)
- Caused by transverse noise along $x$ or $y$ axis: off-diagonal terms in interaction Hamiltonian (noise) drives transitions between $|0\rangle$ and $|1\rangle$
- Energy exchange with an environment with both "up transition rate" $\Gamma_{1\uparrow}$ and "down transition rate" $\Gamma_{1\downarrow}$ (correspond to induced emission and absorption process):

$$\Gamma_1 \equiv \frac{1}{T_1} = \Gamma_{1\uparrow} + \Gamma_{1\downarrow}$$

$$\rho_{BR} = \begin{pmatrix} 1 + (|a|^2 - 1)e^{-\Gamma_1 t} & \alpha\beta^* e^{-\Gamma_2 t} \\ \alpha^*\beta e^{-\Gamma_2 t} & |\beta|^2 e^{-\Gamma_1 t} \end{pmatrix}$$

$$\rightarrow \begin{pmatrix} 1 & 0 \\ 0 & 0 \end{pmatrix}$$

# Longitudinal relaxation

[Krantz *et al.*, *Appl. Phys Rev* **6** (2019)]

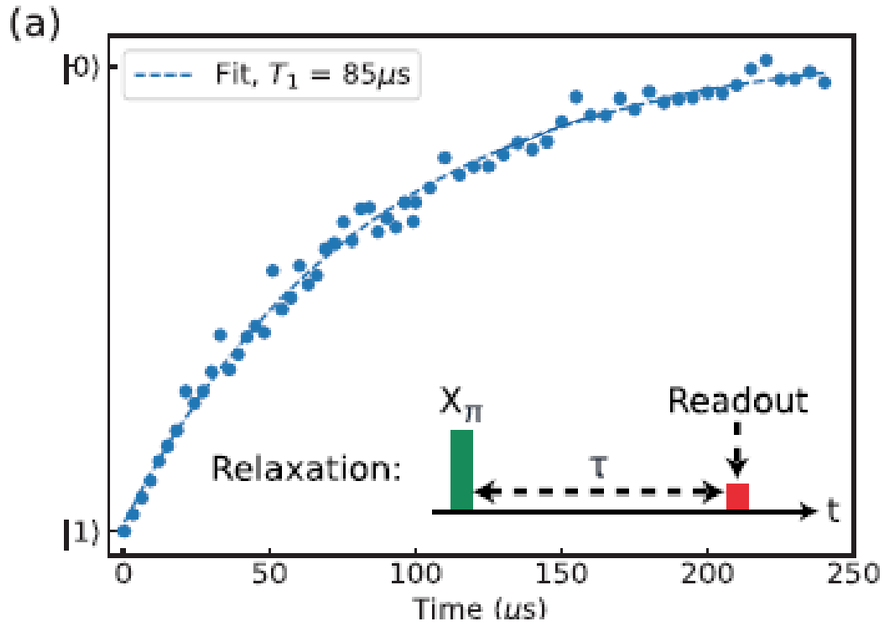


- Detailed balance: $\Gamma_{1\uparrow} = e^{-\hbar\omega_{01}/k_BT}\Gamma_{1\downarrow}$
- Equilibrium qubit polarization

$$p = \frac{n_0 - n_1}{n_0 + n_1} = \tanh\frac{\hbar\omega_{01}}{2k_BT}$$

(at 20mK: $\Gamma_{1\uparrow}$ exponentially suppressed)

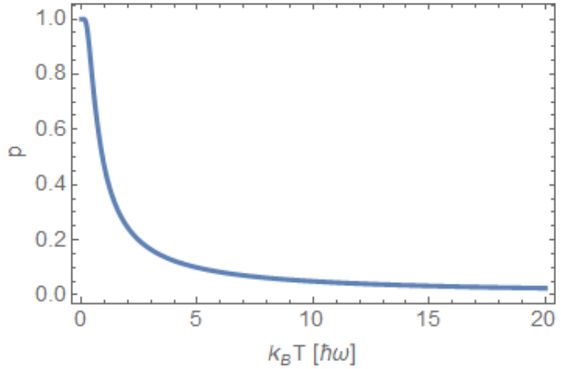


- Caused by noise **at the qubit frequency:**

$$\boldsymbol{\Gamma}_{\downarrow/\uparrow} = S_\omega(\pm\omega_{01})$$

$S_\omega$… noise power spectral density ('how much power at a specific frequency per Hz')

→ typically white noise with short correlation length

+ 1/f noise contribution at low frequencies

$$\rho_{BR} = \begin{pmatrix} 1 + (|a|^2 - 1)e^{-\Gamma_1 t} & \alpha\beta^* e^{-\Gamma_2 t} \\ \alpha^*\beta e^{-\Gamma_2 t} & |\beta|^2 e^{-\Gamma_1 t} \end{pmatrix}$$

$$\rightarrow \begin{pmatrix} 1 & 0 \\ 0 & 0 \end{pmatrix}$$

# Measurement of T1

[Krantz *et al.*, *Appl. Phys Rev* **6** (2019)]

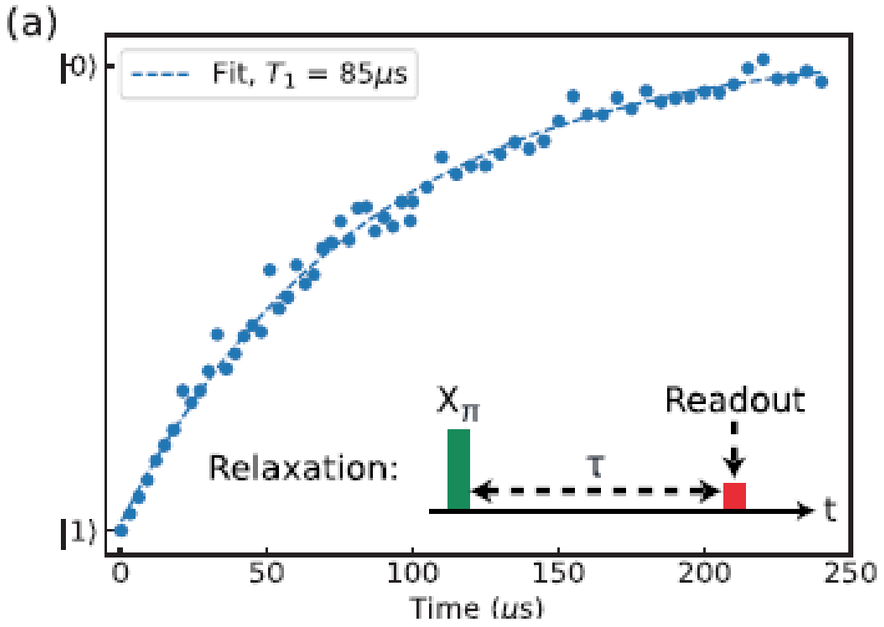


**Protocol:**

- Apply a $\pi$-pulse to populate the excited state.
- Wait for a varying time $\tau$.
- Readout the residual population in the excited state as a function of $\tau$.
- Repeat the experiment to improve the signal-to-noise (SNR) ratio.
- Fit to an exponential decay $f(\tau) = 1 - e^{-\Gamma_1 \tau}$.

# Noise power spectral density

In general: asymmetric power spectral density, quantum noise (see Clerk *et al.*, *Rev. Mod Phys* **82** (2010))

→ negative frequencies: qubit excitation $\Gamma_{1\uparrow}$ (≙ induced absorption)

→ positive frequencies: qubit relaxation $\Gamma_{1\downarrow}$ (≙ induced/spontaneous emission)

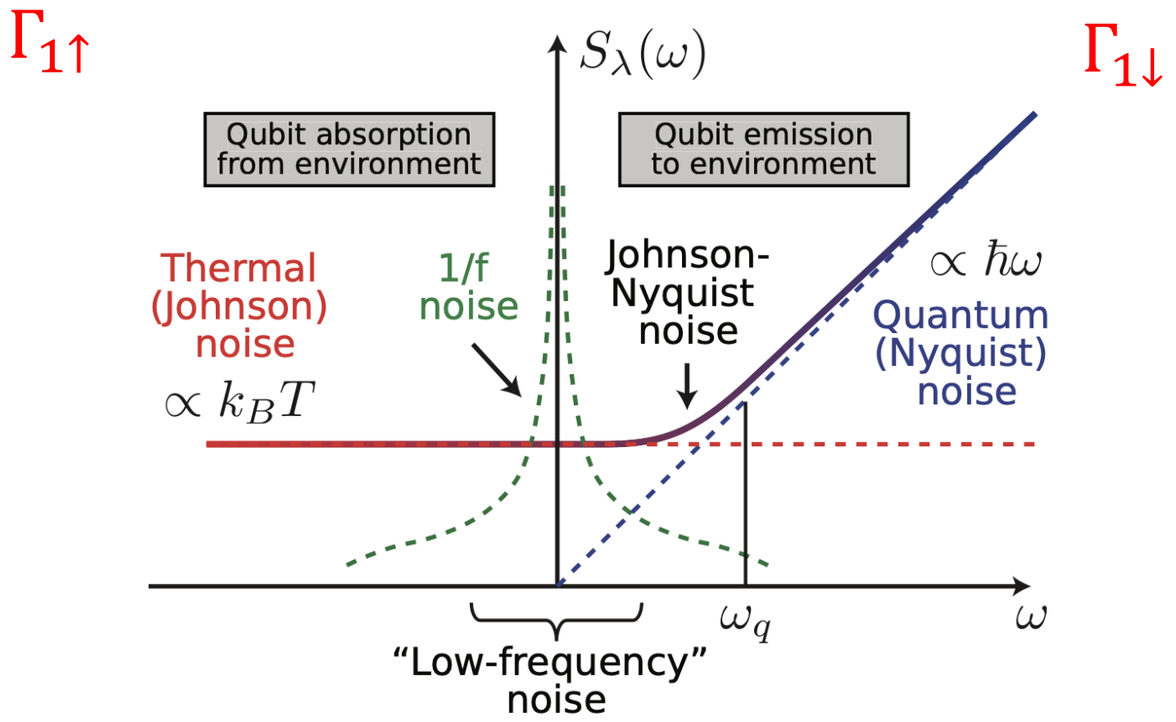


[Krantz *et al. Appl. Phys Rev* **6** (2019)]

# Pure dephasing

[Krantz *et al.*, *Appl. Phys Rev* **6** (2019)]

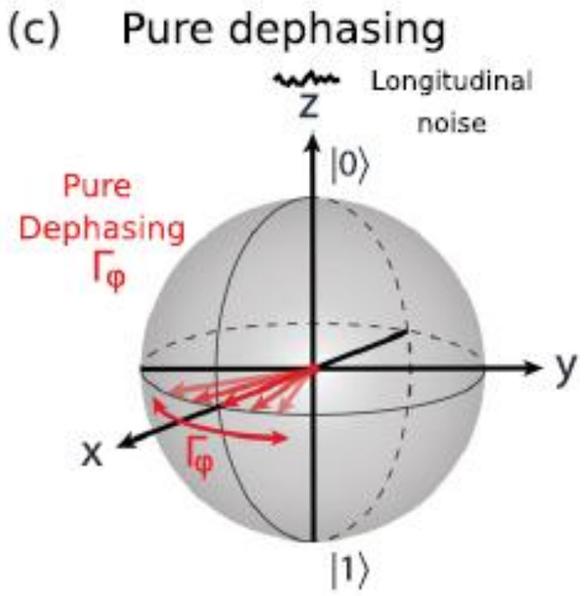


- $\Gamma_\phi = \frac{1}{T_\phi}$ caused by ‘longitudinal noise’ (along $z$ axis)
- Fluctuating qubit frequency
- Not a resonant phenomenon, noise at any frequency can contribute (broadband noise)
- No energy exchange with environment (in principle reversible, e.g., by dynamical decoupling)

$$\rho_{BR} = \begin{pmatrix} 1 + (|a|^2 - 1)e^{-\Gamma_1 t} & \alpha\beta^* e^{-\Gamma_2 t} \\ \alpha^*\beta e^{-\Gamma_2 t} & |\beta|^2 e^{-\Gamma_1 t} \end{pmatrix}$$

$$\rightarrow \begin{pmatrix} 1 + (|a|^2 - 1)e^{-\Gamma_1 t} & 0 \\ 0 & |\beta|^2 e^{-\Gamma_1 t} \end{pmatrix}$$

# Transverse relaxation

[Krantz *et al.*, *Appl. Phys Rev* **6** (2019)]

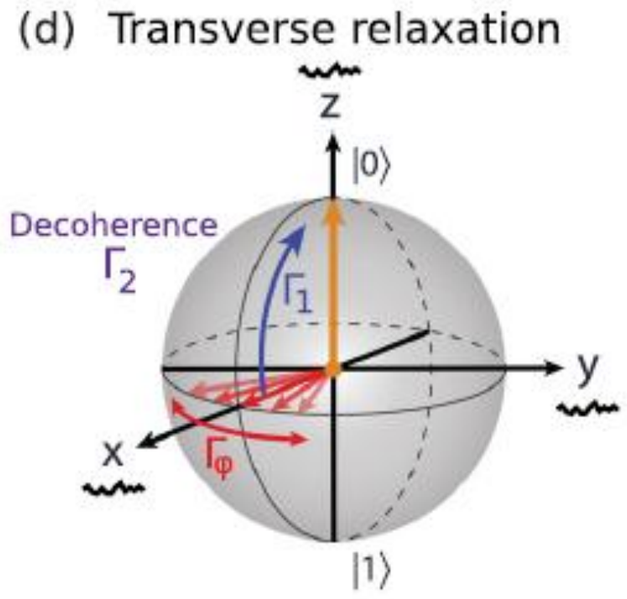


$$\rho_{BR} = \begin{pmatrix} 1 + (|a|^2 - 1)e^{-\Gamma_1 t} & \alpha\beta^* e^{-\Gamma_2 t} \\ \alpha^*\beta e^{-\Gamma_2 t} & |\beta|^2 e^{-\Gamma_1 t} \end{pmatrix}$$

$$\rightarrow \begin{pmatrix} 1 + (|a|^2 - 1)e^{-\Gamma_1 t} & 0 \\ 0 & |\beta|^2 e^{-\Gamma_1 t} \end{pmatrix}$$

- Describes loss of coherence, off-diagonal terms of $\rho$ vanish
- Caused in part by longitudinal pure dephasing, and by transverse noise causing energy relaxation (because with relaxation to ground state comes loss of phase information)
- $\Gamma_2 = \frac{\Gamma_1}{2} + \Gamma_\phi$ (or $\frac{1}{T_2} = \frac{1}{2T_1} + \frac{1}{T_\phi}$)
- $T_2^*$ measured by Ramsey experiment ('$*$' → inhomogeneous broadening plays a role, i.e., quasistatic low-frequency fluctuations)

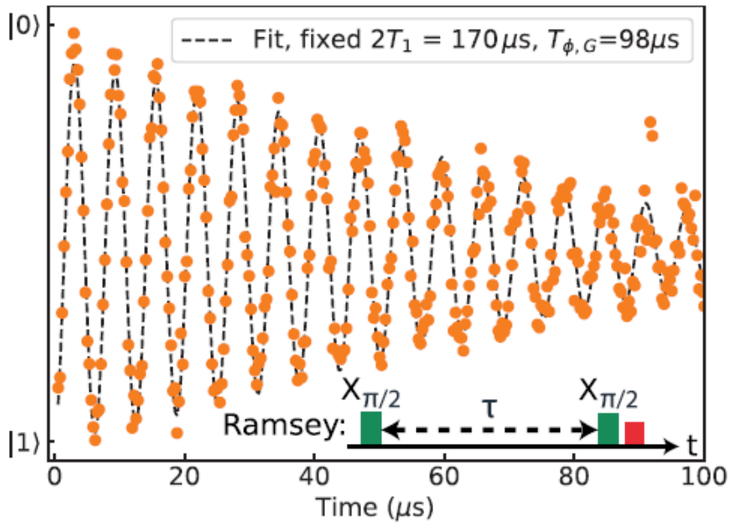

# Ramsey-type measurement

[Krantz *et al.*, *Appl. Phys Rev* **6** (2019)]

**Protocol:**

- Apply a $\frac{\pi}{2}$-pulse about axis in equatorial plane (defines x-axis)
- Wait for a duration $\tau$ (=precession time) (apply identity gate $Id(t)$)
- Apply a second $\frac{\pi}{2}$-pulse
- Measure the population of the excited state.
- Repeat the experiment to improve SNR.
- Fit the decay curve to an appropriate fit function, e.g., exponential. (Warning: Here it becomes tricky because of the frequency spectrum of the noise.)

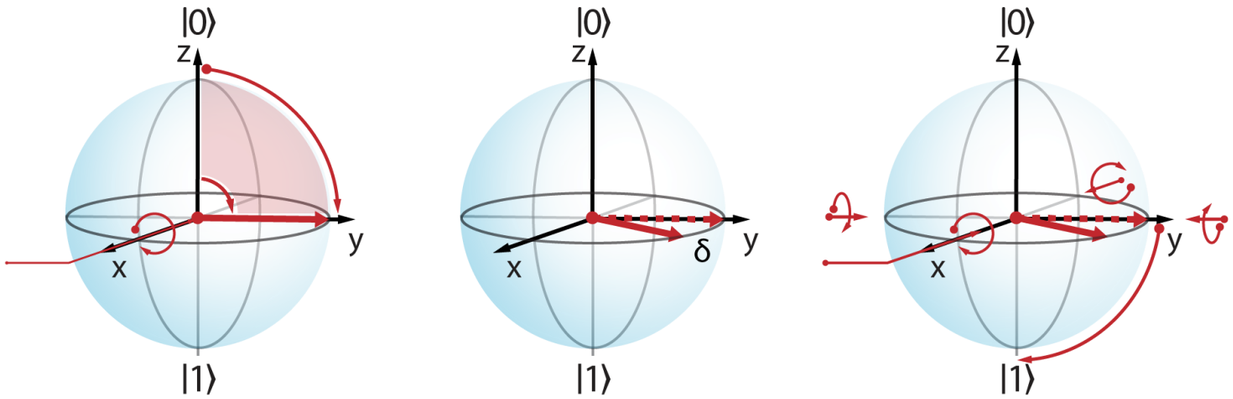


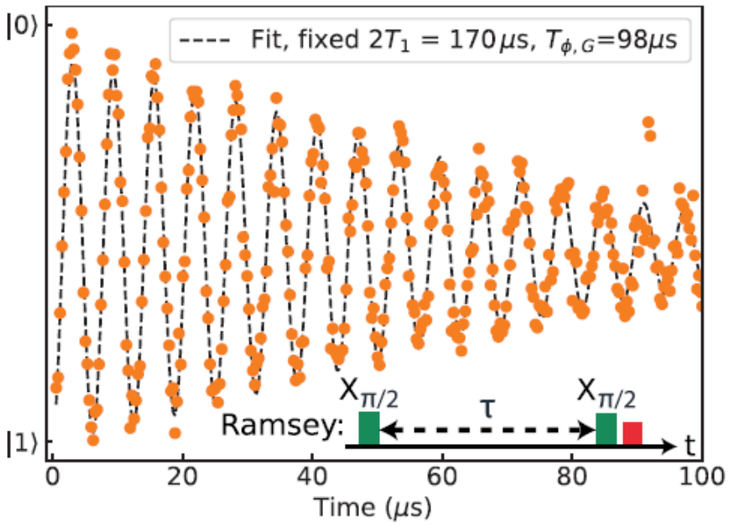

# Ramsey Experiment: Non-exponential decay

[Krantz *et al.*, *Appl. Phys Rev* **6** (2019)]

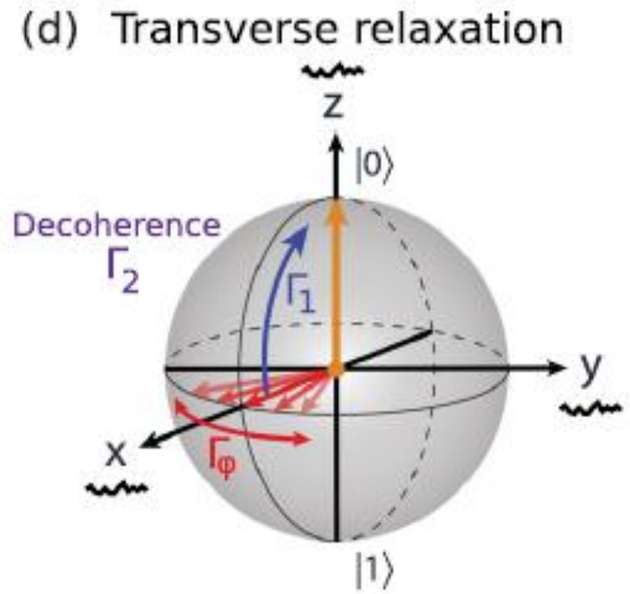


- Ramsey experiment may exhibit non-exponential decay
- Signature of slow 1/f noise, or inhomogeneous broadening (of ensembles) (i.e., either temporal or spatial fluctuations)
- Flux-noise, charge-noise, etc. exhibits typically 1/f-like power spectrum (long-correlation time)
- → Simple exponential decay no longer valid

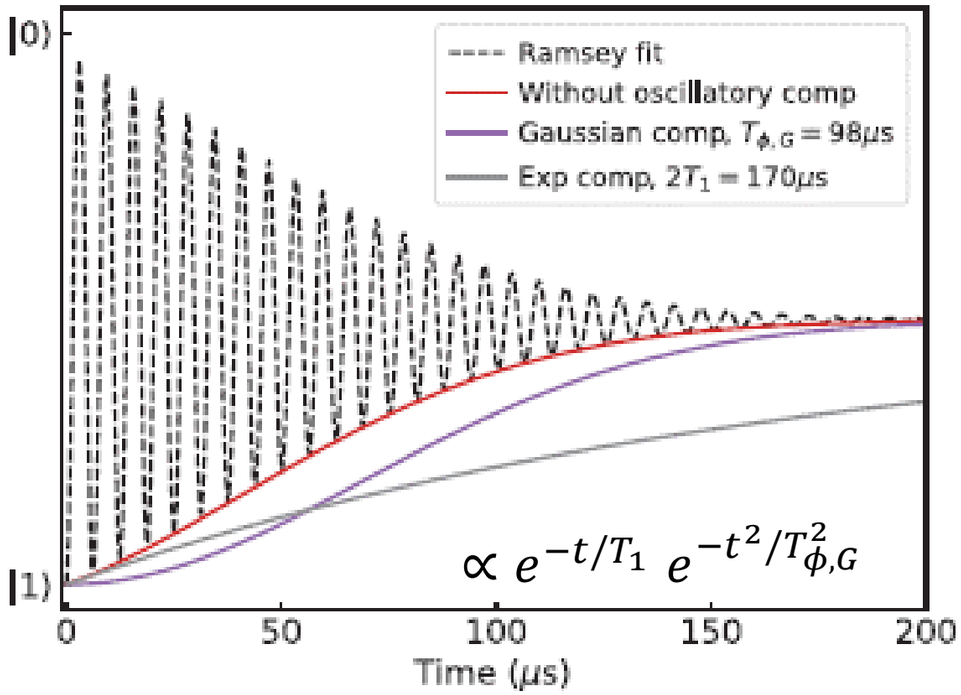

# Hahn echo (Refocusing/Spin echo)

Refocusing scheme: add a $\pi$-pulse in the Ramsey sequence

→ undoes phase accumulation → eliminates slow noise

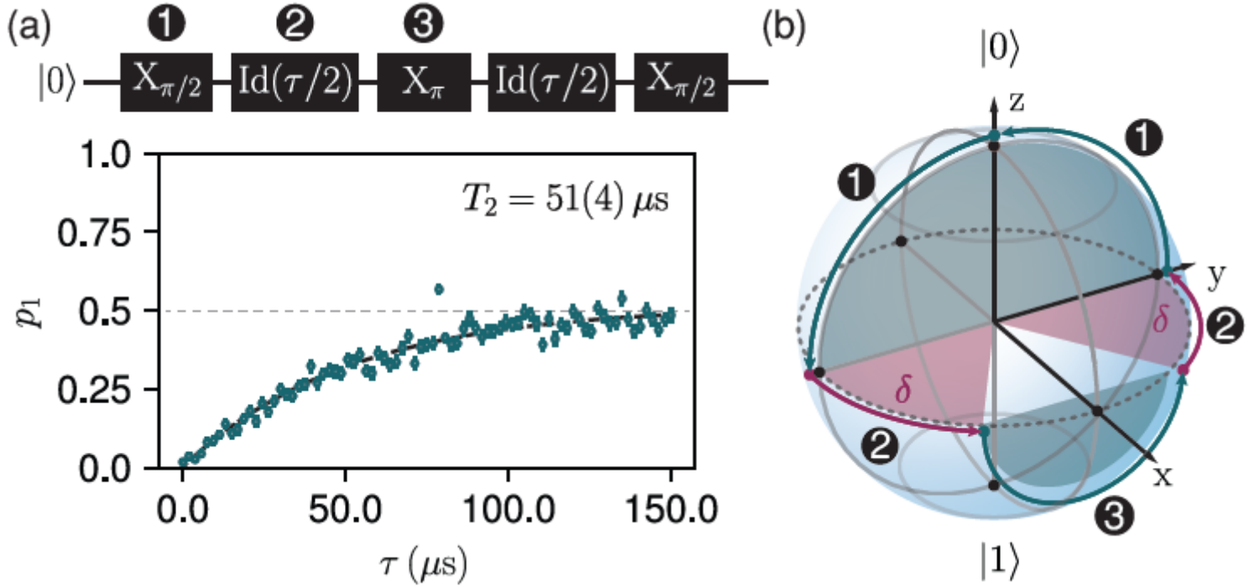





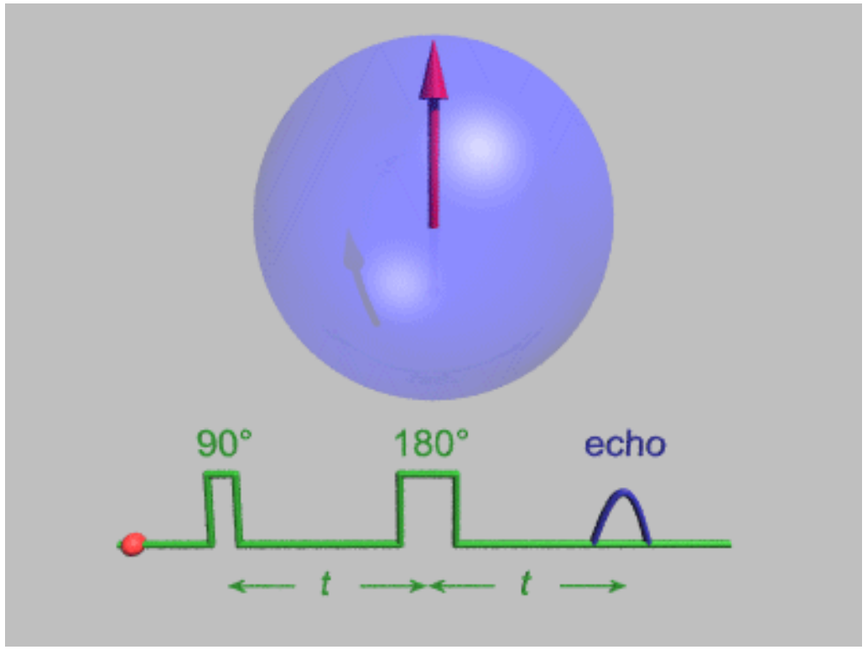


© Wikipedia https://de.wikipedia.org/wiki/Spin-Echo

# Decoherence mechanisms

Which decoherence/dissipation mechanisms are present in a superconducting qubit?

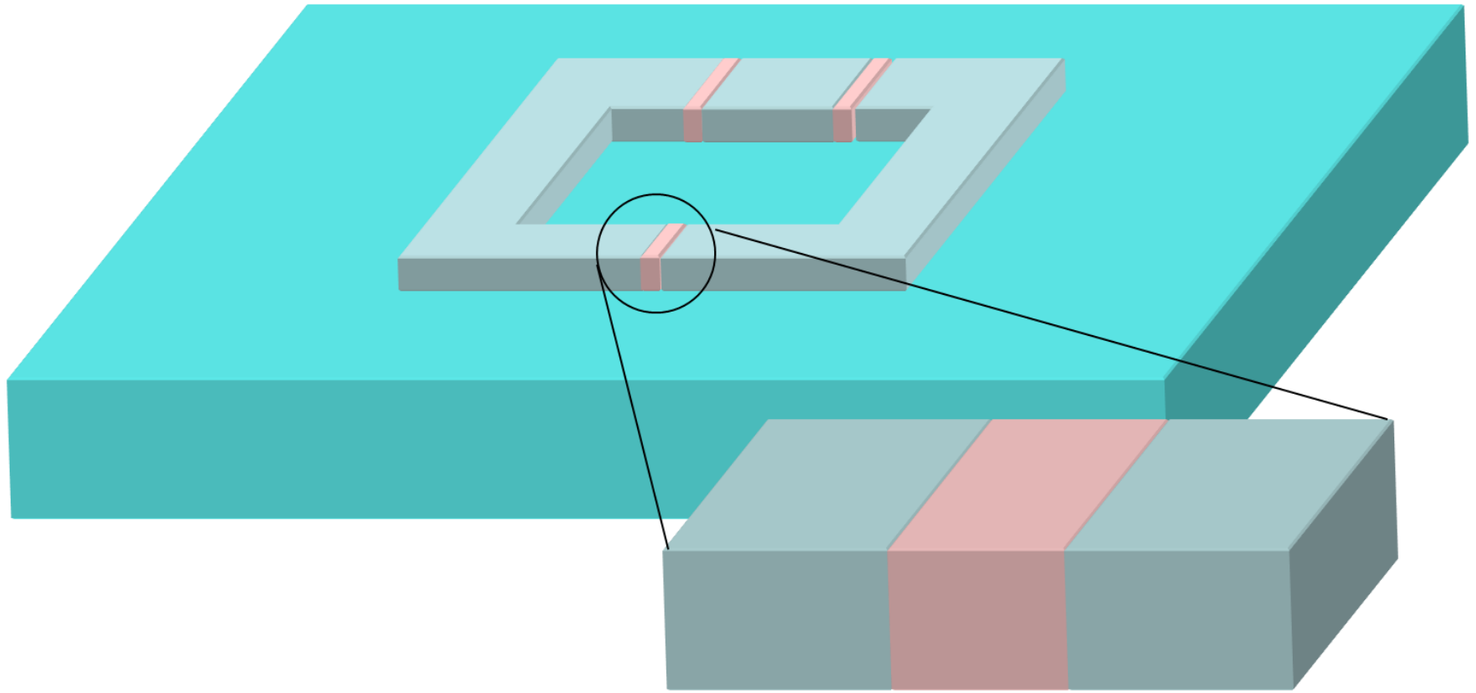

# Decoherence and dissipation

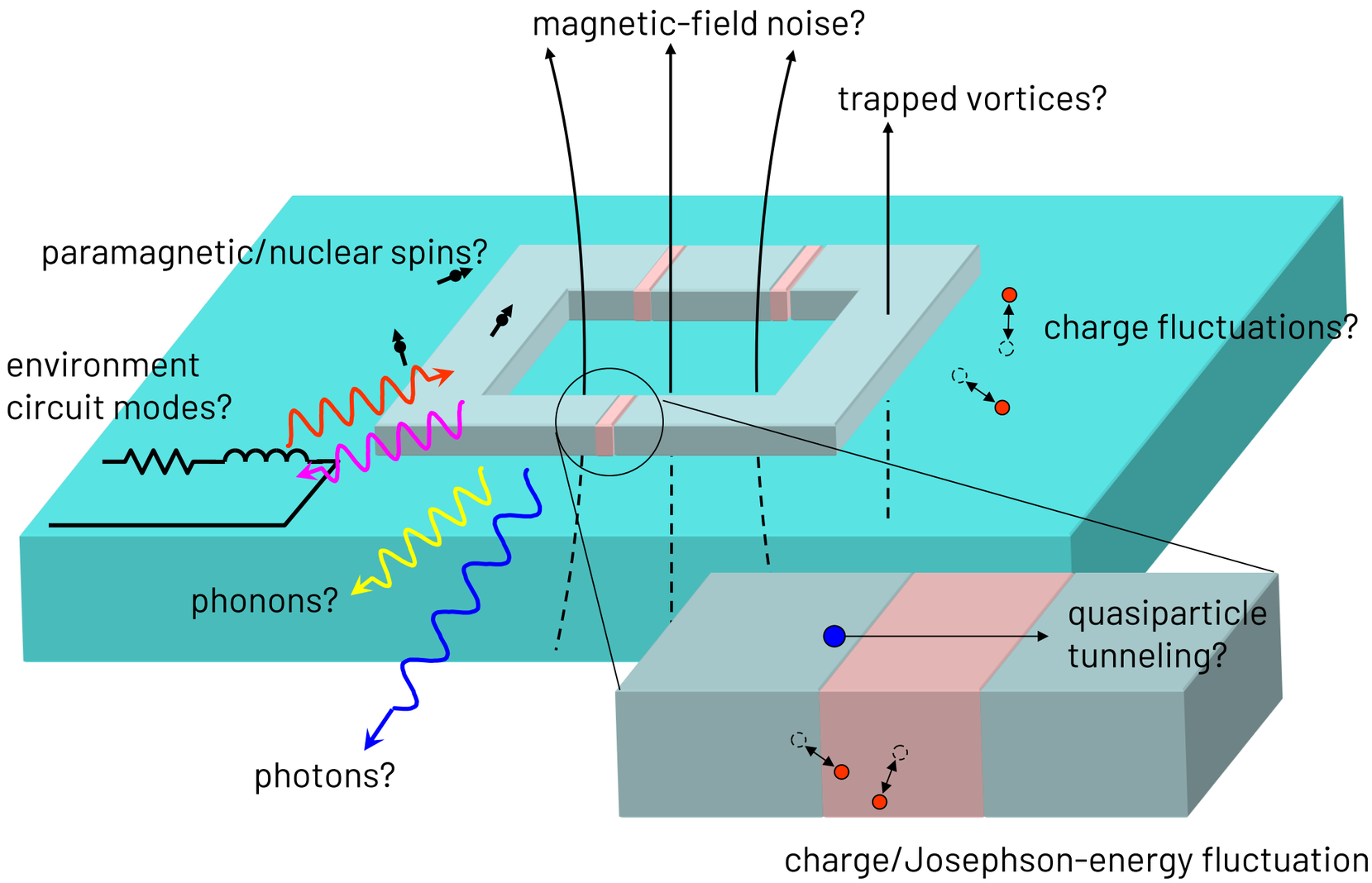


[G. Ithier *et al.*, *Phys. Rev. B* **72**, 134519 (2005)]

# Origin of noise and decoherence

Noise in Hamiltonian parameters leads to decoherence

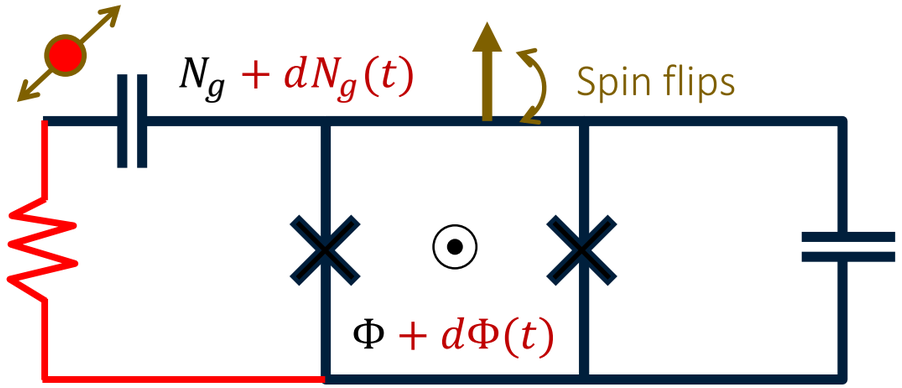


Origin of (stochastic) noise:

[c.f. J. Koch *et al.*, *PRA* (2007)]

1) Electromagnetic (both $T_1$ & $T_2$):
- Johnson-Nyquist due to thermal noise
- Spontaneous emission (quantum noise)

→ described by coupling to E.M. environment (electrical circuit)

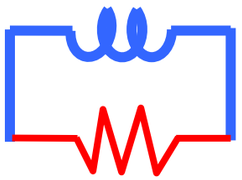

2a) Microscopic (low frequency): responsible for $T_2$
- Charge noise → limitations on $T_2$
- Flux noise → limitations on $T_2$

2b) Microscopic (high frequency): responsible for $T_1$
- Imperfect dielectrics, microwave losses
- Magnetic vortices trapped in the superconducting thin films
- Unpaired electrons (quasiparticles) in the superconductor

Noise mitigation strategy:

1. Avoid noise
2. Lower qubit susceptibility to noise (in qubit design, or by reducing coupling)
3. Use control pulses that are less sensitive to noise

# Sensitivity to (charge/flux) noise

Solutions:

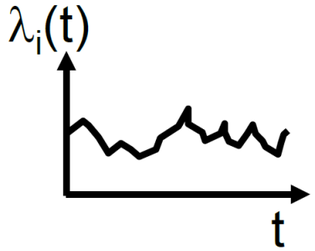


1. Find a point in parameter space with reduced sensitivity to noise:
   → charge (& flux) sweet spot for CPB (only 2nd order sensitive to fluctuations)

Optimal charge bias point at $n_g = \frac{1}{2}$

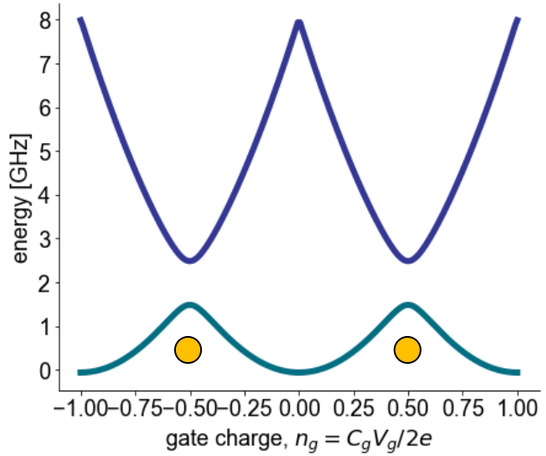


Optimal flux bias point at $\frac{\phi}{\phi_0} = 0$

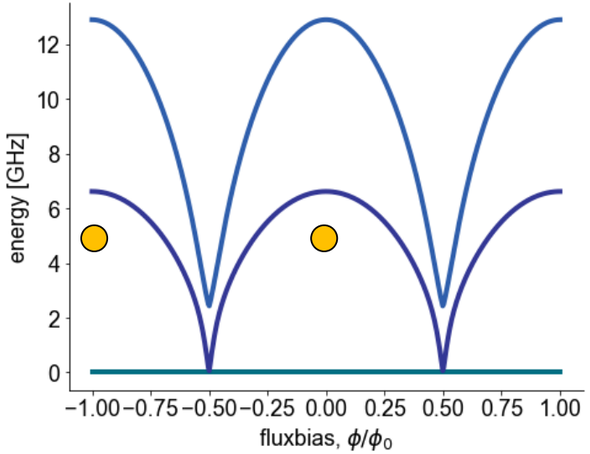


2. Design qubits to lower sensitivity to noise
   → Transmon qubit with large $E_J/E_C$ (optimized CPB)
   → Fluxonium,...
3. Identify noise sources and avoid them (more difficult)
4. Use pulse shapes that are insensitive to errors

# Physics approach: Dissipation and dephasing

## Relaxation / Dissipation:

$$\hat{H}_q = -\frac{1}{2}\,\vec{\hat{\sigma}} \cdot \left( \vec{H}_0(\lambda_0) + \frac{\partial \vec{H}_0}{\partial \lambda}\delta\lambda + \cdots \right)$$

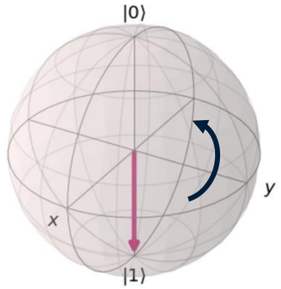



system bath

$D_{\lambda,\perp} = \frac{1}{\hbar}\langle 0|\frac{\partial H}{\partial \lambda}|1\rangle$... transition matrix element

$$T_1^{-1} = \Gamma_1 = \frac{\pi}{2} D_{\lambda,\perp}^2 S_\lambda(\omega_{01})$$ → Fermi's Golden Rule

environmental (bath) density of modes at qubit frequency

## Pure dephasing:

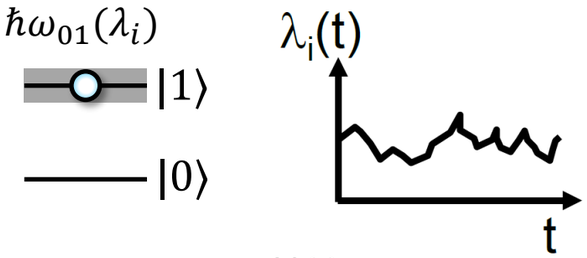


$\alpha|0\rangle + \beta e^{i\phi(t)}|1\rangle$

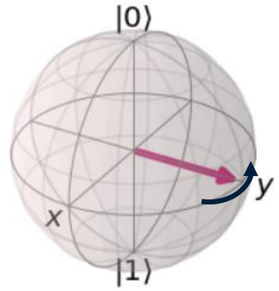


$f(\phi) \equiv \langle e^{i\phi(t)} \rangle \approx e^{-\Gamma_2 t}$... decay function

$$T_2^{-1} = \Gamma_2 = \frac{\Gamma_1}{2} + \Gamma_\phi$$

$$\Gamma_\phi = \pi\, D_{\lambda,\parallel}^2 S_\lambda(0)$$

$$D_{\lambda,\parallel}^2 = \frac{\partial \omega_{01}}{\partial \lambda}$$ Low frequency noise

[G. Ithier *et al.*, *Phys. Rev. B* **72**, 134519 (2005)]

# Noise coupling parameters

[Girvin, Les Houches Lecture Notes; Ithier *PRB* **72** (2005)]

General description of noise coupling to a quantum system $(\eta_j = \delta\lambda_j)$:

$$H(\vec{\lambda}) = H(\bar{\lambda}) + \sum_{j=1}^{n} \frac{\partial H}{\partial \lambda_j}\Big|_{\bar{\lambda}} \eta_j + \frac{1}{2}\sum_{j,k=1}^{n} \frac{\partial^2 H}{\partial \lambda_j \partial \lambda_k}\Big|_{\bar{\lambda}} \eta_j \eta_k + \cdots$$

Single qubit case

(simplest situation; with higher levels and coupling to other modes/qubits it can become complex):

$$H(\vec{\lambda}) = \frac{1}{2}\begin{pmatrix} \lambda_x \\ \lambda_y \\ \omega_{01} + \lambda_z \end{pmatrix} \cdot \begin{pmatrix} \sigma_x \\ \sigma_y \\ \sigma_z \end{pmatrix} = \frac{1}{2}\Big(\underbrace{\omega_{01}\sigma_z}_{H(\bar{\lambda})} + \eta_x\sigma_x + \eta_y\sigma_y + \eta_z\sigma_z\Big)$$

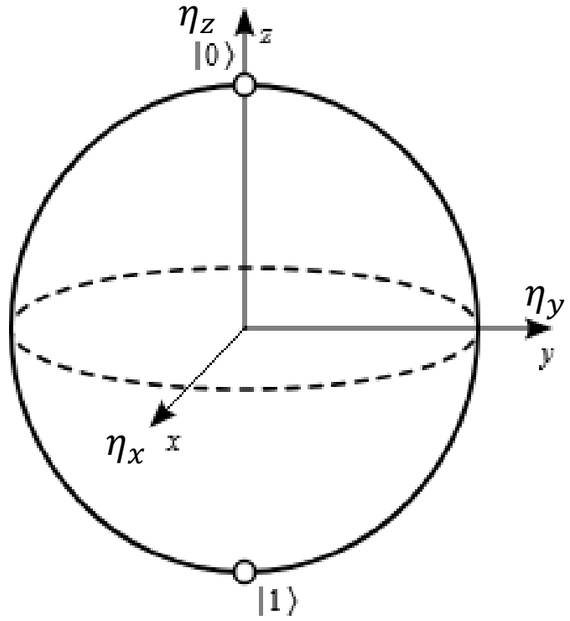


with $\frac{\partial H(\vec{\lambda})}{\partial \lambda_x}|_{\bar{\lambda}_x} \delta\lambda_x = \eta_x\sigma_x$, $\eta_y\sigma_y = \cdots$ and $\bar{\lambda}_{x,y,z} = 0$

$T_1$- Relaxation: Interaction Hamiltonian $\hat{H}_{int} = \frac{\partial H(\vec{\lambda})}{\partial \lambda_x}|_{\bar{\lambda}_x} \delta\lambda_x = \sigma_x\, \eta_x$

relation to $S(\omega)$: via Fermi golden rule $\Gamma_1 \propto \underbrace{\frac{1}{\hbar^2}|\langle 0|\sigma_x|1\rangle|^2}_{(D_{\lambda,\perp})^2} S_\lambda(\omega_{01})$

→ noise power spectral density at qubit frequency is relevant!

# Fermi's Golden Rule

Which part of the decay rate $\Gamma_1 \propto |\langle \Psi_0 | H_c | \Psi_1 \rangle|^2 \; S(\omega_{01})$ can mainly be influenced by fabrication processes?

a) The transition matrix element $|\langle \Psi_0 | H_c | \Psi_1 \rangle|^2$

b) The density of states of the environment $\rho_{env}(\omega_{01})$

c) Both.

# Relaxation

- Fermi's golden rule describes the decay rate from an excited state $\Psi_1$ to ground state $\Psi_0$

$$\Gamma_1 \propto |\langle \Psi_0 | H_c | \Psi_1 \rangle|^2 \, S_{env}(\omega_{01})$$

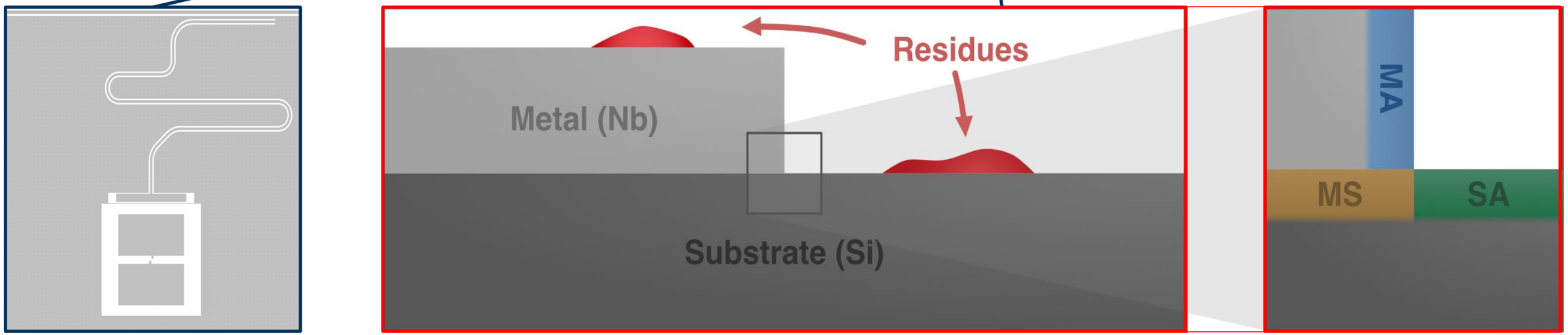


- Transition matrix element from perturbation (environment, TLSs, flux noise,...), can be modified in design
- density of states of the environment (TLSs,...) at transition frequency; one of the main challenges in fabrication

# Contributions to surface losses

Goal: minimize surface losses from dielectric TLS by proper design

Task: Calculate the influence of losses in interface layers, minimize effect on quality factor

$$Q = \frac{\omega}{\Gamma} = \omega T_1$$

$$Q = \left(\frac{1}{Q_{ext}} + \frac{1}{Q_{qp}} + \frac{1}{Q_{bulk}} + \frac{1}{Q_{surface}} + \frac{1}{Q_{etc}} + \cdots\right)^{-1} = \left(\frac{1}{Q_{ext}} + \frac{1}{Q_{int}}\right)^{-1}$$

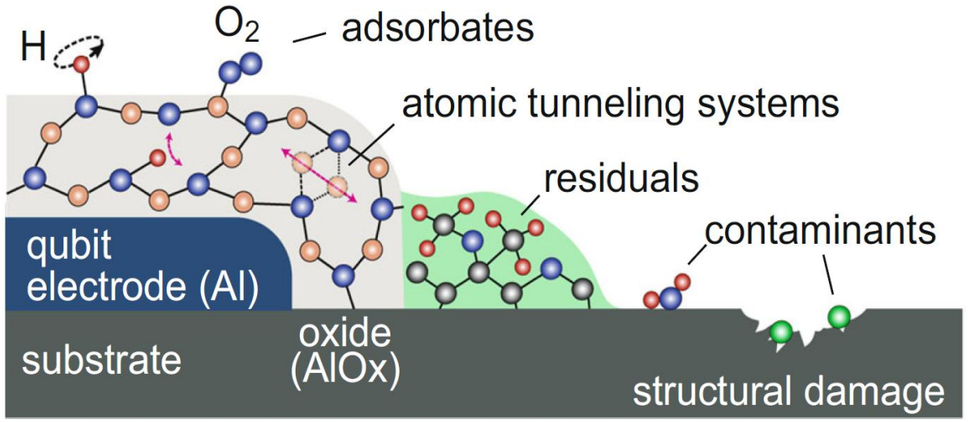


J. Lisenfield *et al., npj Quantum Inf* **5**, 105 (2019)

Quality factor $Q_{surface}$: qualitatively described by loss tangent

$$\tan\delta = \frac{1}{Q_{surface}}$$

Contribution of different interfaces:

$$\tan\delta = \sum_i p_i \tan(\delta_i)$$

$\tan(\delta_i)$... loss tangent of material $i$; $p_i$ ...participation ratio

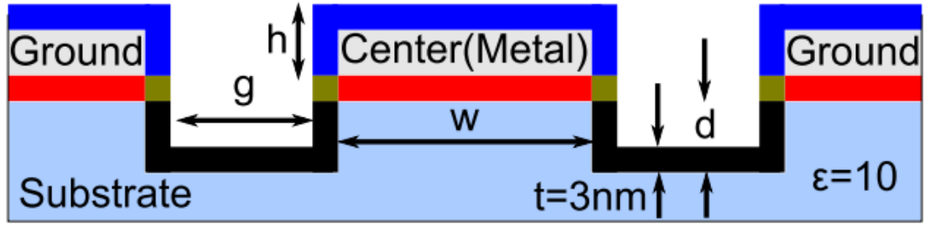


[Martinis, 1107.4698]

Three main categories: **Substrate-Air**, **Metal-Air** and **Metal-Substrate** interfaces (**SA, MA, MS**)

Interface layer t: few nanometers thick
[P. Altoé *et al.*, *PRX Quantum* **3** (2022)]

# Participation ratios - Example

Which geometry has a higher metal-substrate participation ratio (MS)?

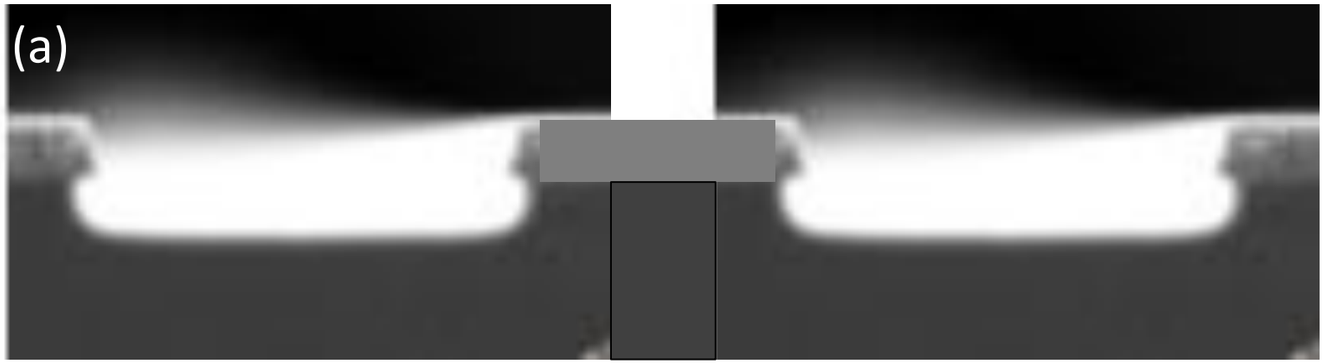


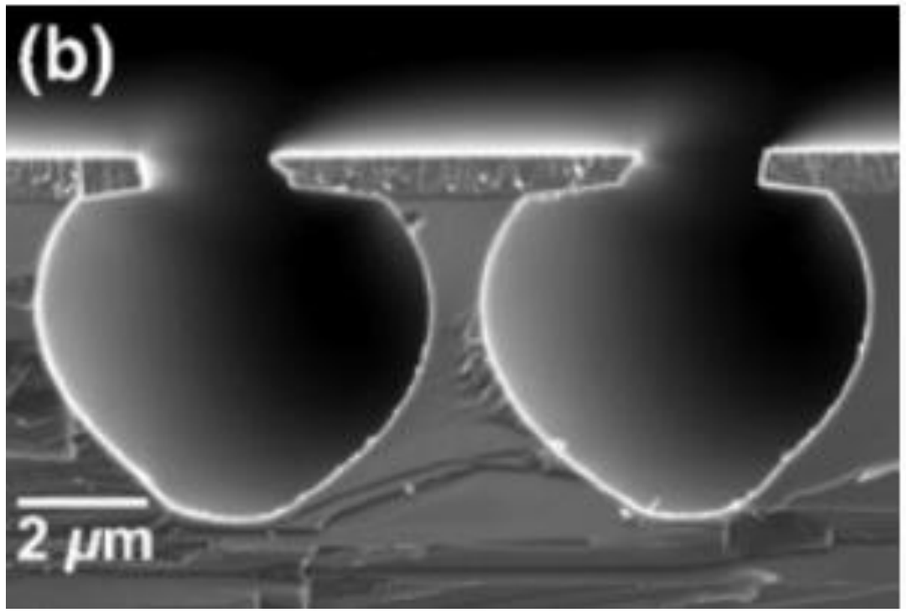

# Participation ratios - Example

Example from MIT – Lincoln Labs [Woods *et al.*, *Phys Rev Applied* **12** (2019)]

TiN Resonator on Si substrate

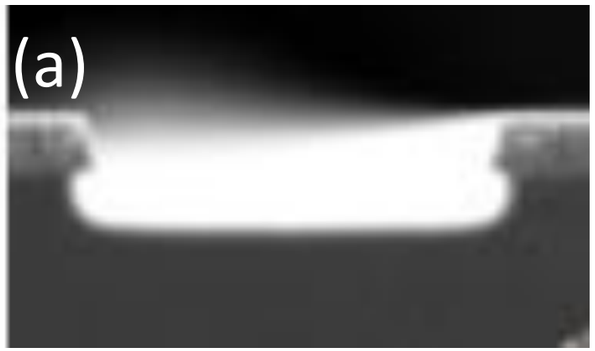


MS-heavy

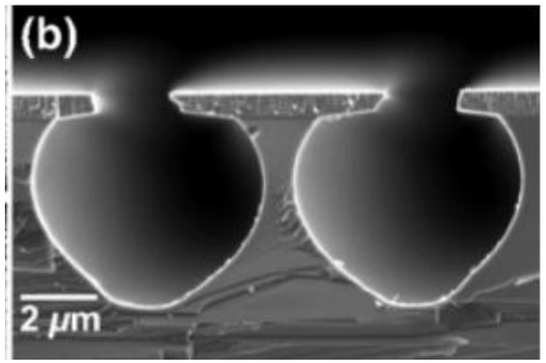


SA-heavy

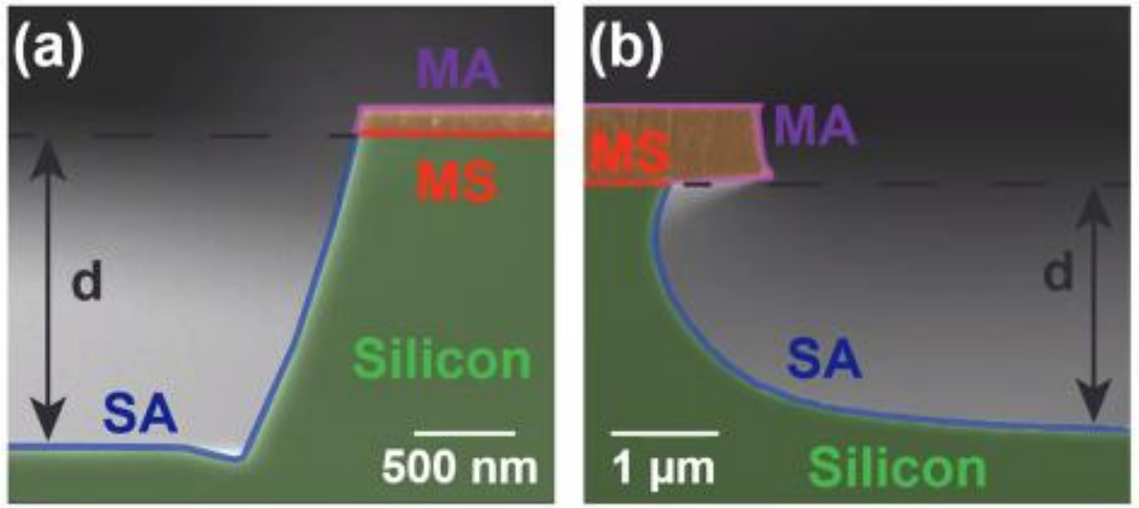


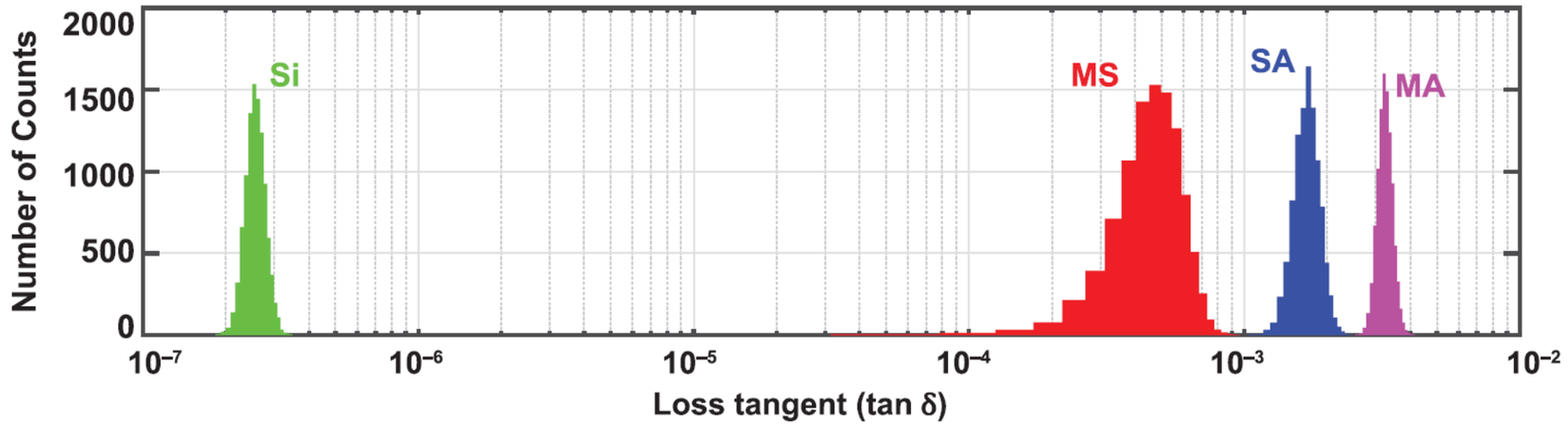

# Qubit geometry

In general:

larger qubits have smaller participation ratios than smaller ones

→ easier to fabricate with high Q-factors

Different designs have different participation ratios:

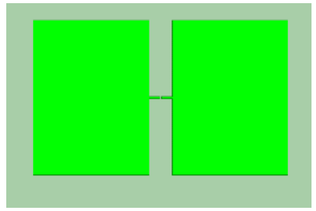

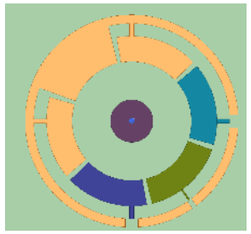

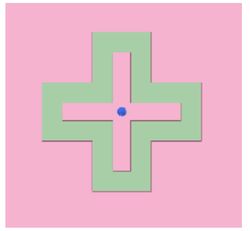

| | PP-Transmon | Coaxmon | X-mon |
|---|---|---|---|
| $p_{MS}$ | $3.51 * 10^{-5}$ | $2 * 10^{-4}$ | $1.38 * 10^{-4}$ |
| $p_{SA}$ | $3.77 * 10^{-5}$ | $1.04 * 10^{-4}$ | $1.76 * 10^{-4}$ |

→ **Think about your qubit design!**

# Qubit $T_\phi$ – longitudinal environmental interaction

Interaction Hamiltonian: $\widehat{H}_{int} = \frac{\partial H(\vec{\lambda})}{\partial \lambda_z}|_{\vec{\lambda}_z} \delta\lambda_z = \sigma_z \, \eta_z(t)$

consider relative phase of a superposition state $|0\rangle + e^{-i\delta\varphi(t)}|1\rangle$

$$\delta\varphi(t) = \int_0^t (\Omega + \eta_z(t'))dt' = \Omega t + \delta\Omega(t)$$

→ fluctuations of the transition frequency $\delta\Omega(t) = D_{\lambda z} \int_0^t \delta\lambda_z(t')dt'$

→ longitudinal qubit's sensitivity $D_{\lambda z} = \frac{\partial H(\vec{\lambda})}{\partial \lambda_z}$ to noise in $\lambda_z$

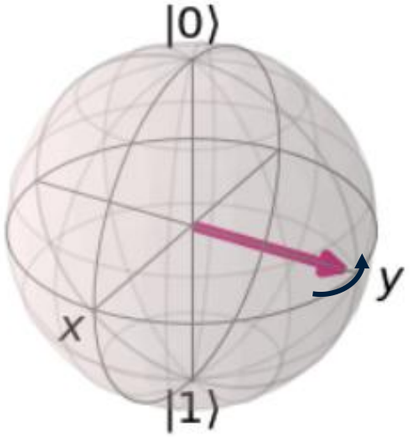


ensemble averaging over a Gaussian-distributed stochastic processes $\delta\lambda(t)$:

$$\langle e^{-i\delta\varphi(t)} \rangle = e^{-i\Omega t - \frac{1}{2}\langle \delta\varphi^2(t) \rangle} \equiv e^{-i\Omega t} e^{-\chi(t)}$$

[e.g., J. Schriefl, Y. Makhlin, A. Shnirman and G. Schön, *New J. Phys* **8** (2006)]

coherence decay function $\chi(t) = -\frac{t^2}{2} D_{\lambda,z}^2 \int_{-\infty}^{\infty} d\omega \; g(\omega) \, S_\lambda(\omega)$ with filter/weighting function $g(\omega)$

non-exponential decay → decay function $e^{-\chi_N(t)}$ with coherence function $\chi_N(t)$ generating pure dephasing

$$\rho(t) = \begin{pmatrix} 1 + (|a|^2 - 1)e^{-\Gamma_1 t} & \alpha\beta^* e^{-\frac{\Gamma_1}{2}t} e^{-\chi_N(t)} \\ \alpha^*\beta e^{-\frac{\Gamma_1}{2}t} e^{-\chi_N(t)} & |\beta|^2 e^{-\Gamma_1 t} \end{pmatrix}$$

# Filter function

Which noise frequencies dominate in a Ramsey-type experiment

a) at $\omega = 0$.

b) at $\omega = \frac{1}{T}$(T… pulse delay)

c) at $\omega = \infty$.

d) at all frequencies

# Dynamical decoupling

Filter function $g(\omega, t)$

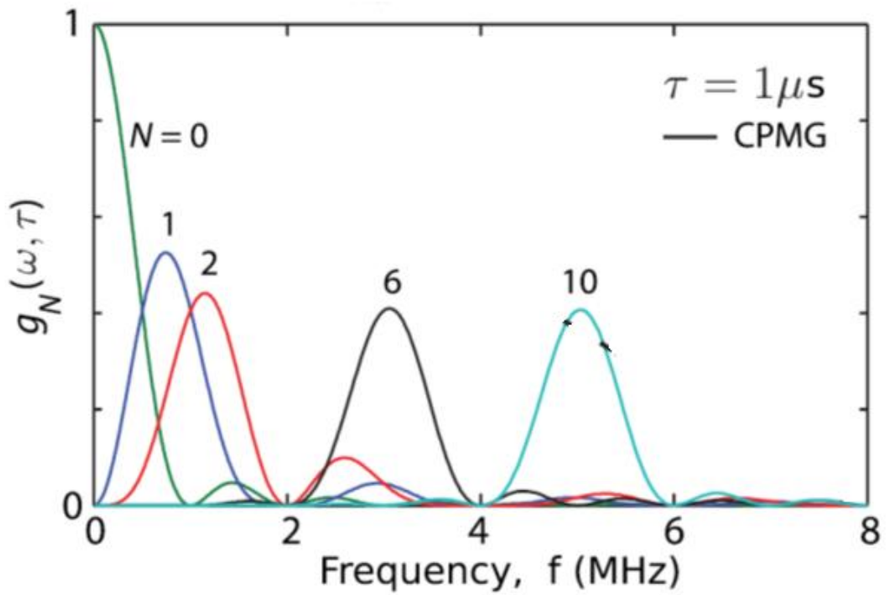


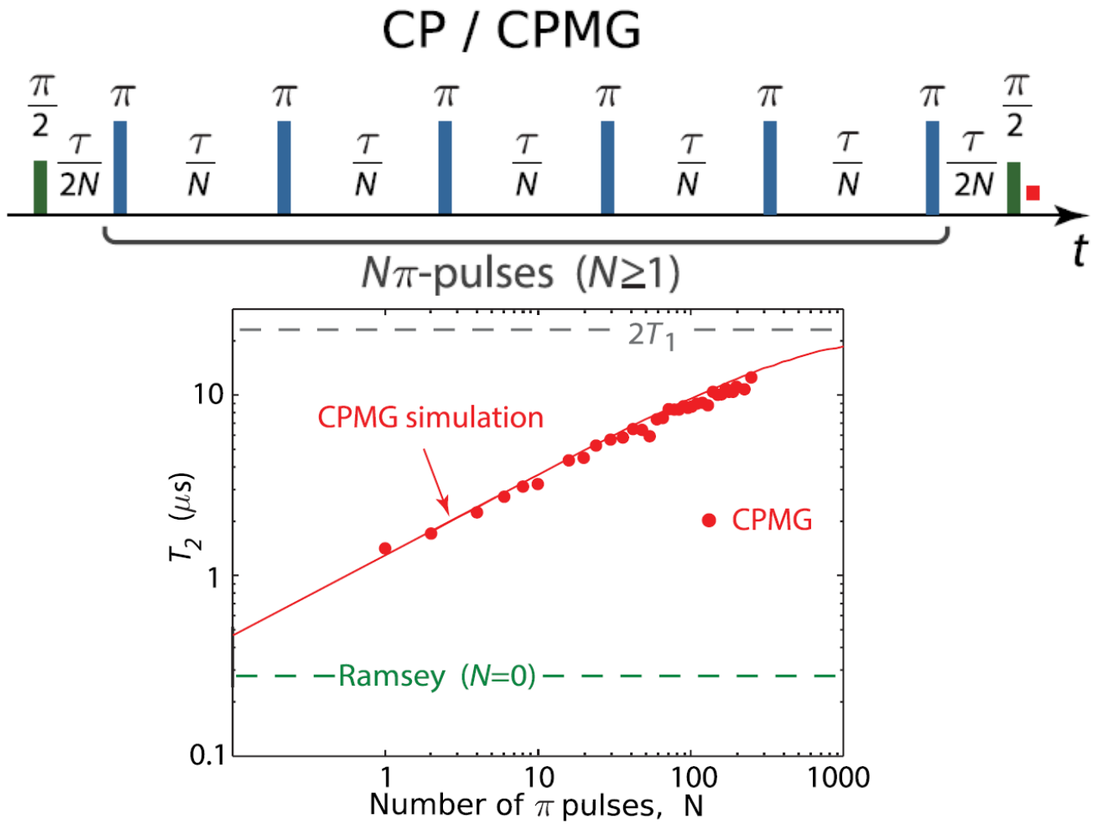


$$g_0(\omega,\tau) = \mathrm{sinc}^2\frac{\omega\tau}{2}, g_1(\omega,\tau) = \sin^2\frac{\omega\tau}{4}\,\mathrm{sinc}^2\frac{\omega\tau}{4}$$

In general: $g_N(\omega,\tau) = \frac{1}{(\omega\tau)^2}\left|1 + (-1)^{1+N}e^{i\omega\tau} + 2\sum_{j=1}^{N}(-1)^j \exp\left(i\omega\delta_j\tau\right)\cos(\omega t_\pi/2)\right|^2$

→ evaluate $\chi_N(t)$ at different $t$ → calculate $S(\omega)$ (not trivial)

[Krantz *et al., PR Applied* 2019; Cywinski *et al., PRB* 2008; Bylander *et al., Nat. Phys* 2011]

# Filter function

Why is the $T_2$-echo time increasing with increasing number of pulses?

(a) Because the noise spectral density is constant.

(b) Because the noise spectral density decreases at higher frequencies.

(c) I don’t know.

# Charge noise

- Ubiqitous in solid-state devices:
  - arises from charged fluctuators in defects, charge-traps
  - Interfaces, junction tunnel barrier, substrate
- E.g., electric field in transmon couples to dielectric defects (see discussion above)
- E-field is transverse to quantization axis
  → responsible for $T_1$ decay (for large $E_J/\mathrm{E_C}$)
  → or $T_2$ as well for smaller $E_J/E_C$
- $PSD$: (1/f + Ohmic [Johnson-Nyqvist] noise)

  at lower frequencies: $S_Q(\omega) = A_Q^2 \left(\frac{2\pi\times 1\mathrm{Hz}}{\omega}\right)^{\gamma_Q}$

  (with $A_Q^2 = (10^{-3}e)^2/Hz$ at 1 Hz and $\gamma_Q \approx 1$)

  at higher frequencies ($> 1GHz$): $S_Q(\omega) = B_Q^2 \left(\frac{\omega}{2\pi\times 1\mathrm{Hz}}\right)$

  (linear)

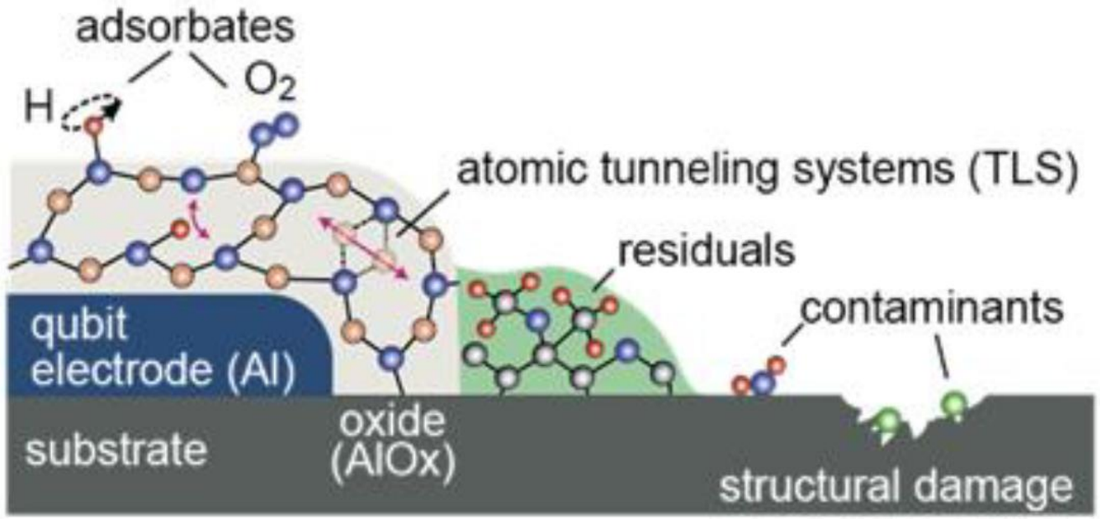


© KIT, Ustinov

# Magnetic flux noise

- Stochastic flipping of spins at the surface of superconducting metals → random fluctuations of the effective magnetic field bias
- E.g., split transmon with fluctuating

  $\omega_{01} = \sqrt{8E_J(\Phi)E_C}$ with $\mathrm{E_J}(\Phi) = E_{J0}\left|\cos\frac{\Phi}{\Phi_0}\right|$

  → Longitudinal noise $(\omega_{01} + \delta\omega)\sigma_z$
- In flux qubit either longitudinal or transversal
- $PSD$: "quasi-universal" 1/f

$$S_Q(\omega) = A_\Phi^2 \left(\frac{2\pi \times 1\mathrm{Hz}}{\omega}\right)^{\gamma_\Phi}$$

with $A_\Phi^2 = (10^{-6}\Phi_0)^2/Hz$ at 1 Hz and $\gamma_\Phi \approx 0.8$
over large frequency range (mHz to > GHz)

- Precise origin of flux noise unclear (and pending issue since decades)
- Potential sources: molecular oxygen or atomic hydrogen
  [Kumar *et al., PR Applied* (2016); de Graaf *et al., PRL* 118 (2017)

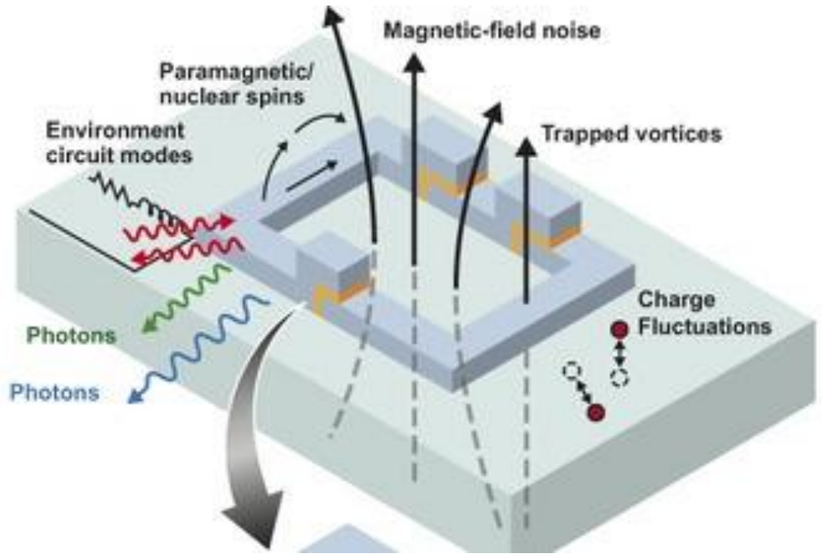


[Oliver and Welander, MRS Bulletin 2013]

# Photon number fluctuations & Quasi-particles

## Photon number fluctuations:

- Residual microwave photons in the cavity
- Dispersive regime – longitudinal coupling $\chi\hat{\sigma}_z\hat{n} \rightarrow$ Pure dephasing at a rate $\Gamma_\phi = \frac{\eta\bar{n}4\chi^2}{\kappa}$

  with average photon number $\bar{n}$ and $\eta = \frac{\kappa^2}{\kappa^2+4\chi\hat{}2}$
- Lorentzian type noise spectral density (white noise)

$$S(\omega) = 4\chi^2 \frac{2\eta\bar{n}\kappa}{\omega^2+\kappa^2}$$

## Quasiparticles:

- Tunneling of quasiparticles through a qubit junction may lead to both $T_1$ or $T_\phi$ depening on qubit type, bias point,...
- Occur naturally because of thermodynamics, exponentially suppressed with decreasing temperature
- Observed $10^{-8} - 10^{-6}$ per cooper pair is higher than expected

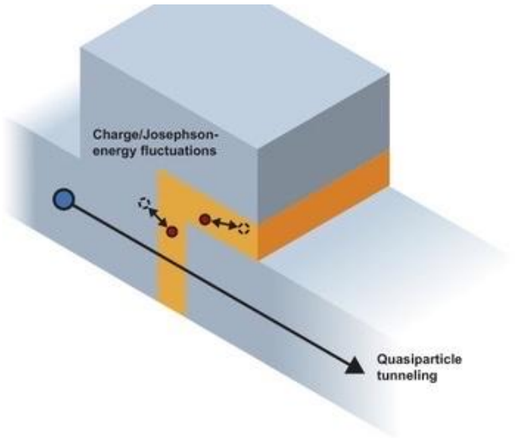

# Superconducting qubits – Trend of lifetime

[Kjaergaard *et al., Ann. Rev. Cond. Mat Phys* **11** (2020); https://arxiv.org/abs/1905.13641]

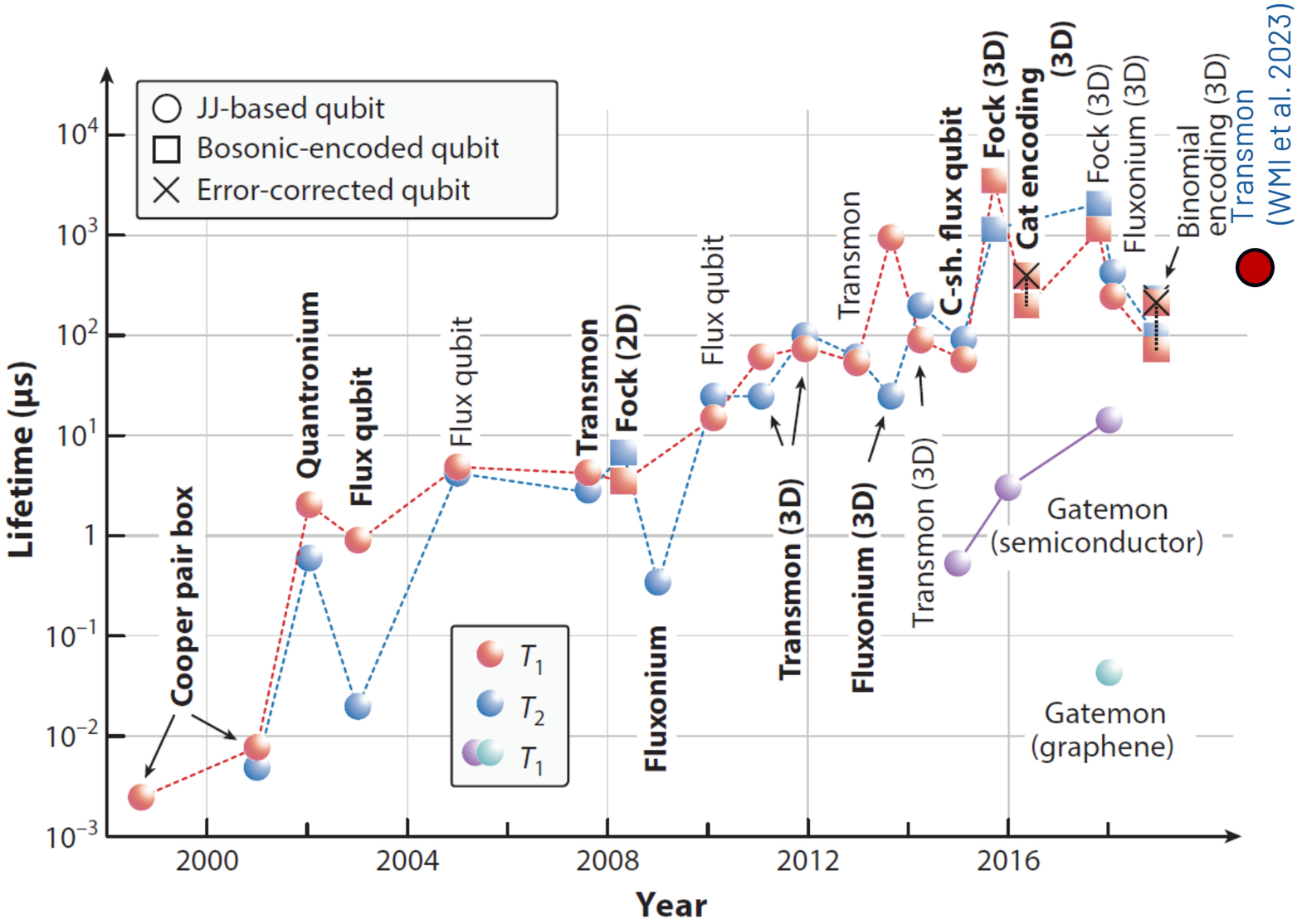

# Qubit Readout

# Superconducting Qubit Readout

Transmission/reflection measurement to determine qubit state:

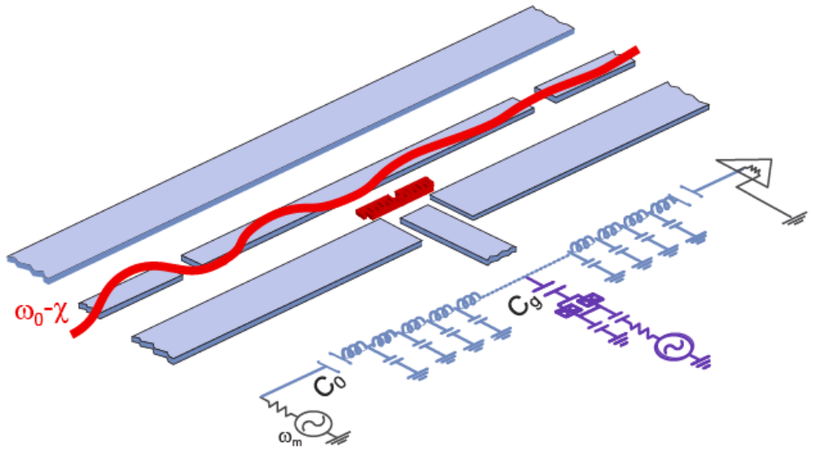


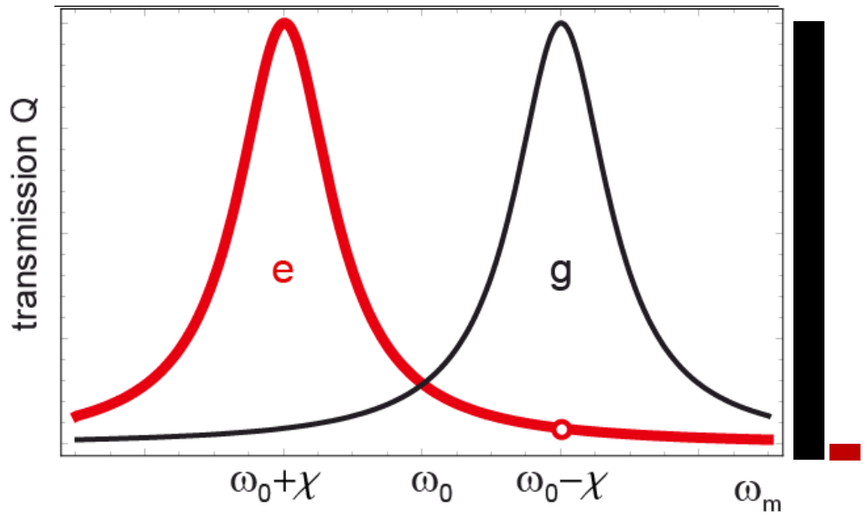


dispersive Hamiltonian

$$H = \hbar(\omega_r + \chi\sigma_z)a^\dagger a + \frac{\hbar}{2}(\omega_q + \chi)\sigma_z$$

with $\chi = \frac{g^2}{\Delta}$ (or $\frac{g^2\alpha}{\Delta\,(\alpha+\Delta)}$ for a transmon)

state-dependent frequency shift

→ $\sigma_z$ determined

# Dispersive regime

resonant:

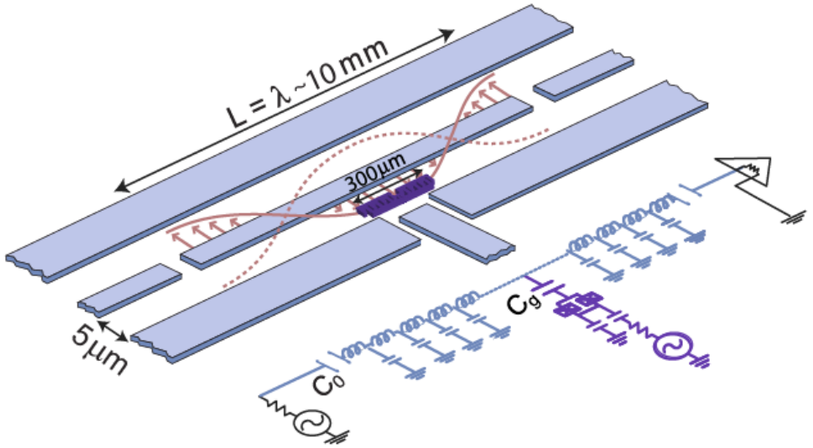


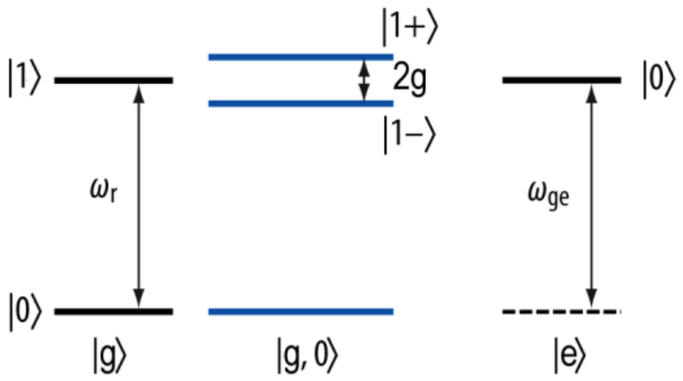


dispersive (qubit detuned from resonance):

$$\Delta = \left|\omega_q - \omega_r\right| \gg g$$

[Blais *et al.*, *PRA* **69** (2004)]

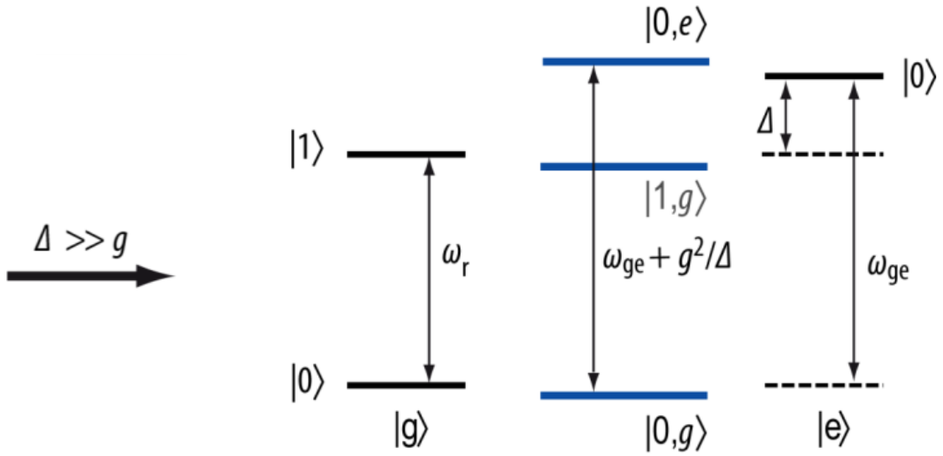

# Dispersive shift

When probing the frequency of the resonator

a) The qubit frequency is shifted by a fixed amount, even without photons in the resonator.

b) The qubit frequency is shifted depending on the mean photon number in the resonator.

c) The qubit frequency is not shifted at all.

# Non-Resonant (Dispersive) Interaction

approximate diagonalization: $|\Delta| = |\omega_q - \omega_r| \gg g$:

$$H = \hbar\left(\omega_r + \frac{g^2}{\Delta}\sigma_z\right)a^\dagger a + \frac{\hbar}{2}\left(\omega_q + \frac{g^2}{\Delta}\right)\sigma_z \quad \text{or} \quad H = \hbar\omega_r a^\dagger a + \frac{\hbar}{2}\left(\omega_q + \frac{g^2}{\Delta} + \frac{2g^2}{\Delta}a^\dagger a\right)\sigma_z$$

Qubit state-dependent cavity frequency shift

Lamb Shift (vacuum fluctuations)

Photon number dependent qubit ac-Stark shift

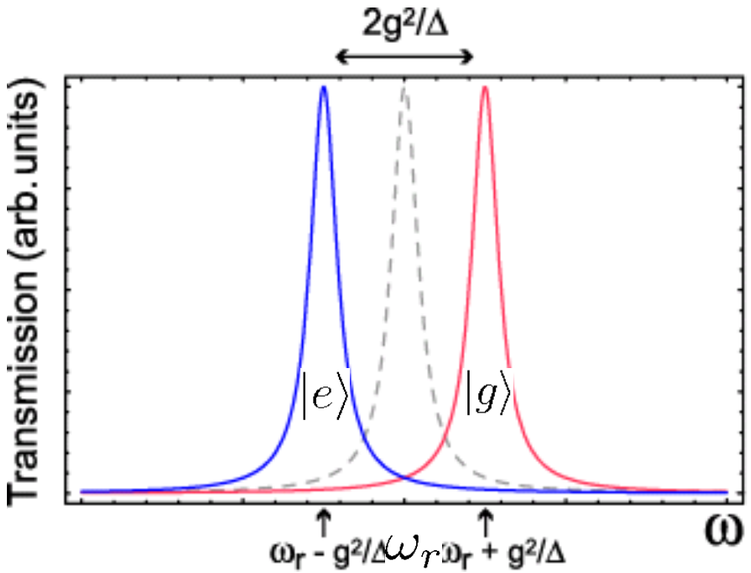


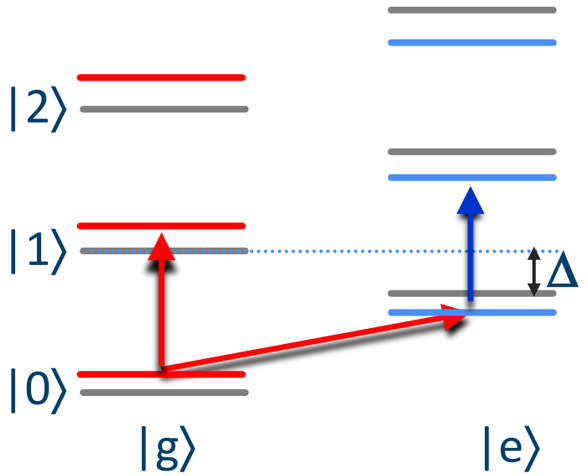


qubit detuned by D from resonator

[A. Blais *et al.*, *PRA* **69**, 062320 (2004)]

# Circuit QED – read out of qubit state

transmission measurement to determine qubit state:

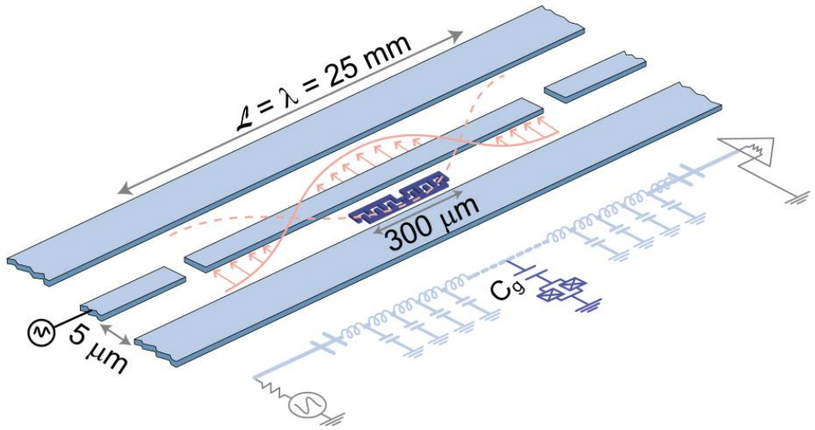


phase sensitive measurement of transmitted microwave:

voltage signal:

$$A(t)\sin\big(\omega_m t + \phi(t)\big) \equiv \underbrace{I(t)}_{A(t)\cos\phi(t)} \sin\omega_m t + \underbrace{Q(t)}_{A(t)\sin\phi(t)} \cos\omega_m t$$

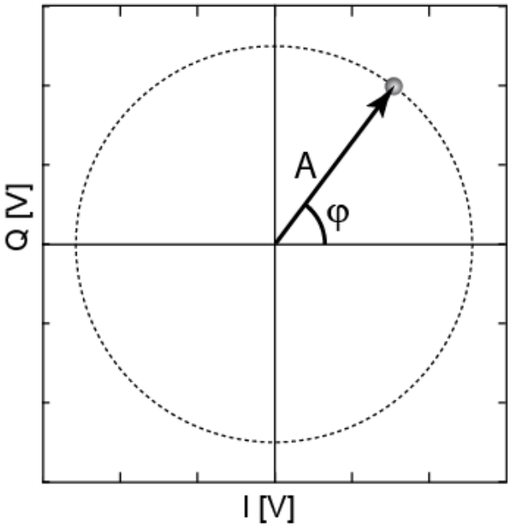

# Superconducting qubits – Readout

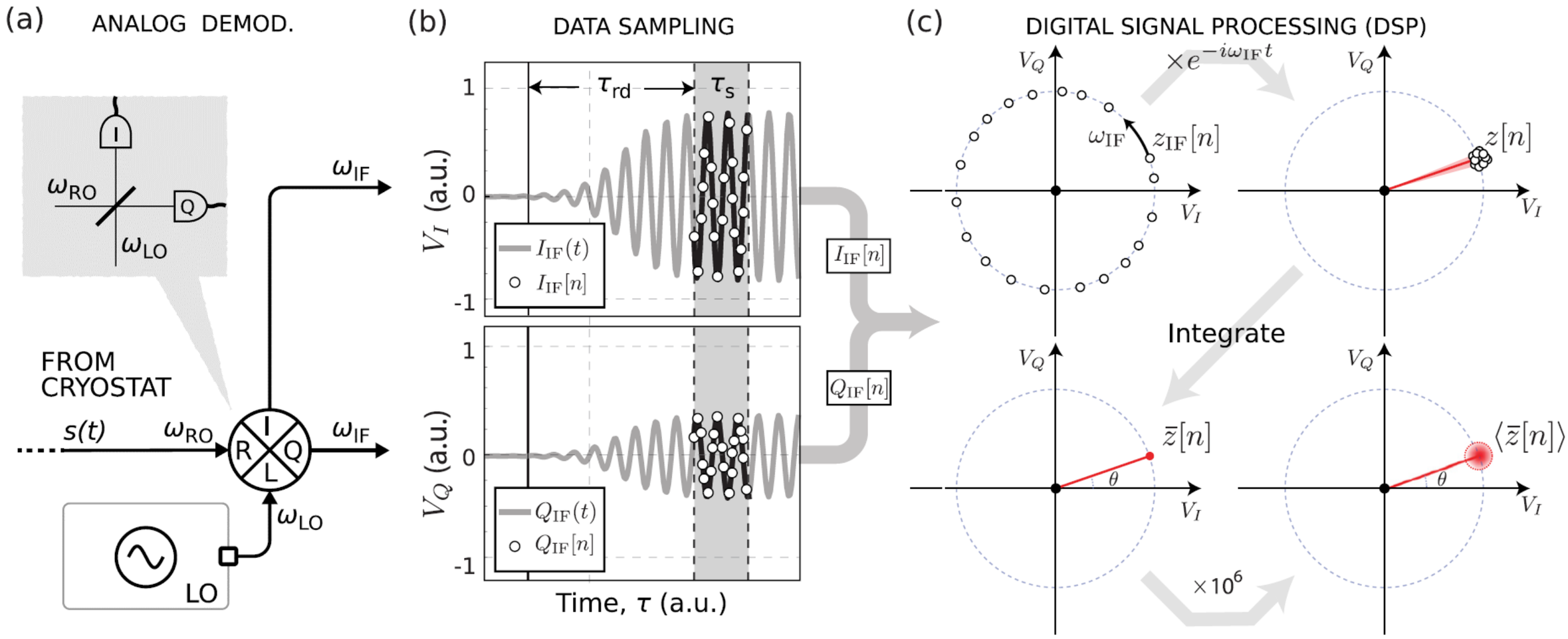


[Krantz *et al., Appl. Phys Rev* **6** (2019)]

# Dispersive read out – reflection measurement

Signal chain for readout:

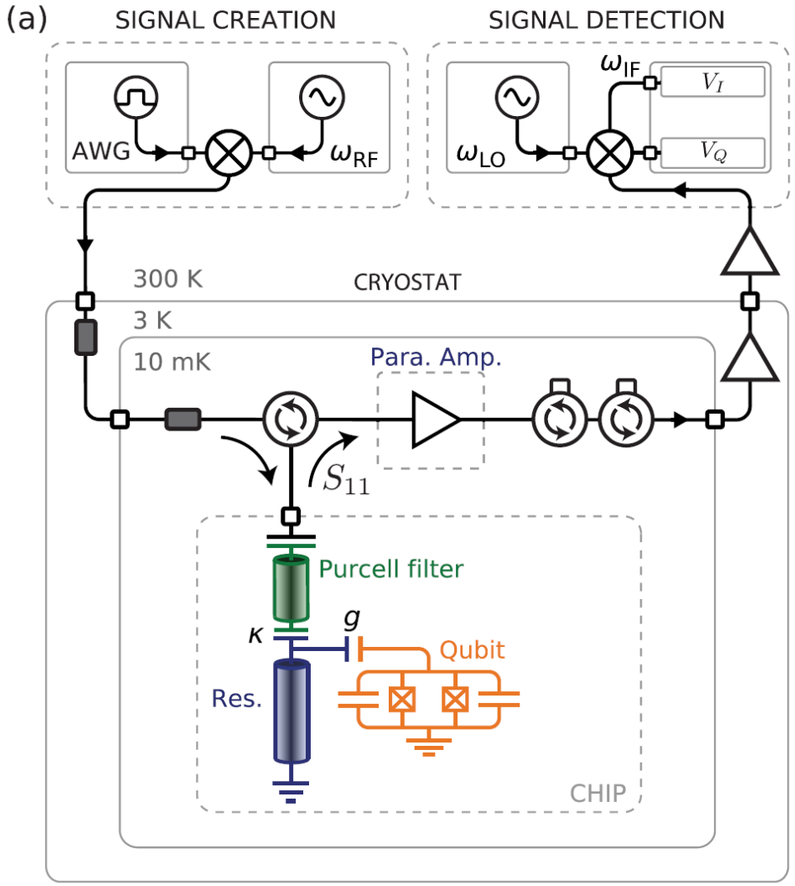


Reflected signal with amplitude $|S_{11}|$ and phase $\theta$:

Two peaks/dips for qubit states $|0\rangle$ & $|1\rangle$,

separated by dispersive shift $\chi$

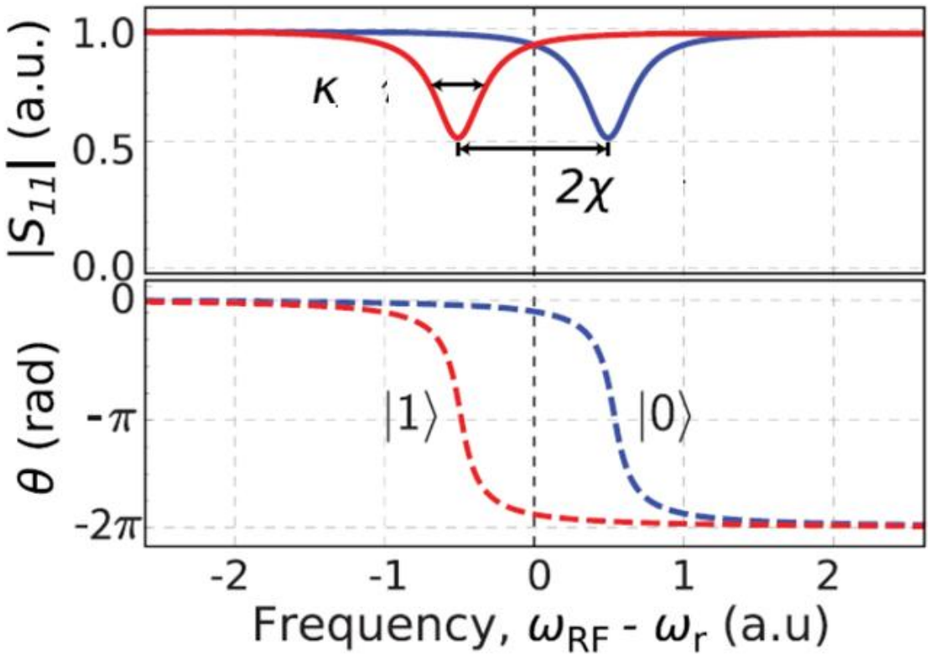


[Krantz *et al., Appl. Phys Rev* **6** (2019)]

# Reflected signal in IQ plane

How does the reflected signal look like in the IQ plane when measuring at $\omega_r$?

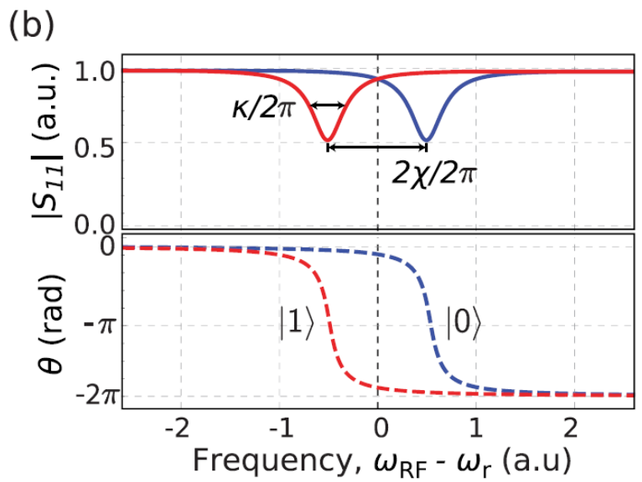


a)

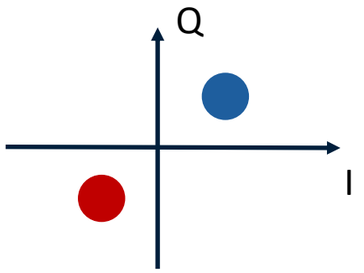


b)

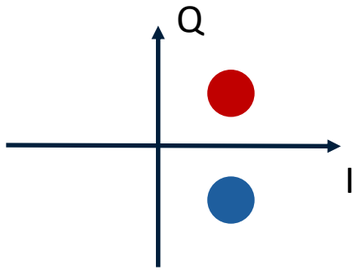


c)

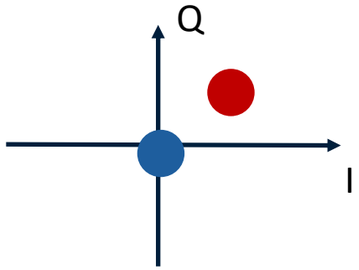

# Dispersive read out – reflection measurement

Signal chain for readout:

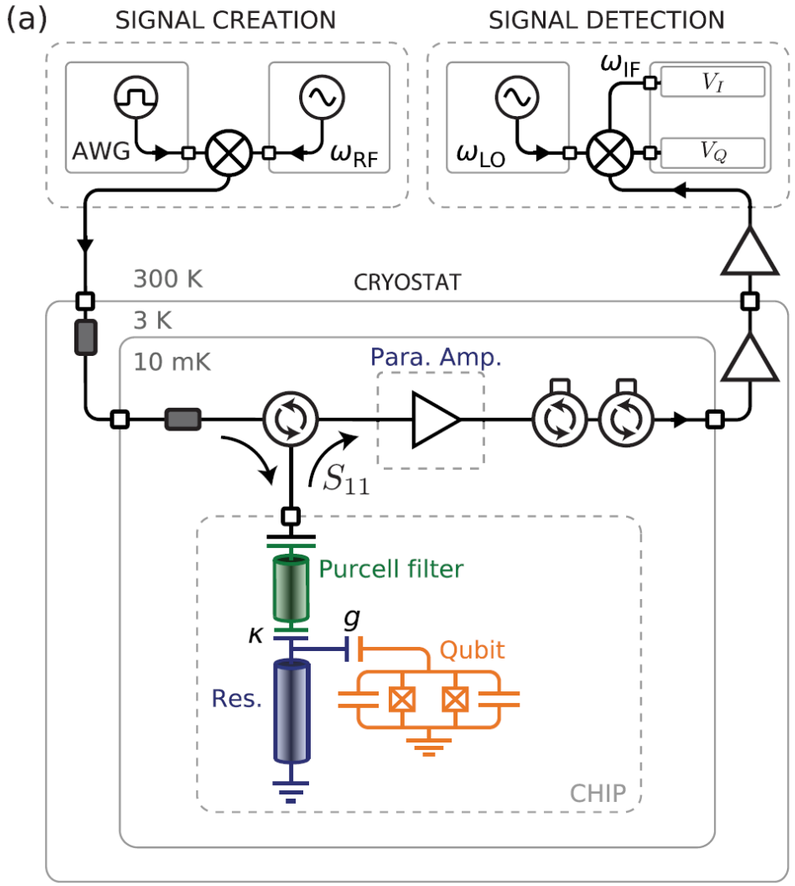


Reflected signal with amplitude $|S_{11}|$ and phase $\theta$:

Two peaks/dips for qubit states $|0\rangle$ & $|1\rangle$,

separated by dispersive shift $\chi$

→ 2 blobs in IQ plane

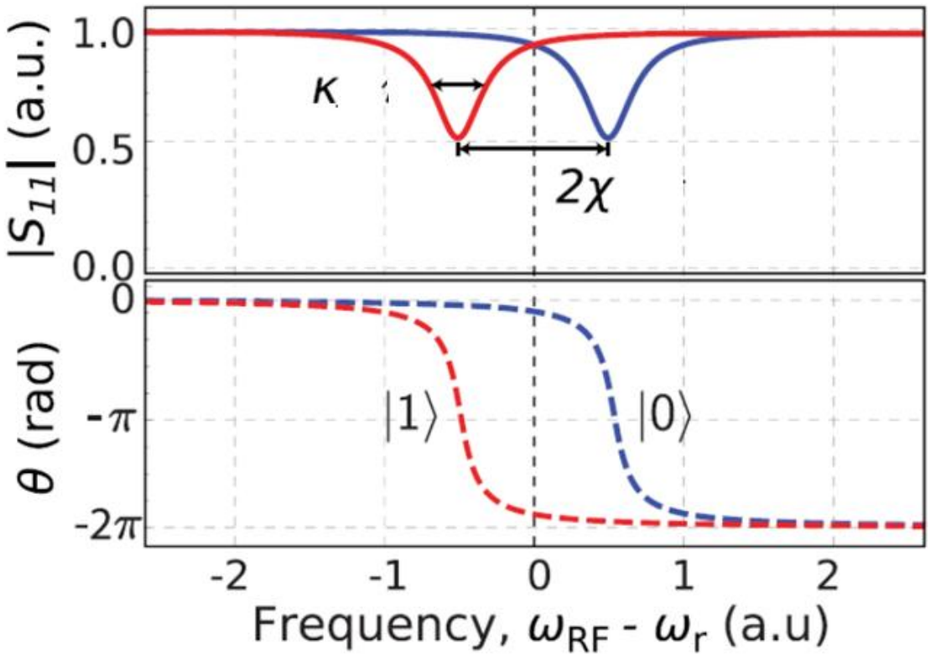


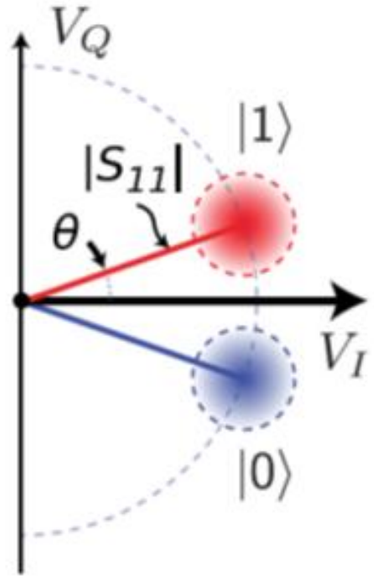


[Krantz *et al., Appl. Phys Rev* **6** (2019)]

# SNR and single-shot measurement

without noise: $|0\rangle$ and $|1\rangle$ can be distinguished for any non-zero dispersive shift

reality: added noise leads to Gaussian distribution in the I/Q plane

[see Clerk *et al.*, *Rev. Mod. Phys.* (2010)]

contribution to noise:

- quantum noise ($\hbar\omega/2$ per unit bandwidth)
- amplifier noise (at least another $\hbar\omega/2$ of qm noise + classical noise)
- classical noise of the signal (drifts, fluctuations)

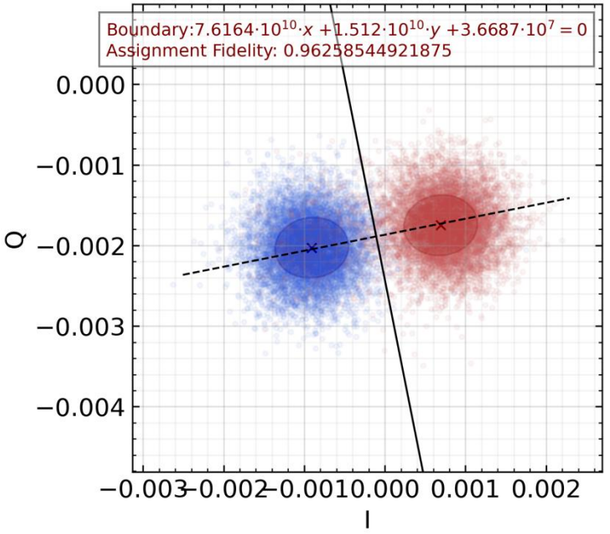


single-shot measurement: discriminate state in each measurement with high fidelity

integrated measurement signal:

finite sampling time to increase signal to noise ratio

note: $T_1$ reduces signal to noise for long integration times

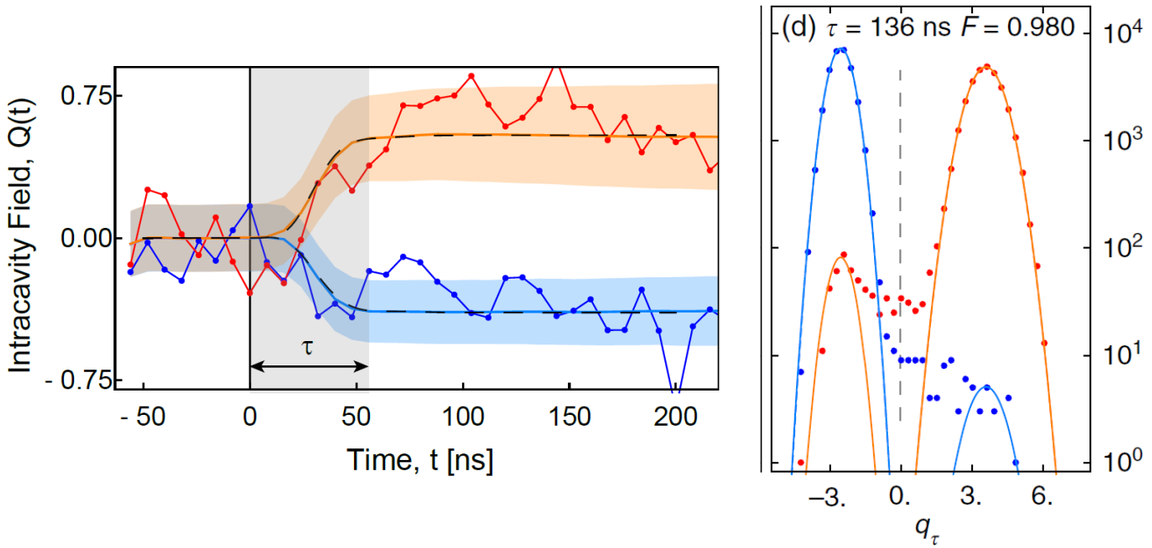


[Walter *et al*, *PR Applied* (2017)]

# Qubit Control

# From Quantum Processor Design to Control

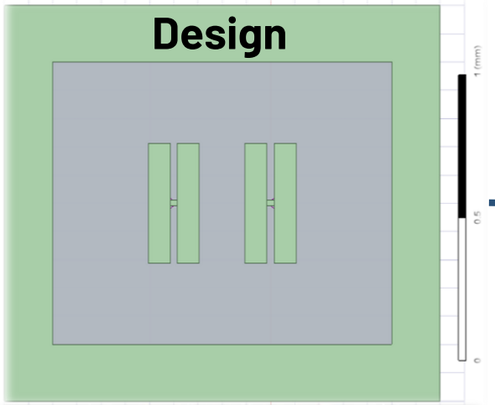



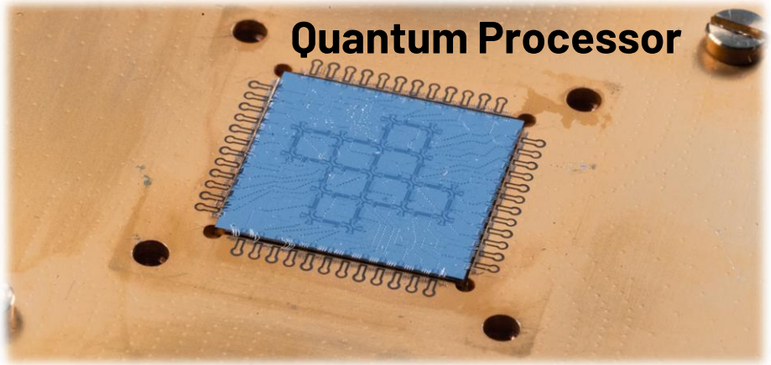


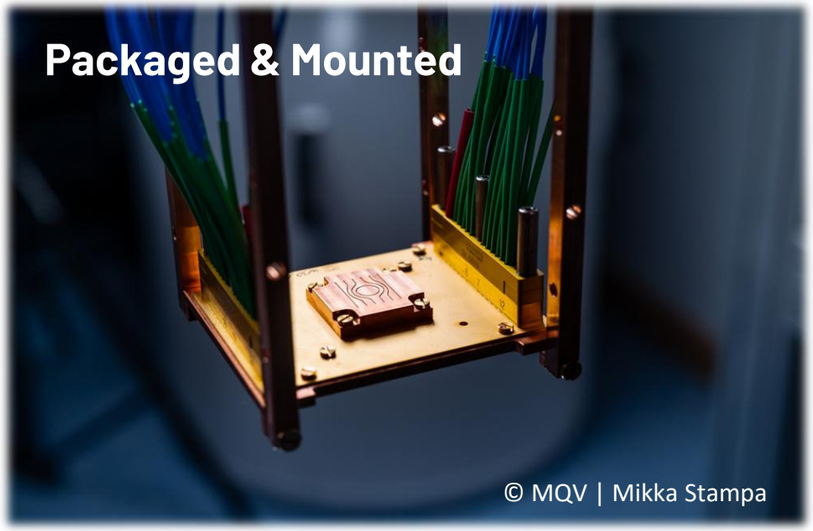


# Superconducting qubit quantum computer setup

Dilution refrigerator to cool qubits to 10 - 15 mK

Cloud access

Local control

QISKIT client

circuit

result

Login node

LAN

PQSC

Microwave electronics

40K

3K

0.9K

0.1K

0.015K

Quantum Processor
(qubits, couplers,
control and readout lines)

# Qubit Control – Single Qubit

apply microwave pulse (capacitive coupling)

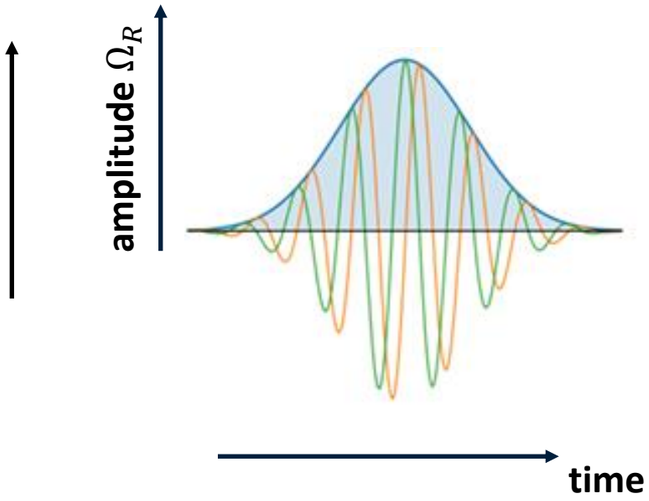


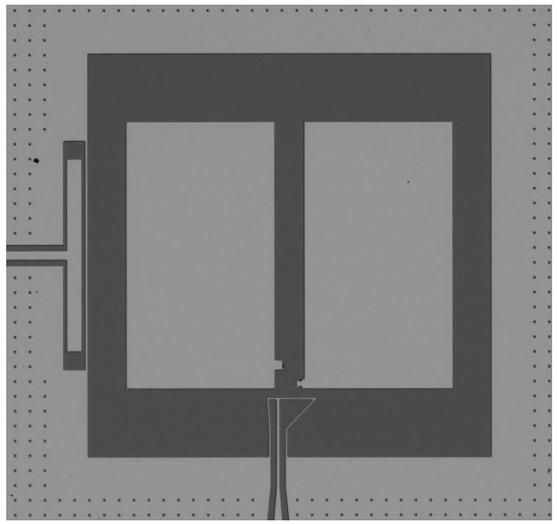

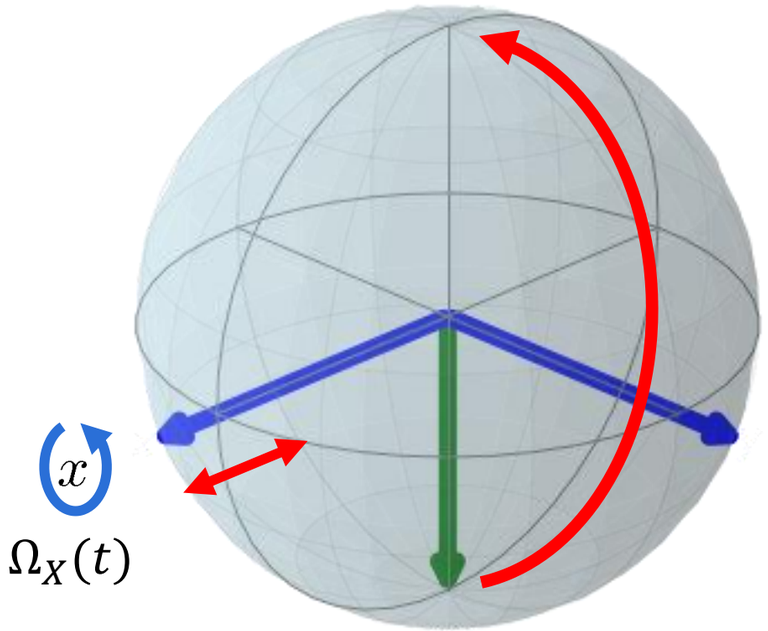


Rabi oscillations:

- Hamiltonian for state manipulation $\hat{H} = \hbar\Omega_x\hat{\sigma}_x + \hbar\Omega_y\hat{\sigma}_y$
- Area under the pulse determines the rotation angle $(X_\pi, X_{\pi/2})$
- Phase $\phi_R$ determines azimuthal angle, e.g., $\phi_R = \frac{\pi}{2} \rightarrow Y_\pi$
- Typical pulse duration: 10-50ns
- Typical fidelities: 99.9%-99.95%

# Rabi Oscillations – X and Y gates

drive at **resonance frequency** with
varying **drive strength Ω** or **duration τ** ($\Omega_x = \Omega, \omega_d = \omega_q$):

effective field $M = (\Omega\cos\phi\,, \Omega\sin\phi\,, 0)$

$X_\pi$ gate (spin flip) for $\theta = \pi$ $\left(\Omega = \frac{\pi}{\tau}\right)$ and $\phi = 0$:

$$H = \frac{\hbar\Omega_x}{2}\sigma_x \rightarrow U = e^{-i\frac{\theta}{2}\sigma_x} \text{ with } \theta = \Omega\,\tau$$

$X_{\frac{\pi}{2}}$ gate (superposition state) for $\theta = \pi/2$ $\left(\Omega = \frac{\pi}{2\tau}\right)$: $U = e^{-i\frac{\theta}{4}\sigma_x}$

$Y_\pi$ and $Y_{\frac{\pi}{2}}$ gate for choice of phase $\phi = \frac{\pi}{2}$

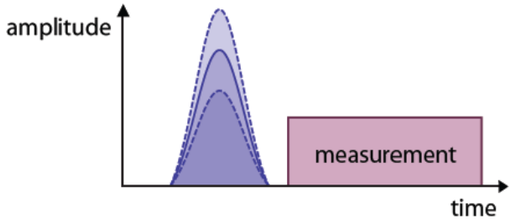


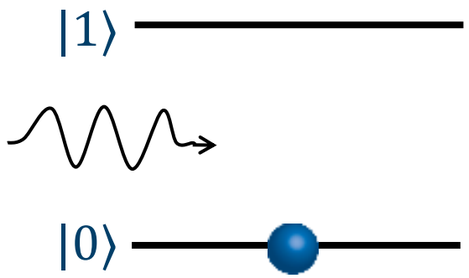


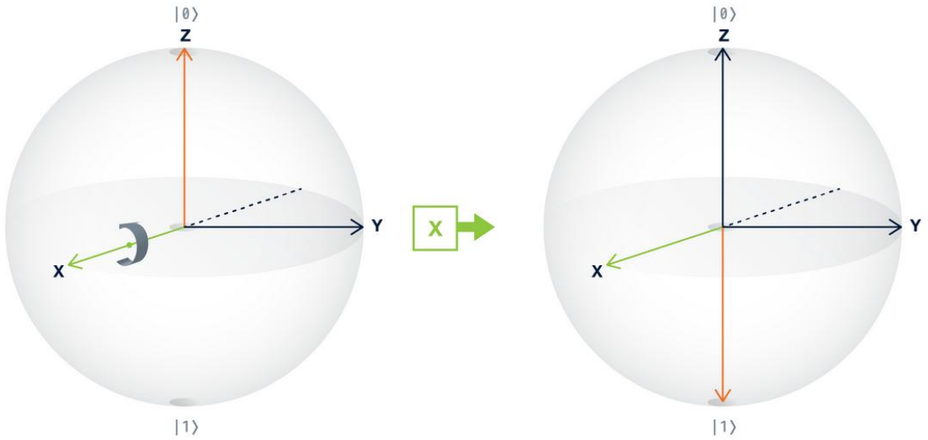


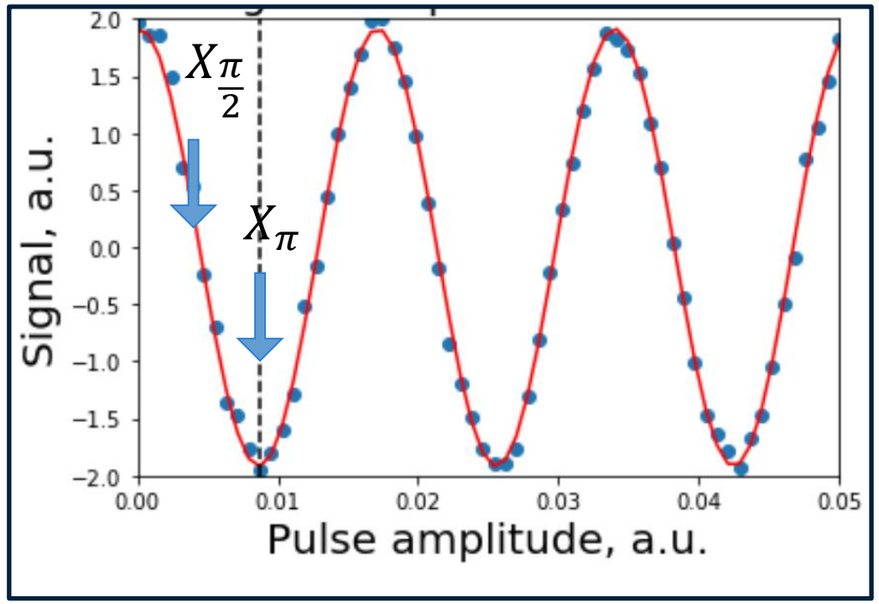

# Virtual Z – gate

extra phase shift $\gamma$ on subsequent gates gives an effective rotation about z-axis (i.e., an extra phase shift)
[McKay *et al.*, *Phys. Rev. A* **96**, 022330 (2017)]

pulse about the x-axis ($X_\theta = e^{-i\frac{\theta}{2}\sigma_x}$) followed by a pulse about a rotated axis with phase offset $\gamma$
($\Gamma_\theta = e^{-i\frac{\theta}{2}(\cos\gamma\sigma_x + \sin\gamma\sigma_y)}$):

$$\Gamma_\theta . X_\theta = e^{-i\frac{\theta}{2}(\cos\gamma\sigma_x + \sin\gamma\sigma_y)} \cdot X_\theta =$$

$$U_z^+(\gamma) \cdot X_\theta \cdot U_z(\gamma) \cdot X_\theta = e^{i\frac{\gamma}{2}\sigma_z} \cdot e^{-i\frac{\theta}{2}\sigma_x} \cdot e^{-i\frac{\gamma}{2}\sigma_z} \cdot X_\theta = Z_{-\gamma} \cdot X_\theta \cdot Z_\gamma \cdot X_\theta$$

→ results in Z-gate $Z_\gamma$ sandwiched between the X gate
(plus an additional $Z_{-\gamma}$ that has to be taken into account for subsequent gates)

Simple example: Ramsey-experiment with different rotation axis of the second $\pi/2$ pulse

Advantage: $\gamma$ can be adjusted in software by setting phase $\gamma$ at the AWG!

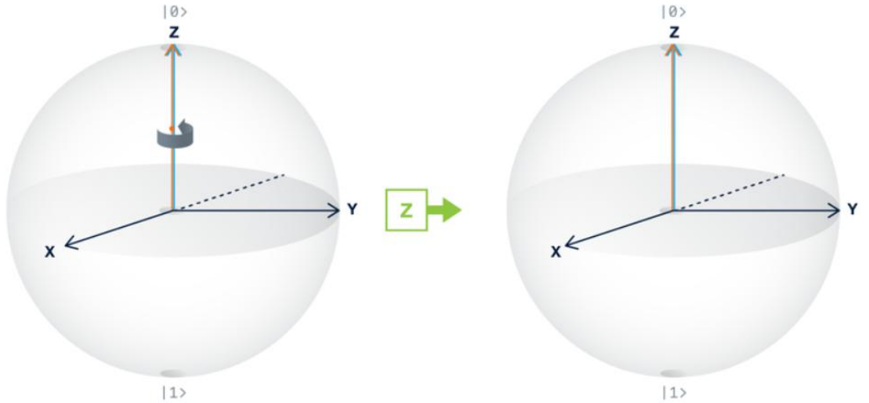

# Questions – constraints on pulses

A transmon resembles more an an-harmonic oscillator than a qubit.
In order to avoid excitation of the 2nd excited state, is a short pulse (large amplitude) or a long pulse (small amplitude) better suited?

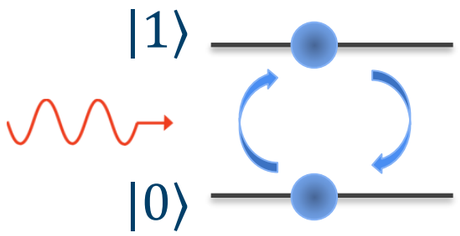


Vs.

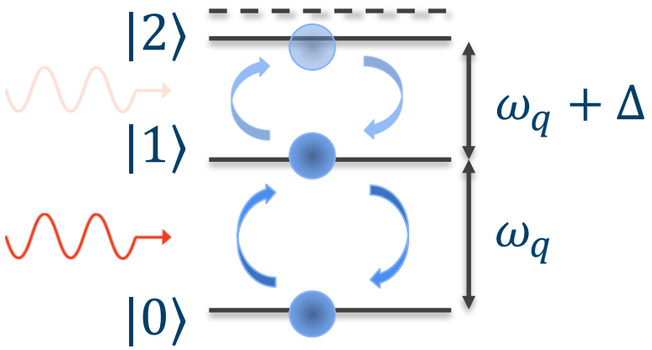

# DRAG pulses – Analytic pulse control

Qubit Hamiltonian:

$$H/\hbar = \frac{\omega_q}{2}\sigma_z + \mathrm{A}(t)\cos(\omega_d t + \phi_d)\sigma_x$$

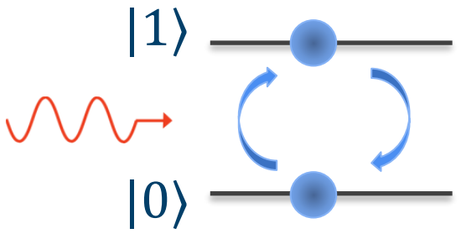


Transmon Hamiltonian:

$$H/\hbar = \omega_{01}|1\rangle\langle 1| + (2\omega_{01} + \alpha)|2\rangle\langle 2| + A\cos(\omega_d t + \phi_d)\,\tilde{\sigma}_x$$

with $\tilde{\sigma}_x = |0\rangle\langle 1| + \lambda|1\rangle\langle 2| + h.c.$

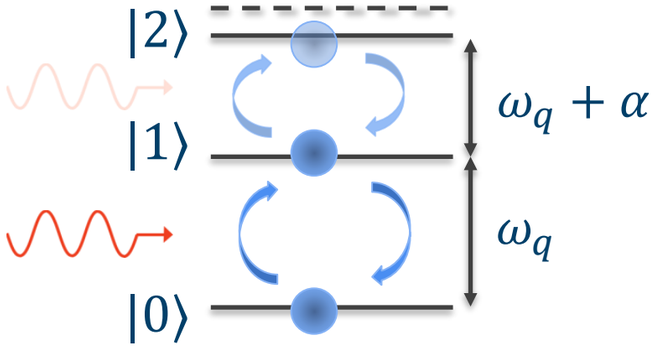


→ drive acts also off-resonantly on the $|1\rangle\langle 2|$ transition

→ leakage and phase-shifts during the pulse

→ pulse control, e.g. by a**nalytic pulse shapes:**

DRAG (Derivative Removal by Adiabatic Gate)

[F. Motzoi *et al.*, *PRL* **103**, 110501 (2009)]

or **numerical optimization of pulse shape**

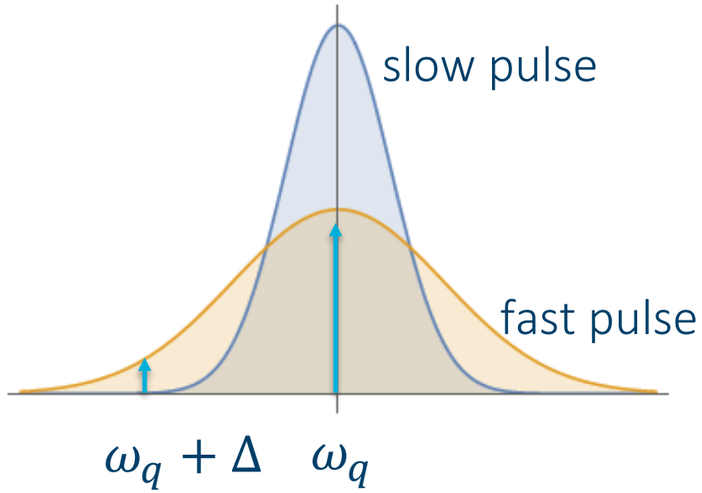

# Questions – constraints on pulses

Think about a realistic implementation of a qubit experiment.
What constraints are prohibiting you as control scientist from exerting the perfect pulse/gate on the system? (2-3 min, discuss with neighbor, I'll collect input and we can discuss)

a) **Bandwidth of pulses:** AWG support typically <2.4 GS/s, mixers have bandwidth of ~500 MHz
b) **Amplitude of pulses – dynamic range**: AWG have up to 16 bit with a maximal output voltage of 2 V
c) **Response function of the system:** Cables, attenuators, filters, amplifier all have certain bandwidth constraints distorting the signal. This has to be taken into account for pulse shaping.
d) **Frequency of carrier:** signal generators up to 20 GHz are affordable
e) **Cross-talk:** signals on selected qubit affects other qubits -> off-resonant driving with weaker amplitude
f) **Noise:** most challenging is 1/f noise, i.e. slow drifts
g) For optimal control: **time delays for updating signals** with new parameter values
h) Etc.

# Two-Qubit Gates

# 2-qubit gats: entangling two qubits

(co-planar waveguide) resonator or coupler circuit can be used as a **quantum bus** to create **entangled** states:

→ instead of direct coupling via capacitance $C_c$, **in-direct / dispersive coupling *J*** mediated by resonant mode

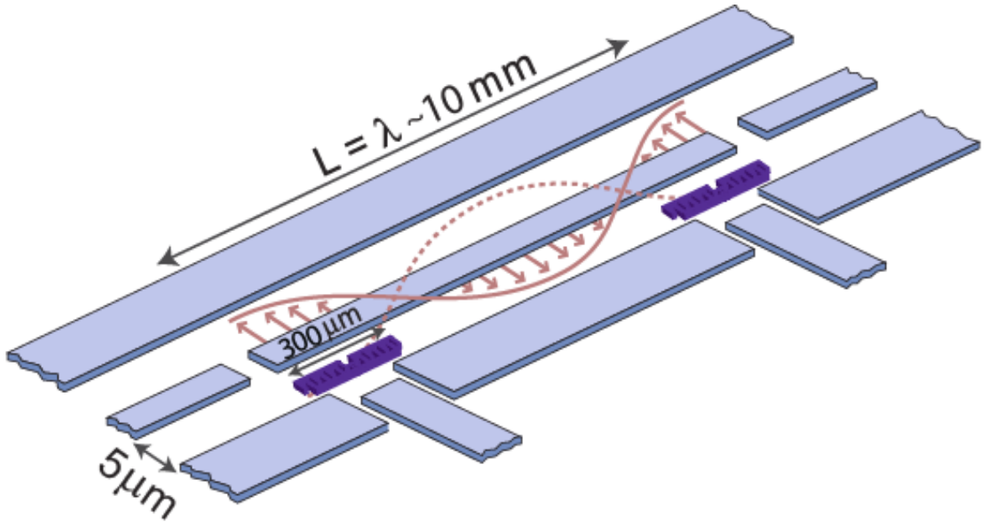


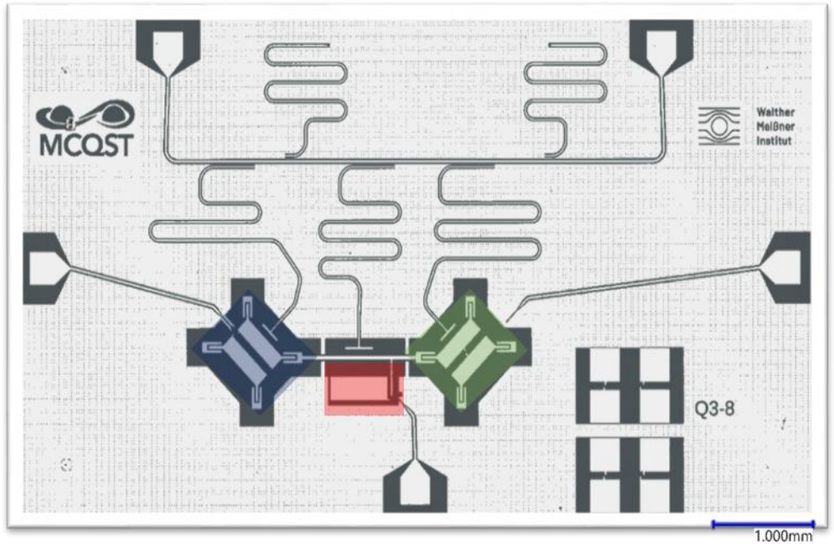


©WMI

# Dispersive two-qubit J-coupling – Energy levels

qubit 1: transition frequency tunable (for transmon: $\omega_{ge} \approx \sqrt{8E_C E_J} = \sqrt{8E_C E_{J,max}|\cos(\pi\Phi_{ext}/\phi_0)|}$)

qubit 2: constant frequency (*e.g.*, $5\ GHz$ )

direct coupling ($g \sim 100 - 200\ MHz$)

mediated J-coupling ($J \sim \frac{g^2}{\delta} \sim 10 - 20\ MHz$, with $\delta = \omega_r - \omega_q^{(1,2)}$)

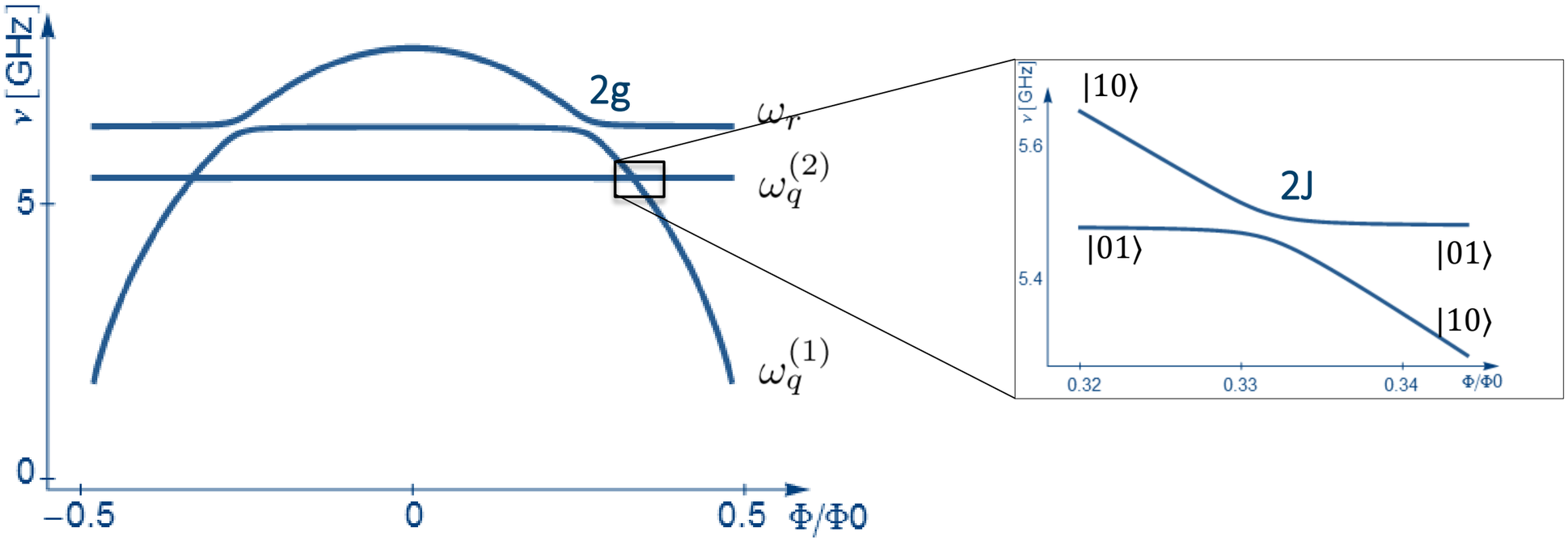


[Majer *et al.*, *Nature* **449** (2007)]

# Avoided level crossing due to qubit-qubit coupling

qubit A swept across resonance with fixed qubit B
cavity mediated coupling leads to an avoided crossing

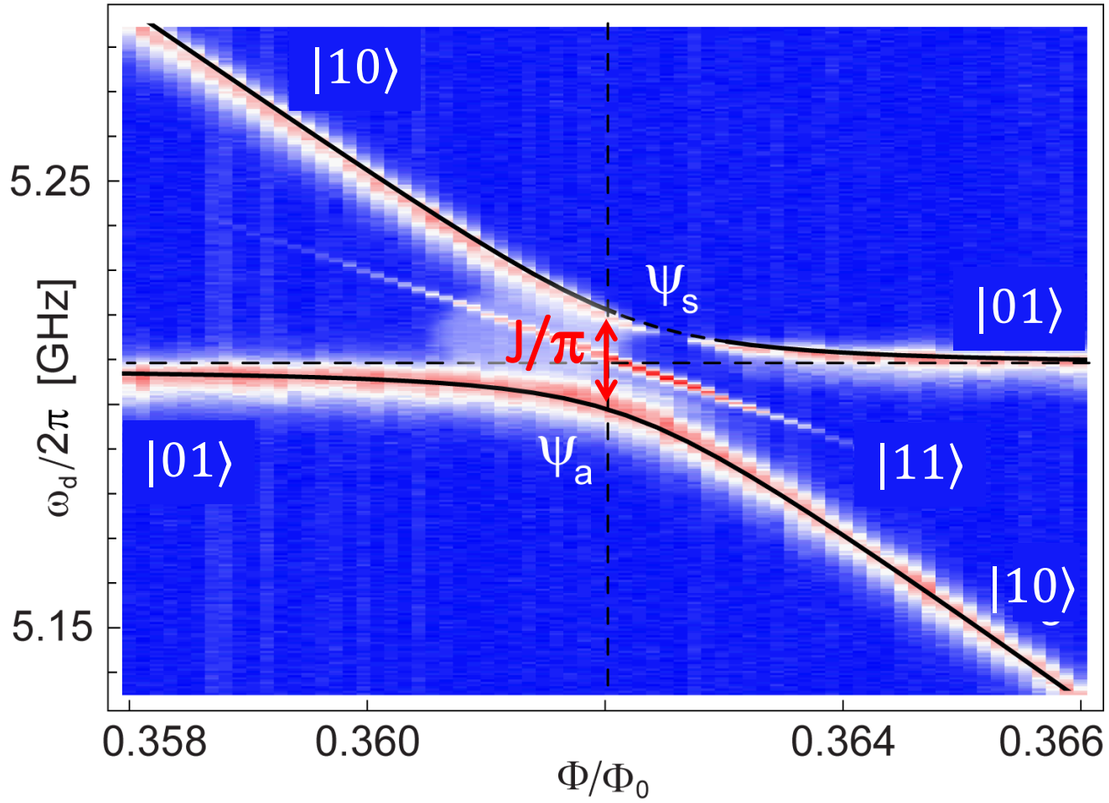


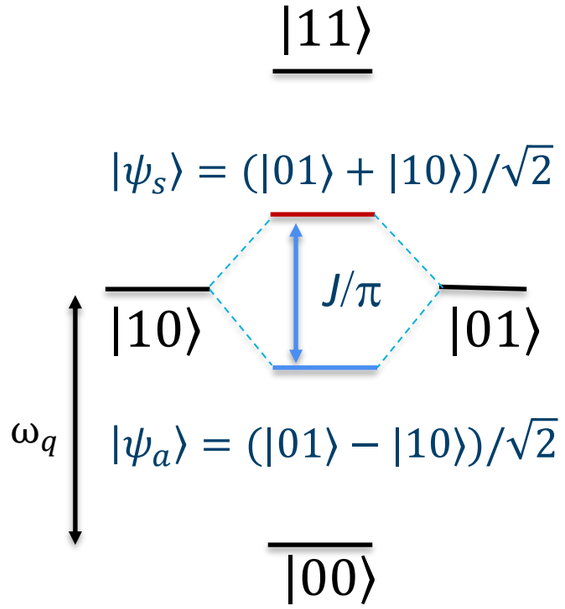


[Filipp *et al.*, *PRA* **83**, 063827 (2011).]

# Adiabatic vs. non-adiabatic

What is the effect on the state if the energy is modified suddenly (non-adiabatically)? What is the effect in the slow (adiabatic) regime?

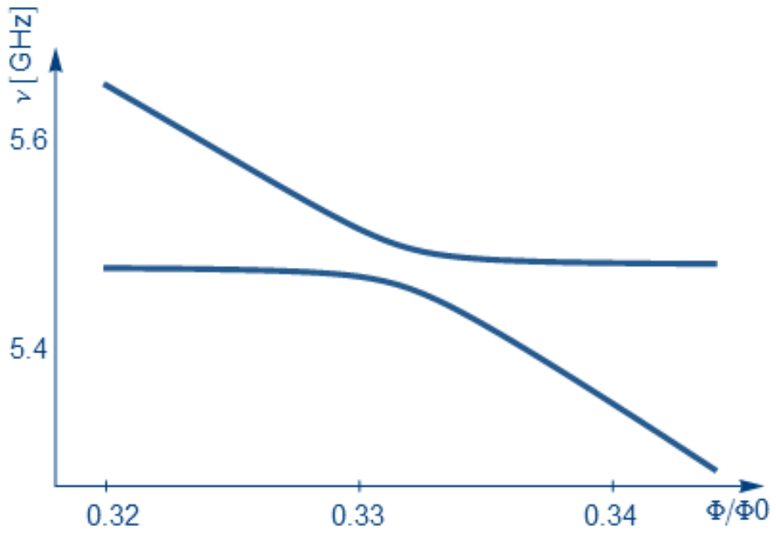

# C-Phase gate using 11 ↔ 02/20 transitions

- $|11\rangle$-level interacts with $|02\rangle$-level
- coupling strength $J_2 \sim 20 - 40\ MHz\ (g \sim 100 - 150\ MHz)$ -> gate duration $\sim 40ns$
- fast, non-adiabatic tuning of qubits into resonance (adiabatic also possible)
- $2\pi$ - rotation after $t = \pi/J_2$
- $|11\rangle$ -state picks up phase $e^{i2\pi/2} = -1$

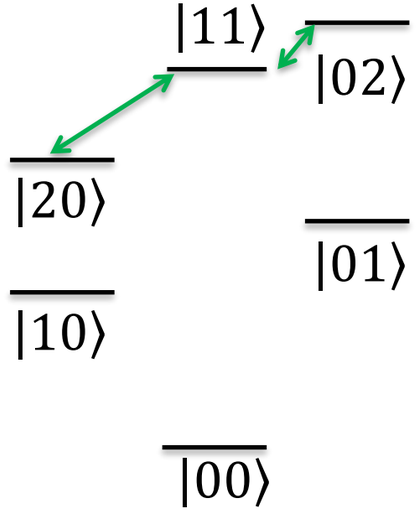


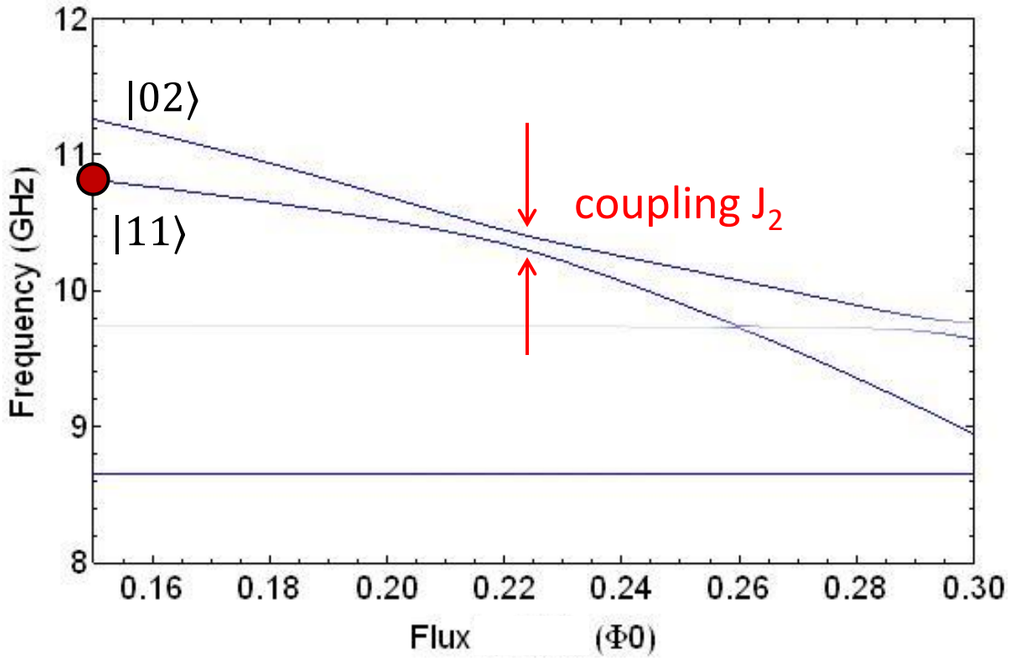


gate operation:

**C-Phase** = universal 2-qubit gate

$$|11\rangle \longrightarrow -|11\rangle$$
$$|01\rangle \longrightarrow |01\rangle$$
$$|10\rangle \longrightarrow |10\rangle$$
$$|00\rangle \longrightarrow |00\rangle$$

$$U_{CPhase} = \begin{pmatrix} 1 & 0 & 0 & 0 \\ 0 & 1 & 0 & 0 \\ 0 & 0 & 1 & 0 \\ 0 & 0 & 0 & -1 \end{pmatrix}$$

# 2-qubit gate: C-Phase gate using $|11\rangle \leftrightarrow |20\rangle$ transition

Similar to iSWAP gate, resonance condition between $|11\rangle - |20\rangle$

coupling Hamiltonian:

$$\mathrm{H}_{\mathrm{cphase}} = J_{20}|11\rangle\langle 20| + h.c. \text{ (or } J_{02}|11\rangle\langle 02| + h.c.\text{)}$$

Adiabatic:

slow, adiabatic change of frequency, no transition to $|02\rangle$
selective energy shift of $|11\rangle$ state caused by coupling
to $|20\rangle$ state leads to accumulation of phase $|11\rangle \rightarrow \mathrm{e}^{\mathrm{iJ_{20}t}}|11\rangle$

Non-adiabatic:

fast, non-adiabatic frequency change
oscillation between states

$$|11\rangle \rightarrow \frac{1}{\sqrt{2}}(|\psi^+\rangle + |\psi^-\rangle) \rightarrow \frac{1}{\sqrt{2}}\left(e^{iJ_{20}t}|\psi^+\rangle + e^{-iJ_{20}t}|\psi^-\rangle\right)$$

rotation on Bloch sphere (basis $|\psi^{\pm}\rangle = (|11\rangle + |20\rangle)/\sqrt{2}$)

return to $(|\psi^+\rangle + |\psi^-\rangle)/\sqrt{2}$ state after time $t = \pi/J_{20}$

non-adiatic return: $|11\rangle$ picks up a minus sign $e^{i\pi} = -1$

[Krantz *et al., Appl. Phys Rev* **6** (2019)]

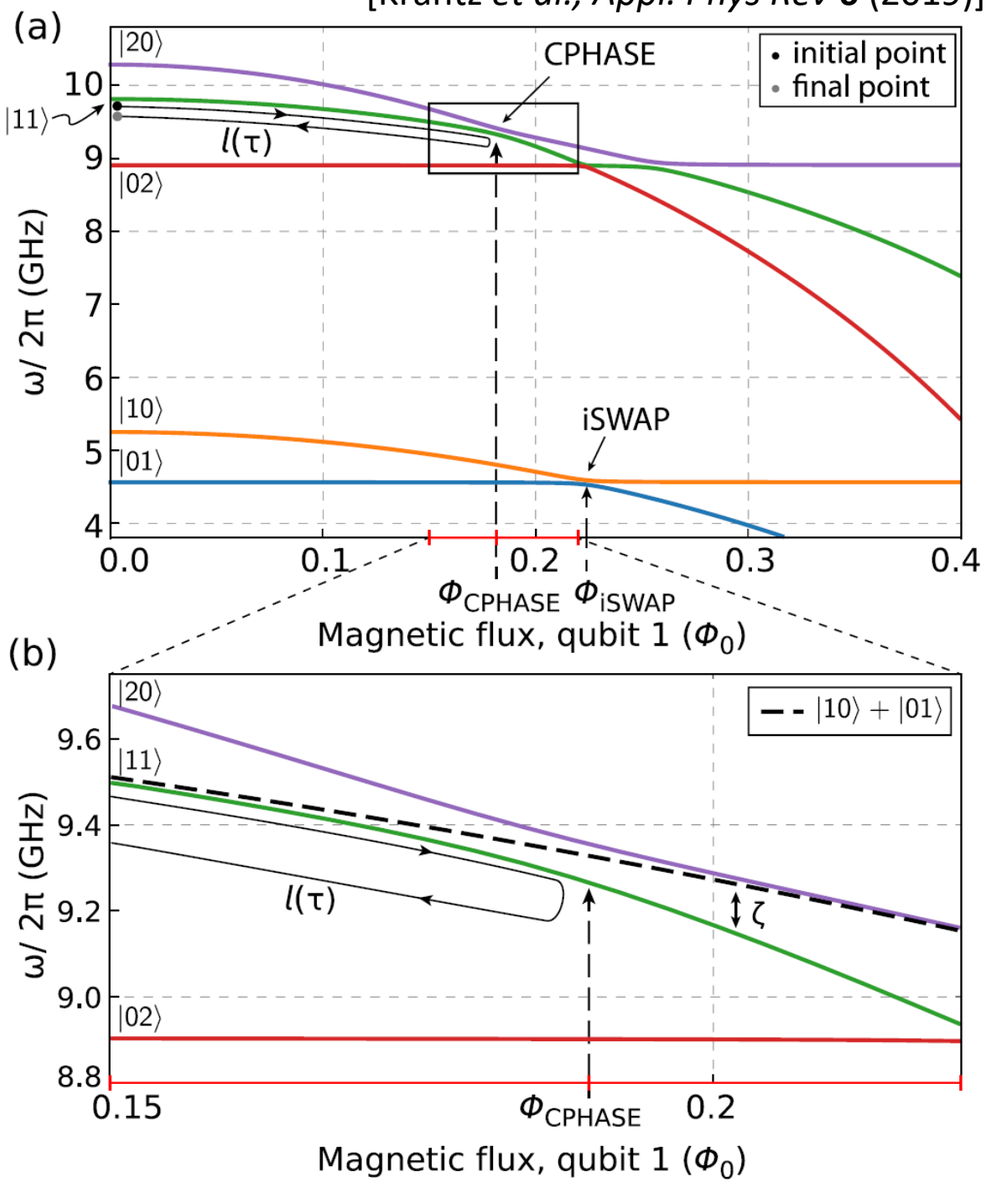

# 2-qubit gate: C-Phase gate using $|11\rangle \leftrightarrow |20\rangle$ transition

resulting unitary operation (adiabatic version)
(including phases acquired by $|10\rangle, |01\rangle, |11\rangle$ relative to ground state $|00\rangle$):

$$U_{ad} = \begin{pmatrix} 1 & 0 & 0 & 0 \\ 0 & e^{i\theta_{10}} & 0 & 0 \\ 0 & 0 & e^{i\theta_{01}} & 0 \\ 0 & 0 & 0 & e^{i(\zeta t+\theta_{10}+\theta_{01})} \end{pmatrix}$$

with frequency difference $\zeta = \omega_{11} - (\omega_{01} + \omega_{10})$

by choosing $\zeta t = \pi$ plus cancellation of single qubit phases (virtual Z-shifts after pulse):

$$U_{CPhase} = \begin{pmatrix} 1 & 0 & 0 & 0 \\ 0 & 1 & 0 & 0 \\ 0 & 0 & 1 & 0 \\ 0 & 0 & 0 & e^{i\pi} \end{pmatrix} = \begin{pmatrix} 1 & 0 & 0 & 0 \\ 0 & 1 & 0 & 0 \\ 0 & 0 & 1 & 0 \\ 0 & 0 & 0 & -1 \end{pmatrix}$$

[Krantz *et al., Appl. Phys Rev* **6** (2019)]

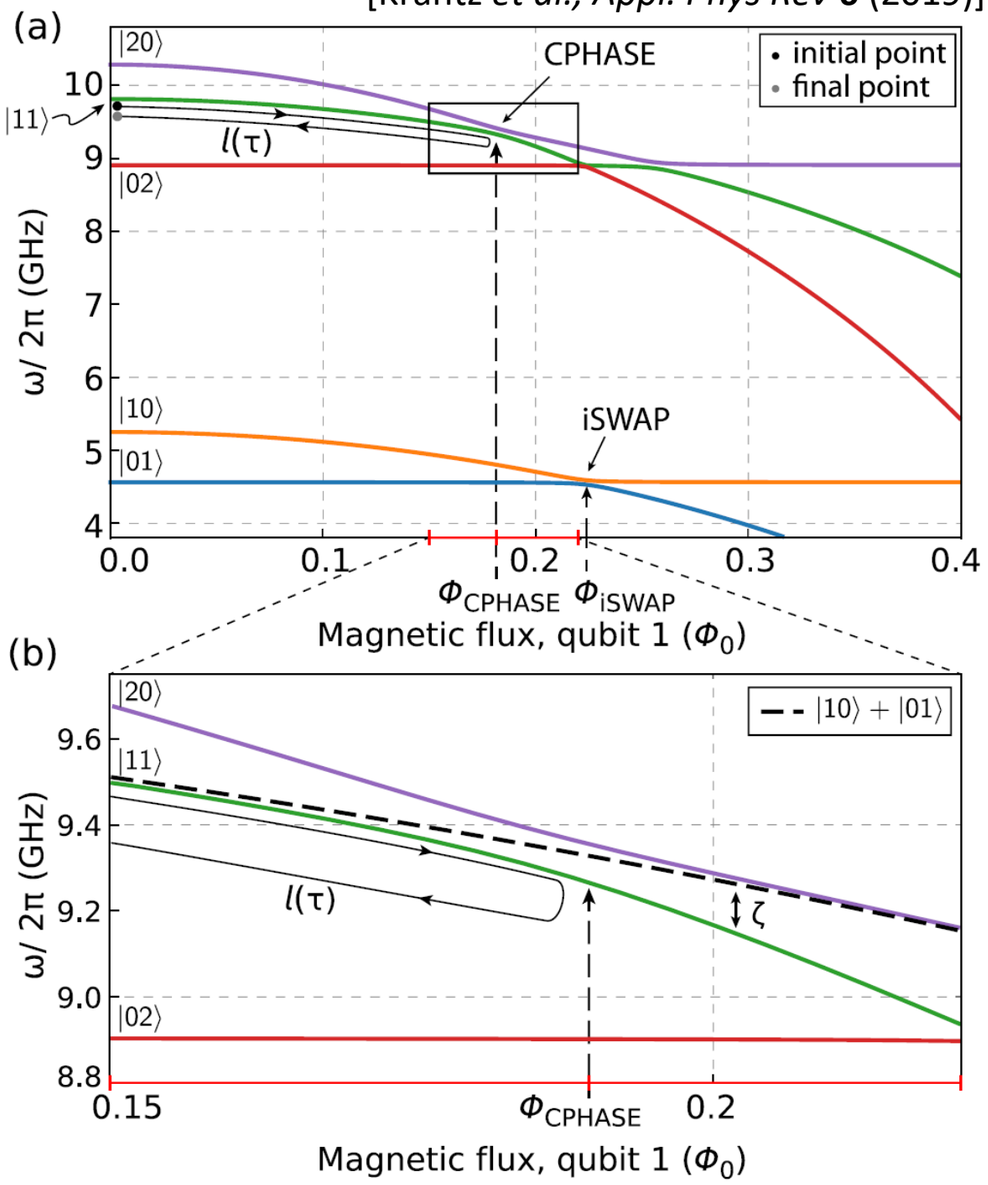

# Two fixed-frequency qubits – one tunable coupler

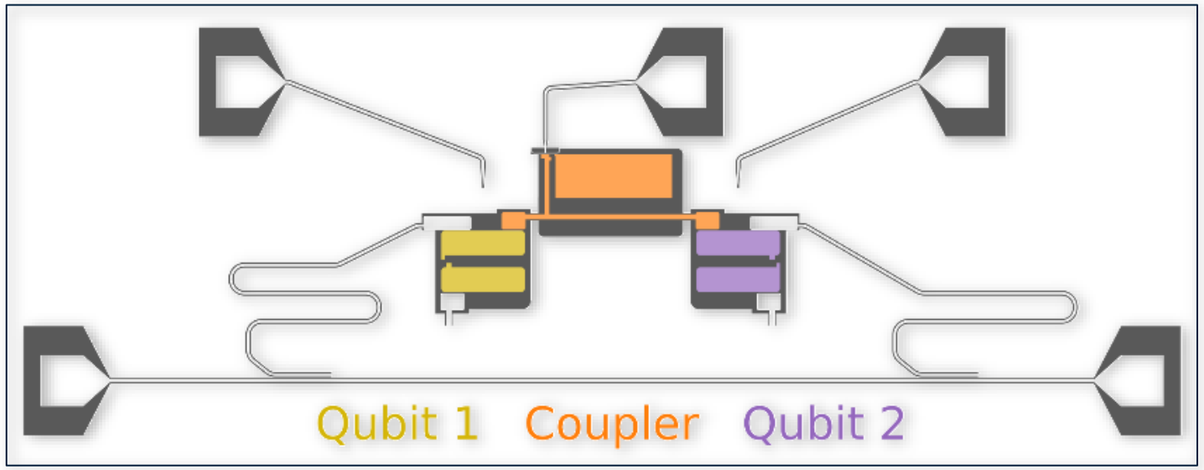


- **Fixed frequency** qubits with control via dedicated **drive lines**
- Two-qubit **CPHASE** gate by adiabatic flux control of **tunable coupler**

| | Frequency $\omega$ | Anharmonicity $\alpha$ | $T_1$ | $T_2^{Echo}$ | $T_2^*$ |
|---|---|---|---|---|---|
| Qubit 1 | 4.115 GHz | -261(1) MHz | 52(4) µs | 111(41) µs | 23(4) µs |
| Qubit 2 | 3.651 GHz | -275(1) MHz | 103(20) µs | 54(11) µs | 5.6(5) µs |
| Coupler | 3.7 - 6.3 GHz | -124 (1) MHz | 16(5) µs | – | – |

# Two-qubit controlled phase gate @ WMI (N. Glaser)

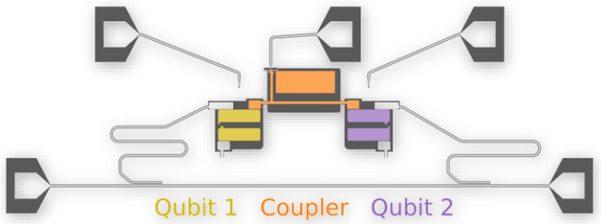


$$U = \begin{pmatrix} 1 & 0 & 0 & 0 \\ 0 & e^{i\alpha} & 0 & 0 \\ 0 & 0 & e^{i\beta} & 0 \\ 0 & 0 & 0 & e^{i(\varphi+\alpha+\beta)} \end{pmatrix}$$

with virtual Z rotations

$$U = \begin{pmatrix} 1 & 0 & 0 & 0 \\ 0 & 1 & 0 & 0 \\ 0 & 0 & 1 & 0 \\ 0 & 0 & 0 & e^{i\varphi} \end{pmatrix}$$

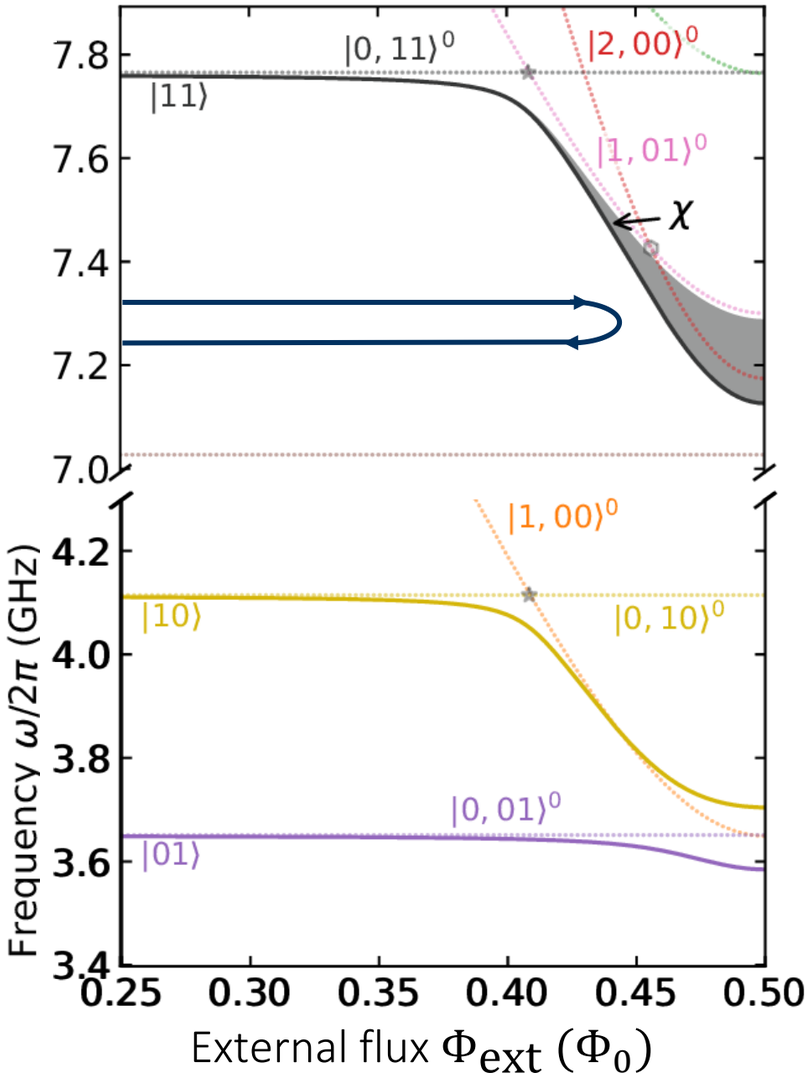


$$\chi = \omega_{11} - (\omega_{01} + \omega_{10})$$

$$\varphi = \int_0^{t_p} \chi\left(\Phi_{\text{ext}}(\tau)\right) \mathrm{d}\tau$$

adiabatic states: $|n_1 n_2\rangle$
bare states: $|n_c, n_1 n_2\rangle^0$

[M. C. Collodo *et al., Phys. Rev. Lett.* **125**, 240502 (2020)
Y. Xu *et al., Phys. Rev. Lett.* **125**, 240503 (2020)
J. Chu & F. Yan, *Physical Review Applied*, **16** (5), 054020 (2021).
Stehlik, J. *et al.*, *Physical Review Letters*, **127** (8), 080505 (2021)]

# Pulse parametrizations

Different pulse shapes**: optimize parameters for highest fidelity (numerical simulation)**

| | #Parameters | Pulse shape | $t_p$ ($\mathcal{F} > 99.9\,\%$) |
|---|---|---|---|
| Gaussian-square | 3 |  | 51 ns |
| Fourier Series | 5 |  | 15 ns |
| Piecewise-constant<br>Using AWG limitations | 22 |  | 9 ns |

Trade-off between parameter count and gate time / fidelity

**C$^3$-toolset:** N. Wittler, *et al., Phys. Rev. Applied* **15**, 034080 (2021)

# Two-qubit (C-Phase) gate optimized pulse shapes

## Gaussian Square

- 3x Shape parameters
- 2x Z-Rotation

Convergence:
40 evolutions (40 min)

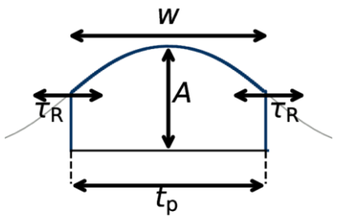


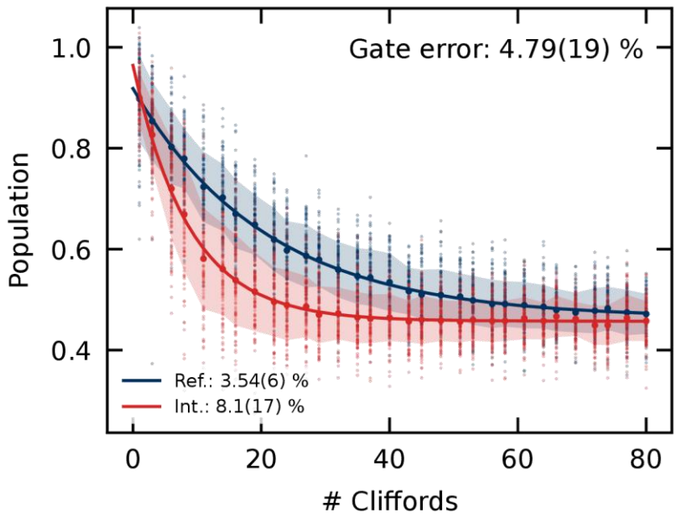


## Fourier Series

- 5x Fourier parameter
- 1x Width
- 2x Z-Rotation

Convergence:
80 evolutions (80 min)

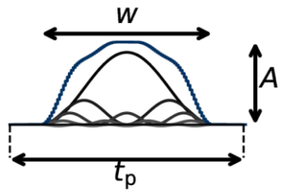


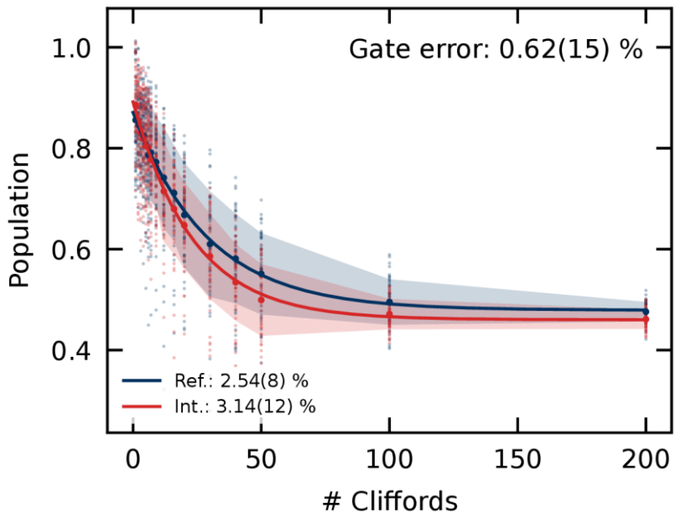


## Linear Interpolation

- 17x Nodes
- 1x Amplitude, 1x Width
- 2x Z-Rotation

Convergence:
260 evolutions (250 min)

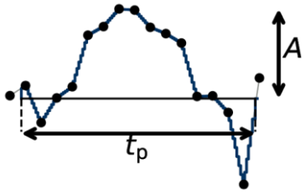


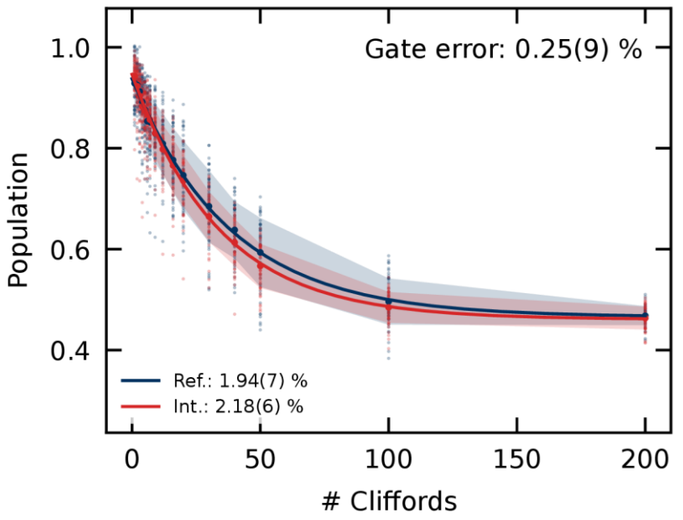


[N. Glaser *et al.*, in prep. (2024)]

# Quantum Error Correction

# The Universal Quantum Computing System

**Idea:**
use error correction schemes
to make a ‘logical’ qubit out
of several ‘good’ physical qubits

$$|0\rangle \rightarrow |00\ldots0\rangle$$
$$|1\rangle \rightarrow |11\ldots1\rangle$$

100-1000 x

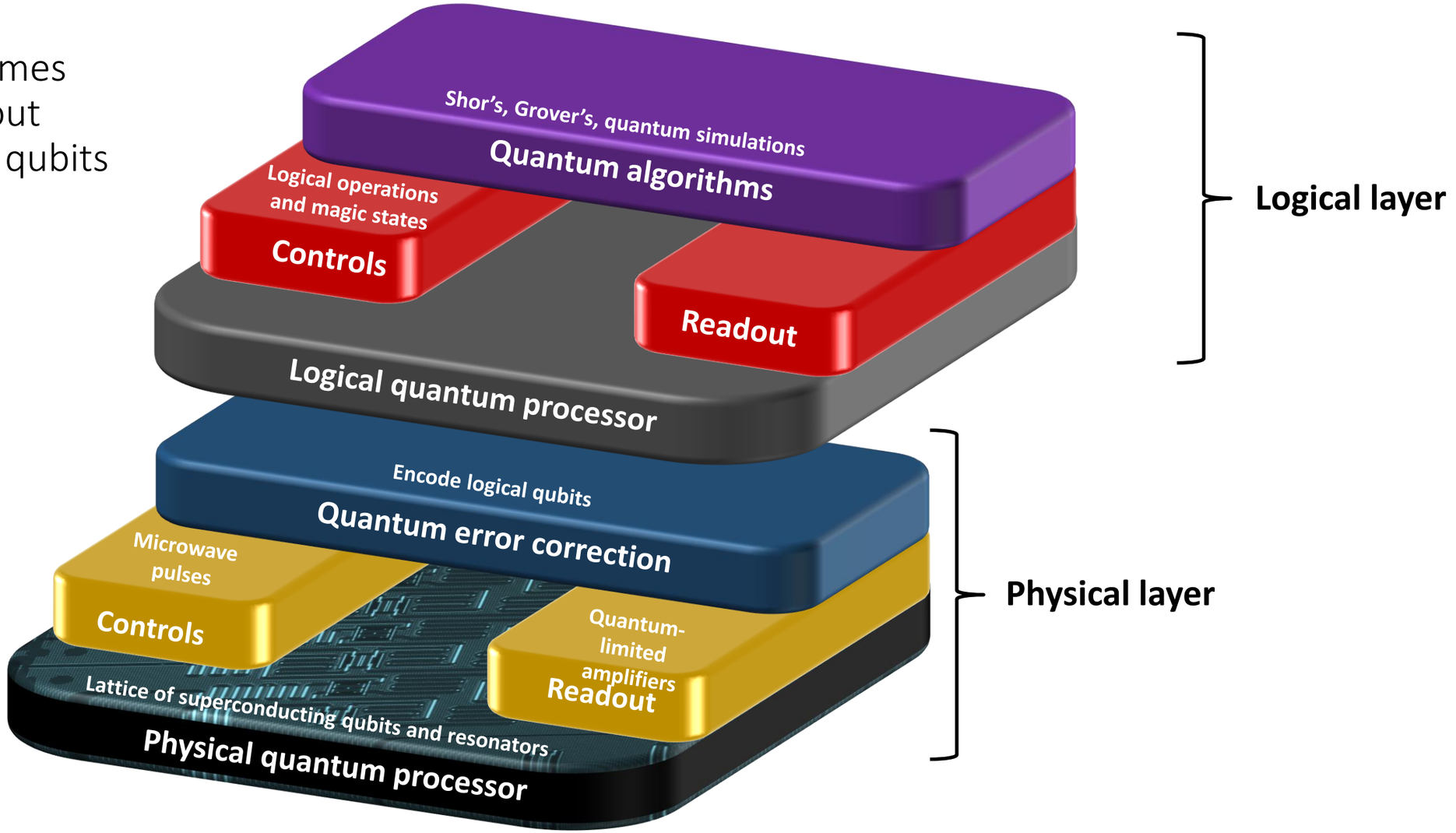


[Gambetta, Chow, Steffen, *npj Quantum Information* **3**, 2 (2017)]

https://ocw.tudelft.nl/course-lectures/3-3-1-quantum-error-correction-codes/

# Repetition Code

**Classical:**

- encode bit value 0 and 1 in *'logical 0'* and *'logical 1'* using multiple bits (*e.g.*, 3)

- assume small error probability $p$ for a bit to flip its value

- majority voting: which value occurs more often determines logical state
  (probability of $\geq 2$ errors $p_e = 3p^2(1-p) + p^3$:
  $p_e < p$ for $p < \frac{1}{2} \rightarrow$ error is reduced)

# Repetition Code

Why is the repetition code not applicable in QM?

No-cloning: encoding scheme needed

Errors are analog: different errors (bit-& phase-flip): must be detected simultaneously

Measurement destroys quantum information

# Repetition Code

**Classical:**

- encode bit value 0 and 1 in *'logical 0'* and *'logical 1'* using multiple bits (e.g. 3)

  $0 \rightarrow 000$ & $1 \rightarrow 111$

- assume small error probability $p$ for a bit to flip its value

  $0 = 000 \rightarrow 001, 010, 100$ or

  $1 = 111 \rightarrow 110, 101, 011$

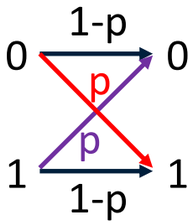


- majority voting: which value occurs more often determines logical state

  (probability of $\geq 2$ errors $p_e = 3p^2(1-p) + p^3$: $p_e < p$ for $p < \frac{1}{2} \rightarrow$ error is reduced)

**Quantum:**

- No-cloning: encoding scheme needed
- Errors are 'analog': different errors (bit-& phase-flip): must be detected simultaneously
- Measurement destroys quantum information

# Repetition Code: Bit-flip channel Encoding

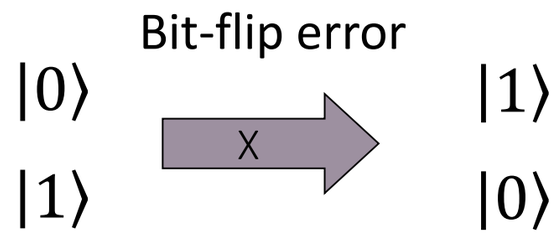


$$|0\rangle \rightarrow |0\rangle_L = |000\rangle$$

$$|1\rangle \rightarrow |1\rangle_L = |111\rangle$$

To detect error: encode 1 bit in multiple (3) bits

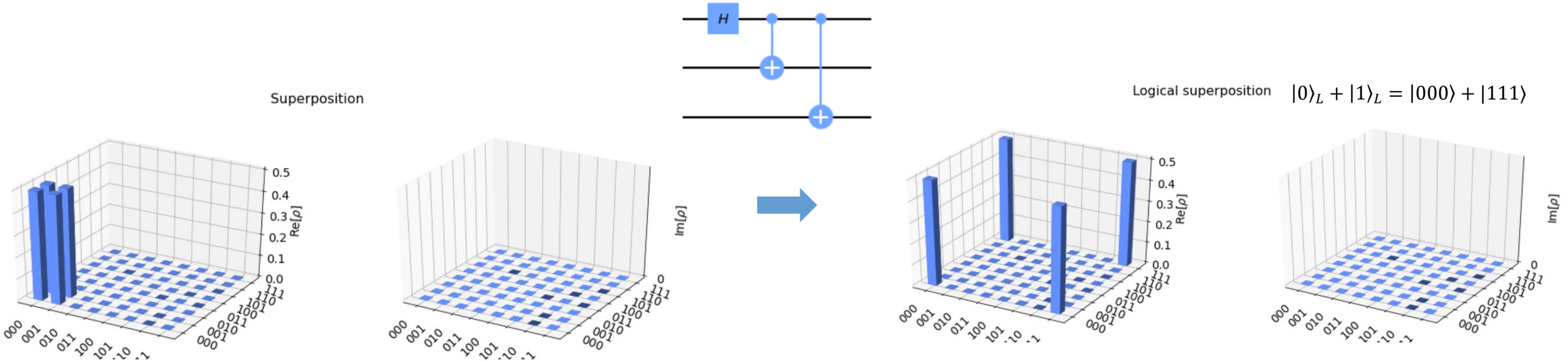

# Repetition Code: Bit-flip channel Encoding

Bit-flip error

$|0\rangle$ → X → $|1\rangle$

$|1\rangle$ → X → $|0\rangle$

$|0\rangle \rightarrow |0\rangle_L = |000\rangle$ → $|100\rangle$, $|010\rangle$, $|001\rangle$

$|1\rangle \rightarrow |1\rangle_L = |111\rangle$ → $|011\rangle$, $|101\rangle$, $|110\rangle$

parity change:

indicates error

To detect error: encode 1 bit in multiple (3) bits


Superposition

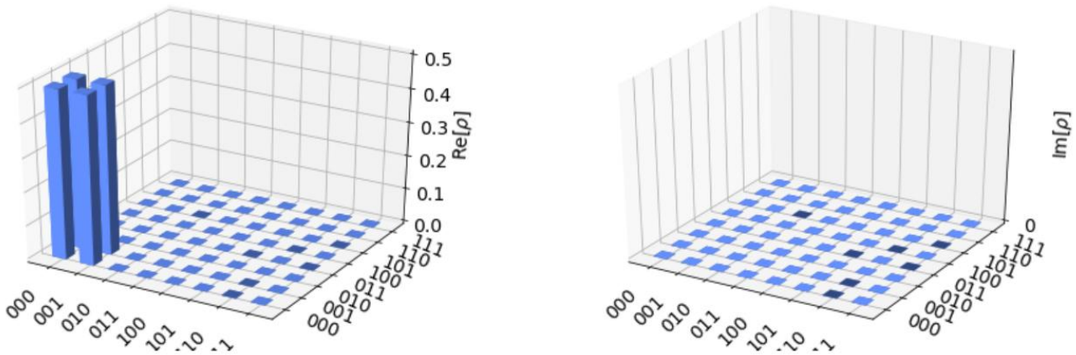


Logical superposition $|0\rangle_L + |1\rangle_L = |000\rangle + |111\rangle$

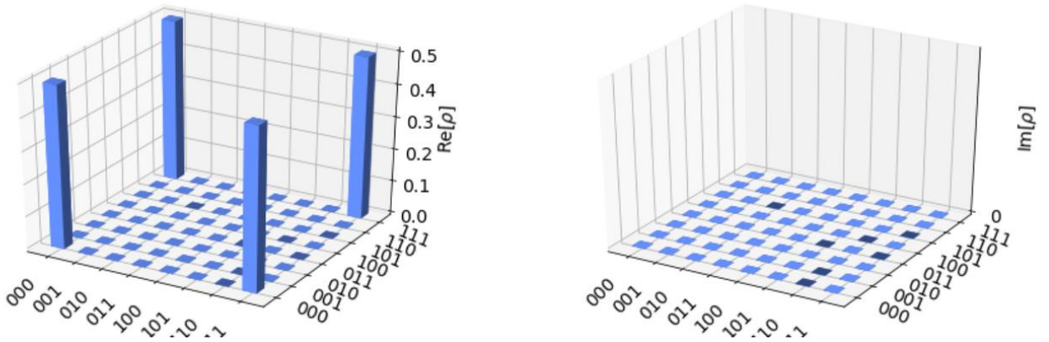

# Repetition Code: Syndrome Measurement / Error Detection

measure $Z_1Z_2$ & $Z_2Z_3$ to identify all possible bit-flip errors

$$|\psi\rangle \propto |000\rangle + |111\rangle$$

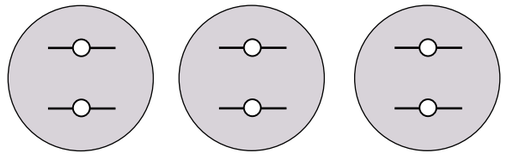

$$\langle Z_1Z_2\rangle = \langle\psi|Z_1Z_2|\psi\rangle = \langle 000|(-1)\cdot(-1)|000\rangle + \langle 111|1\cdot 1|111\rangle = \mathbf{1}$$

$$\langle Z_2Z_3\rangle = \langle\psi|Z_2Z_3|\psi\rangle = \langle 000|(-1)\cdot(-1)|000\rangle + \langle 111|1\cdot 1|111\rangle = \mathbf{1}$$

Bit-flip error qubit 1:

$$|100\rangle + |011\rangle$$

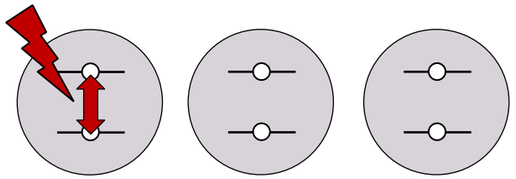

$$\langle Z_1Z_2\rangle = \langle\psi|Z_1Z_2|\psi\rangle = 1\cdot(-1) + (-1)\cdot 1 = \mathbf{-1}$$

$$\langle Z_2Z_3\rangle = \langle\psi|Z_2Z_3|\psi\rangle = (-1)\cdot(-1) + 1\cdot 1 = \mathbf{1}$$

Bit-flip error qubit 2:

$$|010\rangle + |101\rangle$$

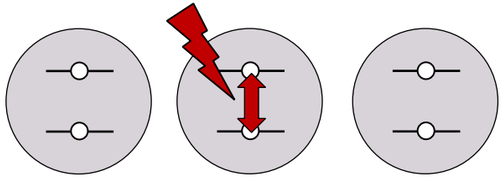

$$\langle Z_1Z_2\rangle = \mathbf{-1}$$

$$\langle Z_2Z_3\rangle = \mathbf{-1}$$

Bit-flip error qubit 3:

$$|001\rangle + |110\rangle$$

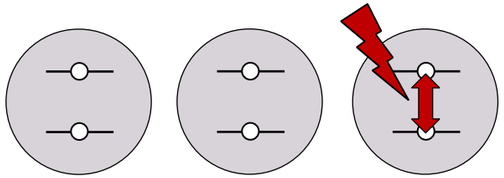

$$\langle Z_1Z_2\rangle = \mathbf{1}$$

$$\langle Z_2Z_3\rangle = \mathbf{-1}$$

# Repetition Code: Syndrome Measurement / Error Detection

measure $Z_1Z_2$ & $Z_2Z_3$ to identify all possible bit-flip errors

$$|\psi\rangle \propto |000\rangle + |111\rangle$$

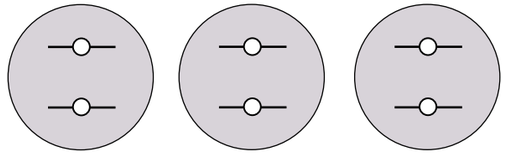

Bit-flip error qubit 1:

$$|100\rangle + |011\rangle$$

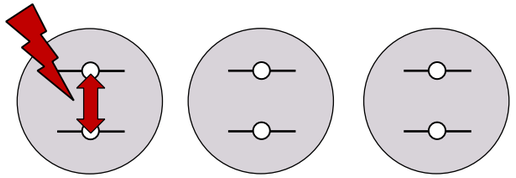

Bit-flip error qubit 2:

$$|100\rangle + |011\rangle$$

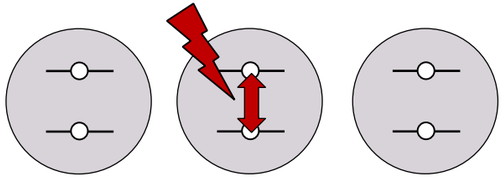

Bit-flip error qubit 3:

$$|100\rangle + |011\rangle$$

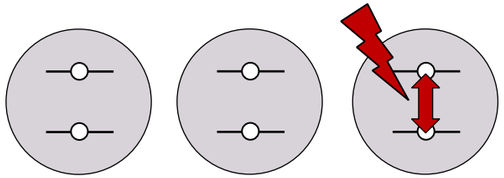

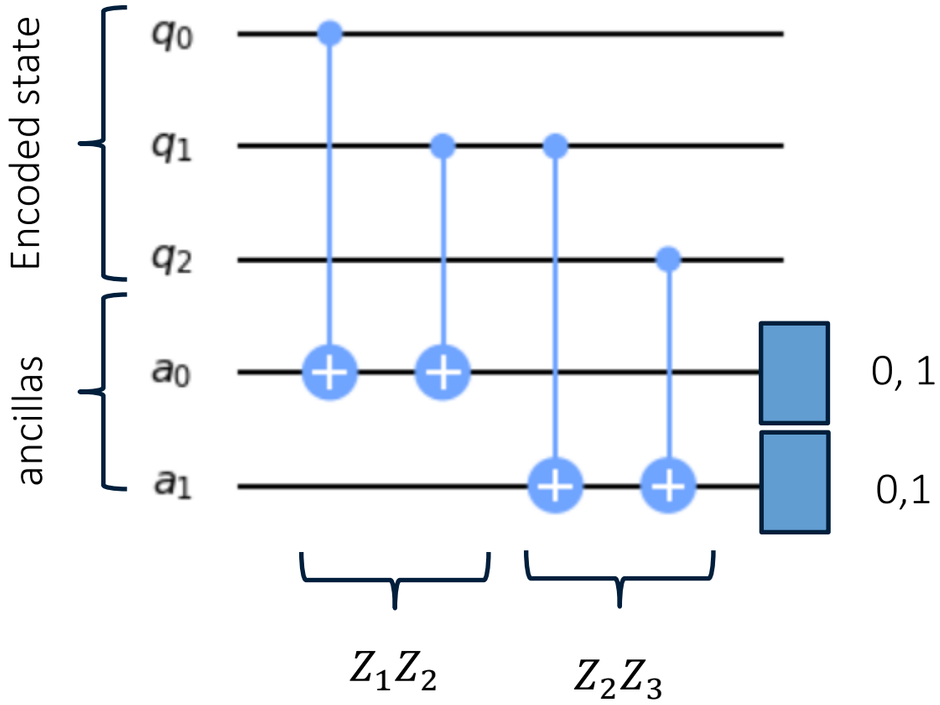


Superposition is not destroyed,
only information about error is extracted!

# Repetition Code: Phase-flip channel Encoding

Phase-flip error

$|+\rangle \xrightarrow{Z} |-\rangle$

$|-\rangle \xrightarrow{Z} |+\rangle$

$|0\rangle \rightarrow |+\rangle_L = |++\,+\rangle \Rightarrow |++\,-\rangle,\ |+-\,+\rangle,\ |-+\,+\rangle$

$|1\rangle \rightarrow |-\rangle_L = |--\,-\rangle \Rightarrow |--\,+\rangle,\ |-+\,-\rangle,\ |+-\,-\rangle$

To detect error: encode 1 bit in multiple (3) bits

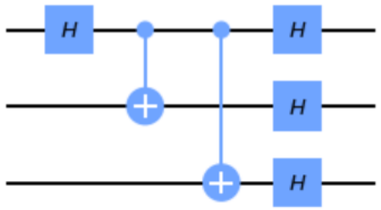


Superposition

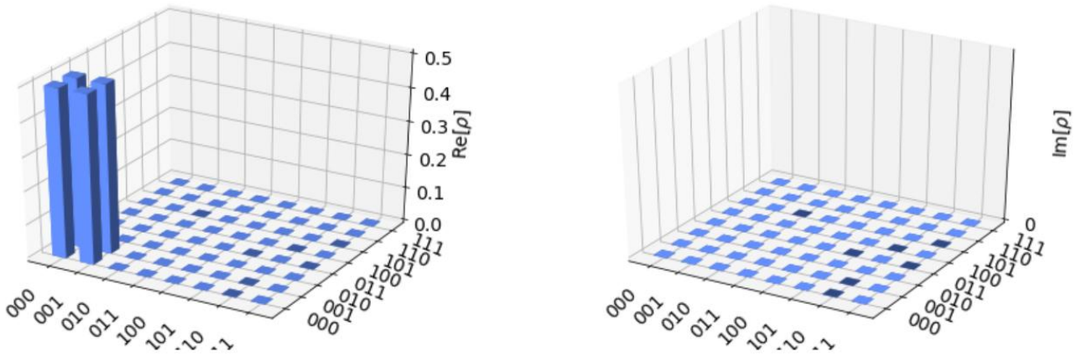


Logical superposition $|0\rangle_L + |1\rangle_L = |++\,+\rangle + |--\,-\rangle$

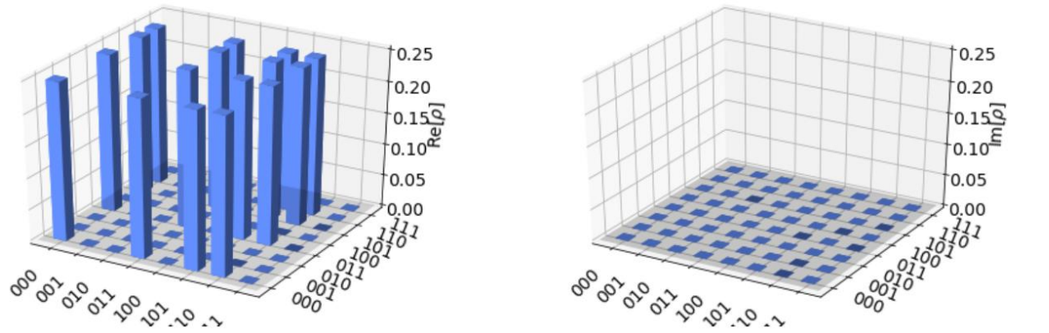

# Repeated Quantum Error Correction (Google AI)

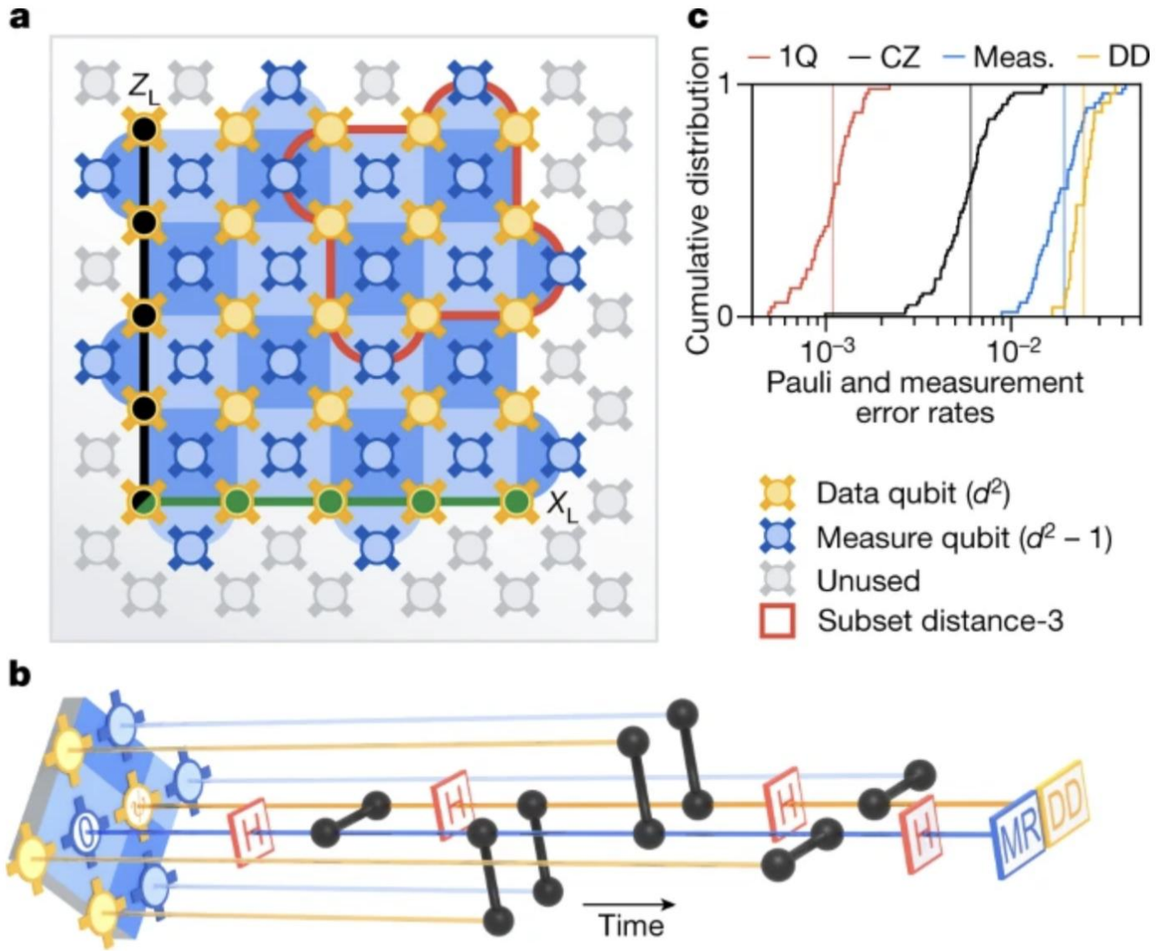


- 72-qubit Sycamore processor (a)
- T1=20$\mu$s, $T_{2,CPMG} = 30\mu s$
- distance-3 & distance-5 surface code
- 49 qubits (25 data, 24 measure) for distance 5
- measure X (b – dark blue) & Z stabilizers (b – light blue)
- Cycle duration: 921 ns
  (25ns single-qubit gates, 34ns two-qubit gates,
  500ns measurement, 160ns reset)

[R. Acharya *et al.*, *Nature* **614** (2023)]

# Error detection cycle

Illustration of a surface code experiment with different types of errors happening

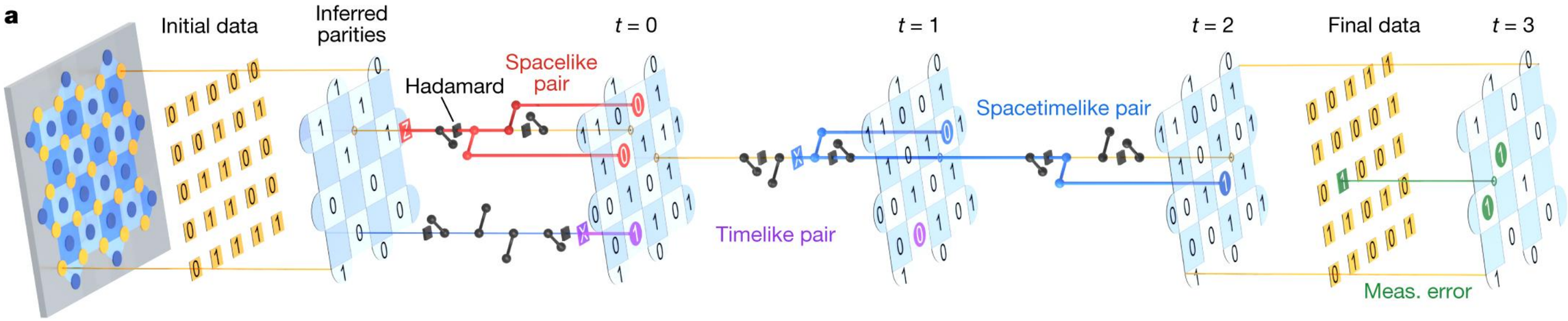


(some) Detection pairs:

1. Z error on data qubit (red) – spacelike pair
2. Measurement error on measurement qubit (purple) – timelike pair
3. X error during CZ gate (blue) – spacetimelike pair
4. Measurement error on data qubit (green) – dected in final Z parities
5. Etc… (more complex patterns for Y errors)

Logical error:
instance succeeds if the corrected logical measurement agrees with the known initial state,
otherwise a logical error has occurred (with probability $p_L$)

# Repeated Quantum Error Correction

Result: first indication that

distance-5 code logical error (2.914)

is (a bit) smaller than

distance-3 code logical error (3.028)!

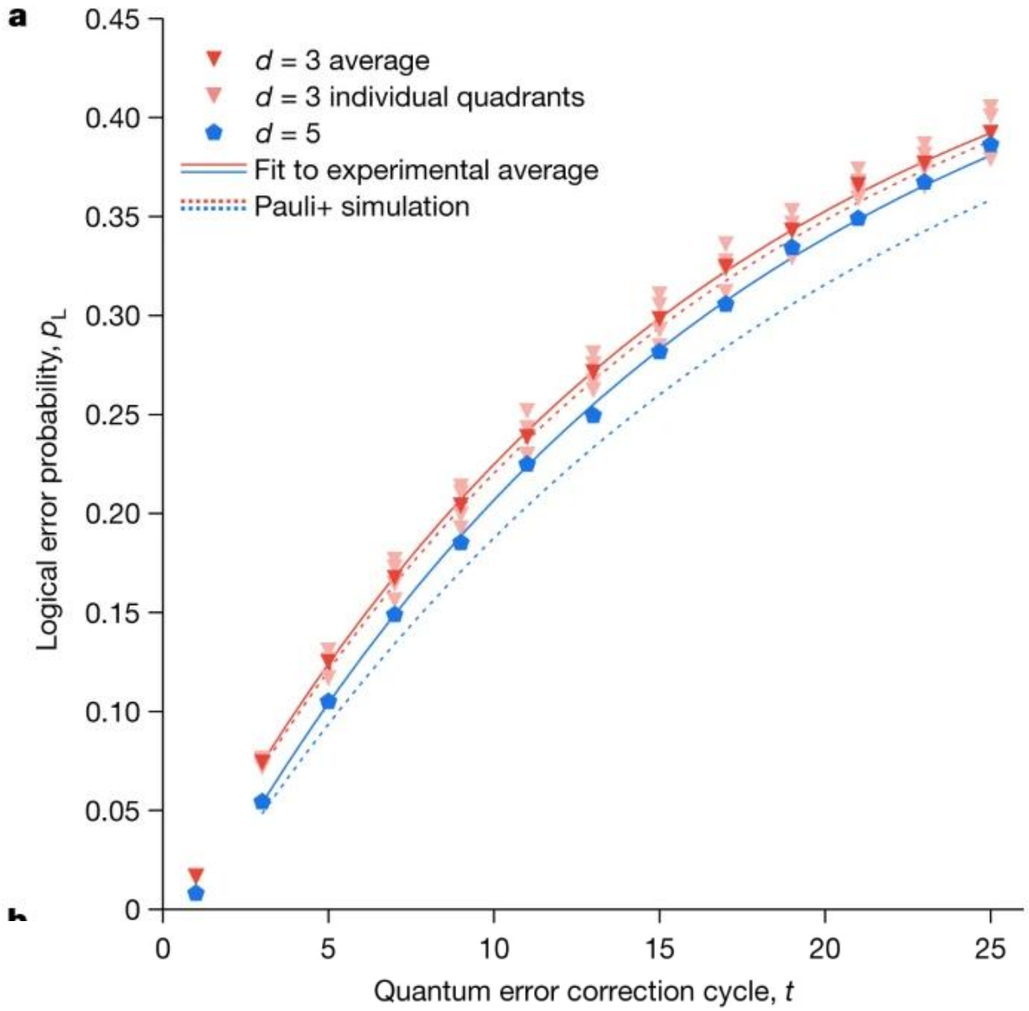


[R. Acharya *et al.*, *Nature* **614** (2023)]

# Challenges ahead

# Challenges ahead (Hardware centric)

Scaling: *guarantee performance at scale*

cross-coupling and cross-talk, uniformity & reproducibility,
scalable control, I/O, size of qubits, thermal budget

Coherence: *maximize lifetime of quantum states*

identification of loss channels and noise sources
(two-level fluctuators, quasi-particles and ionizing radiation, B-field fluctuations), mitigation (by design, by choice of materials, by fabrication)

Control & readout: *coherence-limited high-fidelity gates*

pulse optimization, benchmarking sequences,
multi-qubit operations & extended gate sets

System: *guarantee stable operation conditions*

automated calibration & bring-up, run-time environment,
characterization & verification, quantum/classical integration,
(cryogenic) electronics

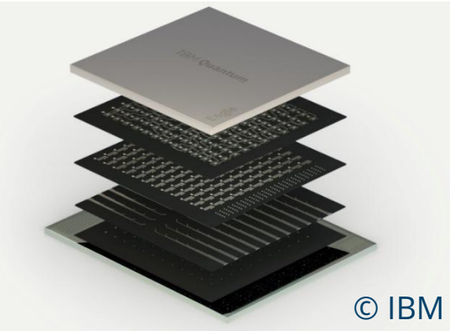
© IBM

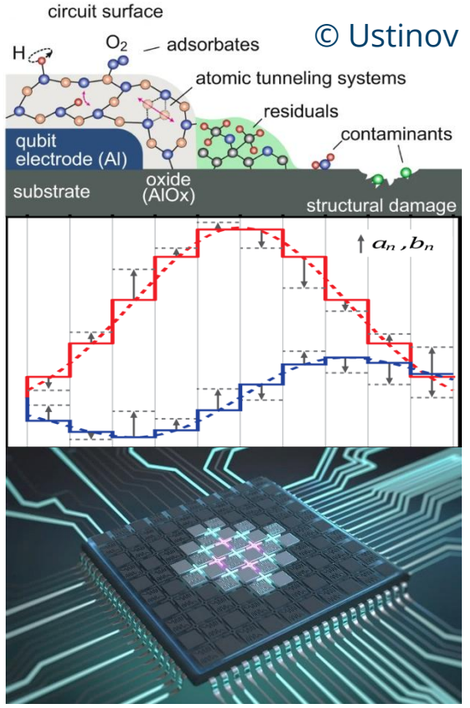

© Ustinov

# Scaling: Reproducibility of Josephson junctions

Josephson junction circuit = qubit

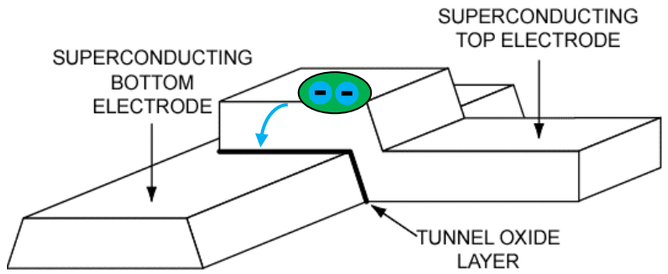


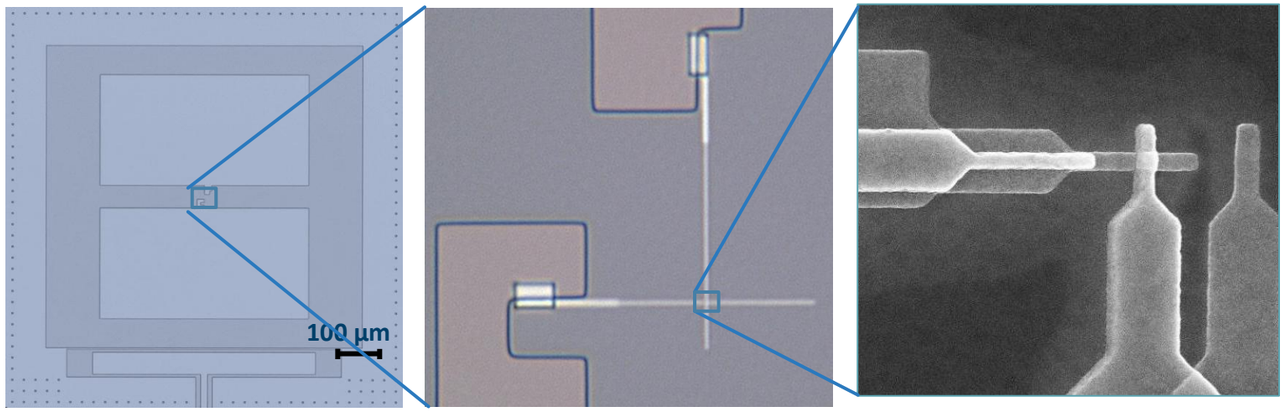


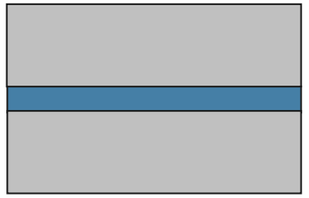

*aluminum*

~ 1nm barrier, $Al_2O_3$

*aluminum*

Qubit frequency: $\omega_q \approx \sqrt{8\,E_J\,E_C} - Ec$ around $5 - 6$ GHz

(charging energy $E_C$; Josephson energy $E_J = \phi_0 I_C$; critical current $I_c \propto A/d$)

Reproducibility: currently $150 - 200$ MHz spread caused by variations of $E_J$ caused (most likely) by lithography uncertainties

Mitigation: improved fabrication, ‘retro-fitting’ of junctions

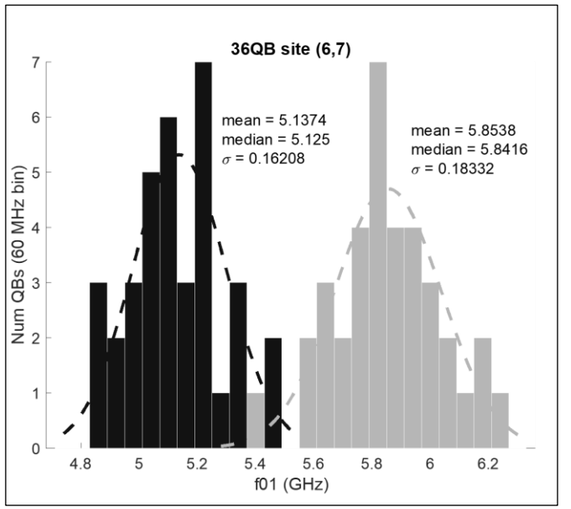

# Coherence: Intrinsic loss ($T_1$)

## Origin:

defects and adsorbates (two-level flucutators)

(mostly) at interfaces

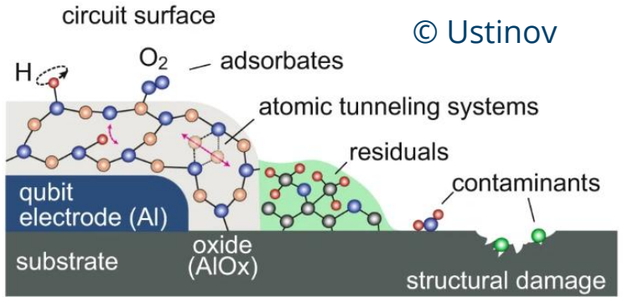


© Ustinov

## Strategy 'design': minimize e-field density on interfaces

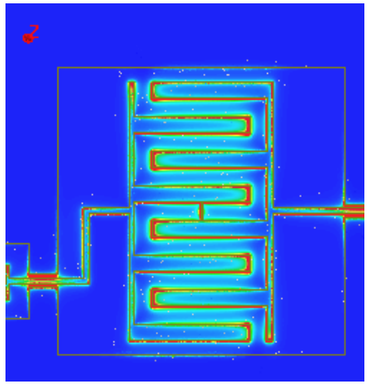

$Q \approx 200 - 500k$

$T_1 \approx 5 - 10\mu s$

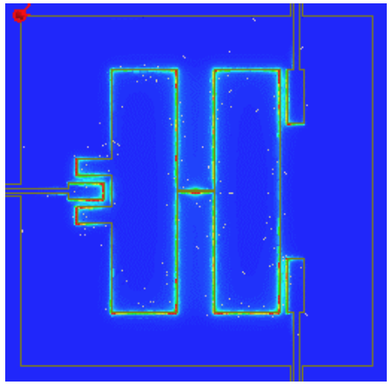

$Q \approx 1.5 - 2.4M$

$T_1 \approx 40 - 80\mu s$

[Wenner 2011; Geerlings 2012; Gambetta 2017 ]

## Strategy 'fabrication': improve technology

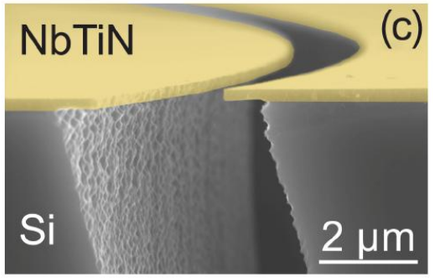


avoid lossy interfaces (trenches, ...)

© Bruno et al 2015

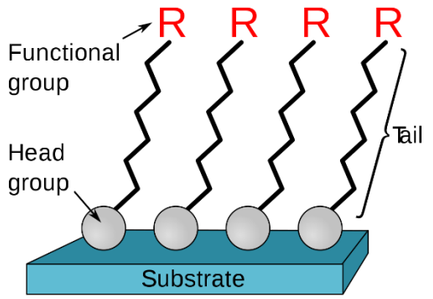


surface treatment (cleaning, passivation,...)

© Wikipedia

# Novel types of qubits

- Fluxonium:
  [Manucharyan *et al.*, *Science* **326**, 113 (2009)]
  single small JJ shunted by a large inductance

- Capacitively-Shunted Flux qubit (CSFQ):
  [Steffen *et al.*, *PRL* **105**, 100502 (2010); Yan *et al. Nat Comm* **7** (2016)]
  Flux-qubit with 3-junction loop,
  capacitively shunted to avoid charge noise

- $0 - \pi$ qubit
  [Brooks *et al.*, *Phys. Rev. A* **87**, 52306 (2013)]
  symmetry protected against relaxation and dephasing

- 'your new qubit'...

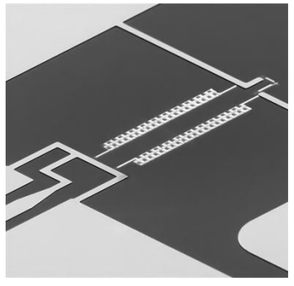

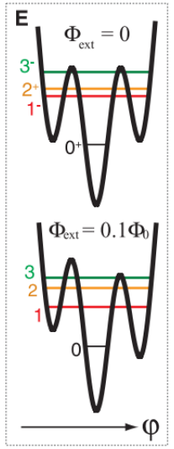


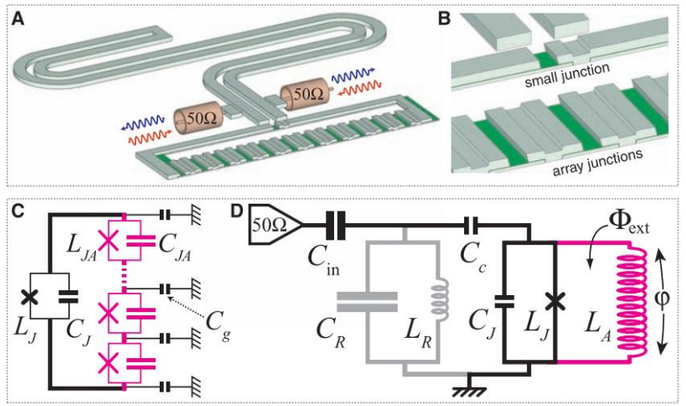


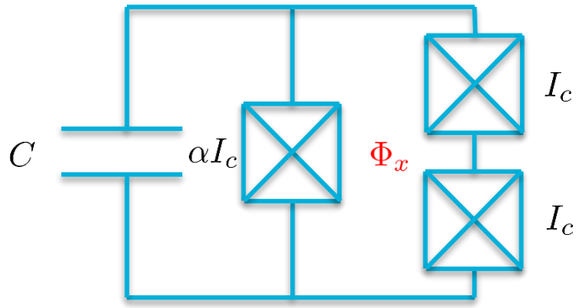


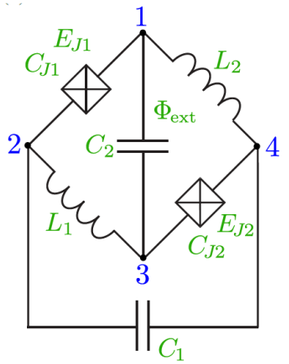

# Scaling: 3D integration

## Requirement for scalability:

- addressability of all qubits (3-5 controls per qubit)
  → would require $> 10^6$ signal lines for universal QC
- reduction of modes in large chips
- reduction of cross-talk

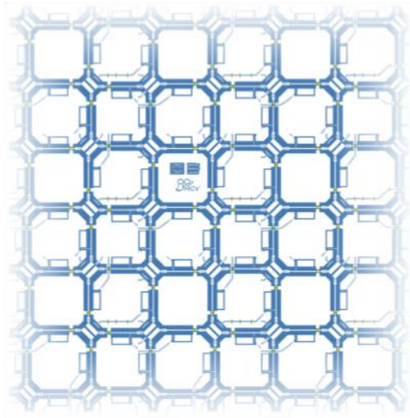

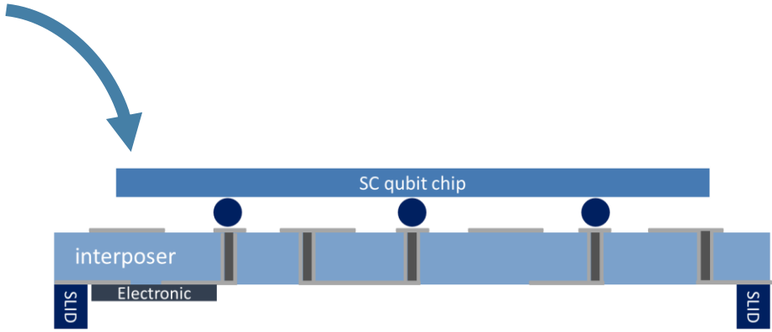


## Technologies in fabrication:

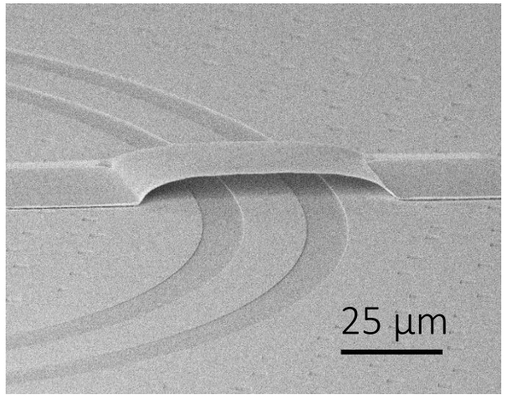


Airbridges

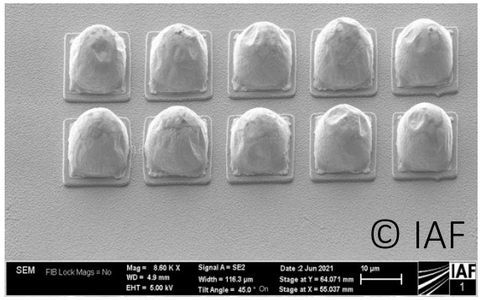


Bump-bonds
(flip-chip)


Thru-silicon vias

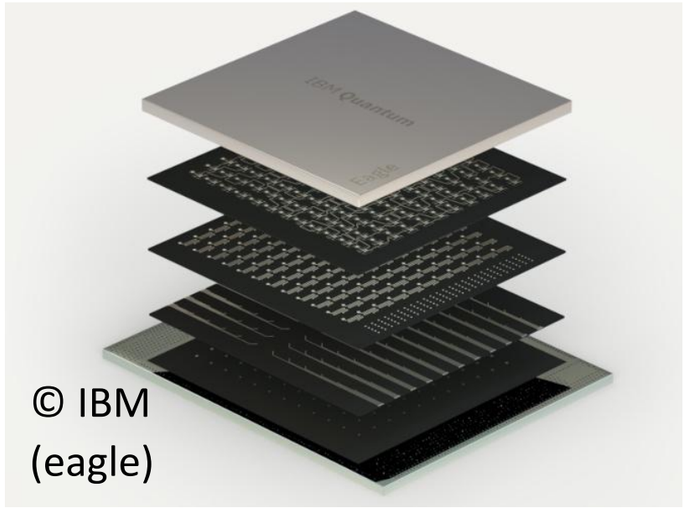

# Scaling: I/O

## Requirement for scalability:

- addressability of all qubits (3-5 controls per qubit)
  → would require $> 10^6$ signal lines for universal QC
- reduction of modes in large chips
- reduction of cross-talk

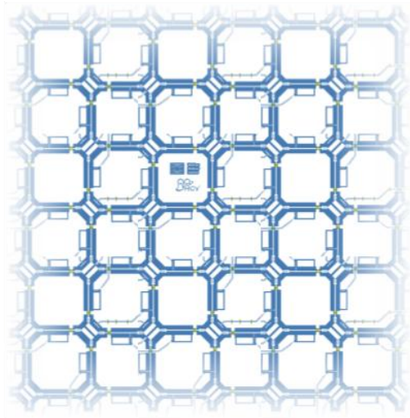

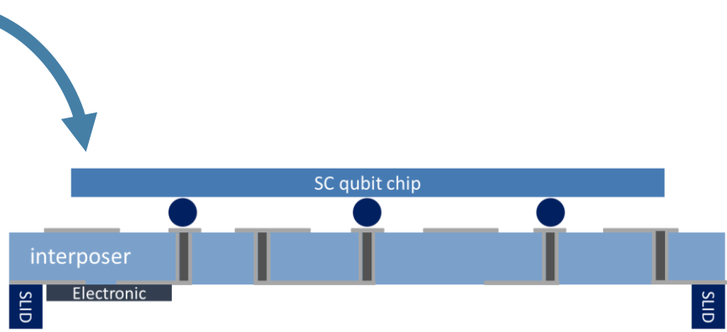


## Technologies for I/O:

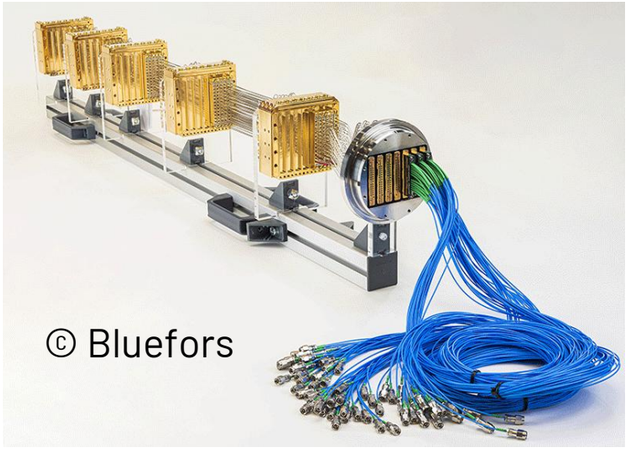


High-density wiring

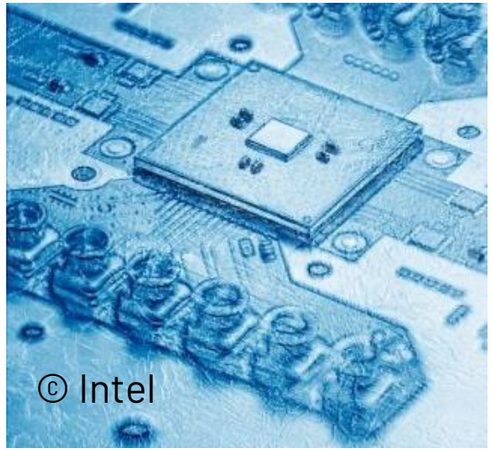


Cryogenic electronics

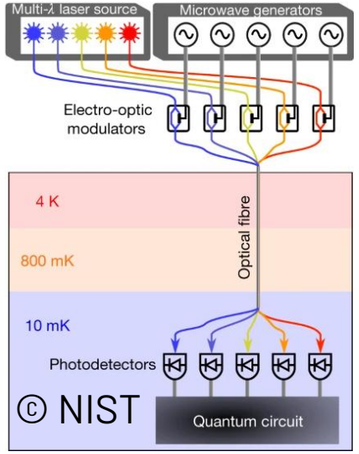


Optical links

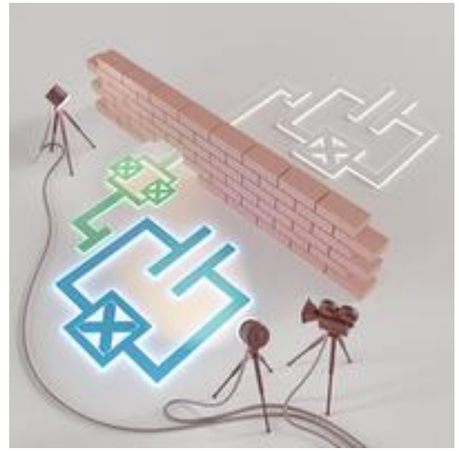

'control' qubits

# Performance at scale

Challenge: **Guarantee excellent performance across entire chip**

Parameters:

- qubit frequency
- qubit coherence ($T_1$, $T_2$)
- control cross-talk
- single-qubit gate fidelity
- two-qubit gate fidelity
- readout fidelity

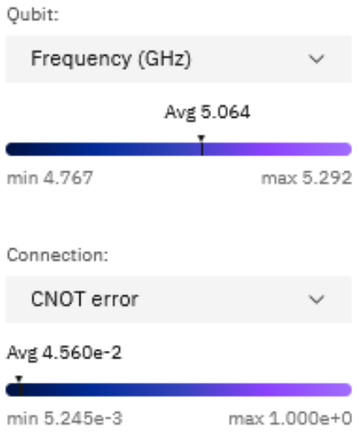


Requires:

- reproducible and uniform fabrication
- efficient calibration and control tools
- scalable (microwave) design methods
- fast and scalable electronics
- excellent shielding
- …

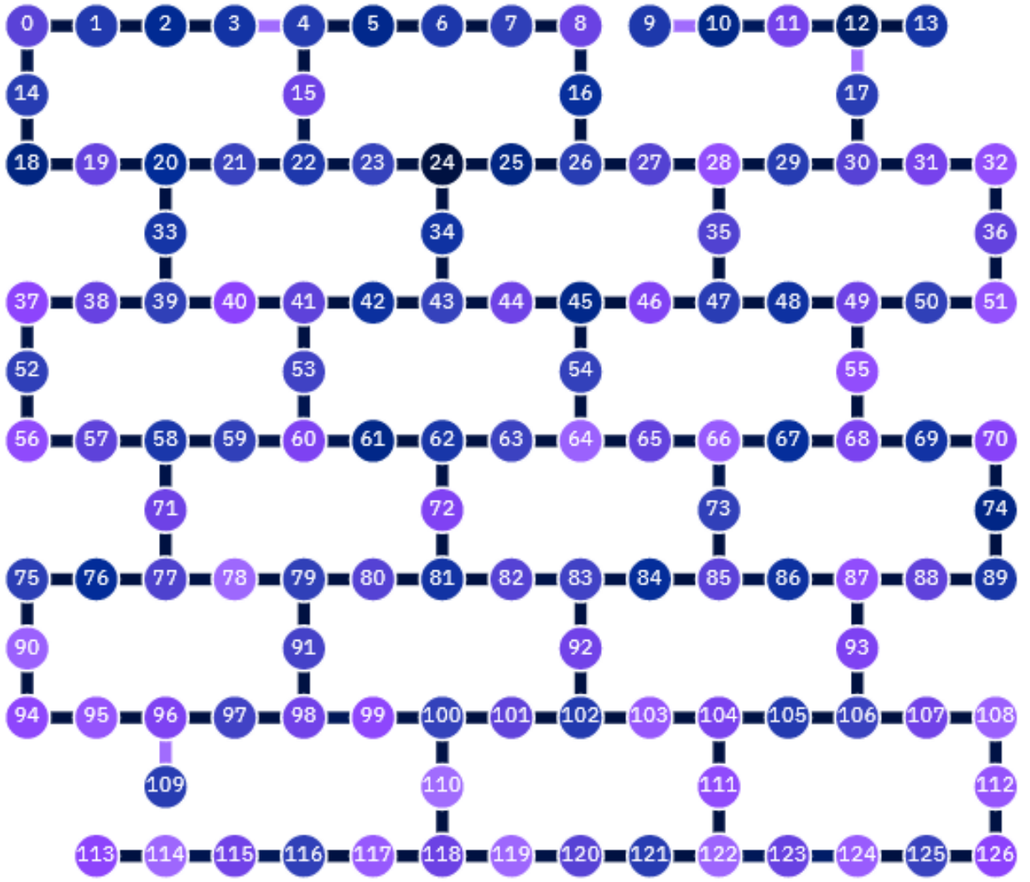


IBM 127 qubit chip ‘Washington’

# Optimal Control for high-fidelity pulses and efficient bring-up

Pulse control to avoid coherent errors
(leakage, cross-talk, stark shifts,...)

Challenge: qubit-specific pulses

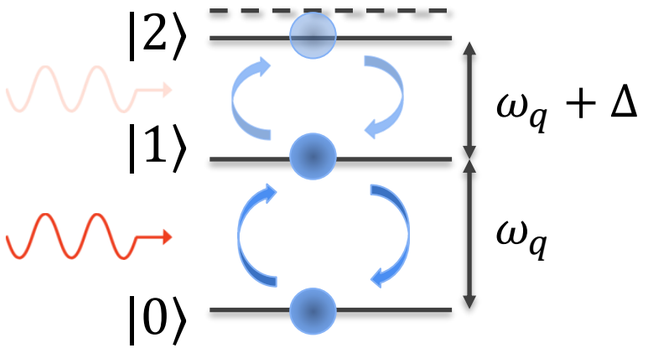


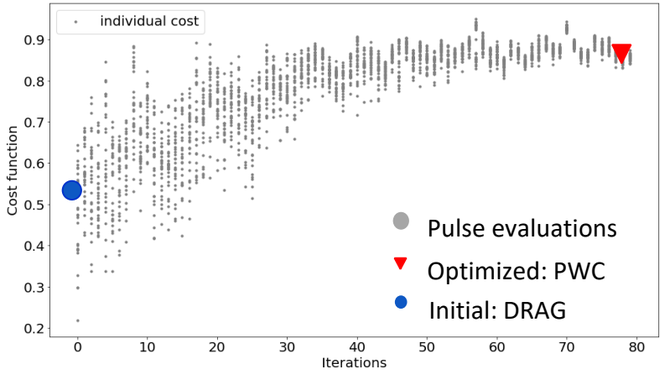


pulse design:
analytical/numerical
control pulses

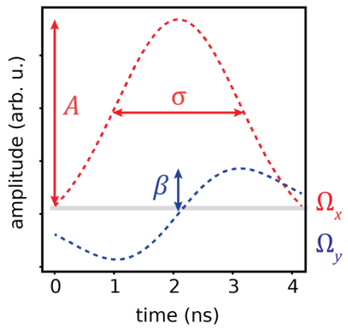



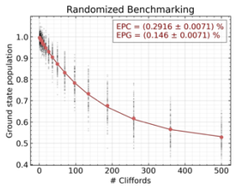


adjust pulse
(gradient free
optimization)

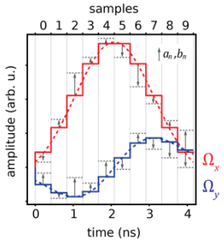


measure fidelity
(randomized benchmarking)

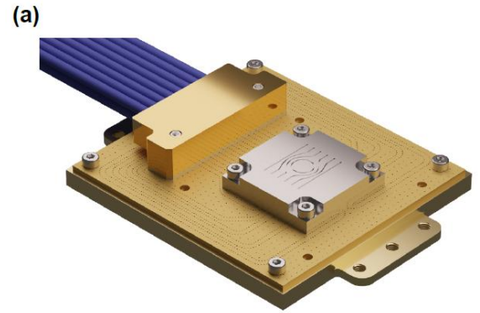


[Egger, Wilhelm 2014; Werninghaus 2021]

# System integration and quantum/classical interfaces

## Hybrid quantum/classical computing:

efficient interfaces for fast optimization (VQE, QAOA) and fast feedback/reset (error correction)

*e.g.* variational quantum eigensolver (VQE)

minimize energy function $\mathrm{E} = \langle\psi(\theta)|H_{mol}|\psi(\theta)\rangle \rightarrow min.$

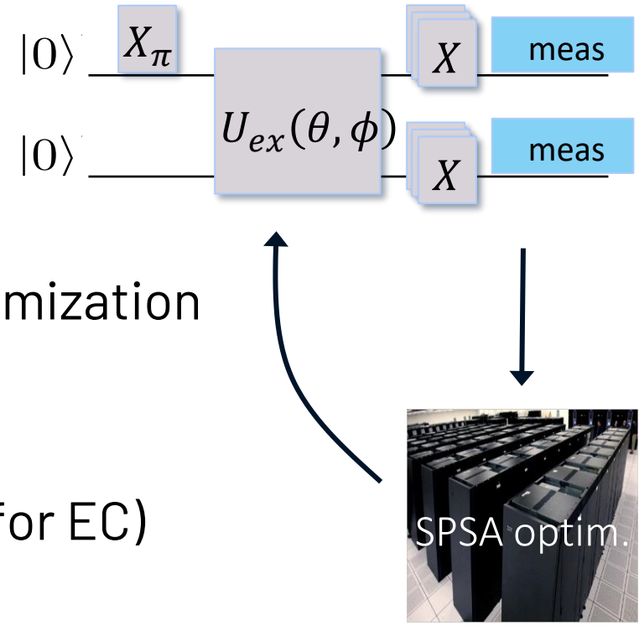


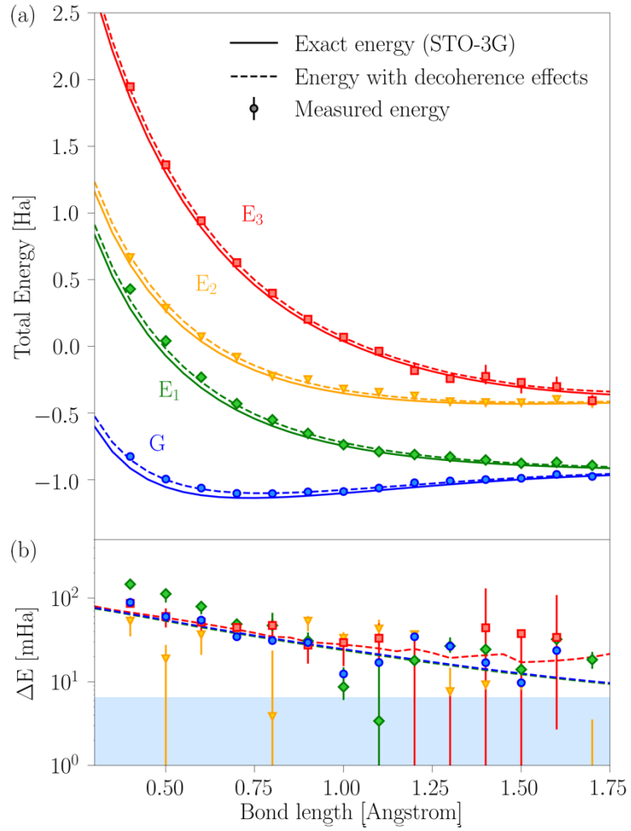


[Ganzhorn et al., PR Applied (2019)]

## Challenges:

- Fast updates of pulses, real-time optimization
- High repetition rates
- System stability
- Fast measurement-based feedback (for EC)

# Grand Challenge: Quantum Computing

## Goal:

**Build computers based on quantum physics to solve problems that are otherwise intractable**

## Roadmap:

### Small-scale (Quantum advantage)

- Research level demonstrations
- Verify chemistry and error correction principles
- Demonstrate ‘Quantum advantage’

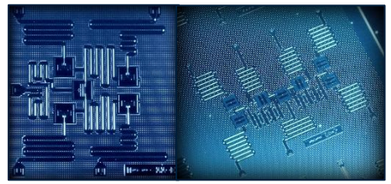

5-8 qubits

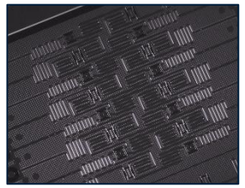

16-20 qubits

### Medium-scale (approximate QC)

- Develop “Hardware-efficient” apps
  - Chemical configurations
  - Optimization
  - Hybrid quantum-classical computers
- No full error correction available

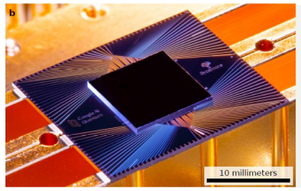


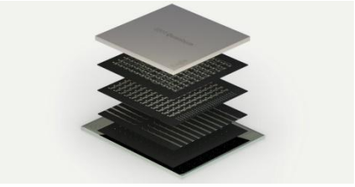

50-100+ qubits

### Large-scale (Universal QC)

Known and proven speed-up:

- Factoring
- quantum molecular simulations
- Speed-up machine learning

Enable secure cloud computing

$10^5$-$10^6$ qubits

# Literature


- Steve Girvin's Les Houche Lecture Notes: https://sites.google.com/site/stevenmgirvin/girvin-les-houches-lecture-notes-drafts
- P. Krantz et al. 'A quantum engineer's guide to superconducting qubits'. Applied Physics Reviews **6**, 021318 (2019), https://arxiv.org/abs/1904.06560
- Nielsen & Chuang, 'Quantum Computation and Quantum Information'. Cambridge Univ. Press.
- 'Learn Quantum Computation with Qiskit', https://qiskit.org/textbook/preface.html'.
- Preskill lecture notes: http://www.theory.caltech.edu/people/preskill/ph229/
- A. Blais et al. 'Circuit Quantum Electrodynamics', https://arxiv.org/abs/2005.12667; Rev. Mod. Phys. 93, 25005 (2021)
- M. Kjaergaard, Superconducting Qubits: Current State of Play Annual Review of Condensed Matter Physics: Vol. 11:369-395, (2020), https://arxiv.org/abs/1905.13641

# Questions

Any questions?

# Quantum Computing: From Theory to Practice

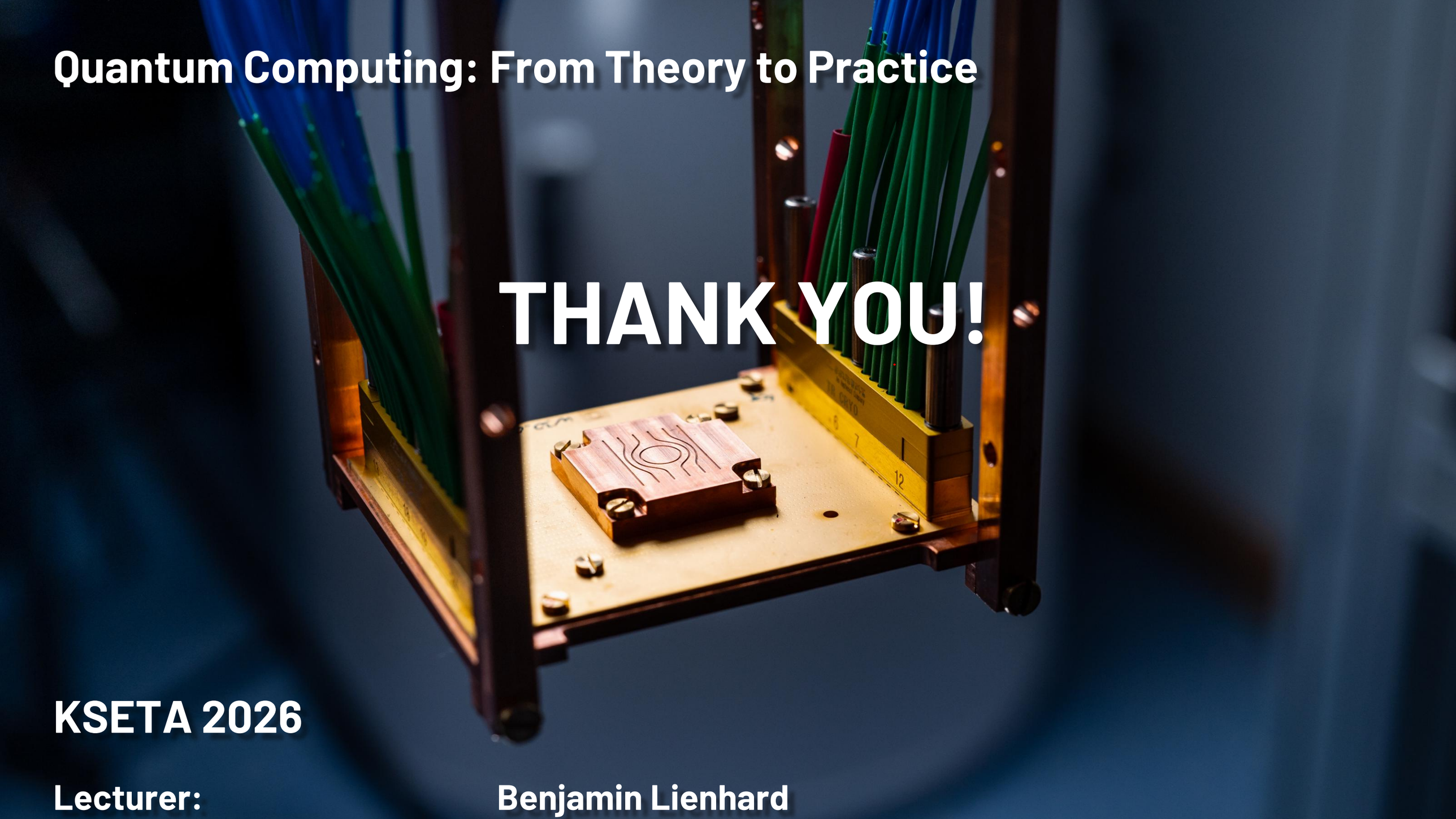

# THANK YOU!

## KSETA 2026

**Lecturer:** Benjamin Lienhard